January 2017

Determination Of Lignin Degradation Products By GC-MS And Thermal Carbon Analysis (tca)

Jan Bilek

DETERMINATION OF LIGNIN DEGRADATION PRODUCTS BY GC-MS AND THERMAL CARBON ANALYSIS (TCA)

by

Jan Bílek

A Thesis

Submitted to the Graduate Faculty

of the

University of North Dakota

in partial fulfillment of the requirements

for the degree of

Master of Science

Grand Forks, North Dakota
December
2017

This thesis, submitted by Jan Bílek in partial fulfillment of the requirements for the Degree of Master of Science from the University of North Dakota, has been read by the Faculty Advisory Committee under whom the work has been done and is hereby approved

Dr. Alena Kubátová

Dr. Evgueni Kozliak

Dr. David Pierce

This thesis is being submitted by the appointed advisory committee as having met all of the requirements of the School of Graduate Studies at the University of North Dakota and is hereby approved.

Grant McGimpsey
Dean of the school of Graduate Studies

December 1, 2017
Date

PERMISSION

Title	Determination of Lignin Degradation Products by GC-MS and Thermal Carbon Analysis (TCA)
Department	Chemistry
Degree	Master of Science

In presenting this thesis in partial fulfillment of the requirements for a graduate degree from the University of North Dakota, I agree that the library of this University shall make it freely available for inspection. I further agree that permission for extensive coping for scholarly purposes may be granted by the professor who supervised my thesis work or, in her absence, by the Chairperson of the department or the dean of the School of Graduate Studies. It is understood that any copying or publication or other use of this thesis or part thereof for financial gain shall not be allowed without my written permission. It is also understood that due recognition shall be given to me and the University of North Dakota in any scholarly use which may be of any material in my thesis.

Jan Bilek

November 22nd, 2017

TABLE OF CONTENTS

LIST OF FIGURES

LIST OF TABLES

LIST OF ABBREVIATIONS

ACN	Acetonitrile
amu	Atomic Mass Unit
BET	Brunauer-Emmett-Teller Isotherm
b.p.	boiling point
BSTFA	N,O-bis(trimethylsilyl)trifluoroacetamide
Da	Dalton
DCM	Dichloromethane
DMSO	Dimethylsulfoxide
DSC	Differential Scanning Calorimetry
EI	Electron Ionization
EtOAc	Ethyl Acetate
EtOH	Ethanol
FID	Flame Ionization Detector
FTIR	Fourier-Transform Infrared Spectroscopy
GC-FID	Gas Chromatography-Flame Ionization Detector
GC-MS	Gas Chromatography-Mass Spectrometry
GC-TCD	Gas Chromatography-Thermal Conductivity Detector
GPC-DAD	Gel Permeation Chromatography-Diode Array Detector
GPC-ELSD	Gel Permeation Chromatography-Evaporative Light Scattering Detector
GPC-RI	Gel Permeation Chromatography-Refractive Index Detector
HPLC-MS	High Performance Liquid Chromatography-Mass Spectrometry
ICP-AES	Inductively Coupled Plasma-Atomic Emission Spectroscopy
i-PrOH	Isopropanol
IS	Internal Standard
K	Kelvin
kJ/mol	Kilojoule per Mole
LLE	Liquid-Liquid Extraction
LOD	Limit of Detection
LOQ	Limit of Quantification
MALDI-TOF	Matrix Assisted Laser Desorption Ionization-Time of Flight
MeOH	Methanol
mM	Milimolar

MW	Molecular Weight
m/z	Mass to Charge Ratio
NIST	National Institute of Standards and Technology
NMR	Nuclear Magnetic Resonance
nNi	Nickel with nm Sized Particles
Pa	Pascal
PAHs	Polycyclic Aromatic Hydrocarbons
p_i	Initial Pressure
ppm	Parts per Million
rpm	Revolutions per Minute
RS	Recovery Standard
SEC	Size Exclusion Chromatography
SEM	Scanning Electron Microscopy
Si/Al	Silica/Alumina
T	Temperature
TCA	Thermal Carbon Analysis
TD	Thermal Desorption
TD-Py-GC-MS	Thermal Desorption-Pyrolysis-Gas Chromatography-Mass Spectrometry
TEM	Transmission Electron Microscopy
TGA	Thermal Gravimetric Analysis
THF	Tetrahydrofuran
TMS	Trimethylsilyl
V	volume
v/v	Volume Ratio
w/v	Weight per Volume ratio
w/w	Weight Ratio
XRD	X-Ray Diffractometry
XRF	X-Ray Fluorescence
µNi	Nickel with µm Sized Particles
ρ	Density
%rel.	Relative Percentage
%wt.	Weight Percentage

ACKNOWLEDGEMENTS

I would like to thank Dr. Alena Kubátová for all her advices and recommendations. Her professional approach helped me to solve not only the lab work related issues, but also problems that I had to deal with in my personal life after coming to a world, which was absolutely new for me. I would also like to thank Dr. Kubátová for even getting a chance to first come for an internship in Summer 2013 and afterwards for becoming her graduate student. Next, I would also like to thank my co-advisor Dr. Evguenii Kozliak for his suggestions, both in experimental work and writing, and for his positive attitude. I also appreciate the support of my third committee member Dr. David Pierce and previous committee members Dr. Julia Zhao and Dr. Yun Ji. I am also grateful for help and cooperation with my research group, especially other lignin researchers Anastasia Andrianova and Keith Voeller and my REU and capstone students Jasmine Kreft, Logan Davis, Shelly Lu and Katie Furey. Besides UND faculty staff and students I would also like to thank Dr. Jan Páca from my Czech alma mater, University of Chemical Technology in Prague, for being the initiator of this long life chapter called "UND".

I am very thankful for the financial support from National Science Foundation (NSF) ND EPSCoR award numbers: Dakota BioCon IIA-1330842 and CSMS IIA-1355466, and the Department of Chemistry at University of North Dakota. Any opinions, findings, and conclusions or recommendations expressed in this thesis are those of the authors and do not necessarily reflect the views of the National Science Foundation or Department of Chemistry.

Besides a lot of knowledge and experience that I gained at UND Chemistry Department, I also appreciate a friendship with many people I met here in Grand Forks, particularly Nastěnka, Sarah, Rahul and Keith.

Ultimately, I would like to express my deepest gratefulness and love to my family members, my mom Irena, my dad Petr and my grandma Zdeňka, and my best friend Evžen, for all their support throughout my whole life.

ABSTRACT

A novel analysis method of lignin and its degradation products was developed based primarily on thermal desorption and pyrolysis coupled with carbon quantification and speciation. Gas chromatography-mass spectrometry (GC-MS) is a traditional method for characterization of the volatile product fraction, however the volatile (thermal desorption) fraction usually contributes less than 10%wt. of the overall product yield. The unique properties of thermal carbon analysis (TCA) allow not only for the analysis of the thermal desorption fraction (200–300 °C), which may further be compared to the GC-MS results, but also for the analysis of higher molecular weight oligomers evolving at pyrolytic temperatures (400–890 °C). In addition, using an oxygenation step (550–890 °C in the presence of oxygen) as the final step, it is possible to evolve the rigid cross-linked oligomers, inorganic carbon and other remaining carbon forms and close the mass balance. The key TCA parameters, drying and purging time, were evaluated in different solvent systems in order to ensure a near-100% recovery of all the lignin degradation products. Furthermore, other factors potentially affecting the TCA profile, such as sample loading, interactions with the sampling surface and initial step temperature, were evaluated.

In the second main part of this study, the lignin hydrotreatment reactions performed in a lab scale, static batch reactor were evaluated using both TCA and GC-MS. The effect of the reaction temperature and the presence of a catalyst, particularly different nickel based catalysts, zeolites, activated carbon and silica-alumina, were studied. The overall yield of monomeric and dimeric degradation products increased with temperature. A promising result was obtained at reactions

conducted at 300 °C in the presence of LaO doped activated carbon and zeolite catalysts, where the total yield of volatiles was 5.3 and 6.3%wt., respectively. In addition, a significant amount of dimers over 1.0%wt. was produced. A good agreement between the GC-MS and thermal desorption fraction of TCA was obtained. Combining the overall TCA yield of carbon with gravimetric data of unreacted lignin lead to a successful mass balance closure.

Ultimately, a complete mass balance closure was also obtained for the solid alkali lignin analyzed by TCA with the newly developed protocol and the results were compared with TGA, proving the excellent TCA analytical performance and selectivity towards the carbon containing species. Another parallel comparison was made using Pyrolysis-GC-MS in order to identify the lignin degradation products contributing to the carbon evolved in each temperature fraction.

CHAPTER 1. INTRODUCTION

1.1 Lignin occurrence, structure and types

Over the last several decades wood biomass has become a topic of interest due to its potential as a possible replacement of petroleum and other fossil fuels in the production of energy and a broad variety of chemicals.[1-2] The plant body material consists of three main parts – cellulose, hemicellulose and lignin. Their percent distribution depends on the particular plant species. Cellulose is the main fraction of the biomass and also the most abundant biopolymer in the world. Its structure is uniform as it is composed of glucose units connected by β-1,4 bonds forming linear chains.[3] Hemicellulose is a polysaccharide consisting of pentoses, such as xylose or arabinose, forming linear chains with occasional short branches. Hemicellulose fibers stabilize the primary cellulose fibers, however compared to cellulose they are shorter (50-200 units) and also less stable due to their amorphous character.[3] Lignin, the second major biomass component, mechanically stabilizes the cellulose and hemicellulose fibers by filling the spaces between them. The lignin structure with all the significant bonds is presented in **Fig. 1**. It is a heteropolymer made of randomly repeating molecules of three aromatic alcohols – coniferyl, sinapyl and *p*-coumaryl alcohol. Their structures are shown in **Fig. 2**. However, instead of breaking down into these particular monomers lignin rather prefers to fall apart into shorter-chain methoxyphenols and their derivatives. Thus from this point, lignin is defined as a biopolymer composed of different methoxyphenols connected by propanoid units.[4-6] Lignin is the second most abundant biopolymer

after cellulose contributing 15–30% wt. to lignocellulosic biomass, moreover it stores approximately 40% of lignocellulose energy.[5] The complex structure of lignin makes it a promising inexpensive and renewable source of energy or chemicals that can be used either by itself or as its monomeric units for polymer production.

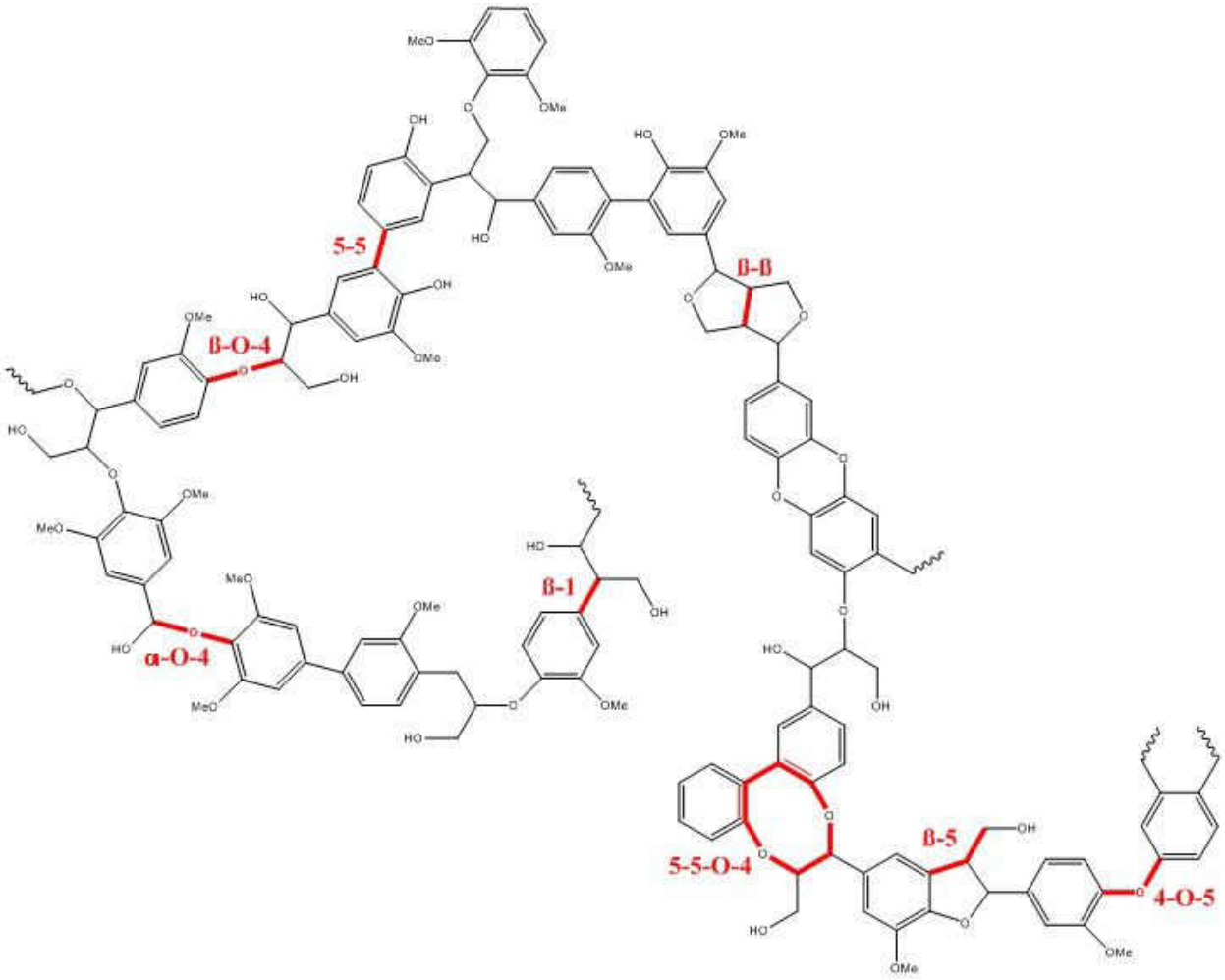

Figure 1: Lignin characteristic structural features

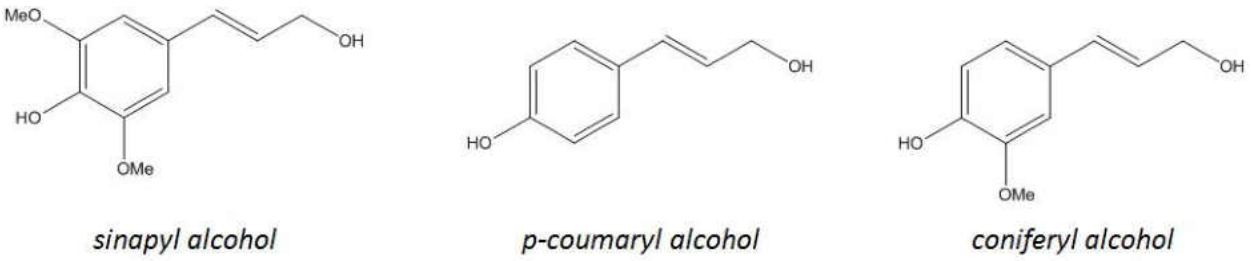

Figure 2: The main structural lignin units: Sinapyl, p-coumaryl and coniferyl alcohol

The lignin structure differs depending on the biomass origin and method of lignin isolation (see **Table 1** for an overview). The most frequently reported lignin types include kraft, soda, lignosulfonate, organosolv, enzymolysis and ionic liquid lignins. The most important industrial lignin sources are either paper manufacturing or upstream processing of biomass in biotechnology. In both processes lignin is obtained as a waste product.[7] The main type of lignin produced in paper industry is kraft lignin.[8] The wooden biomass is heated in the presence of NaOH and Na_2S resulting in a solubilized lignin in the form of a white liquor, which is isolated by precipitation after addition of a strong acid.

The typical characteristics of kraft lignin are a high abundance of hydroxyl groups and high molecular weight up to 200,000 Da. The heating process conducted without Na_2S is known as "soda pulping", i.e., with NaOH alone, and leads to the formation of soda lignin, which is also rich in polar hydroxyl and carboxylic groups, however it is sulfur free compared to kraft lignin. An alternative to the traditional soda pulping called "soda-AQ pulping" uses an addition of anthraquinone to reduce the degradation of carbohydrates, thus making them accessible for a subsequent use, e.g., fermentation and other biotechnological applications.[9] An alkali lignin used in our research is obtained either by cooking the biomass at temperatures of approximately 170 °C with NaOH or with a mixture of NaOH and Na_2SO_4 with subsequent acidification of the black liquor (paper production waste) and its structure is similar to soda lignin.[10]

For some applications, lignosulfonate lignin is preferred due to its high solubility in water. The preparation of lignosulfonate lignin involves a lignocellulose treatment with metals and SO_2 under acidic conditions yielding dissolved lignosulfonates with metal cations.[8] Its disadvantage is a high sulfur content (~5%) that could hamper some applications. Low molecular weight organic solvents and carboxylic acids' application leads to organosolv lignin. Several organosolv pretreatment technologies, such as Alcell, were successfully implemented into the industrial scale.[8] Opposite to kraft lignin, organosolv lignins have virtually no sulfur, a high content of nonpolar moieties and low molecular weight.[10] The handicap of the organosolv process is the harsh treatment conditions used (160–200 °C) leading to significant structural changes.[8-9] This problem can be overcome by using alternative solvents, ionic liquids, i.e., alkyl ammonium or phosphonium salts with low melting points (~100 °C). However, this research is still in progress, since such processes are currently not profitable, especially due to a high cost of the solvent recovery.[8-9]

Lignin can also be obtained by boiling the biomass, typically in the presence of strong mineral acids resulting in hydrolysis lignin.[9] One special variant of hydrolysis lignin is enzymolysis lignin, which is prepared by an application of a complex of hydrolytic enzymes under mild conditions.[11] Such a non-aggressive treatment leads to a lignin that is assumed to retain its native structure.[11] For this purpose, Lewis acids, such as transition metal chlorides or zeolites, might be added during the acidic treatment in order to avoid the production of furfural, which inhibits the enzymatic and microbial performance in the subsequent carbohydrate processing.[12]

Besides hydrolysis, lignin can also be separated from biomass by using strong oxidation agents in combination with an alkaline environment.[13] In the first step of such a process, H_2O_2 is applied followed by ozonolysis in the second step. In the final step, the biomass is treated in the mixture of air and water at a high temperature (around 200 °C) for a short time resulting in the

removal of the remaining hemicellulose, leaving lignin as a precipitate.[13-14] However, as a result of this treatment, the lignin structure becomes highly fragmented and the resulting biphasic mixture contains many byproducts, such as aldaric, aldonic or phenolic acids and low molecular weight aliphatic carboxylic acids, e.g., acetic acid.[13]

Besides chemical methods of lignin recovery from lignocellulose materials, physical methods may also be used, however in industry they are less preferred due to their higher costs and lower efficiency.[8] Pyrolysis lignin is produced from the biomass exposed to a high temperature about 450 °C at a short time of approximately 2 s.[8] Even though the pyrolysis lignin might have unique properties for the production of chemicals, which could not be obtained when using other lignin types, the immense fuel consumption still prevents it from being widely available.[8] Probably the most commonly used biomass physical treatments are fiber explosion techniques, such as steam or acid assisted explosion. In a steam explosion process, the wooden biomass is initially treated with steam at 180–230 °C at pressures of 1.38–3.45 MPa for 1–20 min followed by a sudden pressure release. Such a pressure drop causes the fibers to swell out.[8, 15] The lignin structure modified by the steam explosion provides a large amount of phenolic hydroxyl and carboxylic groups. By contrast, the number of β-O-4 bonds, which are the most frequent within the lignin structure, is significantly decreased.[8, 16] Regarding the molecular weight, the steam explosion lignin is similar to organosolv lignin and since no sulfur containing agents are used, the resulting lignin is sulfur free. [8] However, this process suffers from an extensive damage of fibers during the explosion and further research has to be conducted considering the complications with the separation of the lignocellulose components after the treatment.[15-16] An alternative of the steam explosion is a fiber explosion assisted by an acid or base, e.g., SO_2 or NH_3, respectively. Compared to the traditional steam explosion, these methods usually require a lower temperature (~100 °C)

and the resulting lignin is a better substrate for an enzymatic treatment and fermentation, considering the low amount of inhibitors.[17-18]

Table 1: Lignin types and their properties

Type of lignin	MW (Da)	Characteristics	Methods of isolation and consequences	Annual production (tons)	References
Kraft	Up to 200,000	Low sulfur content High amount of phenolic hydroxyl groups Stilbene and biphenyl structures Missing diphenylmethane and vinyl aryl ether moieties Quinone and catechol structures (Oxidative conditions) Minimal amount of cellulose and hemicellulose compared to acid treatment Suitable for enzyme treatment	150–180 °C at high pH created by addition of NaOH or Na_2S Swelling of cellulose and hemicellulose fibers after the ester bond cleavage Extensive β-aryl bond cleavage	6,000,000–9,000,000	8-10, 19-23
Soda	~8,000	Sulfur free Less suitable for enzyme treatment than Kraft Less efficient degradation than Kraft Potentially high silicate and nitrogen content	Similar conditions as for Kraft (150–180 °C cooking with NaOH), but without the addition of sulfur containing compounds	5,000–10,000[a]	8-9, 19-20, 23-25
Lignosulfonates	6,900–62,000	Soluble in water High sulfur content High amount of polar functional groups: hydroxyl, carboxylic, sulfonic The lignin structure changes less than during kraft process Electrolytic properties High ash content	Cooking at pH 2-12 with $MgSO_3$ or $CaSO_3$ environment	1,200,000	8-9, 22-23, 26

Table 1 continues: Lignin types and their properties

Type of lignin	MW (Da)	Characteristics	Methods of isolation and consequences	Annual production (tons)	References
Organosolv	900–5,400	Hydrophobic Sulfur free High purity Low polydispersity Relatively high moisture content (7.5%)	Wood material subjected to organic solvent at ~ 160-200 °C, usually alcohols or carboxylic acids Lignin obtained by the condition change (pH, temperature, concentration) followed by precipitation	70,000[a]	8-10, 26
Enzymolysis	7,500–100,000	Environmentally friendly More reactive than kraft or lignosulfonate Presence of plant secondary metabolites (mild treatment)	Wooden biomass treated with hydrolytic enzymes at ambient conditions maintaining the initial lignin structure	Compared to Kraft and organosolv higher (exact values not found)	9, 11, 27-28
Ionic liquid	~2,000	Similar to organosolv Low ash amount (0.5 – 2.0%) Carbohydrate free ~1.5% sulfur	Cooking with ionic liquids (alkylbenzenesulfonates, DMSO, N-methylimidazole) at ≥100 °C Recovered by addition of regular solvents (water, acetonitrile) Low recovery (<50%)	Not reported	9, 29-30
Steam explosion	~2,000 Da	MW similar to organosolv lignin Sulfur free Number of β-O-4 bonds significantly decreased Large amount of hydroxyl and carboxylic groups	Biomass treated with steam at 180–230 °C at 1.4–3.5 MPa for 1–20 min followed by a sudden pressure release Complicated separation of each biomass component after the process	Not reported	15-17, 31-32

[a]annual production reported only for one factory

1.2 Methods for lignin degradation

Due to its structural diversity, lignin decomposition is expected to lead to formation of a broad spectrum of both monomeric and oligomeric compounds.[33] The final product composition, reaction selectivity and yield of the desired products depend on many variables such as reaction temperature, time, type of lignin, wood source, reaction solvent, catalyst used, etc.

The main approaches used for lignin decomposition are pyrolysis and especially thermal hydrotreatment, as it appears to be more promising.[34] The greatest technological obstacles of all these methods are weak reaction selectivity, low yield of monomers, insoluble char formation and repolymerization of final hydrotreatment products.[35]

1.2.1 Lignin pyrolysis

Pyrolysis is a simple method for the degradation of not only lignin, but also other biomass components. Solid lignin sample is thermally treated without a solvent, resulting in a liquid fraction called pyrolytic oil, a gas portion and a solid remainder (char and coke).[36-37] Since lignin is the most thermally stable lignocellulose component, the pyrolysis conditions are harsher than for cellulose or hemicellulose.[38] Different literature sources additionally split the definition of pyrolysis into three distinct processes operated at different temperatures and pressures: 1) liquefaction conducted at 200–350 °C and 5–20 MPa, 2) pyrolysis conducted at 650–800 K and 0.1–0.5 MPa and 3) gasification conducted at more than 900 K.[36, 38-39] The liquid portion consists mostly of alkylbenzenes, alkylphenols and alkoxyphenols, particularly substituted guaiacols and syringols, and low molecular weight aliphatics, such as methanol, acetone or acetaldehyde.[40-42] The gases produced during lignin pyrolysis are mainly CO and CO_2 formed from carbonyl and carboxylic groups, water and gaseous alkanes, such as CH_4 or C_2H_6.[37] Additionally, during the

oxidation processes hydrogen is evolved, thus together with CO it can potentially be used for syngas production to make artificial petroleum products.[40] The solid part consists of the product of anoxic processing (coke) and char, which is a highly thermally stable aromatic polycyclic conglomerate formed via inter and intramolecular condensation.[40, 43]

Ether bonds, especially β-O-4 bonds (the most common) and α-O-4, and hydroxyl groups attached to β and γ-C are particularly prone to be cleaved at low temperatures (200–400 °C).[44-45] The most common mechanisms to cleave the ether bonds are free-radical homolytic cleavage, intramolecular elimination and molecular rearrangement.[46-47] The homolytic cleavage of methoxy groups occurs approximately at 450 °C.[45] The C-C bonds are the least likely to break and very high temperatures are needed to accomplish that.[37] Obviously, the final product composition is affected by the lignin type and its source due to a varied abundance of typical lignin bonds and presence of functional groups specific for the particular isolation technique and plant species.[36, 42, 48] Liu et al. reported the simple phenolics to be the major products of soda alkali and Alcell organosolv lignin pyrolysis, since both consist mainly of β-O-4 bonds.[33] Guo et al. discovered that the lignin molecular weight controls the final product distribution.[49] They conducted pyrolysis of four different alkali lignin fractions ranging from less than 1 kDa to >10 kDa. The low molecular weight lignin provided the highest yields of gaseous products and simple phenolics, while the higher molecular weight lignin mainly promoted the formation of alkylguaiacols.[49] Wang et al. claimed that in alkali lignin the ether bonds were relatively stable, while when conducting the pyrolysis of organosolv lignin, they became amenable to scission.[50] The pyrolytic mechanism is also affected by a particle shape and size, since heat and mass transfer differ on the surface and within the particle.[51]

Fast pyrolysis is considered to be the most powerful pyrolytic technique. It is performed in the temperature range of 600–1,000 °C at a very short residence time of 0.5–10 s, using a heating rate of 10–200 °C/s in the absence of oxygen.[36] The minimum temperature required to decompose the lignin macromolecule by fast pyrolysis is 400–450 °C.[36, 44] The average percentage of the oil obtained is 40–60%, the amount of gas produced is usually 8–20%, however when conducting the fast pyrolysis at heating rates of several thousand °C/s, the liquid portion can increase up to 80%.[36] Despite the high oil yields, such steep heating rates are not manageable on the industrial scale. Additionally, the lower heating rates are also preferred in kinetic studies, because the analytical methods used (e.g., TGA) are not able to acquire relevant information in such short time periods.[52]

Ojha et al. conducted fast pyrolysis of alkali lignin at 400, 500, 600 and 700 °C applied for 2–30 s. The amount of guaiacols decreased with increased temperature (84.0%rel. at 400 °C and 54.8%rel. at 700 °C), while at higher temperatures a significant amount of simple phenols and PAHs was evolved.[52] Geng et al. treated alkali lignin by fast pyrolysis in the presence of nickel formate in a fixed bed reactor at 300, 400, 500 and 600 °C with a nitrogen gas residence time of 1s. The pyrolytic products were analyzed by Py-GC-MS at the same temperatures set for 10s with a heating rate of 20 °C/ms. Similar to Ojha's group, the guaiacol, alcohol and aldehyde content decreased with increased temperature, while the alkylphenols and PAHs contents increased. Nair et al. subjected alkali lignin to fast pyrolysis at 500 °C in the presence of TiO_2, ZrO_2 and CeO_2 catalysts. For the optimal conditions using TiO_2, the amount of guaiacols obtained reached 36-37%wt. For the experiments varying the lignin:TiO_2 ratio, the char contribution was 30–46%wt.[44] Nevertheless, testing lignin model compounds by Bai et al. claimed that the fast pyrolysis conditions also favor the condensation reactions. According to their research, lignin fast pyrolysis might lead to an increased amount of dimers, since higher molecular weight compounds, such as

phenylcoumaran, stilbene or biphenol, turned out to be more stable.[53] Jiang et al. reported the formation of stable dimer intermediates produced during lignin pyrolysis by intramolecular elimination.[46]

Transition metal oxides were observed to increase the oil yield and change the product distribution in favor of simple phenolics.[38, 44] The most probable reason is the formation of hydroxyl radicals that initiate the phenolics' generation by a free radical attack.[44]

In chapter 1.2.2, zeolites will be mentioned regarding their acid properties increasing the monomer yields and minimizing the char formation. Their acidic character may also be be useful used in case of lignin pyrolysis. In the first step, the free radicals attack the C-C and C-O bonds, providing low molecular weight intermediates, which are stabilized by adsorption inside the zeolite pores, thus avoiding the condensation reactions.[36, 38] The zeolite acidity can be regulated by the pore size and accessible surface area. The disadvantage that applies not only for zeolites, but also other catalysts, such as metal oxides, is the char being formed inside the pores, poisoning the catalyst.[37, 54] Shen et al. reported an extensive formation of aromatics in the absence of oxygen containing functional groups from black liquor pyrolysis using zeolites.[55] This observation was made by Zhang et al. when degrading organosolv lignin.[56] Ohra-aho and co-workers degraded Kraft lignin in the presence of two zeolites with varied acidity, particle and pore size. In comparison to Pd/C catalyst the zeolites promoted significant demethylation and demethoxylation. Due to zeolites' acidic character (hydrogen donor), the double bonds were reduced. This process was particularly hindered by the addition of a Pd/C catalyst. The lignin and catalyst characterization were performed by analytical Py-GC-MS at 600 °C for 2 s. Analytical Py-GC-MS is a popular device among the researchers for both lignin characterization and catalyst

performance evaluation, because the degradation studies are conducted at similar conditions as the industrial biomass processing.[39, 48, 57-58]

Besides acids, bases can be used both for hydrotreatment and pyrolysis to increase the depolymerization activity.[37] Peng et al. reported a significant decarboxylation, decarbonylation and dealkylation of unsaturated alkyls from alkali lignin during base catalyzed pyrolysis. Additionally, when strong concentrated bases, such as KOH or NaOH were used, mainly alkylphenols were yielded due to an increased demethoxylation activity.[59]

1.2.2 Lignin hydrotreatment

Hydrotreatment approaches can be differentiated based on the additives or catalysts employed into several categories using: 1) acids and bases, 2) different solvents, 3) hydrogen donors or 4) using solid catalysts with an emphasis on transition metal catalysts and their oxides, sulfides and phosphides.

1.2.2.1 Acid and base catalyzed hydrotreatment

Generally, both acidic and basic lignin degradation are rarely conducted without a presence of any co-solvent, hydrogen donor or solid phase catalyst. Initially, acid catalyzed degradation was used for the prior separation of lignin from lignocellulose rather than specifically for lignin degradation.[37] Later, the acid catalyzed degradation was applied on lignin itself. A strictly acidic environment without any additives was mostly used for the mechanistic and characterization studies of lignin model compounds and not for the intact lignin.[60-61]

Typically, during acidic lignin hydrolysis the less frequent α-aryl ether bonds are cleaved faster than the predominant β-aryl ether bonds, since they have a lower activation energy.[37] The acid concentration does not have a significant effect in this case.[37] An obstacle diminishing both

acid and base catalyzed lignin hydrotreatment efficiency are condensation reactions (repolymerization).[37] One way to address this issue is to capture the reactive intermediates, especially aldehydes, by using diols, which are present in the sugar fraction after the lignocellulose separation.[62] As a result, acetals are produced. Alkyl aromatics or cyclic compounds can be obtained by reducing the starting material at a hydrogen atmosphere in combination with a 5% Ru/C catalyst.[38] Finally, monomeric aromatics, such as toluene or methylanisole, can be recovered upon decarbonylation and subsequent dimer cleavage by a reaction with iridium and phosphine containing complexes.[61] Another possibility of minimizing the repolymerization is to use capping agents protecting the free hydroxyl groups, such as phenol at high temperatures (~300 °C) or boric acid.[62]

Besides using strong mineral acids, lignin decomposition can also be achieved in the presence of Lewis acids, especially metal chlorides, acetates and triflates. However, the presence and selection of a solvent is crucial for the proper reaction performance, since a Brønsted acid (hydrogen donor) has to be formed, otherwise the monomeric fraction yield is low and insoluble char formation becomes significant.[63] Gűvenatam et al. discovered that soda lignin treated at 400 °C in supercritical water in presence of Lewis acids provided at most 6.9 %wt. of bio-oil, mainly consisting of catechols (3.1 %wt.). The highest bio-oil yield of 6.9 %wt. was obtained by using $FeCl_2$ as a catalyst.[63] Generally, in experiments using aqueous solutions, metal chlorides were the most effective catalysts, while the metal triflate $Sc(OTf)_3$ provided only 1.8 %wt. of monomers.[63] A similar observation was made by Hepditch and Thring, who decomposed solvolysis lignin in water at high temperature (255–305 °C) in the presence of $NiCl_2$ and $FeCl_3$.[64] The highest amount of bio-oil was 17.5 %wt., with an excessive char formation. By contrast, only a minimal amount of gas products was formed.[64] When supercritical ethanol was used by Gűvenatam et al. as a

solvent at 400 °C, the char yield was minimal and the Lewis acid type affected mainly the products distribution, since most of the feedstock was converted into monomers. Metal acetates led the reaction selectivity towards ketones (41–67 %wt. of bio-oil), while metal acetates and triflates generated mainly aliphatic products (in case of triflates, 67-75 %wt. of bio-oil). The yield of obtained bio-oil ranged from 1.8 to 9.4%wt.[63]

The most probable reason for the char elimination observed in the incorporation of the ethanol molecule into the final product via dehydration catalyzed by a Lewis acid, oligomerization and hydrogen transfer reactions.[37, 63] In addition, triflates are able to form a large variety of products by catalyzing Diels-Alder reactions, Friedel-Craft acylations, aldol condensation or Michael reaction.[62] Their advantage is that they also work efficiently in the aqueous environment. Gűvenatam et al. achieved almost complete lignin degradation in a 1:1 (v/v) EtOH/water mixture when using different metal triflates.[62] The oxygen containing reactive intermediates of lignin hydrotreatment were subjected to triflation with a subsequent deoxygenation leading to carbocations, which were stabilized by an alkylation reaction with ethanol.[62] The most abundant type of compounds in the final product mixture were aliphatics again (57–89%rel. of GC-elutable products).[62]

The effect of Lewis acids may be intensified by the use of ionic liquids. Their greatest merit is the ability to completely solubilize not only lignin, but also other lignocellulose components.[60] In addition, ionic liquids support carbocation evolving reactions and promote the aryl-ether bond cleavage.[37] The ionic liquid acidic treatment affects mainly β-O-4 bonds in both phenolic and non-phenolic moieties.[60] After the hydrotreatment, they can be separated and used again without a loss of performance.[65] The main obstacles of using the ionic liquids are related mainly to the

downstream processing. The stirring has to be designed well, since the medium is very viscous. Other engineering challenges are the product separation and solvent recycling.[60, 65]

Another type of acids used in lignin degradation studies are carboxylic acids.[38, 66] They are used in combination with either water or alcohols, such as methanol, ethanol or isopropanol.[66-67] The presence of a solvent (mostly alcohol) is important for two reasons. Since alcoholysis is the main degradation mechanism, the alcohol first provides hydrogen atoms to initialize the hydrogenolysis of aryl ether bonds resulting in the production of oligomers with a MW of 1,100–1,600 Da.[67] Second, the presence of alcohol decreases the amount of char by lowering the oxygen content in the final products due to a hydrodeoxygenation activity.[67] Consequently, the carboxylic acid catalyzes the hydrogenolysis of oligomers yielding monomeric species.[67] In order to stabilize the reactive oxygen containing intermediates, solid acids, such as silica alumina or zeolites are usually implemented. They play the role of a Lewis acids, as mentioned in the previous paragraph, however compared to regular metal salts their propensity to become the corresponding Brønsted acids is higher. They are also highly available and cost efficient.[67]

The most frequently employed carboxylic acid in lignin hydrotreatment is formic acid. Formic acid is either thermally or catalytically converted into CO or CO_2 and H_2, which is responsible for the hydrogenolysis.[68] It is usually used in combination with either alcohols[67-69] or water.[66, 70] In order to enhance the degradation efficiency, carbon supported metal catalysts, mainly Ru, Rh, Pd, Ni and Pt, are used to increase the hydrodeoxygenation activity.[66-68, 70] Kloekhorst et al. obtained 31.7 %wt. of initial feedstock of monomeric species with minimal char formation using organosolv lignin treated at 400 °C for 4h in iso-propanol/formic acid 1:1 (w/w) mixture in presence of Ru/C catalyst.[68] Kristianto et al. applied 5 %wt. Ru on C support to hydrolysis lignin in supercritical ethanol at 350 °C for 60 min with an addition of formic acid at an acid: lignin ratio of 3:1 yielding

66.3 %wt. of biooil, which contained 6.1 %wt. of monomers.[67] Liguori and Barth achieved a char and coke free mixture of phenolics when employing different Pd based catalysts in formic acid and water mixture at 300 °C for 2 hours with an addition of a solid superacid Nafion SAC-13.[70] The purpose of superacids in lignin chemistry is to break down the produced monomers even more to low molecular weight hydrocarbons and methanol that can be used as fuels. The highest obtained overall content of guaiacol, resorcinol and pinoresinol was 17.6% of initial feedstock.[70]

Hydrotreatment conducted by low cost, widely available bases, such as LiOH, NaOH or KOH is one of the most accessible ways for the selective monomeric production with a minimized repolymerization.[37] However, the fact that acidic phenolics are produced has to be considered, since the neutralization of the base (catalyst) may occur. Erdocia et al. claimed that formosolv and acetosolv/formosolv lignin treated with NaOH with water yielded less monomers and led to a higher char formation than acetosolv lignin due to the weakening of the base catalyst by the presence of formic acid.[4] One of the possibilities how to overcome this undesired phenomenon is to use the capping agents mentioned above.[38] Roberts et al. implemented boric acid as a capping agent during NaOH catalyzed lignin degradation yielding 52% of the bio-oil obtained containing 85% of low molecular weight compounds, while without the use of H_3BO_3 only 36% of oil containing less than 30% of simple phenolics.[71] Boric acid promotes mainly the dimers' formation by the intermediate stabilization, by contrast in the case of phenols the repolymerization is also blocked, but the demethoxylation or dealkylation pathways of the intermediates may still occur.[38, 72] Another way to prevent the char formation is combining a base and an organic acid as catalysts at mild conditions or developing multiphase reactors allowing one to extract the product directly from the reaction mixture followed by distillation, chromatography and crystallization in order to purify the products.[73] The hydroxide treatment without a catalyst affects particularly the most

common and the least stable β-O-4 bonds. The degradation rate increases with the base strength.[37, 73]

The hydrotreatment reactions are mostly conducted under high pressures and temperatures, especially when no catalyst is present and strong inorganic bases are used. In such cases a large portion of gaseous products might be produced due to side reactions.[38] Several base-catalyzed experiments in the aqueous phase performed in the pressure range of 90–315 bar and temperature range of 240–370 °C supported this point.[4, 71-72, 74] Erdocia et al. obtained 26%wt. of catechols in bio-oil with the highest yield of bio-oil 18.5%wt. when working with acetosolv and formosolv lignin at 300 °C in the 4%wt. aqueous solution of NaOH.[4] Organosolv lignin in combination with NaOH addition in water was also used by Roberts et al. resulting in the formation of up to 9% GC-able compounds.[71] Beauchet et al. used the same reaction system obtaining up to 19% of GC-able fraction from kraft lignin.[74] Toledano et al. also used a mixture of water and NaOH applied on organosolv lignin yielding up to 57% of GC-able species.[72] Using water as a solvent for base catalyzed lignin hydrotreatment is convenient due to its low cost and wide availability, however the reaction rate in phenols or alcohols appears to be higher because of the solvolysis effect.[37, 74] Furthermore, the overall product yield varies less than for the experiments performed in water. Nevertheless, the organic solvents also promote the addition reactions, e.g., the aromatic ring alkylation or the formation of low molecular weight carboxylic acids.[75]

Since the solubilized bases, such as NaOH or KOH, complicate the separation of the reaction products, solid bases, e.g., MgO, can be used. However the solid base surface is more prone to cause repolymerization than the dissolved homogenous bases.[2, 69] Narani et al. used MgO-La_2O_3 catalyzed Kraft lignin degradation in supercritical methanol yielding 80% of methanol (MeOH) soluble oil, 9% dichlormethane (DCM) soluble solids and negligible amount DMSO soluble solids

with no char formation, while using acidic or neutral catalysts, such as activated carbon or zirconite, up to 20% of char was formed.[69] Long et al. added MgO to a tetrahydrofuran (THF) solution. After performing the treatment at 250 °C for 15 min 38% of char stayed in the mixture. When water was added, all the lignin became solubilized and the product contained 13.2%wt. of initial feedstock of monomers.[2]

Recently, organic bases caught an attention, e.g., 1-butyl-2,3-dimethylimidazolium chloride or 1,5,7-triazabicyclo[4.4.0]dec-5-ene (TBD), where the N atoms act as nucleophiles attacking α and β C atoms in the quinone moiety, which is expected to be the main intermediate of the β-O-4 cleavage.[37, 76] Organic bases can also be used in combination with acids for the whole lignocellulose complex degradation when the acid promotes the polysaccharide cleavage and the base catalyzes the lignin breakdown.[37]

1.2.2.2 Hydrogen donors and solvolysis

In chapter 1.2.1.1, hydrogenolysis was mentioned to be one of the main processes occurring during the lignin depolymerization. In order to cleave the bonds by hydrogenolysis, a hydrogen source is needed. This can be simply solved by using hydrogen gas.[35] Long et al. worked in a pressurized batch system with organosolv lignin in methanol with an addition of NaOH and Ru/C catalyst at 260 °C and 40 bar H_2 atmosphere for 4 h yielding 12.7%wt. of phenolic monomers and 6.1%wt. of aliphatic alcohols.[35] Kim et al. conducted an organosolv lignin hydrotreatment in sub- and supercritical EtOH at 200–350 °C at 2-3 MPa of hydrogen atmosphere for 20–60 min. The highest amount of simple phenolics obtained was 9.7%wt.[77]

Since the use of gaseous hydrogen is related to strict safety precautions, high temperature, pressure requirements and the hydrogen generators are expensive, external hydrogen donors are usually employed.[78] Hydrogen donors not only supply hydrogen, they also play the role of a

solvent, thus preventing repolymerization by stabilization of reactive radical species, decreasing the char formation and they partially deoxygenate lignin.[24] Commonly utilized hydrogen donors are carboxylic acids, such as formic or acetic acid.[66-67, 70]

One of the non-traditional hydrogen donors that became attractive in recent years is tetralin. Tetralin has been used as a stabilizer of radical species formed during fuel production from petroleum and coal liquefaction.[78-79] Tetralin gained an attention due to its high boiling point and ability to form stable naphthalene when releasing hydrogen at hydrocracking conditions, thus not causing any side reactions with the hydrotreatment products.[80] Toledano et al. used tetralin and formic acid in the presence of several transition metal catalysts to decompose organosolv lignin at mild conditions employing microwave heating.[81] Both hydrogen donors provided a comparable total yield of monomers of approximately 1% wt.[81] Kim et al. disintegrated organosolv lignin in the presence of either tetralin or isopropylalcohol at temperatures 300, 350 and 400 °C. The amount of monomers yielded was 6–12% wt. of initial feedstock[79] Thring and Breau performed hydrocracking of organosolv lignin at 370–410 °C in the presence of tetralin yielding up to 50% of degraded lignin. Addition of a Ni-W catalyst improved the yield of the gaseous products, however the yield increase of phenolics in the liquid phase was negligible.[80]

Another important parameter responsible of the product yield and selectivity is solvent selection. The degradation reactions occur mostly at sub- or supercritical conditions, when the solvent provides a better solubilization ability. In addition, the solvent can be easily separated and the reaction setup also allows for use of additional hydrogen donors, such as acids.[82] At such conditions, water is a solvent of particular interest, not only because of the economical aspect, but also because of the unique properties that can be readily controlled by changing temperature and pressure.[83] Supercritical water dissolves organics and gases produced during the hydrotreatment,

however inorganic salts become insoluble.[83] In addition, Takami et al. confirmed that the monomeric reaction products in the presence of supercritical water suppress the char formation.[84]

Wahyodiono et al. performed degradation of alkali lignin in near-critical and supercritical water at 350–400 °C and 25–40 MPa. At 400 °C the reaction yielded 30.5 %wt. of catechol, 3.3 %wt. of phenol, 8.8 %wt. of *m*- and *p*-cresol and 3.7 %wt. of *o*-cresol in the bio-oil.[83] Pinkowska et al. conducted an alkali lignin hydrotreatment in sub- and supercritical water using a lab scale batch reactor at 280–390 °C for up to 4 h, obtaining a maximum yield of 11.2%wt. of guaiacol, 11.1%wt. of catechol, 4.2%wt. of phenol and 7%wt. of different cresol isomers in initial lignin.[85] Hidajat et al. performed a hydrotreatment of Kraft and hydrolysis lignin at 330 °C for 30 min in subcritical water and supercritical MeOH in the presence of bases (NaOH, KOH and Na_2CO_3). The Kraft lignin treated in supercritical MeOH provided 7.8%wt. of aromatics and 28.5%wt. of char. The aromatics consisted mainly of methoxylated species, due to a high MeOH methoxylation ability. The amount of char in subcritical water decreased to 15.8%wt. and the aromatics yield increased to 17.9%wt. The aromatics consisted mainly of alkylcatechols.[86] The reason for such differences are a lower dielectric constant of MeOH (lower polarity) at these certain reaction conditions, causing the bases in MeOH to precipitate and possible neutralization of the basic catalyst by the acidic reaction products.

Another option is a solvolysis by sub/supercritical alcohols. They form a sub/supercritical fluid at relatively low pressures and temperatures (200–350 °C) depending on a particular solvent.[87] They also exhibit a good heat transfer, low toxicity, ability to dissolve high molecular masses, low char formation and prevention of repolymerization.[79, 87-88] Besides lignin, they can also solubilize other lignocellulose components.[89]

Since the organic solvents do not provide sufficient hydrogen donor capacity, they are usually combined with acid catalysts. Riaz et al. subjected a hydrolysis and kraft lignin to supercritical EtOH with an addition of formic acid. 85%wt. yield of bio-oil was obtained and the oxygen content was decreased by 44% at 350 °C applied for 30 min.[90] Another related issue is that the presence of hydrogen provided by the donors can be used to regenerate the protonated form of the solvent instead of hydrogenolysis of the ether bonds in lignin.[91] Warner's group solved this problem by using Cu and La doped hydrotalcite when degrading organosolv lignin in supercritical MeOH.[91]

Recently, the application of supercritical CO_2 was evaluated due to its ability to form a supercritical fluid at a relatively low temperature and pressure (31 °C, 7.4 MPa), low cost, safe use and power of dissolving a wide range of chemicals. Gosselink's group degraded an organosolv lignin in a mixture of supercritical CO_2, acetone and water at 300 °C and 100 bar for 3.5 hours obtaining 10–12%wt. of monomeric aromatics.[92] Numan-Al-Mobin et al. confirmed that CO_2 affects the reaction selectivity, since with different water:CO_2 the percent contribution of each monomeric product changed. The guaiacol yield at the 1:5 water:CO_2 ratio reached 28%rel., while at 1:1 it was only 18%rel.[93]

1.2.2.3 Transition metals catalyzed reactions

Either supported or unsupported transition metal catalyst significantly affect the hydrotreatment product yield and selectivity, since every metal catalyzes specific reaction pathways.[88, 94] In this study, nickel based catalysts were of the major interest. Nickel has a high industrial potential for its low cost, broad availability, high activity and compatibility with a wide range of solvents.[95] Regarding the reaction selectivity, nickel is mainly known as a powerful hydrogenolysis and hydrodeoxygenation catalyst.[58, 95-96] This property is especially important when the lignin degradation products are thought to be used as a fuel, where a high content of

hydrocarbons with a minimized amount of oxygen is preferred.[95] Jin et al. evaluated the hydrodeoxygenation activity of various nickel catalysts on anisole, a lignin model compound.[95] The experiments were conducted at relatively mild conditions: 180–200 °C and 0.5–3.0 MPa H_2 pressure. All the tested catalysts exhibited hydrogenation and hydrodeoxygenation activity to some extent, however the catalyst support was proven to be the crucial parameter determining the reaction selectivity. Ni supported on activated carbon and mesoporous silica drove the reaction via the hydrogenation of the aromatic ring yielding cyclohexylmethylester, while Ni on regular SiO_2 the hydrodeoxygenation product cyclohexane is the major.[95] Forchheim's group evaluated catalytic properties of Raney Ni using guaiacol and catechol as starting reagents. At 250 °C and 1 MPa H_2 pressure cyclohexanol and phenol were obtained as the main products.[96]

Another significant nickel properties are a capability to decrease the char formation and the biooil oxygen content.[58] Forchheim et al. also claimed that the nickel catalyst presence increases the gaseous products amount.[96] This observation is particularly convenient, when the main goal of the lignin degradation is gasification, e.g. for syngas production. Tsodikov et al. applied a microwave heating providing an average temperature of 700–750 °C on kraft lignin mixed with Ni nanoparticles without the solvent presence yielding 65%wt. of syngas of H_2/CO 1:1 composition.[97] Geng et al. also confirmed that the Ni based catalyst can be used for lignin pyrolysis (without the solvent), when subjecting alkali lignin to temperatures 300–600 °C. At 600 °C without the catalyst presence the liquid products yield reached 21.2%wt. After the addition of nickel formate the liquid fraction amount increased to 30.2%wt. and the solid residue content was lowered by 2.3%wt.[58]

The initial goal of our research was to find conditions (mainly to find the proper catalyst) to yield as high concentration of monomers and dimers as possible regardless the product

composition and close the mass balance of all the fractions produced. **Table 2** summarizes the remarkable studies focusing on the product quantification, where nickel based catalysts were used to degrade lignin. All the experiments were conducted at higher temperatures of at least 120 °C and increased pressure. Gaseous hydrogen atmosphere was mostly used to provide additional hydrogen needed for hydrogenolysis.[5, 24, 27, 69, 80, 94, 96, 98-107] In some studies an inert atmosphere of either nitrogen[98, 108] or argon[109] is used. Monometallic catalysts are rarely used, the only nickel catalyst applied in degradation studies, which might be considered to be monometallic, is Raney nickel (activated Ni catalyst slurry in water).[27, 98, 105, 107] The published studies were mainly performed using metal catalyst on zeolites,[69, 98, 110] silica,[106, 111-112] alumina,[24, 100-101] silica-alumina,[80-81, 100-101] activated carbon[69, 94, 103-104, 113] and other support materials. In experiments performed without the inorganic support bimetallic catalysts are mostly used.[99, 114]

There are several obstacles, which complicate the direct comparison of the data. For our research, we have been using Kraft alkali lignin, however the reported studies use also different lignin types, e.g. solvolysis,[5, 111] soda,[63, 94] enzymolysis[27, 98] or lignosulfonate lignin,[103] which obviously affects the amount and distribution of the reaction products. Some studies do not even start with pure isolated lignin, but with the unseparated wooden biomass.[103, 115] In some quantification papers, the catalyst screening is conducted on a lignin model compound instead of lignin itself, since it is easier to evaluate the reaction mechanism and kinetics.[96, 116]

Another complication in comparing the data obtained by different researchers is a lack of agreement of how to present the results. One of the most important criteria characterizing the degradation process efficiency is the bio-oil yield. However, there are multiple definitions of bio-oil. Probably the most accurate one defines the bio-oil as a product fraction soluble in an organic solvent.[63, 81, 110, 112] The common bio-oil yields are in a range of units of %wt. to approximately 30

%wt.[63, 81, 110, 112] Nevertheless, the overall amount of degradation products is mostly reported as % of organic/liquid phase or % of conversion/solubilization, which includes not only the amount of degradation products dissolved in the organic solvent, but also the solvent itself.[27, 98, 103] Other index that is not presented uniformly is the yield of low molecular weight compounds/monomers. The most comprehensible way to report the yield of monomers is as a %wt. of initial lignin, however many researchers show their data in normalized %, which do not account for different detector response of each compound.[24, 80, 100-101] In addition, these normalized abundances of the reaction products are usually related to the organic/liquid phase, not to initial lignin.[80] Also, many studies are not comprehensive regarding the analysis of a broad range of products, but they focus only on the most abundant products, e.g. guaiacol, phenol and catechol,[96, 111] or they quantify the degradation products as a specific group with common properties, i.e. phenols, guaiacols, saturated and unsaturated compounds.[103, 105, 113] The biooil and monomers recoveries were presented in %wt. of initial feedstock, when the authors presented their data in these units or when the recalculation was possible, otherwise the data in **Table 2** are shown in units published in the particular work, since the recalculation is not possible due to incompatibility of the units.

Table 2: Nickel catalyzed lignin hydrotreatment experiments

Type of lignin	Reaction solvent and additives	Catalyst	Reaction conditions	Yield of bio-oil	Yield of monomers	Reference
Organosolv	Water	NiRu, NiRh, $Ni_{85}Pd_{15}$	1, 12 h; 130 °C; 1 MPa H_2	Not reported	Up to 3.3 %wt.	[5]
Enzymolysis	MeOH or EtOH/water 5:2 (v/v)	**Raney Ni** with acidic zeolites	5-140 min; 207-307 °C; 2.7 MPa p_i, 9–27 MPa final pressure (H_2 or N_2)	48-64%wt.	12.9%wt. for Raney Ni	[98]
Enzymolysis	0.75 M NaOH + dioxane/water	**Raney Ni**	3.5 h; 120–200 °C; 2 MPa H_2	16.7%wt. (no NaOH)	3.6–4.4 mmol/g of OH groups	[27]
Organosolv	Water, MeOH	NiMO supported on pure and ZrO_2 doped mesostructured silica	1 h; 200–350 °C; pi 101 kPa, otherwise not reported	Aqueous fraction after reaction up to 10%	7.2%wt. of syringol	[111]
Kraft, organosolv, Inbicon	Supercritical t-BuOH	Pt/C, Pd/C, Ru/C, Ni/C and other transition metals supported on activated carbon (Pt, Pd, Ru)	40 min; 350 °C; 3 MPa p_i, max pressure 15 MPa in H_2	49.5% wt. (Ni/C)	8.6%wt. (Ni/C)	[104]
Organosolv	Water with addition of NaOH (0–2.7 eq.)	Ni_7Au_3	2, 4 h; 130, 160 °C; 1 MPa H_2	Not reported	Up to 10.9%	[99]
Organosolv	Tetralin, formic acid	2–10%wt. Ni, 2%wt. Pd, 2%wt. Pt, 2%wt. Ru supported on silica/alumina	30 min; 140 °C (microwave); 101 kPa	max 30%wt. (10% Ni)	0.4% wt. (10% Ni)	[81]

Table 2 continues: Nickel catalyzed lignin hydrotreatment experiments

Type of lignin	Reaction solvent and additives	Catalyst	Reaction conditions	Yield of bio-oil	Yield of monomers	Reference
Alkali	Water:EtOH 1:1 (v/v)	Ni doped tungsten phosphide supported on activated carbon (Ni-WP/AC), WP, WP/SiO2, WP/AC, Fe-WP/AC	2 h; 280 °C; 2 MPa	~50%wt. of organic phase	0.5%wt. of phenols (Ni-WP/AC)	[113]
Organosolv + other biomass fractions	Glycerol, diethylene glycol (1:1 w/w) and 3%wt. of *p*-toluenesulfonic acid used for liquefaction, tetralin for subsequent hydrotreatment	$NiMo/Al_2O_3$, Ni/SiO_2-Al_2O_3, Pd/Al_2O_3, Pd/C, MoS_2	100-190 min; 350 °C; 8 MPa H_2	After the reaction liquid and condensed water fraction together up to cca 98% wt. (200 °C)	%rel. sorted by functionalities (based on FTIR)[a]	[100]
Organosolv + other lignin fractions	Glycerol, diethylene glycol (1:1 w/w) and 3%wt. of *p*-toluenesulfonic acid used for liquefaction; tetralin, 2-propanol, phenol, *m*-cresol, anthracene, cyclohexanol, xylene and pyridine for subsequent hydrotreatment	$NiMo/Al_2O_3$, Pd/Al_2O_3, Pd/C, Ni/SiO_2-Al_2O_3, MoS_2	60-200 min; gradual increase to max T 300 °C; 8 MPa H_2	After the reaction liquid and condensed water fraction together up to cca 95% wt. (300 °C in tetralin)	%rel. sorted by functionalities (based on FTIR)[a]	[101]

Table 2 continues: Nickel catalyzed lignin hydrotreatment experiments

Type of lignin	Reaction solvent and additives	Catalyst	Reaction conditions	Yield of bio-oil	Yield of monomers	Reference
Soda	Supercritical water and ethanol	$NiCl_2$, $Ni(Oac)_2$, $FeCl_2$, $CuCl_2$, $CoCl_2$, $AlCl_3$, $Fe(OAc)_2$, $Cu(OAc)_2$, $Co(OAc)_2$, $Sc(OTf)_3$ (Lewis acids)	4 h; 400 °C; pressure not reported	11%wt. (Al(Otf)3 at 400°C)	6.2%wt. ($NiCl_2$); 7.1%wt. ($Ni(OAc)_2$)	63
Solvolysis	Tetralin	6%Ni/19%W on silica/alumina	15–120 min; 370–410 °C; 1 MPa H_2 p_i, otherwise not reported	Less than 50% of lignin solubilized, DCM organic fraction 4-8%	Only relative abundances in DCM fraction (catechol most abundant 21.9%rel.)[a]	80
Acidolysis, alkali	Ionic liquid BMIM OAc, methanol, EtOAc, water	nano Ni, Fe_3O_4–$(NiMgAlO)_x$ and $(NiAlO)_x$, NiO nanosheet	6,24 h; lab T, 180 °C; 0.1-1 MPa of H_2	Only % of solubilization: Up to ~94% (nano Ni)	Only % of *m/z* distribution: Up to 60% of GC-elutables in 100–500 *m/z* range (nano Ni)[a]	102
Soda	Tetralin	Alumina supported NiMo sulfide	5 h; 350 °C, p_i 2 MPa, final 8 MPa of H_2	~65% of liquid products (5 h w/ catalyst)	Only %rel. abundance of functionalities (NMR and FTIR characterization)[a]	24
Enzymolysis	Near-critical water	Raney Ni	30, 120, 270, 1200 min; 25-400 °C; 1 MPa H_2	Not reported	1.6% wt. of guaiacol, phenol and catechol (400 °C)	96

Table 2 continues: Nickel catalyzed lignin hydrotreatment experiments

Type of lignin	Reaction solvent and additives	Catalyst	Reaction conditions	Yield of bio-oil	Yield of monomers	Reference
Lignosulfonate	Water, cyclohexane, i-PrOH, 1,4-dioxane, MeOH, EtOH, Propylene glycol, glycerol, ethylene glycol	Ni/AC, NiLa/AC, NiPt/AC, NiCu/AC, NiPd/AC, NiCe/AC, Ni/MgO, **Raney Ni**, Ni/MCM-41	2 h; 200 °C; 5 MPa H_2	Only % of conversion (solubilization): Up to 75%	Only selectivity (%rel.) of major products (4-propyl and 4-ethylguaiacol): Up to 95% [a]	103
Soda	Supercritical MeOH, EtOH, 2-propanol	Ni/C, Pt/C, Pd/C, Ru/C	40 min; 350 °C; 3-19 MPa (H_2)	50.0–60.2%wt. of liquid phase (Ni/C)	9.4–10.9%wt. (Ni/C)	104
Kraft	Supercritical MeOH, EtOH, 2-propanol	NiW, NiMo, CoMo on zeolite, activated carbon and MgO/LaO	8 h; 320 °C; 3.5 MPa H_2	MeOH soluble oil 40-82%wt. (NiW, NiMo)	16.5–28.5%wt. (NiW, NiMo)	69
Kraft	MeOH:water 1:1 (v/v), addition of NaOH (1.7 mM)	HZSM zeolite w/wo Ni	7 h; 220 °C; 0.1 MPa Ar	33.8-44.9%wt. EtOAc soluble products, 16.0-19.1%wt. water soluble products	21% wt. (Ni doped zeolite with 1.7 mmol NaOH)	109
Kraft	MeOH, EtOH, THF, i-PrOH	TiN-Ni (1, 10 and 50% Ni/Ti molar ratio)	1.5–4.5 min; 150 °C; 2.5 MPa	28-71%wt. of organic phase	Not reported	117
Organosolv	MeOH	Ni/C (11%wt. Ni)	6 h; 200 °C; 0.2-0.9 MPa N_2	Not reported	6-32%wt.	108
Organosolv	Formic acid	10% Ni on SBA-15 mesoporous silica support	30 min; 150 °C (100 W microwave heating); pressure not reported	12–35%wt.	~1%wt.	112

Table 2 continues: Nickel catalyzed lignin hydrotreatment experiments

Type of lignin	Reaction solvent and additives	Catalyst	Reaction conditions	Yield of bio-oil	Yield of monomers	Reference
Organosolv	2-PrOH, Methylcyclohexane, MeOH	**Raney Ni**	8 h; 200–300 °C; 0.7 MPa H_2	27–83% solubilization	Only selectivity of saturated and unsaturated products	[105]
Hydrolysis	Water, MeOH, EtOH, i-PrOH	3 types of Ni doped and 4 types of Al doped mesoporous silica	2–8 h; 260–320 °C; 1 MPa H_2	49.3–79.9%wt. of liquid fraction	3.9–17.8%wt.	[106]
Hydrolysis	Supercritical EtOH	$NiOMgAlO_y$ (30%wt. of NiO), $Co_3O_4MgAlO_y$, 4 types of $CuOMgAlO_y$ differing by CuO doping	4 h; 400 °C; pressure not reported	Not reported	10.8%wt. (with NiO)	[118]
Bio, Eucalyptus, Hardwood (isolation technique not reported)	Formic acid	H-ZSM-5 zeolite doped with 2, 3.5 and 5% NiO	1 h; 180 °C; pressure not reported	5–20%wt.	7.2–11.4%wt.	[110]
Organosolv	Subcritical water	5 **Raney Ni** catalysts	3 h; 360 °C; 7 MPa H_2	~40–60%wt.	4.8–10.2%wt.	[107]
Soda	Supercritical EtOH	15 different NiO/SiO_2 combined with Ni_2P	4 h; 340 °C; 20 bar N_2 or H_2	11–44%wt.	3–53%wt. of biooil	[119]
Alkali	Supercritical EtOH	$CuMgAlO_x$, Ni_2P/SiO_2, Ni/SiO_2, Ni/amorphous Si/Al	4 h; 340 °C; 10–30 bar N_2 or H_2	8–52%wt.	2–26%wt.	[120]

Table 2 continues: Nickel catalyzed lignin hydrotreatment experiments

Type of lignin	Reaction solvent and additives	Catalyst	Reaction conditions	Yield of bio-oil	Yield of monomers	Reference
Alkali	Subcritical water/subcritical CO_2, subcritical water/subcritical N_2	NiO, Ce doped SC stabilized ZrO_2	10 min; 100–400 °C; 22.1 MPa	Not reported	%rel., guaiacol and vanillin most abundant	[121]
Organosolv	Supercritical EtOH	FeB, NiB, FeNiB	2 h; 320 °C; pressure not reported	Not reported	%rel.; propylguaiacol, propenylguaiacol and propenylsyringol most abundant	[122]
Enzymolysis	MeOH/water	**Raney Ni**/$Cs_xH_{3-x}PW_{12}O_{40}$	3 h; 250-280 °C; 3 MPa H_2	9.5–45.7%wt. of aqueous phase	~13–22.5%wt.	[123]
Softwood pine	Water	Ni, Ru, Fe, Cu and Zn doped zeolites	4 h; 250 °C; 4 MPa H_2	Only % of conversion	Up to ~35%wt. of hydrocarbons	[124]
Organosolv	MeOH	Ni, Ni/Fe, Fe, Pd, Pt and Ru supported on activated C	6 h; 180–240 °C; 2-10 MPa H_2	Not reported	~4–23%wt.	[125]

[a] shown as normalized % of GC-elutable compounds

1.3 Methods of analysis

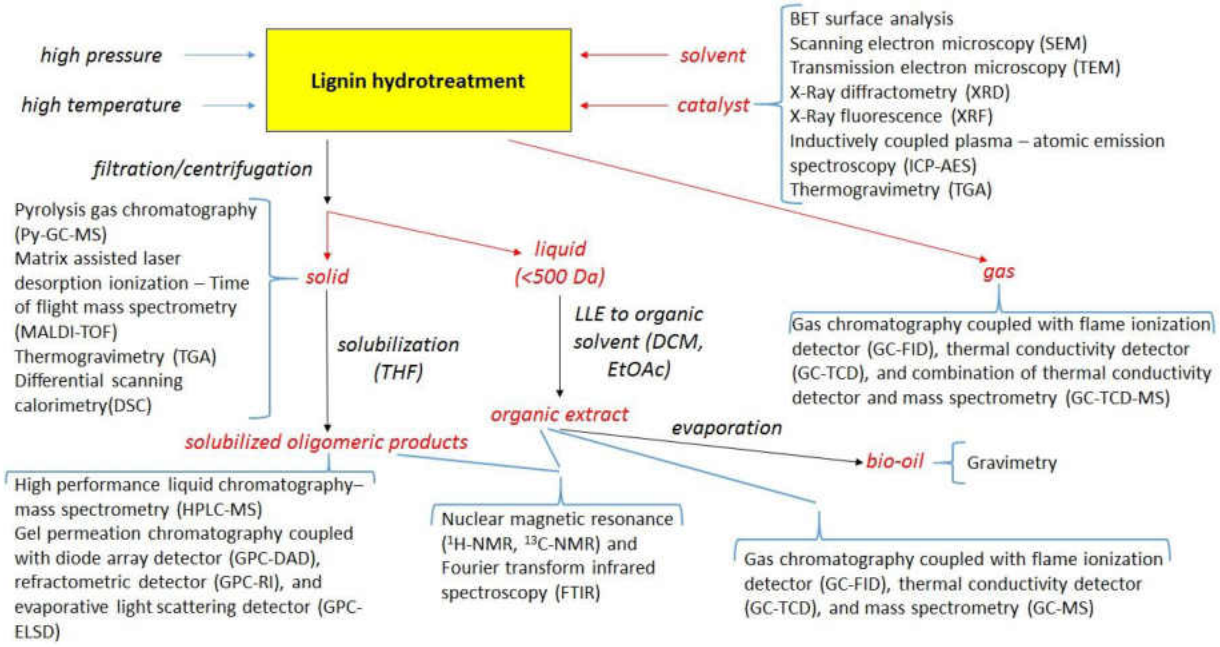

Figure 3: Analytical methods used for lignin and its degradation products

A diagram describing the typical suite of analytical methods used for lignin degradation products and the reaction mixture (catalysts) is presented in **Fig. 3**. The hydrotreatment lignin reaction usually results in a multiphase batch of components, which have to be separated first. The produced gas is either collected in Tedlar bags or the reactor setup allows for a transfer of the gaseous products directly into the analytical device.[68, 126] The solid residue is separated from the liquid phase by either filtration or centrifugation.[12, 73, 88]

Assuming that the liquid portion consists of degradation products dissolved either in water or an aqueous phase with organic solvent, a liquid-liquid extraction to an immiscible organic solvent has to be performed in order to analyze the volatile fraction (<500 Da) by GC-MS, GC-TCD or GC-FID.[63, 94, 127-128] The common solvents used are DCM or ethylacetate.[63, 98, 128-129] In case of water-organic solvent reaction mixtures, the organic solvent can be separated by vacuum filtration

and the two fractions can be treated separately.[98] The aqueous fraction contains low molecular weight lignin degradation products in the form of oil droplets. After the water evaporation, their % wt. yield can be obtained by gravimetry and reported as "bio-oil", i.e., product portion extractable to organic solvent, however, not all the bio-oil components are GC-elutable.[98]

The solid hydrotreatment fraction (filtration residue or centrifugation pellet) is usually rinsed with the reaction solvent and either dried for a gravimetric measurement in order to close the mass balance or further dissolved for additional characterization.[98] The solid portion consists of coke (product of burning without the presence of oxygen), as well as non-degraded and modified lignin. Since both the non-degraded and modified lignin consists mainly of higher molecular weight oligomers or polymers (> 500 Da), LC systems are used for the analysis.[128, 130] One of the main parameters characterizing both intact lignin and the degradation fractions is molecular weight. The different lignin fractions are mainly separated by using size exclusion chromatography (SEC), especially by gel permeation chromatography (GPC).[35, 94, 128, 130] GPC is a separation method used for organic soluble compounds (the mobile phase is an organic solvent). Therefore, when the solid reaction products are being analyzed, they have to be solubilized, mostly in THF.[128, 130] The commonly used detectors employed with GPC are refractometric (RI)[35, 81, 128] UV-Vis/diode array (DAD)[1, 94, 128] and evaporative light scattering detector (ELSD).[131] Since these detectors obviously do not provide mass spectral information, a calibration using commercially available standards has to be performed.[130] However, there are no lignin standards for MW measurement available, therefore polystyrene standards are mostly used.[130] Alternatively, liquid chromatography (HPLC) coupled with mass spectrometry is applied on lignin degradation products, particularly those of lower molecular weight.[128, 132] Electrospray ionization is used in this case to ionize and vaporize

the higher molecular weight lignin products.[98] Jiang et al. were able to analyze the lignin degradation products of MW up to 1500 g/mol.[98]

The most of chemical information about solid lignin samples is provided by Py-GC-MS. By applying a preset temperature program for the thermal decomposition of the sample, accompanied with the GC separation and MS detection, it is possible to identify the degradation products specific for a certain temperature fraction, thus allowing to reveal the degradation mechanism or estimate the bond energies.[33, 36] A common non-chromatographic method of lignin MW determination used mostly for solid samples is matrix assisted laser desorption ionization (MALDI) coupled with time of flight (TOF) mass analyzer.[98, 128-129, 133] However, MALDI-TOF suffers from several issues complicating the data processing and correct mass determination. The laser used for MALDI causes excessive fragmentation of both analyte and matrix leading to a large amount of fragments.[134-135] As a consequence, the abundance of the molecular ion is significantly decreased and the mass spectra is characteristic by an intensive background noise in mass range <1000 Da.[134-135] Regular polymer thermal properties tests, such as thermogravimetry (TGA) or differential scanning calorimetry (DSC), can also be applied for solid lignin samples.[136]

The gaseous degradation products, e.g., CO, CO_2, CH_4, C_2H_6, C_2H_4 or C_3H_8 are mainly analyzed using GC accompanied with TCD and FID detector.[94] Due to the fact that the TCD is a non-destructive detector, Joffres et al. used GC-TCD-MS for the analysis of gaseous lignin degradation products.[24]

For lignin characterization, regarding the functionalities, the main techniques used are NMR (^{1}H NMR or ^{13}C NMR)[35, 137-138] and FT-IR.[128, 136-137, 139] They are applicable for both the liquid and the solid product fractions after the solubilization.

Many lignin degradation studies using a catalyst also conducted the catalyst characterization. The particle surface area, the pore diameter and volume are measured by adsorption isotherms, mostly BET.[111, 129] The results obtained by BET can be confirmed by obtaining the catalyst images using scanning electron microscopy (SEM)[139] or transmission electron microscopy (TEM).[5] The crystalline structure is determined by X-ray diffraction measurements (XRD) usually using Cu radiation.[5, 129] The amount of individual components, as well as the evaluation of their % decrease during the catalyst recycling, can be evaluated by using X-ray fluorescence (XRF) or inductively-coupled plasma-atomic emission spectroscopy (ICP-AES).[127, 139] The same as for lignin, the catalyst thermal properties can also be studied, e.g., by TGA.[139]

1.4 Statement of Purpose

The main aim of the presented work was to develop a new method for the analysis of lignin and its degradation products by TCA with regards to the maximum recovery of all the degradation products and successful mass balance closure. For this purpose, the drying and purging time of a wide range of lignin model compounds in various solvents were evaluated. In addition, other factors potentially affecting the TCA profile, such as sample loading, surface interactions and initial step temperature were investigated.

In the second part of the study, lignin hydrotreatment experiments performed in a static batch reactor were studied. The goal of the hydrotreatment studies was to evaluate the effect of the reaction temperature and the presence of catalyst, particularly different nickel based catalysts, zeolites, silica-alumina and activated carbon, on the product yield and distribution. GC-MS was used for the product characterization, however the disadvantage of this analytical technique is that only volatile species are detected. Therefore, a parallel comparison with TCA was implemented in order to quantify the remaining fractions of lignin degradation products, which are not GC-elutable. Moreover, the TCA includes an oxygenation step, where the least volatile lignin derived polymers and inorganic carbon are supposed to be evolved. Thus, the TCA may become a suitable method for the complete mass balance closure of lignin degradation products.

Finally, the newly developed TCA protocol minimizing the analyte losses was compared to the old protocol using longer purging and drying times. In order to identify the lignin degradation products contributing in the amount of carbon evolved in each temperature fraction, Py-GC-MS was applied.

CHAPTER 2. EXPERIMENTAL PART

2.1 Materials

The organic solvents used in this study involved DCM, MeOH, acetonitrile (ACN) and THF of GC or HPLC grade, all purchased from VWR (Airlington Heights, IL, USA). Deionized water was obtained from distilled water further purified using Direct-Q 3 UV system purifier (Millipore, Billerica, MA, USA) claiming the purity below 5 ppb of organic carbon. For the thermal carbon analysis (TCA) method optimization following standards were used: guaiacol (99%), syringol (99%), levoglucosan (99%), vanillin (99%), homovanillyl alcohol (99%), vanillic acid (97%), phenol (99%), methylguaiacol (98%), propylguaiacol (99%), syringaldehyde (98%) and pinoresinol (≥ 95%). All the chemicals were purchased from Sigma-Aldrich (Milwaukee, WI, USA). Bicreosol was synthesized at UND chemistry department.[140] For the TCA calibration purpose, sucrose (99%) purchased from Alfa Aesar (Ward Hill, MA, USA).

Besides already mentioned guaiacol, syringol, vanillin, homovanillyl alcohol, vanillic acid, phenol, methylguaiacol, propylguaiacol and syringaldehyde following standards were used for GC-MS calibration: *p*-cresol (99%), 4-ethylphenol (97%), 4-propylphenol (99%), mequinol (99%), vinylguaiacol (98%), acetovanillone (98%), homovanillic acid (98%), isoeugenol (99%), 4-ethylguaiacol (98%). All of the standards were purchased from Sigma-Aldrich (Milwaukee, WI, USA) except mequinol purchased from Pfaltz&Bauer (Waterbury, CT, USA). *o*-terphenyl (99%) used as an internal standard (IS) and 4'-chloroacetophenone (97%) used as a recovery standard

(RS) were both purchased from Sigma-Aldrich (Milwaukee, WI, USA). TD-14 was synthesized at UND chemistry department. For the derivatization of hydroxyl groups N,O-bis(trimethylsilyl)trifluoroacetamide (BSTFA) derivatization grade reagent purchased from Sigma (Milwaukee, Wisconsin, USA) was used.

For hydrotreatment experiments alkali lignin from Sigma-Aldrich (Milwaukee, WI, USA) was used. The elemental analysis of alkali lignin was performed by Atlantic Microlab, Inc. (Norcross, GA, USA) resulting in 64.14% C, 5.79% H, 1.39% S and 0.46% N. For the catalyst screening following Ni based catalysts were used: <50 μm particle Ni (99.7%), <100 nm particle Ni (99%) and <1 mm Ni on silica/alumina purchased from Sigma-Aldrich (Milwaukee, WI, USA). 50% Raney Ni activated catalyst slurry in water was purchased from Acros Organics (NJ, USA). The properties of the nickel based catalysts used in lignin degradation studies are shown in **Table 3**. 6 different silica-alumina based catalysts obtained from Dr. Seames's group from UND Chemical Engineering department were tested, i.e., undoped silica-alumina and silica-alumina doped with 1% Cu, 1% Ni, 1% Li, 1% Ga and 1% Fe, respectively. LaO, MoO and CoO doped activated carbon and zeolite catalysts were obtained from Dr. Raynie's group from SDSU Chemistry Department.

Table 3: Particle diameter and surface area of Ni based catalysts used in lignin degradation studies

Catalyst name	Particle diameter	Surface area (m^2/g)	Manufacturer
μNi	<50 μm	2-5	Sigma-Aldrich
nNi	<100 nm	27.8	Sigma-Aldrich
Ni on Si/Al	<1 mm	190	Sigma-Aldrich
Ni slurry	Not specified	~100	Acros Organics

2.2 Methods

2.2.1 Lignin hydrotreatment reactions

2.2.1.1 Static batch reactor setup

The lignin hydrotreatment experiments have been conducted in a lab scale batch reactor consisting of a GC oven (Hewlett-Packard GC5890) and rotary part made of Leeson permanent magnet DC gearmotor (Grafton, WI, USA) equipped with Dayton DC speed control. The rotor part was implemented in the thermally insulated door of the reactor. The heated part of the rotor contains five holders, where stainless steel vessels with the reaction mixture can be placed. The vessels were stirred at approximate rate of 3 rpm in order to provide sufficient mixing of the reaction mixture. The stainless steel vessels were purchased from Parker (Cleveland, OH, USA). Each vessel had a length of 6.325 cm and an internal diameter of 0.71 cm. The vessels were sealed with two stainless steel caps of 1.1 mL volume. The volume of the vessel without the caps was 2.5 mL resulting in the final volume of the sealed vessel 4.7 mL. The schematics of the static batch reactor are presented on **Fig. 4**.

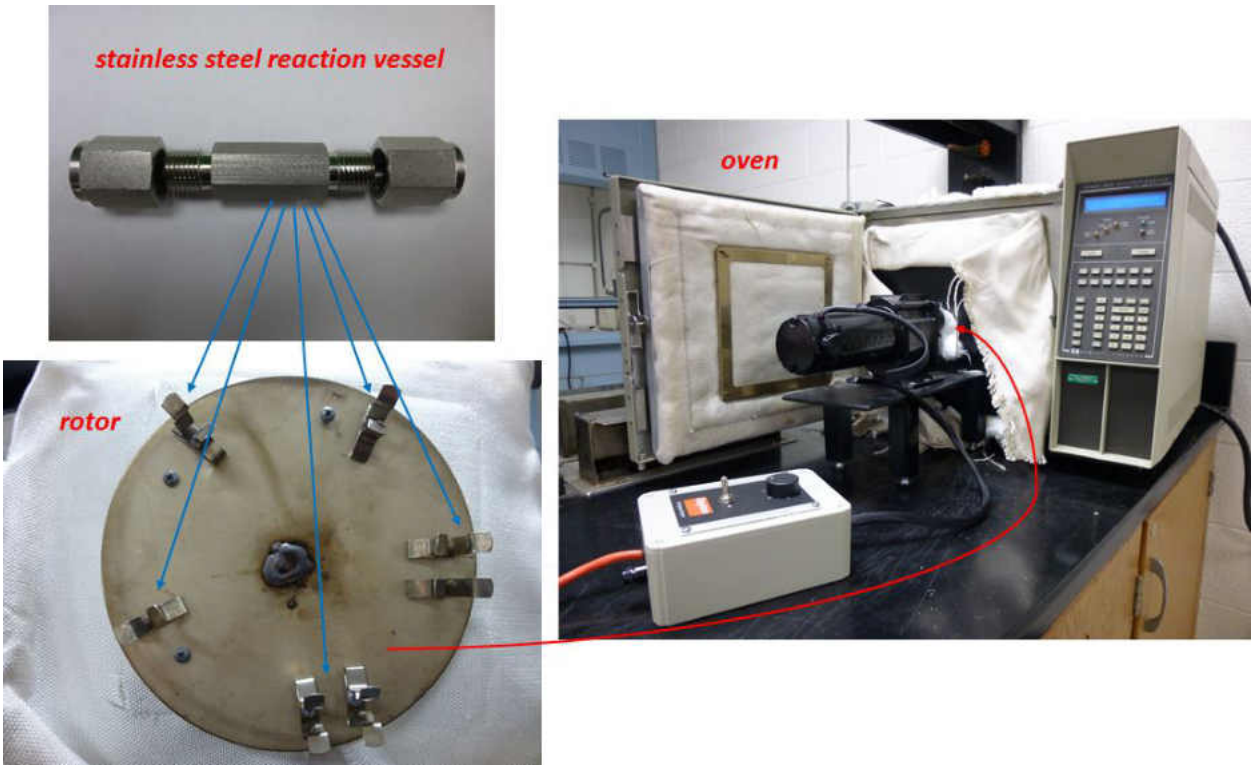

Figure 4: Static batch reactor setup

2.2.1.2 Lignin hydrotreatment reaction conditions

For both catalyzed and non-catalyzed lignin hydrotreatment reaction water was used as a solvent. In the first, non-pressurized experiment 0.10 ± 0.01 g of lignin was vortexed with ~6 mL of water for 2 min. For the reactor experiments the lignin amount and the water volume were calculated with regards to working in subcritical conditions. For all the reactor experiments the body of vessel was completely filled with the mixture. However the presence of the sealing caps ensured sufficient headspace that was important to maintain the gas/liquid equilibrium, which was crucial in order to maintain subcritical conditions and to avoid any potential safety issues resulting from the excessive pressure in the vessel. The procedure how to determine the pressure and the portion of the liquid phase inside the vessel in order to ensure the operation at safe conditions is shown in **Appendix I**. Four different reaction temperatures were studied: 200 °C, 250 °C, 275 °C

and 300 °C. For 200 °C experiments 0.1 ± 0.01 g of lignin and 3.2 mL of water were used and the internal pressure was 16 bar. For the reactions conducted at 250 °C, 275 °C and 300 °C, 0.25 ± 0.01 g of lignin and 2.9 mL of water were used, the internal pressure was 40, 59 and 86 bar, respectively. For the catalyst screening, 0.25 ± 0.01 g of lignin, 0.1 ± 0.01 g of catalyst and 2.9 mL of water were used.

A set of five reaction vessels was usually prepared for every reaction experiment to be able to obtain replicate data even in the case of a leak. In order to avoid the leak, a 7 cm long Teflon tape was attached around both threads and the vessel caps were properly tightened. After the vessels were placed into the reactor the temperature was gradually increased to the final temperature. A separate vessel with incorporated temperature probe was placed in the GC oven to determine the actual temperature in the vessels. The heating times needed to reach the reaction temperature were 5.9 min for 200 °C, 8.5 min for 250 °C, 10.0 min for 275 °C and 11.6 min for 300 °C. At the point of reaching the final temperature in the GC oven the reaction time was started. The reaction time of all the reactions was set to 30 min. Since additional time, approximately 5 min, was required to heat the vessel interior to 300 °C, the actual reaction time at constant temperature of 300 °C was 25 min. After the reaction was finished, the reaction vessels were carefully removed and cooled down by a stream of cold tap water. In the next step one of the vessel caps was loosened to release the pressure and the liquid content was transferred to a vial. The vessel was rinsed properly with the reaction solvent to obtain the final theoretical volume of 7 mL of the aqueous extract. A 1 mL aliquot was taken afterwards and a liquid-liquid extraction procedure provided in part 3.2.1.3 was conducted.

Since the aliquot used for extraction did not undergo any filtration, a gravimetry procedure was implemented in order to account for the amount of solid particles present in the aqueous extract

and in the vessel after the liquid portion recovery. The reaction vessels were weighed several times throughout the whole procedure; at the very beginning the vessels were weighed empty, afterwards they were weighed filled with lignin, water and catalyst before the reaction and finally after the reaction to detect potential leaks. After the liquid content recovery the vessels were weighed and then dried at 50 °C to constant weight and weighed again. From the gravimetric data, the tentative amount of unreacted lignin and the real volume of the aqueous extract needed for quantification of lignin degradation products could be calculated.

One reaction was conducted in different solvent than water. The experiment was inspired by the work of Jiang et al.[98] Five stainless steel vessels filled with ~0.25 g of alkali lignin and ~0.1 g of Raney Ni slurry. Afterwards, a mixture of MeOH/water 5:2 (v/v) was added. Three vessels were filled fully (2.9 mL of the mixture), another two were half full. The reaction was conducted for 30 min at 275 °C. Similarly as the experiments conducted in water, the rinsing process after the reaction was performed with the reaction mixture and the theoretical volume of the final extract was 7 mL.

After the liquid portion was recovered, the vessels were dried at 50 °C to constant weight and the solid residue amount was evaluated. The liquid extract was consequently filtered using Teflon syringe filters. The filtration was followed by vacuum evaporation of MeOH. In the next step, the collected MeOH fraction was dehydrated using an addition of a small amount of anhydrous Na_2SO_4. The separated water portion was then subjected to an extraction with EtOAc, following a vacuum evaporation of the resulting EtOAc extract.

The number of sample preparation steps was minimized in the next experiment in order to decrease potential sample losses. Instead of EtOAc, DCM was used as an extraction solvent. Two different sets of a DCM extract were prepared. The first was prepared directly from the

MeOH/water extract right after the hydrotreatment. The second one was prepared from the bio-oil after the solvent evaporation.

2.2.1.3 Liquid-liquid extraction procedure

In order to be able to analyze the hydrotreatment samples by GC-MS the aqueous solution has to be extracted to an organic solvent, therefore an extraction method to dichloromethane was established.[141] First, a 1 mL aliquot was transferred and 50 μL of recovery standard RS (10,000 ppm 4-chloroacetophenone solution in MeOH) was added. Afterwards, the mixture was spiked with approximately 10 μL of glacial acetic acid to set pH around 4 in order to obtain protonated form of analytes, which is more likely to be extracted to relatively nonpolar DCM. The pH probe had to be washed with deionized water to wash out potential recovery standard attached to the probe. The resulting acidified aqueous solution was then transferred to a test tube and extracted three times with 1 mL DCM. The resulting 3 mL total volume of DCM extract was then transferred to a new test tube and 75 μL of internal standard IS (10,000 ppm solution of o-terphenyl in DCM) was added. The internal standard concentration in the DCM extracts from the hydrotreatment experiments was the same as in the calibration mixtures. In the final step an aliquot of DCM extract with internal standard was transferred to an autosampler vial and ready for GC-MS analysis.

2.2.2 BSTFA derivatization procedure

The lignin DCM extracts prepared using the protocol in section 2.1.3 were mixed with the BSTFA reagent in 1:1 (v/v) ratio. Subsequently, the mixture of the DCM extract and BSTFA was placed into the oven heated at 70 °C and the derivatization reaction was conducted over night (12 hours).

2.2.3 Direct GC-MS analyses

GC-MS analysis were conducted on an Agilent Technologies GC5890 system (Santa Clara, CA, USA) equipped with an Agilent Technologies MS 5975C detector and HP-5MS capillary column with nonpolar stationary phase of 45 m length, 0.25 mm internal diameter and 0.25 μm film thickness. The following temperature program was set: initial temperature 50 °C hold for 1 min followed by 40 °C/min gradient up to 80 °C followed by second gradient 25 °C/min up to 320 °C hold for 7 min. Splitless injection with 0.2 min splitless time and 0.2 μL injection volume were used for the sample introduction. The injector temperature was set at 300 °C and the transfer line temperature at 280 °C. Helium was used as a carrier gas. The column flow was set to 1.5 mL/min, the septum purge was set to 3 mL/min. The mass spectrometer parameters were set as follows: solvent delay 4 min, mass range 33–500 amu, quadrupole temperature 150 °C and electron ionization (EI) source 230 °C.

An internal standard calibration was implemented. For this purpose a set of seven calibration solutions was prepared starting commonly at approximate concentration of 500 w/v and ending at 0.7 ppm for every calibration standard including RS, where the concentration of 500 ppm corresponded to 300% recovery in the samples. The calibration mixtures underwent a serial dilution by a factor of 3. The final GC-MS sample contained 400 μL of the solution and 10 μL of IS solution, which corresponds to the amount of IS in the GC-MS samples prepared from lignin extracts.

2.2.4 Thermal-Desorption-Pyrolysis-GC-MS (TD-Py-GC-MS)

2.2.4.1 TD-Py-GC-MS instrumentation and principle

The TD-Py-GC-MS was performed using Pyroprobe 5200 Series obtained from CDS Analytical, Inc. (Oxford, PA, USA). The main idea is to thermally decompose the sample in the

pyroprobe in the sequence consisting of certain temperature steps mimicking TCA. Consequently, the analytes evolved by either simple vaporization or by thermal decomposition are passed through the transfer line heated at 300 °C to the GC-MS. By using this approach, the degradation products for each temperature fraction can be identified, thus providing an information about the mechanism of the lignin molecule cleavage.

2.2.4.2 TD-Py-GC-MS sample preparation

The lignin model compounds solutions were prepared either in DCM (mequinol, guaiacol, syringol, bicreosol) or MeOH (levoglucosan and vanillic acid) possessing approximately the same concentration as the solutions used for TCA method development, i.e. ranging from 5670 to 9224 ppm giving 20 µg of C per 5 µL of the solution loaded for all of them.

The aqueous hydrotreated lignin samples did not undergo any additional sample preparation. The loaded volume was also 5 µL. The solid alkali lignin from Sigma was also not subjected to any further treatment. An internal standard solution of 100 ppm *o*-terphenyl in DCM was used. The spiked volume was 3 µL.

2.2.4.3 TD-Py-GC-MS method parameters

The initial lignin model compounds experiments were performed using 200, 300, 890 and 1200 °C final probe temperature steps. Before the probe coil started heating up, the pyroprobe interface element had to be heated to its final temperature. For all the pyroprobe methods the initial interface temperature initial hold time was set to 0. In reality, after every analysis the interface was cooled to approximately 50 °C. For the 200 °C step the final interface temperature was also set at 200 °C, for 300 °C step at 300 °C and for 890 and 1200 °C at 350 °C, respectively. A ballistic heating rate was applied for the interface. After the interface reached the final temperature, the

probe coil started heating up at 10 °C/s heating rate and the final temperature was kept for 30s. For every method the initial probe temperature was set at 40 °C. After the interface residence time, which was kept for 2.5 min in every method, the 8-way valve position switched and the sample was not evolved onto the transfer line heated at 300 °C anymore. The valve oven temperature was set at 320 °C. Since the analyses were performed in pyroprobe (direct) mode, the trap heating was turned off.

For the solid alkali lignin and hydrotreated lignin samples, two additional methods with 400 and 500 °C probe temperatures were implemented in order to mimic the TCA lignin ramp. The interface final temperature for both methods was set at 350 °C.

Before the sample was spiked onto the glass wool in the quartz tube placed in the probe, the coil was pulled out and cleaned at 1200 °C for 5 s. Afterwards, a waiting period of 5 min was required until the sample introduction in order to avoid analyte losses by evaporation. DCM samples were subjected to 50 °C for 30 s and all the runs were performed without using a solvent delay. MeOH and water samples were not dried, since the long drying time might lead to analyte losses, similar to long drying times before TCA analysis. A solvent delay time of 4.25 min for the first step at 200 °C was used instead.

A split injection onto the GC column was used for all the Py-GC-MS runs. For the lignin and lignin hydrotreatment samples a split ratio of 10:1 was used. The lignin model compounds' profile was evaluated using 10:1 and 50:1 split ratio. The same temperature program as described in section 2.2.2 were used for the GC-MS analysis. The detected mass range of the MS was broadened from 10 to 550 amu in order to monitor air related gases (water, N_2, O_2 and CO_2).

2.2.5 GC-MS data processing

For the data acquisition, ChemStation software was used. NIST library was chosen to help facilitating the identification of analytes. The list of all the lignin degradation products separated by functionalities in the order of elution including their molecular weights and formulas and the target and confirmation ions used for the peak integration are shown in **Table 4**.

The quantification was performed in Microsoft Excel based on the peak area corrected with the IS peak area using two separated calibration curves for low and high concentration, i.e. approximately 0-20 (w/v) and 20-500 (w/v), respectively. The coefficient of reliability R^2 never decreased below 0.95. The standard deviation of a calibration curve was calculated using the "steyx" function in Excel. The "low slope" was calculated with one order of magnitude of LOD using the "slope" function in Excel. The limit of detection (LOD) and quantification (LOQ) were calculated using following equations:

$$LOD = \frac{3 * steyx}{low\ slope}$$

$$LOQ = \frac{10 * steyx}{low\ slope}$$

Finally, the concentrations in the DCM extracts were recalculated with extraction recoveries and converted into %wt. of initial lignin.

Table 4: Lignin degradation products, their molecular formula, molecular weight, retention time, target and confirmation ions and relative intensities of confirmation ions

Analyte	Molecular weight (g/mol)	Molecular formula	Retention time (min)	Target ion, confirmation ions (relative intensities)
		phenols		
phenol	94	C_6H_6O	4.52	94(100), 66(34), 65(25), 39(18)
methylphenol	108	C_7H_8O	5.10	107(100), 108(85), 77(30)
ethylphenol	122	$C_8H_{10}O$	5.66	107(100), 122(25), 77(25)
propylphenol	136	$C_9H_{12}O$	6.20	107(100), 136(25), 77(15)
propenylphenol	134	$C_9H_{10}O$	6.73	134(100), 133(90), 107(60), 77(45)
		guaiacols		
guaiacol	124	$C_7H_8O_2$	5.23	109(100), 124(88), 81(68), 53(16)
methylguaiacol	138	$C_8H_{10}O_2$	5.86	138(100), 123(94), 95(32), 67(18)
mequinol	124	$C_7H_8O_2$	5.97	109(100), 124(90), 81(65), 53(15)
ethylguaiacol	152	$C_9H_{12}O_2$	6.36	137(100), 152(70)
vinylguaiacol	150	$C_9H_{10}O_2$	6.56	135(100), 150(98), 107(72), 77(70)
eugenol	164	$C_{10}H_{12}O_2$	6.80	164(100), 149(32), 103(27), 131(27)
propylguaiacol	166	$C_{10}H_{14}O_2$	6.85	137(100), 166(25), 122(11)
isoeugenol-isomer	164	$C_{10}H_{12}O_2$	7.07	164(100), 149(30), 131(20)
isoeugenol	164	$C_{10}H_{12}O_2$	7.29	164(100), 149(30), 131(20)
propylguaiacol-isomer	166	$C_{10}H_{14}O_2$	7.35	137(100), 166(20), 122(15)

Table 4 continues: Lignin degradation products, their molecular formula, molecular weight, retention time, target and confirmation ions and relative intensities of confirmation ions

Analyte	Molecular weight (g/mol)	Molecular formula	Retention time (min)	Target ion, confirmation ions (relative intensities)
4-(ethoxymethyl)guaiacol	182	$C_{10}H_{14}O_3$	7.86	137(100), 138(50), 123(40), 182(30)
hydroxypropenylguaiacol	180	$C_{10}H_{12}O_3$	8.76	137(100), 180(50), 124(45), 91(40)
guaiacyl carbonyls				
vanillin	152	$C_8H_8O_3$	7.06	151(100), 152(97), 81(23), 109(18)
acetovanillone	166	$C_9H_{10}O_3$	7.51	151(100), 166(46), 123(20)
acetonylguaiacol	180	$C_{10}H_{12}O_3$	7.93	137(100), 180(20)
guaiacyl acids				
vanillic acid	168	$C_8H_8O_4$	7.85	168(100), 153(74), 97(29), 125(19)
homovanillic acid	182	$C_9H_{10}O_4$	8.21	137(100), 182(39),122(14)
dimers				
diguaiacylethane	274	$C_{16}H_{18}O_4$	11.06	274(100), 137(500)
$C_{16}H_{14}O_6$	302	$C_{16}H_{14}O_6$	12.04	302(100), 259(15)
diguaiacylethene	272	$C_{16}H_{16}O_4$	12.29	272(100), 211(10)
guaiacyl-homovanillin dimer	316	$C_{18}H_{20}O_5$	12.31	137(100), 316(30)
diguaiacylethyne	344	$C_{19}H_{20}O_6$	13.75	137(100), 344(30)
others				
syringol	154	$C_8H_{10}O_3$	6.76	154(100), 139(45), 96(25), 111(25)
ethylcatechol	138	$C_8H_{10}O_2$	6.96	123(100), 138(30), 77(15), 91(10)
veratraldehyde	166	$C_9H_{10}O_3$	7.50	166(100), 165(70), 95(25), 151(10)

Table 4 continues: Lignin degradation products, their molecular formula, molecular weight, retention time, target and confirmation ions and relative intensities of confirmation ions

Analyte	Molecular weight (g/mol)	Molecular formula	Retention time (min)	Target ion, confirmation ions (relative intensities)
homovanillyl alcohol	168	$C_9H_{12}O_3$	7.73	137(100), 180(20), 122(15)
dimethoxyacetophenone	180	$C_{10}H_{12}O_3$	7.91	165(100), 180(55), 137(20), 122(10)
		recovery standard		
4-chloroacetophenone	154	C_8H_7OCl	6.14	139(100), 111(46), 141(33), 154(21)
		internal standard		
o-terphenyl	230	$C_{18}H_{14}$	9.40	230(100), 229(65), 215(38), 228(36)

2.2.6 Thermal carbon analysis

2.2.6.1 TCA operational principle

Lab OCEC (Organic Carbon Elemental Carbon) aerosol analyzer was obtained from Sunset Laboratory Inc. (Tigard, OR, USA) and used for TCA. This instrument was originally designed for thermal optical analysis of atmospheric particulate matter. For purpose of this study, the optical feature was not used as we have been targeting only organic carbon determined by the flame ionization detector (FID).

The operation of the analysis is shown in **Fig. 5**. In the first step, either a liquid or solid sample was placed on the Pall Flex 2500QAT-UP tissue quartz filter (Pall Corp, East Hills, NY, USA) of 1.5 cm^2 area. The filter was prebaked in the furnace over night at 500 °C in order to clean the filter from the moisture and volatile carbon containing impurities, which might affect the analysis results. Before the analysis, the filter underwent another cleaning step inside the TCA oven at 890 °C, both with and without oxygen (see **Appendix II**). Consequently, the proper instrument

performance was checked by the analysis of a sucrose with known amount of carbon. Samples dissolved in organic solvents required an additional drying step, since organic solvents also contain carbon atoms that affect the result. In the next step, the filter with the introduced sample free of organic solvent was introduced into the main TCA oven.

Table 5: TCA operational softwares and their main properties

Software version	Offline purging time (s)	Online purging time (s)
OCEC828	40	120
OCEC828NoPurge	2	2 (variable, when volatiles are analyzed)
OCEC828_2+2	2	2

The analysis was controlled by three different versions of software obtained from Sunset lab Inc. listed in the **Table 5** enabling different modes of operation and data acquisition, particularly affecting Off and Idle and Helium phase. The different version of software controlled the valves and time purging atmospheric CO_2 prior or as part of the analysis. Previously, the TCA device had been designed for the analysis of aerosols in the atmosphere. The implementation of the purge step in the data acquisition allowed us for the detection of ambient CO_2, as well as volatile species evolved at low temperatures. Due to a trace level of aerosols in the air, typical instrumental design employed a purging (Off and Idle) step at the beginning of the analysis, because the presence of ambient CO_2 and carbon containing impurities would significantly affect the results (see **Appendix III**). This approach was also used in initial characterization of lignin and lignin degradation products. Following the offline purging, the system switched to Purge online (Helium phase) ensuring that the FID signal was stable (see **Appendix IV**), then the analysis started and the software acquired the data while still being in Helium phase, i.e., the valve configuration did not change. During Off and Idle phase no carbon form was passed through the methanizer oven and therefore no FID signal was obtained. During Purge online the main helium stream passed through all three ovens, however the software did not collect any data. In the helium phase the sample in

the main oven was heated up according to the programed temperature sequence and different temperature fractions were being evolved from the sample. The vaporized sample components were carried in the helium stream first to the back oven, where all the carbon forms were catalytically converted into CO_2 using MnO_2 oxidation catalyst at 870 °C. CO_2 carried in the helium stream was consequently mixed with hydrogen gas and catalytically converted into methane in the methanizer oven by Ni catalyst at 500 °C. After the last temperature step at Helium phase, a mixture of helium/oxygen 90/10 (v/v) was introduced to the system (Oxygen phase) and the carbon species that were evolved neither in lower temperature thermal desorption steps or pyrolytic steps without oxygen were burned out leaving the clean filter in the main oven (see **Appendix V**). Finally, a mixture of 5% methane in helium was introduced to the system (Calibration gas phase) and a calibration peak potentially used as an internal standard appeared on the thermogram (see **Appendix VI**). The main oven cooled down to the ambient temperature and the system switched back to Off and Idle state waiting for a new sample. For the detailed procedure describing the TCA operation see the operational manual in **Appendix VII**. The manual contains a guide for the data processing using Excel templates, which provide higher precision and better control when integrating response areas due to more sophisticated baseline settings. Previously, Origin software was used in order to process TCA data. The data processing procedure in Origin software is described in **Appendix VIII.**

The TCA calibration was conducted using serial dilution of a sucrose solution. The calibration ranged from 0.1 µg to 80 µg of C. Two separated calibration curves were made for low and high C amount, i.e. 0.1-5 µg and 5-80 µg, respectively. The calculated LOD and LOQ were 0.2 and 0.6 µg of C, respectively.

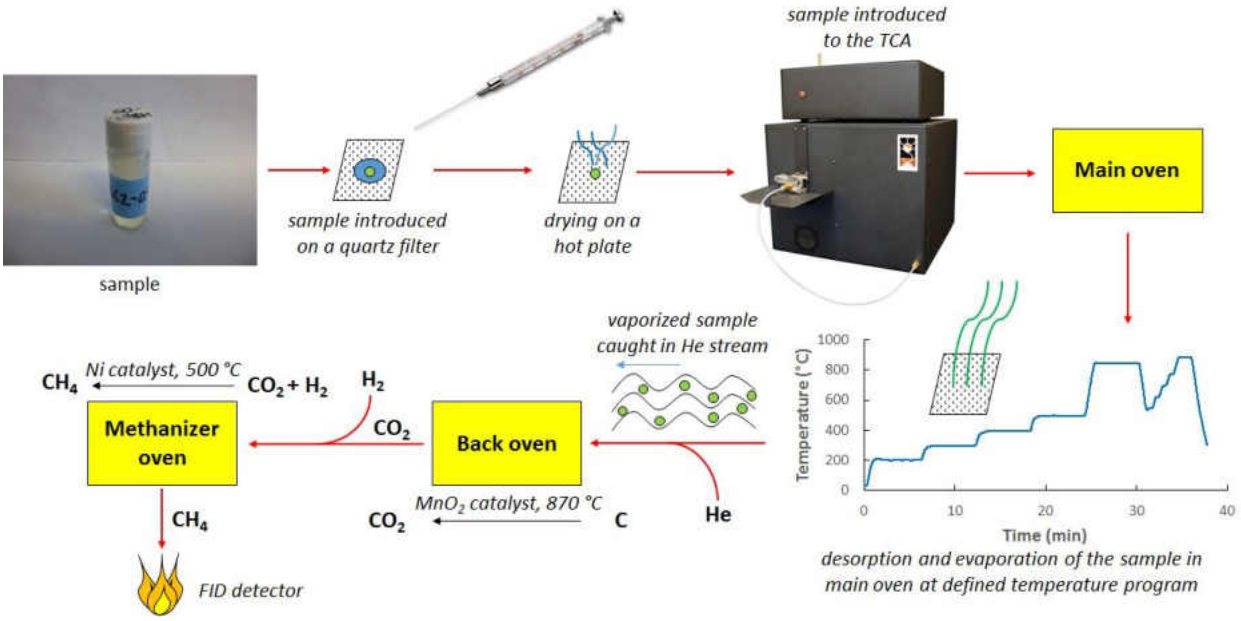

Figure 5: TCA operation diagram (Helium phase)

2.2.6.2 TCA method development

The TCA thermogram can be separated into several distinct fractions. All these fractions are shown in the thermogram in **Fig. 6**. During 200 and 300 °C temperature steps without oxygen the thermal desorption fraction (TD) is evolved. Since the GC oven temperature program reaches similar temperatures, the TD fraction % wt. of carbon evolved can be compared to GC-MS results (GC-elutable fraction). Therefore, the TD fraction is supposed to be consisted mainly of volatile monomeric and dimeric phenolics. In the second significant, pyrolytic, fraction (400 – 890 °C without oxygen) oligomers are evolved. Species that are not evolved in either TD or pyrolytic fraction, such as elemental carbon or potentially highly cross-linked polymers, are burned out from the quartz filter at 550 – 890 °C step with oxygen (coked fraction).

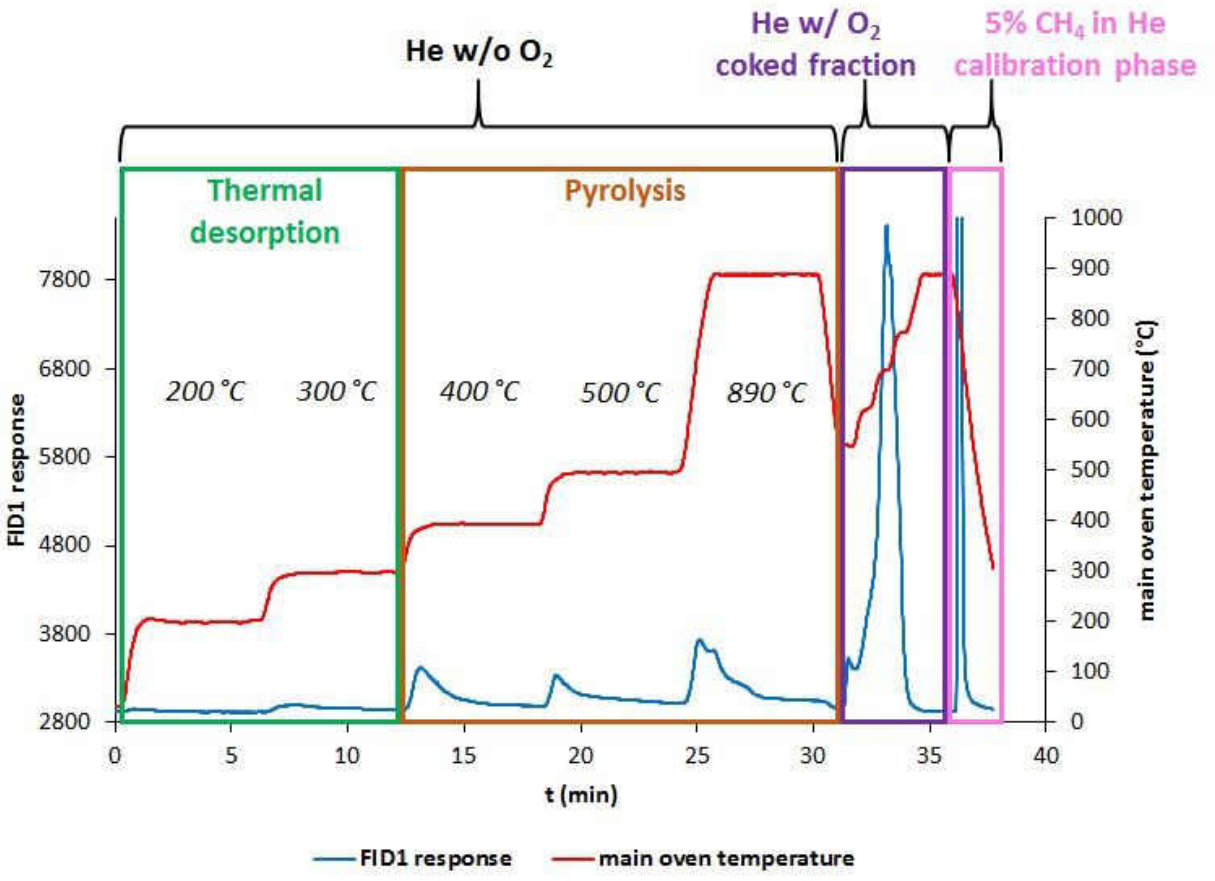

Figure 6: TCA thermogram with distinct carbon fractions

The original "lignin ramp" parameter started with 2.7 min purging (40 s offline and 2 min online) followed by the first data acquisition step at ambient temperature for 10 s proceeded with two TD steps of 200 and 300 °C for 6 min with approximate heating rate of 5 and 2 °C/s, respectively. The pyrolytic steps employed were 400, 500 and 850 °C for 6 min each. The heating rates below and above 500 °C were 2 and 6 °C/s, respectively.

Once the TD and pyrolytic steps were performed without the presence of oxygen in the He atmosphere, the main oven was cooled to 550 °C with an approximate cooling rate of 7 °C/s. Finally, the oxidizing agent mixture of He with 10% of O_2 was introduced to burn out the residual mass (coked fraction). The oxygenation phase involved several short steps starting at 550 °C for

45 s followed by 625 °C for 45 s, 700 °C for 45 s, 775 °C for 45 s and 890 °C for 120 s. In the final lignin ramp the ambient step was lengthened to 6 min and the last pyrolytic step was increased to 890 °C maintained for 12 min.

The lignin model compounds were first studied using a short method including a 10 s long ambient step and both TD steps lasting 120 and 75 s with an approximate heating rate equal to the original "lignin ramp." The pyrolysis section of the temperature program was limited to 700 °C for 75 s with a 5 °C/s approximate heating rate. This pyrolytic temperature was later increased to 890 °C. For the evaluation of the initial temperature step effect another two parameter files starting at 100 and 300 °C for 120 s were created. The parameter starting at 100 °C additional TD step at 300 °C for 75 s. The parameter starting at 300 °C did not include more TD steps. In further TCA optimization the ambient step time was increased from 10 s first to 1 min and finally to 6 min. The TD fractions were subsequently studied at times of 2.5 and 6 min and the 890 °C (pyrolytic) fraction at 4 and 6 min. The final program for the "short standard" method involves ambient temperature step for 6 min followed by 200 and 300 °C TD steps both for 4 min, pyrolytic step at 890 °C for 6 min and oxygenation step with O_2 with same settings as in "lignin ramp."

The effect of interaction between different functionalities during the drying step was studied using the "short standard" parameter. The DCM mixtures were dried at 4 min. The first DCM mixture tested contained the most volatile lignin standards: 1,071 ppm of phenol, 1,930 ppm of guaiacol, 2,474 ppm of methylguaiacol and 1,620 ppm of ethylguaiacol. A sample amount corresponded to 17.6 µg of C. In the second DCM mixture the ratio of volatile to less volatile compounds was increased to approximately 1:1, i.e., 6,965 ppm of guaiacol, 1,471 ppm of syringol, 2,687 ppm of vanillin and 2,394 ppm of syringaldehyde. A sample amount corresponded to 26.2 µg of C. Finally, an aqueous solution containing 1,009 ppm of phenol, 2,960 ppm of

vanillin and 2,728 ppm of syrigol was analyzed after a prior drying of 7 min. A sample amount corresponded to 20.4 µg of C.

The carbon loading effect was evaluated in the 3.3 to 39.0 µg of C range for lignin model compounds and in 1.9 to 41.0 µg of C for solid alkali lignin. For the lignin model compounds the original "short standard" temperature program with 700 °C step and the original "lignin ramp" were the initial parameters used. The pyrolytic temperature was later increased to 890 °C. The solid alkali lignin loading effect was evaluated using the final "lignin ramp".

The initial temperature effect experiments were conducted using 15.6 – 20.5 µg of C loading. The parameters applied began with original "short standard" method with 700 °C pyrolytic step, which was later increased to 890 °C.

The substrate effect was studied for both quartz filter sides, i.e. smooth and rough, and glass boat without the filter use for syringol. The "short standard" parameter with 890 °C pyrolytic step and original short step times was applied.

Due to a variety of functionalities the lignin model compounds possessed, they had to be dissolved in different solvents. The standards were dissolved in DCM, except vanillic acid, homovanillyl alcohol, levoglucosan and pinoresinol, which were dissolved in MeOH. Several experiments with bicreosol were also performed in ACN. Since an organic solvent contains C atoms, it cannot be introduced to the TCA machine, therefore a drying step prior the analysis has to be implemented. The initial drying time for organic solvents was 4 min. Subsequently, the drying time was evaluated for 1.5, 1 and 0.5 min. The initial drying time used for aqueous solutions was 7 min, including the hydrotreated lignin samples. Since water molecule does not contain any C atoms, the water samples were not dried at all in the further method development.

Another crucial parameter that has an impact on the % wt. recovery is the purging time. The original purging time was set to 2.7 min (40 s offline purging followed by 2 min online purging). Since the OCEC828 software does not allow the user to set a certain purging time, the Sunset Laboratory reprogrammed the software upon our request to minimize the purging time to 2 s for both online and offline purging (0 could not be set due to valve switching). The first modified software kept the offline purging at constant time of 2 s, however the online purging time was variable depending on the sample volatility. The set time for online purging was also 2 s, but when a volatile sample was being analyzed, the system did not begin the data acquisition until the FID signal was stable. Therefore, one more modified software was obtained with both offline and online purging set at 2 s, regardless the analysis parameter or the sample properties.

2.2.7 Thermal gravimetry analysis (TGA)

For TGA analysis, a SDT Q600 TGA instrument (TA Instruments, New Castle, DE, USA) was used. First, approximately 20 mg of solid Sigma alkali lignin was placed onto an aluminium boat. The sample was run in triplicate. The temperature program contained 6 temperature steps; 25, 200, 300, 400, 500 and 850 °C, each of them held for 5 min. The nitrogen flow was set at 100 mL/min. The amount of coked fraction was calculated from the difference between the lignin introduced at the beginning and the amount of mass left after the 850 °C step.

2.2.8 Lignin repolymerization tests

Initially, four different mixtures were prepared, each one of them in triplicate. Two mixtures were prepared in the static batch reactor. 0.25 g of solid Sigma alkali lignin was heated at 300 °C for 30 min at 3 rpm approximate mixing rate in 2.9 mL of water and mixture of MeOH/water 5:2 (v/v), respectively. The aqueous (aqueous/MeOH) extract recovery after the reaction was

conducted according the procedure explained in section 3.2.1.2, except increasing the rinsing solvent volume in order to obtain the final theoretical volume of extract 10 mL, ensuring sufficient amount of sample for continuous screening. The same mixture composition was also prepared at ambient temperature.

The freshly prepared triplicates of the four mixtures were immediately analyzed by TCA using the long purging time of 2.7 min in combination with the original "short lignin standard" parameter consisting of 10 s long ambient step, 200 °C step for 2 min, 300°C for 75 s, pyrolytic step at 700 °C for 75 s, cooling down to 550 °C for 45 s and oxygenation step starting at 550 °C up to 890 °C for 5 min, including the same heating and cooling rates described in chapter 3.2.6.2. Before the analysis a sample aliquot was filtered over a Teflon syringe filter. The amount of the sample loaded onto the quartz filter was 5.0 μL. The aqueous samples were not subjected to any drying, the samples containing organic solvents were dried for 4 min. Afterwards, the samples were placed onto a shaker, stirred at 700 rpm and in one week intervals remeasured. 19 days after the initial mixtures were prepared, a triplicate of another two suspensions was made: 0.25 g lignin in 10 mL of THF and 10 mL of water/ACN 1:1 (v/v), respectively. The second sample set was stirred at the same conditions as the first one and the regular analysis continued in one week intervals for another 42 days. Consequently, the each mixture set was split into one suspension, which was kept being stirred on the shaker; one where a few drops of 6M HCl was added and then the suspension was kept stirred on the stirrer too and one suspension, which was left on the bench without stirring subjected to the sunlight. The TCA measurement then continued in one week intervals for another 25 days.

Last set of samples for the repolymerization testing was prepared using the static batch reactor at 300 °C for 30s applied on 0.25 g of lignin in 2.9 mL of THF/water 1:1 (v/v) mixture. After the

reaction, the vessel was rinsed with the reaction solvent obtaining 10 mL theoretical volume of the liquid extract (25,000 ppm of lignin). Consequently, an aliquot of the mixture was diluted by factor of 10 and the second testing mixture set (2,500 ppm) was obtained. The samples were stirred continuously at 700 rpm and weekly analyzed by TCA using the "short standard" parameter with 890 °C pyrolytic step and 4 s total purging time for next 25 days. The spiked for diluted solution was 10 µL and for the concentrated solution 5 µL.

CHAPTER 3. RESULTS AND DISCUSSION

3.1 TCA method development

3.1.1 Solvent control evaluation and minimizing the solvent contribution

To ensure high accuracy and precision for sensitive carbon determination potential sources of contamination need to be assessed and minimized. The TCA sample analysis is performed in various solvents depending on reaction studied and extraction protocol employed. Thus, in this study the contribution of the following solvents: DCM, MeOH, ACN and THF and the drying time need prior to the analysis was evaluated (summarized in **Appendix IX-XII** and **Fig. 7**).

Initially, the protocol for the analysis of organic solvent containing samples, including the DCM extract from the batch reactor experiments, included drying for 4 min at 50 °C on a heating plate and the software with long purging time (~40 s offline and 2 min online purging) was used for the analysis (see "OCEC828" software in **Table 5**). For aqueous solutions a drying time of 7 min was initially used. Such drying time was sufficient to dry out the solvent, however the low recoveries of volatiles (explained in the chapters 4.1.2 and 4.1.3) suggested that the decrease in the drying time should be tested in order to minimize the analyte losses and the solvent contribution at the same time. The issue with the volatiles losses was later solved by application of minimized drying and purging time and implementation of ambient temperature step into the analysis parameter (see chapters 4.1.2 and 4.1.3).

Based on the results from the analysis of solvent blanks the drying time was decreased as follows: for DCM 30 s and for THF, MeOH and ACN 1.5 min. For water, the drying time was eliminated, since the water vapors at such small volumes (loading volume max. 10 µL) should not affect the FID signal. Thus, the aqueous solutions were spiked onto the filter and analyzed immediately without any drying. No fluctuations of the FID signal caused by the water presence were observed the method development. The thermogram of syringol (7.9 µg of C) dissolved in water analyzed by "short standard" parameter without prior drying does not show any sudden increase or decrease of the FID signal within one temperature step caused by water vapors presence (**Appendix IX**). Nevertheless, it was observed that the laser transmittance and reflectance is affected during the analysis of the aqueous samples. Therefore, if the laser signal is needed, it is recommended to dry the sample completely.

The carbon in solvent control experiments was primarily evolved at pyrolytic temperatures. Since the filter was cleaned in the main oven before the solvent blank analysis at 890 °C, both w/ and w/o O_2, and the FID signal remained stable on the baseline, suggesting that this C increase in higher temperature fractions might be most probably caused by carbon containing impurities from air, which were adsorbed onto the filter during the drying on the heating plate. The presence of particulate matter containing organic aerosols and inorganic (black) carbon in the air is well known and has been described in many publications.[142-144] An approximate amount of C evolved at TD fractions was around the LOD level (~0.2 µg of C for all the calibration curves measured), suggesting that the organic solvent was vaporized. **Fig. 7** demonstrates that a relatively significant FID response (usually 0.5–1.0 µg of C) could be usually observed at the highest pyrolytic step (700-890 °C w/o O_2) and at the oxygenation step (550–890 °C w/ O_2).

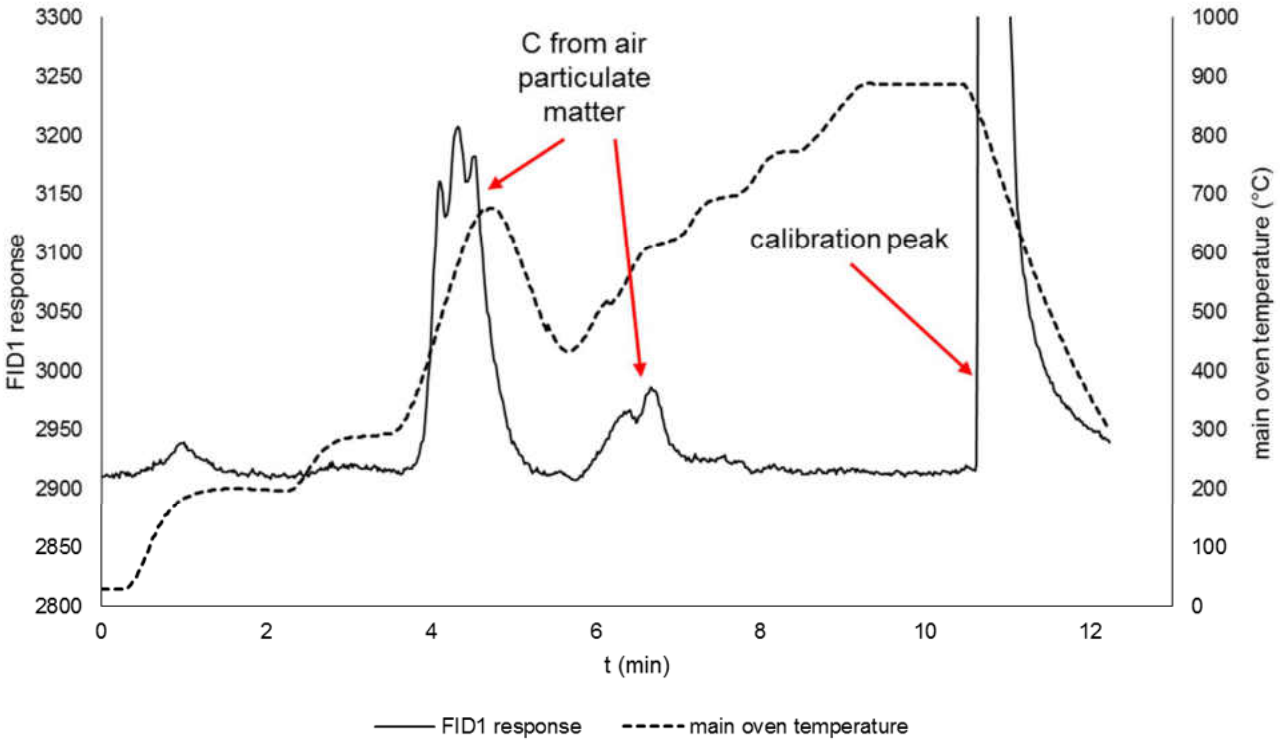

Figure 7: TCA solvent control; 5 µL of DCM dried for 4 min and analyzed using 2 min 40 s purging time

There is no evidence of changes in the evolved C amount with regards to the changes of the spiked volume, drying time or the temperature of the initial step[141], which was proven by the analysis of DCM solvent controls prepared in summer time. For all the analysis the C amount contained in TD fraction (starting either at 100, 200 or 300 °C) was lower than the LOD (<0.1 µg of C). The amounts of C observed in the highest pyrolytic fraction (700 °C w/o O_2) and in the coked fraction are presented in **Appendix X**, for each set of conditions the analysis was performed in duplicate. Generally, it can be claimed that the total C amount in solvent blanks does not exceed 1.0 µg of C.

Another set of filter and DCM blanks was run in the winter time in order to evaluate possible humidity effect, since the outside air in winter tends to be dry. The exposure time of the filter blanks was 30 s. The DCM solvent blanks were evaluated for two injection volumes, 5 and 10 µL,

which were spiked onto the filter and then dried for 30 s. The intraday repeatability was tested using a triplicate of runs for all the studied conditions. In order to evaluate the interday repeatability, the analyses were performed 3 days in a row. The average of the triplicate data for these 3 consecutive days for the filter blank and DCM blank with 5 and 10 µL spiked, respectively, are presented in **Appendix XI**.

Together with the weather monitoring, the effect of the gloves manipulation was evaluated. As shown in **Appendix XII**, the gloves contact with a filter causes a significant increase of carbon evolving at 890 °C w/o O_2, probably due to nitriles evolving from the material or C containing impurities from air adsorbed on the surface. Therefore, it is necessary to handle the filter with a tweezer every time.

Regarding the DCM blanks, the C amount evolved at TD temperatures and oxygenation phase never exceeded LOD levels (~0.3 µg of C). However, in all three figures there are apparent increases of C evolved at 890 °C w/o O_2. Due to the variation of the individual blanks at the pyrolytic fraction, the local concentration and particle size distribution in the lab might not be uniform.

Since the concentration and the particle size of the organic particulate matter in the air may be affected by the weather conditions, e.g. by the ventilation system or window opening[145-146], the weather was being monitored during the three days of blank measurement and could not be correlated with the results obtained.

Discrepancies in the amount of C evolved at 890 °C w/o O_2 were observed in case of filter blanks and DCM solvent blanks at 10 µL injection volume, which might be related to the weather change, since it was the only day with precipitations. However, for the 5 µL spiked volume of DCM the highest pyrolytic fraction is relatively consistent with the other fractions, whereas a

sudden increase was observed on the second day. A significant increase compared to the regular values was also observed for the 10 μL of DCM on the second day, confirming that the TCA blank results are probably not significantly affected by the outside weather. Since the appearance of the outliers with the increased amount of C does not have any consistent pattern, the outliers are probably caused by the changing local concentration of carbon containing air particles. The reason for such changes might be the air flow in the lab caused by the ventilation system. Non-uniform air composition in the lab might be also caused by varying flow rate caused by the fluctuations of temperature or particle/moisture concentration.

In conclusion, before analyzing any samples it is crucial to analyze a solvent blank using the same drying and purging time, injection volume and the same parameter file as for the sample itself. During the data processing, the amount of C evolved in the blank run has to be subtracted from the amount of C evolved in the sample run to ensure that only the analytes of interest contribute to the quantified C.

3.1.2 Evaluation of analyte evaporation losses

Table 6: TCA lignin model compounds' recoveries at different drying times

Analyte	Solvent	Spiked volume (µL)	C introduced (µg)	Drying time (min)	Average % recovery
Propylguaiacol	DCM	5	19.0	4	81.7 ± 3.4
Propylguaiacol	DCM	5	19.0	1.5	85.5 ± 1.7
Propylguaiacol	DCM	5	19.0	0.5	107.2 ± 3.8
Methylguaiacol	DCM	5	18.2	4	29.3 ± 0.2
Methylguaiacol	DCM	5	18.2	1.5	71.9 ± 2.3
Methylguaiacol	DCM	5	18.2	0.5	102.4 ± 1.4
Guaiacol	DCM	5	20.3	4	6.1 ± 4.0
Guaiacol	DCM	5	20.3	1.5	9.9 ± 4.7
Guaiacol	DCM	5	20.3	0.5	51.5 ± 1.5
Guaiacol	water	5	19.8	7	9.6 ± 0.6
Guaiacol	water	5	19.3	0	69.8 ± 1.9
Phenol	DCM	10	22.0	4	1.9 ± 0.3
Phenol	water	5	20.3	7	23.4 ± 6.4
Phenol	water	5	20.3	0	85.2 ± 1.6

The purpose of the drying time evaluation is to observe possible differences in the recoveries of different compounds with different properties. In section 4.1.1 the question of the solvent interfering with the sample results was discussed. The drying time has to be minimized for two reasons. First, the residue of organic solvents increase the amount of quantified C and second, excessive drying time might lead to losses of volatile organic compounds. The lignin model compounds studied during the TCA method development contained a large variety of functionalities (phenols, guaiacols, guaiacyl acids, guaiacyl carbonyls and others), which determine their unique properties. In addition, the molecular weight range of the standards tested was relatively broad starting with phenol (MW= 94 g/mol) and ending with pinoresinol (MW= 358 g/mol), which affects also their boiling point and relative volatilities.

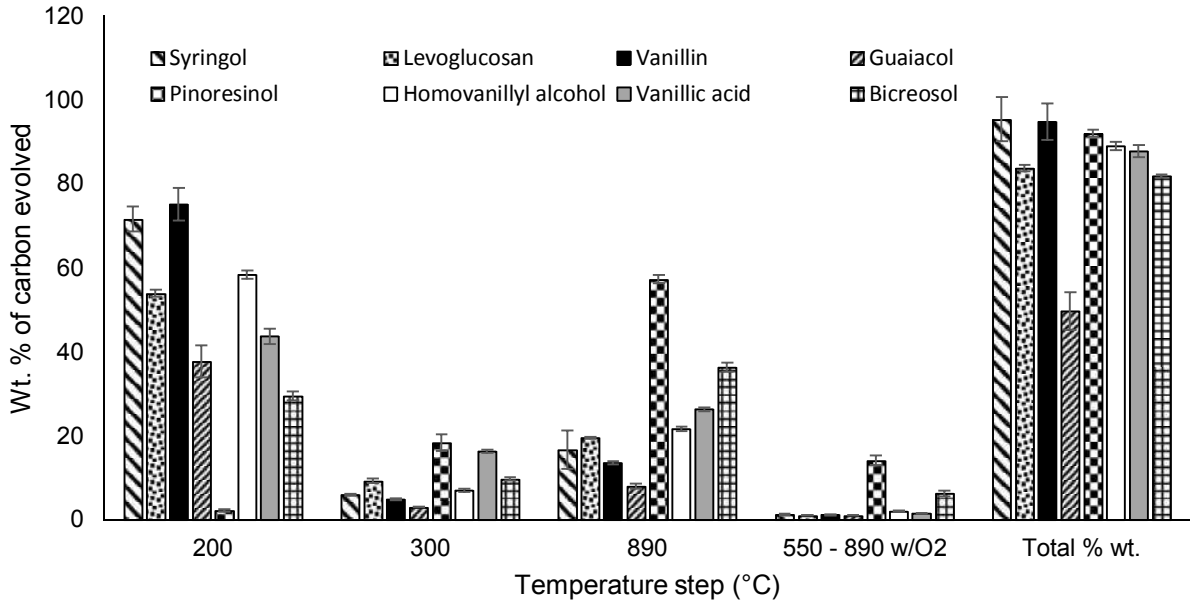

Figure 8: The TCA recoveries of lignin model compounds (%wt.) dissolved in DCM and MeOH dried prior to the analysis for 30 s and 1 min 30 s, respectively. An approximate loading of 20 µg of C was introduced on the filter and 2 min 40 s long purging time was used.

The TCA profile was examined using 2 min 40 s purging time and minimal required drying time for each solvent and the results are presented in **Fig. 8**. By applying the "short standard" parameter for the TCA analysis, we discovered that such conditions are sufficient to fully recover relatively stable model compounds of high molecular weight. Either full or near full recoveries were achieved for all of the compounds but guaiacol. This problem was later solved by minimizing the purging time (see chapter 4.1.3). Besides the analysis parameters, such as initial step temperature and duration of temperature steps discussed in section 4.1.6, we proved that the analyte properties (structure and functionalities) may also have an influence on the pyrolyzed and coked fraction. A significant increase of pyrolyzed and coked fraction compared to other standards was observed for the least volatile compounds (bicreosol and pinoresinol). Their behavior may be explained by a higher propensity to interact with the filter surface and by their higher molecular weight and molecular size, which determine their higher stability at lower temperatures. This

phenomenon is apparent on the pinoresinol TCA profile, which does not evolve almost any C at 200 °C. Also polar derivatives (homovanillyl alcohol and vanillic acid) exhibited a slight increase of the pyrolyzed and coked fraction.

As mentioned before, higher molecular weight, less volatile lignin standards, i.e. pinoresinol, bicreosol, levoglucosan, vanillin, homovanillyl alcohol, vanillic acid and syringol, provided either complete or near-complete mass balance closure, which is documented in **Appendix XIII-a** showing a syringol thermogram after 4 min drying time. An abundant fraction of C is evolved at 200 °C. This fraction contributes to the final %wt. recovery with 80.2 ± 0.6%wt. of C evolved, suggesting that syringol is relatively thermally stable at 4 min drying time and 2 min 40 s purging time.The drying time evaluation continued with the testing of guaiacol and its derivatives. Their behavior at different drying times is summarized in **Table 6**. The most thermally stable alkylguaiacol was expected to be propylguaiacol (MW= 166 g/mol, b.p.= 125–126 °C). However, even in case of propylguaiacol in DCM, the 4 min drying time did not fully recover the analyte. In order to obtain the 100% recovery, it was necessary to decrease the drying time to 30 s, which is a minimum drying time required for DCM.

When a comparable amount of methylguaiacol (MW= 138 g/mol, b.p.= 220 °C) was subjected to 4 min drying, a more than two times lower amount of C was recovered than in the case of propylguaiacol. However, limiting the drying time to 30 s was sufficient to fully recover the analyte, similar as for propylguaiacol. **Appendix XIII-b** shows a methylguaiacol thermogram dried at 4 min and compared to a similar amount of syringol dried at the same drying time, the fraction of C evolved at 200 °C is significantly less abundant (10.9 ± 4.8%wt. vs. 80.2 ± 0.6%wt.).

Guaiacol (MW= 124 g/mol, b.p.= 204-206 °C) is one of the most abundant lignin degradation products and its proper quantification and a full recovery in TCA is crucial for the reliability of

the results. However, it is also one of the most volatile standards. Guaiacol in DCM was almost completely vaporized at 4 min drying (see **Appendix XIII-c**) and 30 s of drying recovered only slightly over half of the C content. The original drying time used for aqueous samples (7 min) applied on the guaiacol aqueous solution (~20 μg of C) did not significantly increase the recovery compared to the DCM mixture dried with the original time for organic solvents (4 min). The highest recovery of guaiacol obtained with the long purging time (2 h 40 min) was 69.8 ± 1.9%wt. after the aqueous solution was analyzed without drying, suggesting that the drying step is not the only factor where low molecular volatiles are being lost.

The last compound tested for potential drying losses was phenol (MW= 94 g/mol, b.p.= 182 °C). In GC-MS analyses, phenol had the shortest retention time (see **Fig. 26)** and thus was expected to be the most volatile compound tested. In different words, phenol played a role of a marker determining the lowest possible recovery for certain conditions. Drying the DCM solution at 4 min did not recover almost any phenol and even the aqueous solution analyzed without any prior drying did not provide a full recovery. Taking into account the results obtained with guaiacol, it can be summarized that minimizing the drying time to the smallest possible value does not solve the vaporization losses of phenol, alkylphenols and guaiacol, i.e., not only the drying step is responsible for their incomplete recovery.

Ultimately, mixtures containing lignin model compounds of different functionalities and concentrations were analyzed for potential interaction effects increasing the recovery. First, a DCM mixture containing the most volatile lignin standards, i.e. phenol, guaiacol, methylguaiacol and ethylguaiacol yielded an average recovery of 17.6 ± 6.6%wt. Consequently, the amount of less volatile standards was increased to an approximate ratio of 1:1. The mixture contained guaiacol, syringol, vanillin and syringaldehyde and an average recovery of 53.4 ± 6.6%wt. was obtained

Since the DCM mixtures did not provide any apparent increase in recovery, an aqueous solution containing phenol, vanillin and syrigol was analyzed and an average recovery of 70.1 ± 1.9%wt. was obtained. The mass losses during the analyses of the three mixtures correspond to the amount of vaporized phenol, guaiacol and alkylguaiacols, according to their expected recoveries obtained in the previous experiments with single analytes, suggesting that there is not any apparent interaction effect between different functionalities that would significantly affecting the recovery.

3.1.3 Purging effect

Since the drying time minimization did not solve the mass losses of simple phenolics, the purging time started being considered the most likely factor responsible for additional vaporization of analytes, especially because the default purging time (2 min 40 s) was not changed since the instrument was acquired.

As a confirmation of the purging time being responsible for the further losses of analytes, a guaiacol aqueous solution was analyzed without a prior drying step. An FID signal was observed during the "Purge online" phase (see section 3.2.6.1. and "Helium phase" in Appendices for details). The FID1 current was increased dramatically since the very beginning of the online purging, proving that the analyte losses were caused by the He flow. As a result, another two versions of the operational software with minimized purging time were obtained.

Fig. 9 compares the %wt. of C distribution for guaiacol solution in DCM (20.3 µg of C) dried for 30 s at 40 °C analyzed by the three different operational softwares showing that when a seemingly essential purging step (originally implemented to remove the ambient CO_2 prior to the analysis) was eliminated and combined with a decreased drying time, the vaporization losses were minimized, even for the most volatile lignin standards. In addition, the implementation of the longer ambient temperature step instead of the shortened purging time allowed us to monitor the

ambient CO_2 and some analytes, such as phenol and guaiacol (see also section 4.1.6). After 30 s drying at 40 °C and 4 s total purging time an average recovery of 96.1% was obtained for guaiacol in DCM (20.3 µg of C). Compared to the softwares with the long preset purging time, the latest version provides almost twice higher abundance of 200 °C fraction, confirming the importance of the purging time.

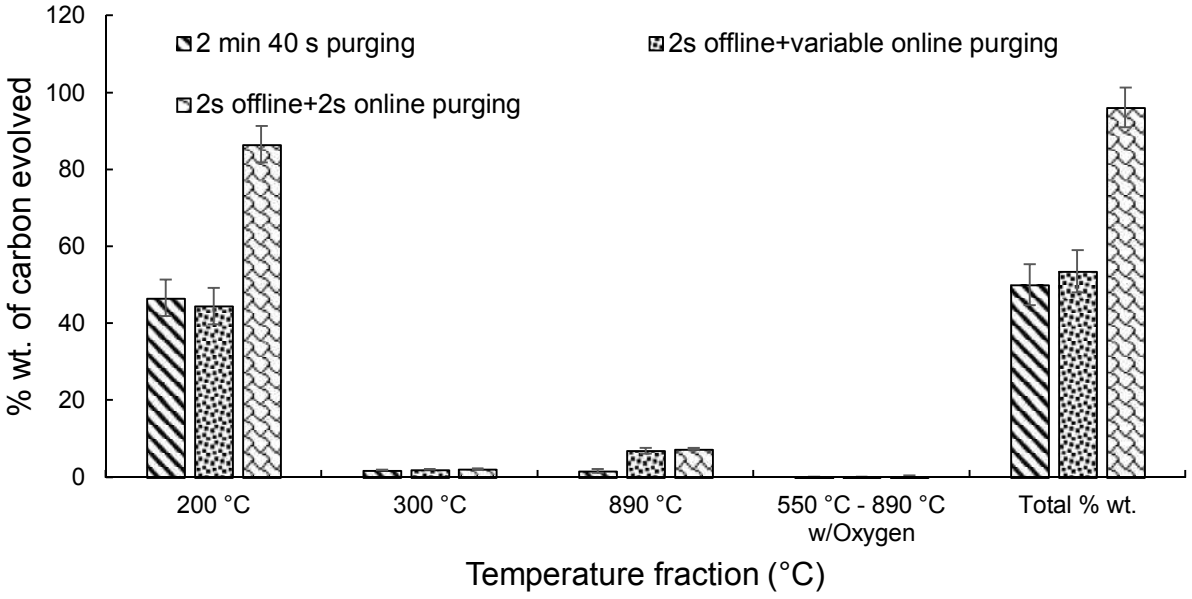

Figure 9: TCA operational software comparison; TCA profile of guaiacol in DCM; 20.3 µg of C loaded, 30 s drying at 40 °C, 200 ° C initial step

Fig. 10 shows a thermogram of guaiacol dissolved in DCM, obtained using 30 s drying time at 40 °C and 4 s total purging time. There are two important observable patterns. First, a thin and relatively tall peak appears at the very beginning of the data acquisition. Most probably, this peak belongs to the ambient CO_2, which is a consequence of limited purging time. The thermogram (**Fig. 10**) shows that the peaks of ambient CO_2 and the analyte can be separated. Thus, the ambient CO_2 was accounted for by subtracting a blank with no analytes using the same conditions and analysis parameter as for the sample itself.

Compared to the FID response to the particulate matter evolving mainly at 890 °C w/o O_2, solving the issue of CO_2 peak has one advantage. There is a relatively good separation between the CO_2 peak and guaiacol evolved at ambient temperature and even though a small portion of the ambient guaiacol co-elutes with CO_2, the peak separation allows the user to exclude the CO_2 peak from the quantification by simply narrowing the integration area, which is not possible in case of organic particulate matter co-eluting with the analytes (**Fig. 10**). By monitoring the CO_2 peak every analysis it can be claimed that its peak area is not uniform from sample to sample, however the C amount rarely exceeded 1 μg. The fluctuation of the peak size (C amount) is probably caused by different local concentration of CO_2 in the lab caused by air flow (non-uniform air composition) or researchers breathing in the lab.

The second important feature of **Fig. 10** is a monitoring of lignin and lignin model compounds at ambient temperature with an included 6 min long ambient temperature step at the beginning of the analysis. In order to accomplish this, the blower constant controlling the He flow responsible for cooling of the main oven had be increased from 0 to 8, since the thermal insulation between the main oven and the back oven (870 °C) could not stop the heat transfer completely (see **Appendix XIV** and **XV** for details). By analyzing guaiacol with the limited purging time and long ambient step, it was discovered that 65.1%wt. of the spiked C evolves already at ambient temperature. The data were compared to phenol in water (20.2 μg) analyzed w/o drying and similar profiles were acquired (see **Fig. 11**). In the case of phenol, 71.9%wt. of C evolved at ambient temperature and at 200 °C 22.1%wt. of C was evolved. However, a more important observation is that 99.7%wt. average recovery was obtained. Considering that phenol is the most volatile lignin standard studied, we can claim that by applying our TCA method we can obtain nearly 100% recovery for all the aqueous lignin reaction mixtures.

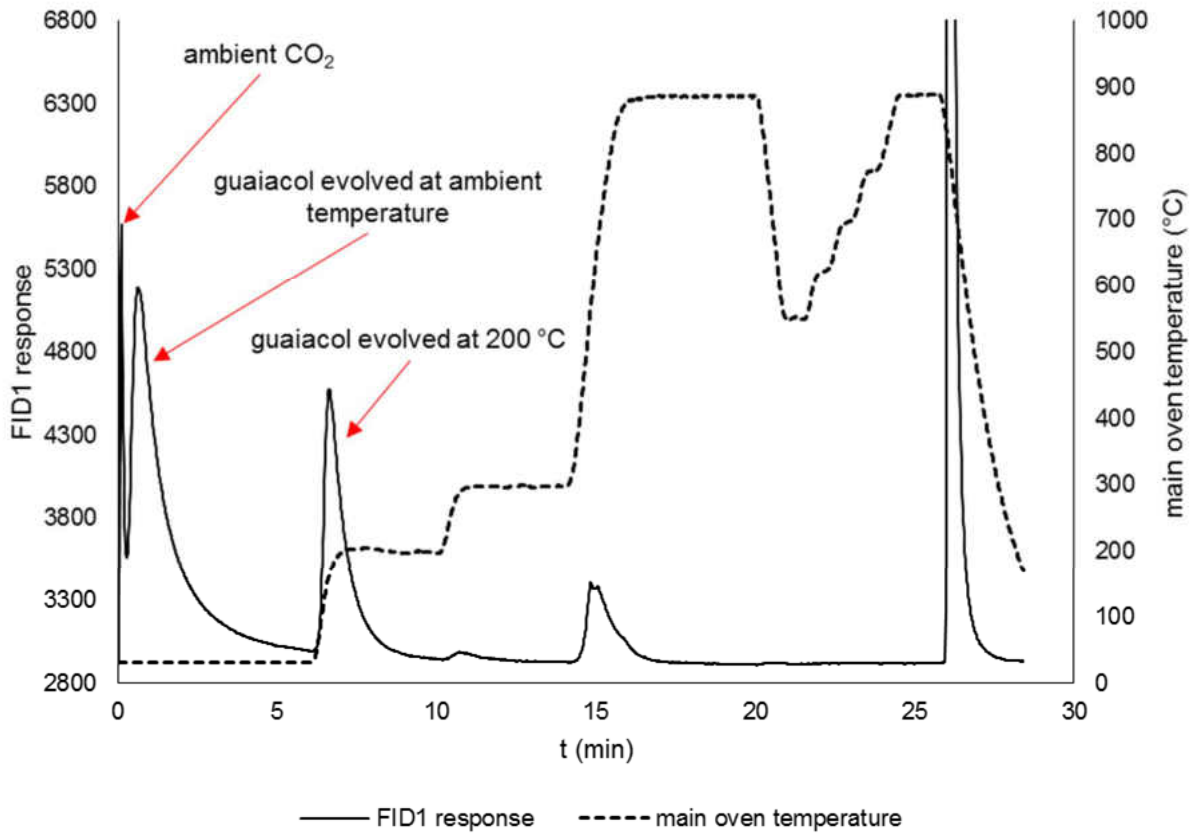

Figure 10: TCA thermogram of guaiacol in DCM; 20.3 µg of C, 30 s drying at 40 °C, 4 s total purging time.

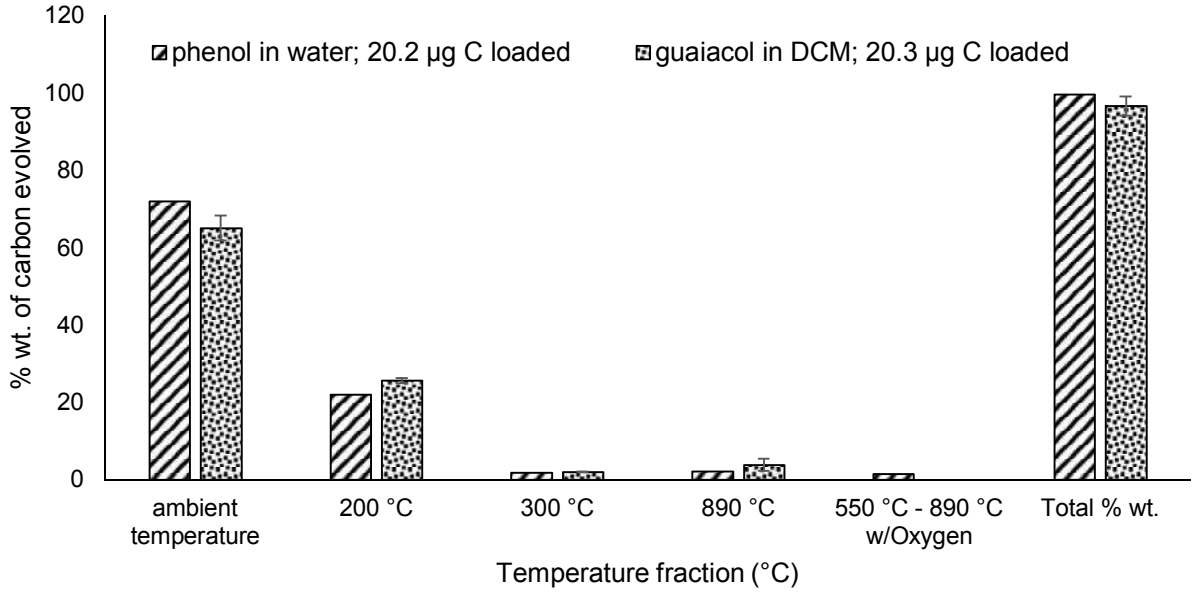

Figure 11: Comparison of TCA %wt. C distribution of guaiacol vs. phenol; guaiacol in DCM dried for 30 s at 40 °C, phenol in water not dried, 4 s total purging time was used.

Interestingly, mequinol (MW= 124 g/mol, b.p.= 243 °C), a guaiacol isomer differing from guaiacol by the position of the methoxy group, exhibited a similar recovery (95.8%wt.), but significantly different TCA profile (**Appendix XVI**). Besides the CO_2 peak, a negligible amount of C was evolved at ambient temperature, whereas most of the mass evolved at 200 °C. The difference in the TCA profiles is caused by higher boiling point and lower vapor pressure of mequinol compared to guaiacol.

3.1.4 Effect of carbon loading on the TCA profile

To assess the impact of sorption and desorption from the filter on the TCA profiles, the thermal profiles were compared for a different loading of relatively non-volatile lignin standards, syringol, vanillin and bicreosol (**Fig. 12**). The temperature profiles for the pyrolytic fraction were more detailed introducing additional 400 and 500 °C steps besides 870 °C, to differentiate the types of pyrolyzed carbon. For both syringol and vanillin a full recovery was obtained for both loadings, howeverthe fraction evolved for lower loading at the TD temperatures was smaller, and the corresponding increase was observed at pyrolytic temperatures. This trend was even more pronounced for the dimeric bicreosol. The observed pyrolysis appears to be due to the analyte retention caused by non-specific, strong analyte adsorption to the surface of the quartz filter. Once the active sites are saturated (when using higher loadings), this effect is negligible. It was previously suggested to use an optimal loading of approximately 20 µg of C for the TCA analysis.[141]

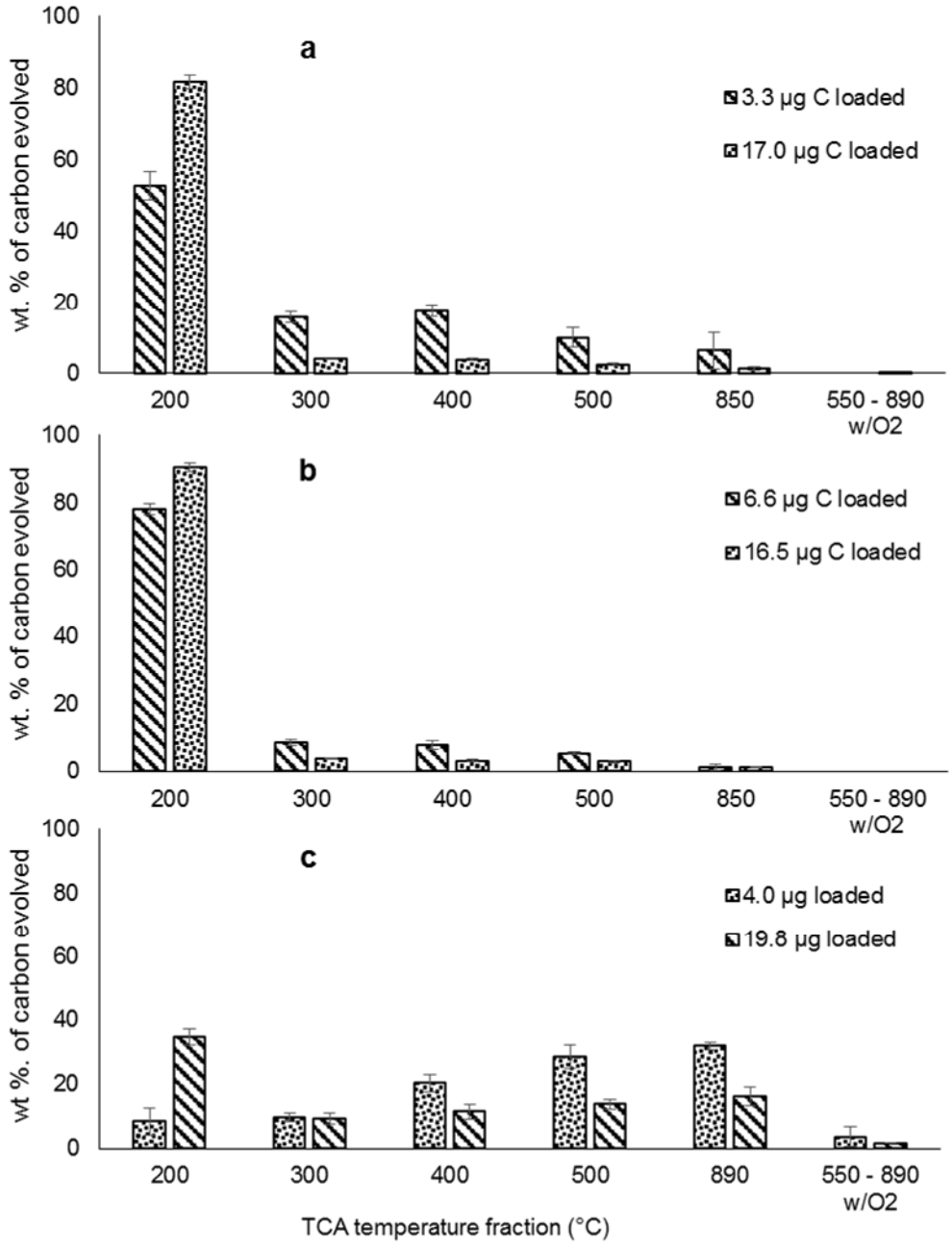

Figure 12: Effect of C loading on evaluation of %wt. of lignin model compounds introduced in DCM over different temperature fractions, a) syringol, b) vanillin, c) bicreosol. The solutions were dried at 40 °c for 30 s and 2 min 40 s purging time was used for the analysis.

3.1.5 Surface adsorption effect

Syringol %wt. of C distribution was evaluated regarding possible surface interactions. A comparison was made using a new quartz filter freshly prebaked in the oven and an old filter left in an aluminum foil wrapped Petri dish for several weeks. In addition, an effect of the filter side was tested. Besides the regularly used rough filter side, the sample was also spiked onto the smooth side. Finally, the syringol solution was introduced onto a bare glass boat. The results are presented in **Fig. 13**. A full recovery of syringol was obtained for all the studied conditions. The TCA profiles were similar and showed statistically insignificant differences between the data sets with the most abundant 200 °C fraction.

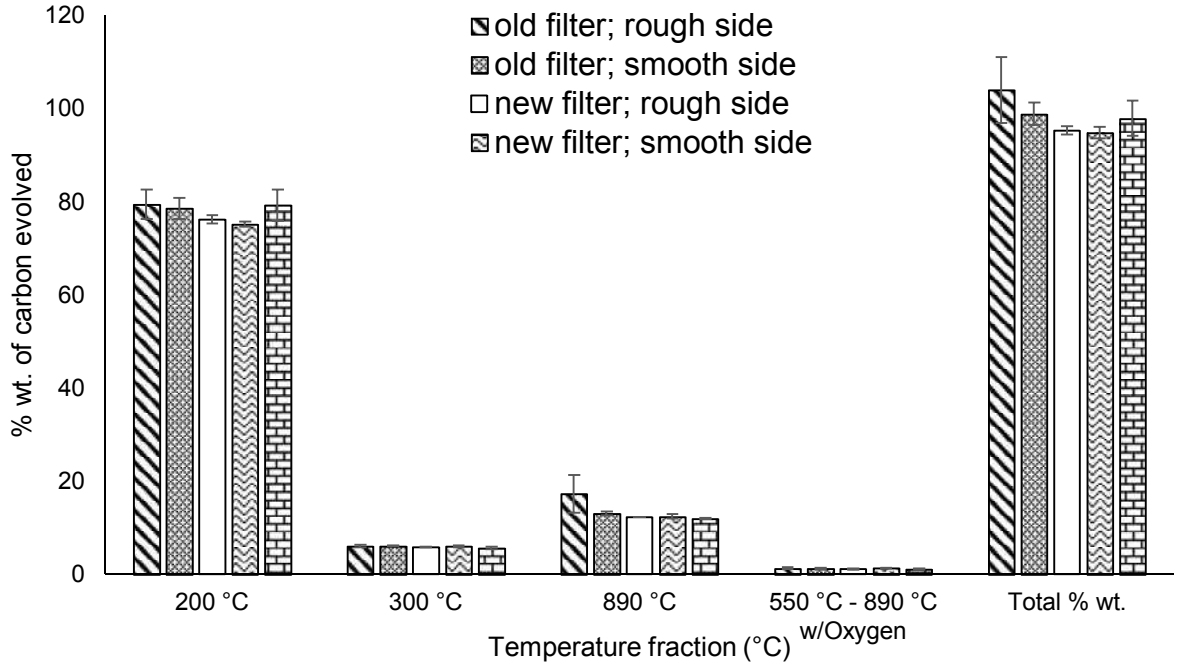

Figure 13: TCA surface effect evaluation of syringol in DCM; 20.5 µg of C loaded, drying time of 30 s and purging time of 2 min 40 s was used.

The adsorption behavior was also evaluated for bicreosol in DCM using the rough side of the quartz filter and also the bare glass boat (see **Fig. 14**). The same average recovery of 98.3%wt. was calculated for both conditions, however for the bicreosol spiked on the bare glass boat a higher

amount of C evolved at 200 °C was obtained (48.5 vs. 37.2%wt.). Conversely, in the case of bicreosol spiked onto the filter, the pyrolyzed and coked fractions were more abundant (36.9 vs. 28.9%wt. and 10.1 vs. 6.9%wt., respectively), suggesting that for the least volatile standards, such as bicreosol, there is a noticeable surface interaction with the quartz filter decreasing the amount of quantified monomers and dimers (TD fraction).

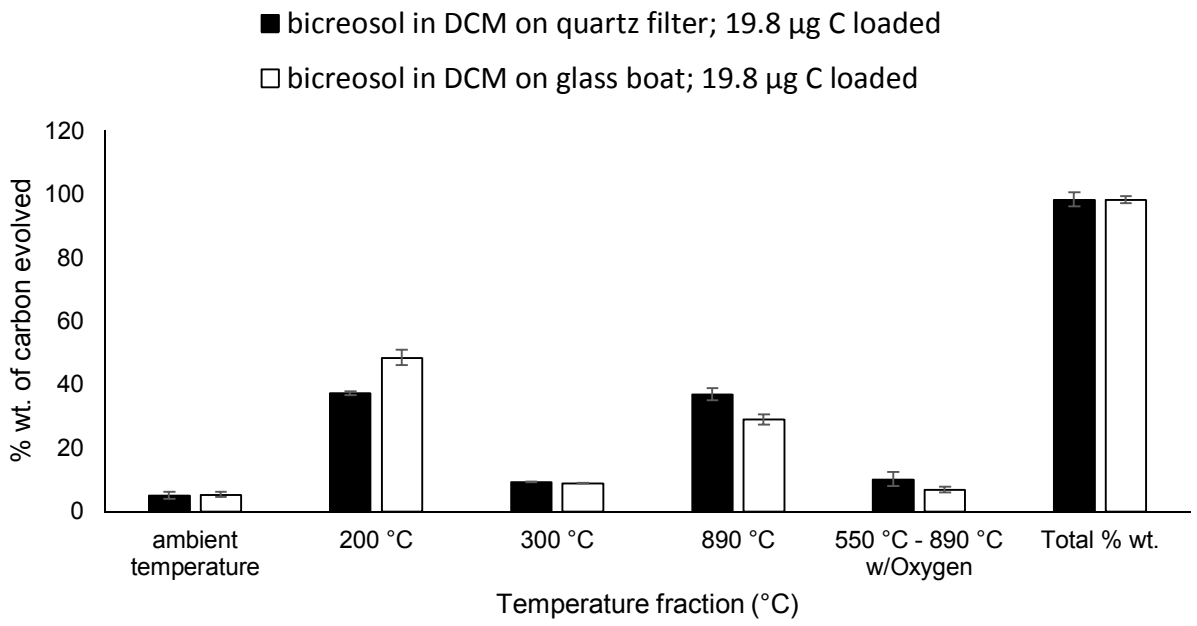

Figure 14: TCA surface effect evaluation of bicreosol in DCM; 19.8 µg of C loaded, drying time of 30 s and purging time of 2 min 40 s was used.

3.1.6 Temperature programming

The first TD step in the TCA temperature program was evaluated for four compounds (**Fig. 15**), potential lignin decomposition products, with a goal to minimize both the pyrolyzed and coked fractions when lower initial temperatures are applied to prevent the analyte polymerization. Contrary to our expectations, the pyrolyzed/coked fractions did not differ whether the programming started with 100, 200 or 300 °C. We also observed that the last temperature fraction obtained under the He atmosphere, at 850–890 °C, cannot be eliminated or replaced with any lower

temperature steps, as then this fraction would subsequently evolve with oxygen, thus artificially increasing the share of this “coke” fraction.

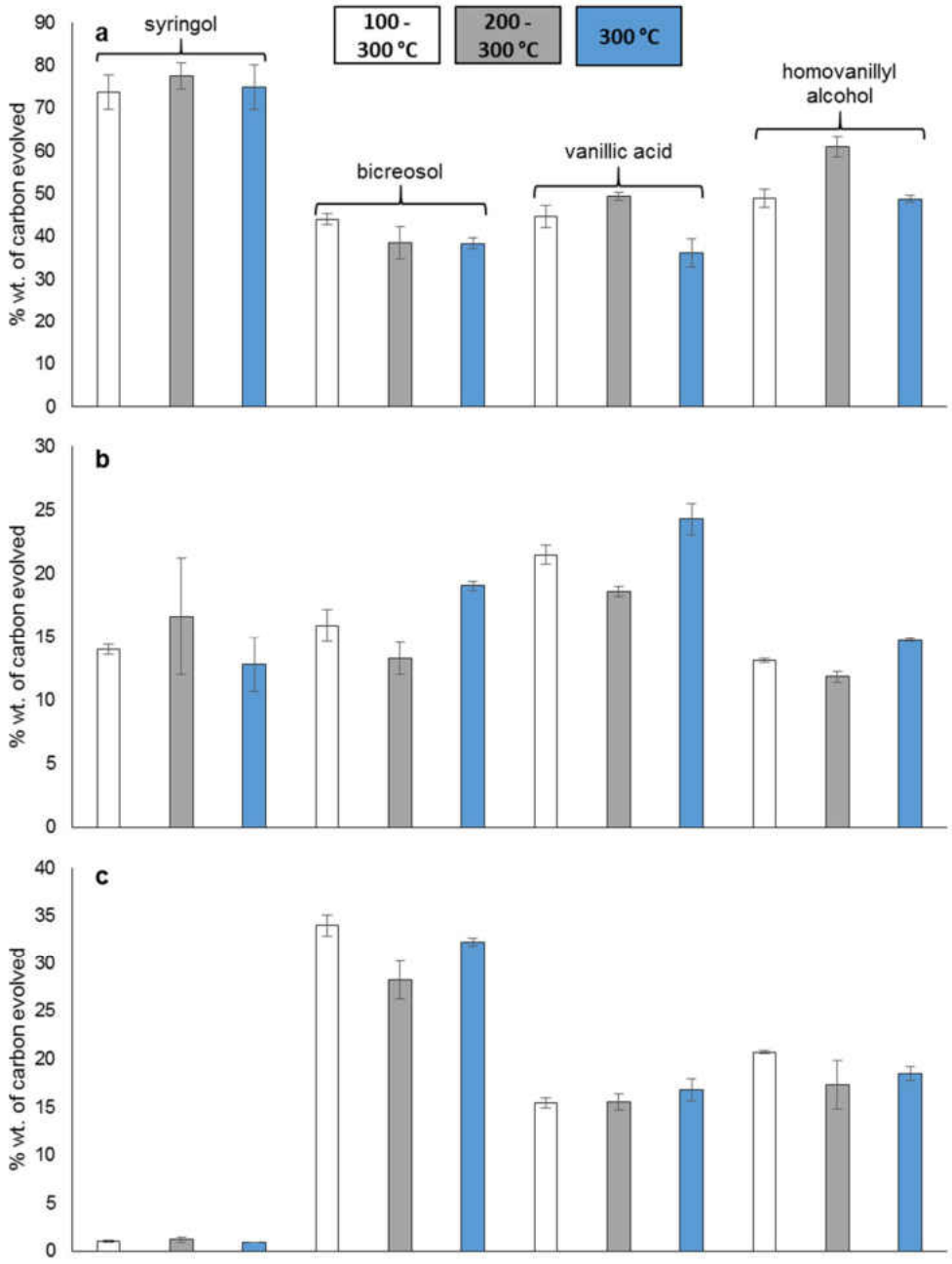

Figure 15: Recovery of lignin model compounds (wt. %) depending on the TCA initial temperature step; comparison of TCA profiles starting the thermal desorption with 100 & 300 °C , 200 and 300 °C, and 300 °C. the recoveries are compared for a) thermal desorption step, b) pyrolytic 700–890 °C and c) coked (550–890 °C w/oxygen) temperature fractions. Approximately 20 µg of carbon was loaded for each standard. For syringol, bicreosol and vanillic acid (DCM solutions) 30 s drying time was used. For homovanillyl alcohol in MeOH 1 min 30 s drying time was used. 2 min 40 s long purging time was used for all the standards.

Another important parameter of the temperature programming is a temperature step time ensuring evolution of all carbon at particular temperature, especially in case of the most abundant fractions, i.e. pyrolyzed and coked fraction in lignin. The importance of their correct distinction was discussed in the previous chapter. As observed in **Appendix XVII-a**, a lignin analyzed by the original "lignin ramp" evolves a significant amount of coked fraction, which is caused by insufficient time of the last pyrolytic step (6 min). The evidence is apparent on the sudden decrease of FID signal with the decreased main oven temperature, suggesting that not all the C was evolved. Other feature of **Appendix XVII-a** is a tailing tendency of the FID signal, suggesting possible repolymerization, causing a lack of time to evolve all the C.

Therefore, additional 6 min were added in order to recover all the pyrolytic C. In **Appendix XVII-b**, there is not any apparent decrease of the FID signal with the decreased main oven temperature observed between the last pyrolytic and oxygenation step anymore. In addition, the amount of the coked fraction is minimal compared to all the pyrolytic fraction (400–890 °C w/o O_2).

3.1.7 TCA application on solid alkali lignin

The solid alkali lignin evolves a significant amount of pyrolyzed and coked C (, as shown in **Fig. 16**. Such a high amount of pyrolyzed and coked C (27.0 ± 6.0%wt. and 46.5 ± 4.0%wt. of initial C for lower loading and 15.8 ± 1.8%wt. and 52.5 ± 1.6%wt. of initial C for higher loading, respectively) is mainly owing to lignin related oligomers and polymers that are expected to be evolved at pyrolytic and oxygenation conditions due to their rigid structure and high molecular weight. However, the increase of C in these particular fractions may also be caused by a repolymerization of monomeric species.[38, 63] Interestingly, a relatively large amount of C was

evolved in the TD fraction (0.9–1.5%wt. at 200 °C and 2.5–3.3%wt. at 300 °C, respectively), proving that monomeric and dimeric species are present in solid alkali lignin.

A satisfactory mass balance was obtained for all the solid alkali lignin TCA analyses. The amount of loaded sample did not seem to impact TD fractions and lower pyrolytic temperatures, however some shift occurred between the highest pyrolytic step and the coked fraction (**Fig. 16**), which is similar observation as for lignin model compounds (**Fig. 12**). The observed increase in the coked fraction at higher loadings is possibly due to a competition of evaporation with polymerization reactions becoming more pronounced for large samples.

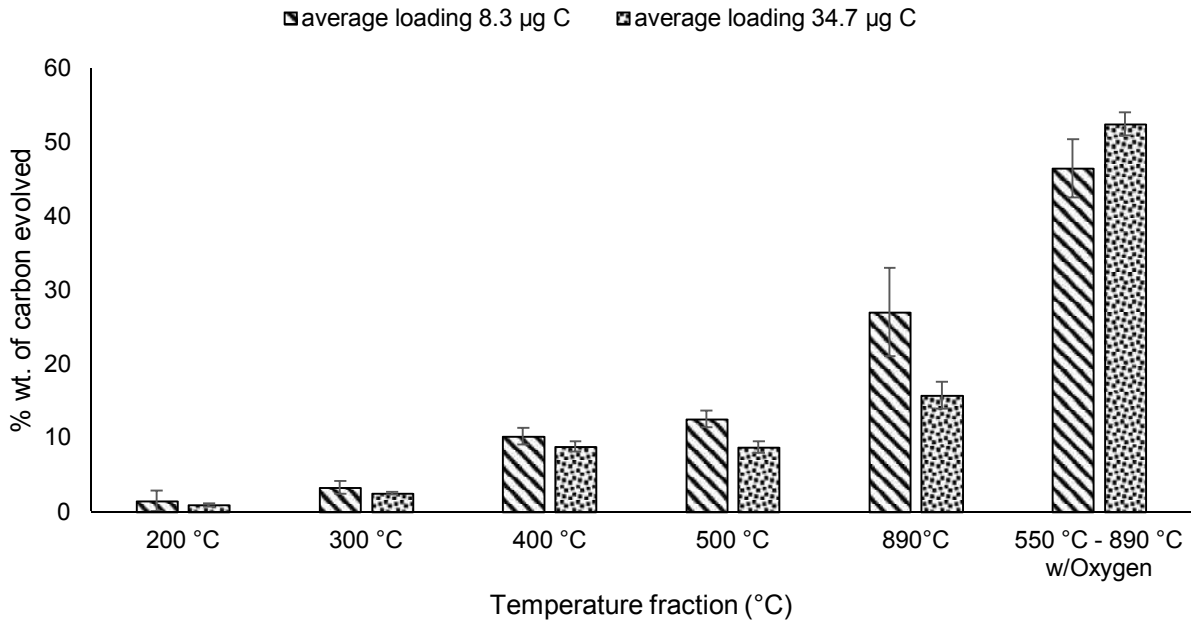

Figure 16: Evaluation of solid alkali lignin loading on its TCA profile. Analysis performed with 2 min 30 s purging time without prior drying.

The solid alkali lignin was later analyzed by newly developed TCA method with short purging time. A similar profile to the lignin analyzed with long purging time was obtained, including the most questioned TD fraction, where slight losses were expected due to the vaporization of simple phenolics during the purging. However, 1.1 ± 0.1%wt. and 3.2 ± 0.1%wt. of C was evolved at 200

and 300 °C, respectively, which are the data similar to those obtained with the long purging time. Moreover, **Fig. 17** shows a negligible amount of C evolved at an ambient temperature, suggesting that monomeric phenols and guaiacols mostly contributing to the mass losses at ambient temperature, as investigated in sections 4.1.2 and 4.1.3, are not present in large amounts in solid alkali lignin.

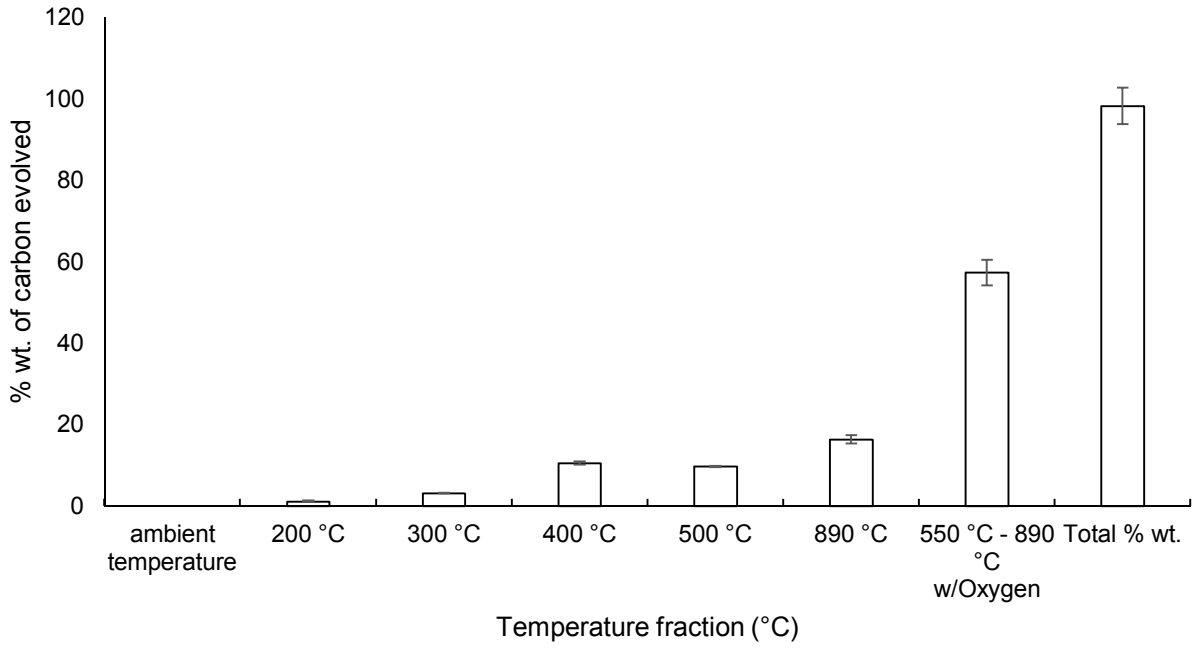

Figure 17: TCA profile of solid alkali lignin (37.6 µg average amount of C). 2 min 30 s purging time was used for the analysis without prior drying.

3.1.8 Comparison of TCA vs. TGA analysis of solid alkali lignin

TCA analysis data of higher loading of solid alkali lignin (~34.7 µg of C) were compared to TGA results (~20.3 mg of lignin; 13.0 µg of C). The results are shown in **Fig. 18**. A similar amount of mass/carbon was evolved at 500 °C and in the coked fraction. However, at lower temperatures the TGA evolved significantly higher amount of mass. The discrepancies in data may be explained by different operational principle of the two analytical techniques. The TCA is selective towards

C containing analytes, while the TGA analyzes the mass loss in time in general (non-specific analysis), including moisture, salts, sulfur, other carbon-free species and oxygenated compounds, which have usually 10-15% greater MW.[147] Sigma alkali lignin contains about 5%wt. of moisture and based on the elemental analysis performed by Atlantic Microlab, Inc., it contains approximately 1.4% of sulfur, which together with other carbon-free species possibly causes higher TGA mass losses compared to TCA.

Another advantage of TCA over TGA is an oxygenation step allowing for quantification of elemental and coked carbon, whereas in TGA the oxygenation step is missing and the coked fraction has to be calculated from the difference, assuming 100% mass balance.

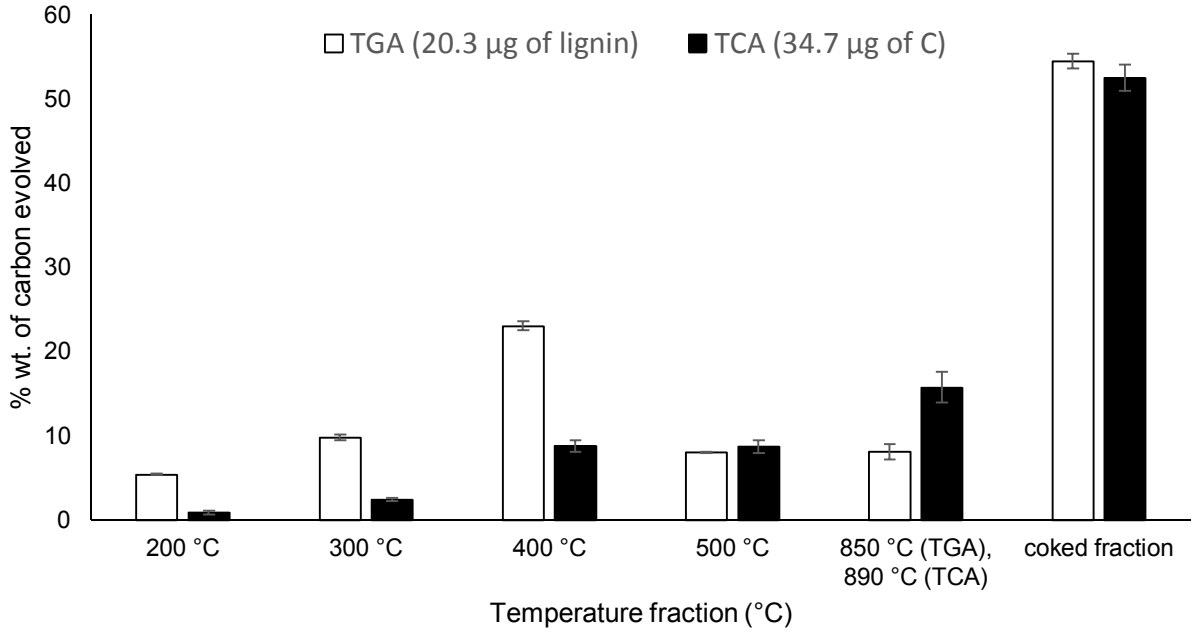

Figure 18: Comparison TCA vs. TGA analysis of solid alkali lignin. TCA analysis was performed using 2 min 40 s purging time without prior drying.

Appendix XVIII shows TGA profiles of solid alkali lignin (average loading 20.3 µg) analyzed in triplicate. Consistent data with minimal fluctuation in temperature program were obtained.

3.2 Lignin repolymerization investigation

The TCA is a convenient method for the analysis of lignin repolymerization, assuming that during the repolymerization process the monomeric compounds' amount decreases, while they are converted into higher molecular weight oligomers and polymers. Therefore, a decrease of C in TD fraction and increase of pyrolytic and potentially coked C should be observed. There was not any significant change in the %wt. of C distribution observed throughout the monitoring in the mixture of lignin in MeOH/water 5:2 (v/v) (**Fig. 19**) and neither later prepared mixtures in THF nor ACN/water 1:1 (v/v) at lab temperature, which were expected to dissolve higher portion of lignin (confirmed by increased total %wt. of C), provided any proof of repolymerization (**Fig. 20**), since there was no observable difference between the weekly measured TCA profiles.

The lignin repolymerization probably did not occur due to a low concentration of monomeric and dimeric species (the TD fraction in **Fig. 19**). The desired effect was not observed even in lignin mixtures treated at 300 °C, which had the TD fraction more pronounced, thus higher concentration of monomers, which could possibly merge. The visual observation of the lignin mixtures also had a negative effect.

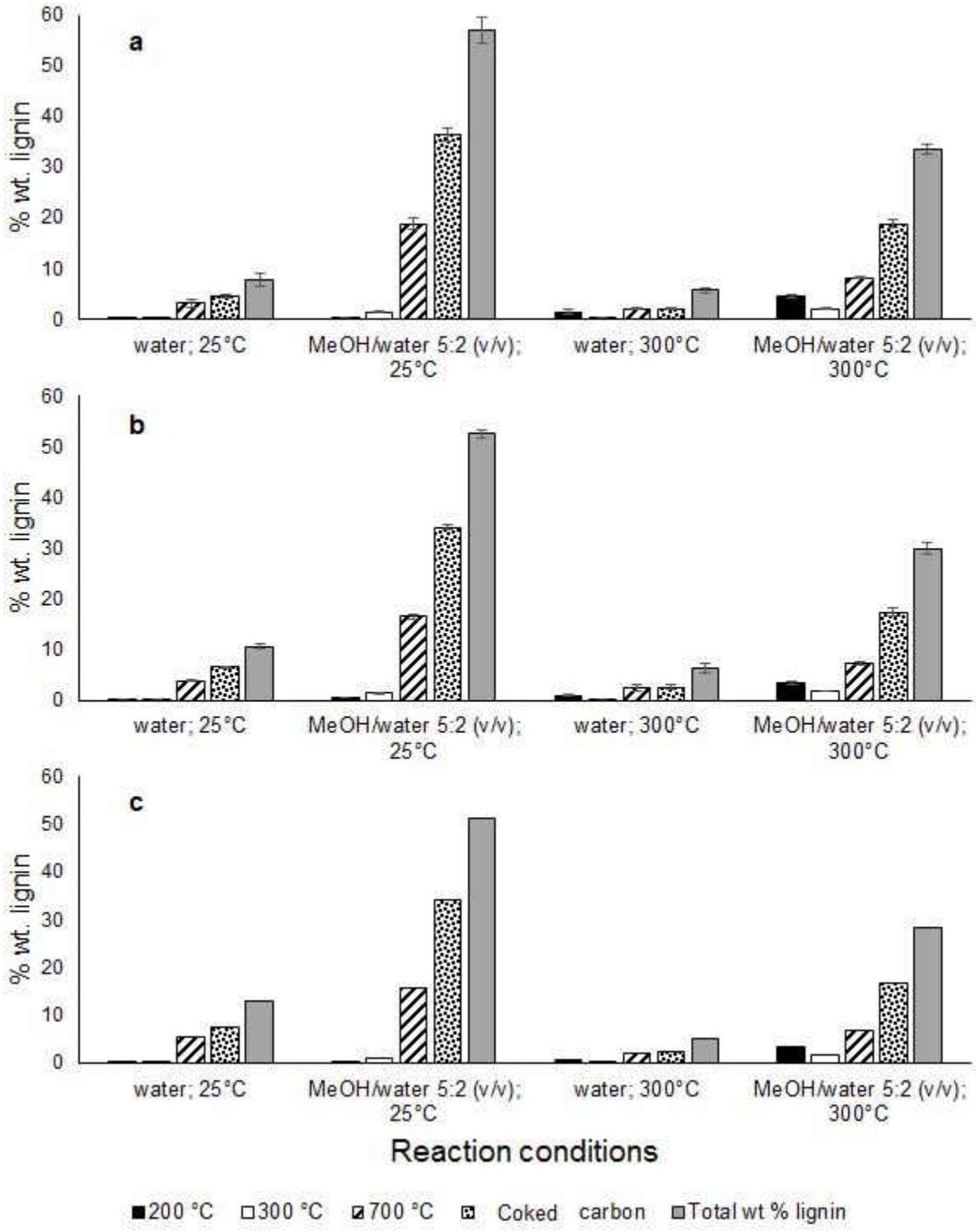

Figure 19: Lignin repolymerization in different solvent systems evaluated by using TCA, 1. mixture set, a) day 1, b) day 27, c) day 61

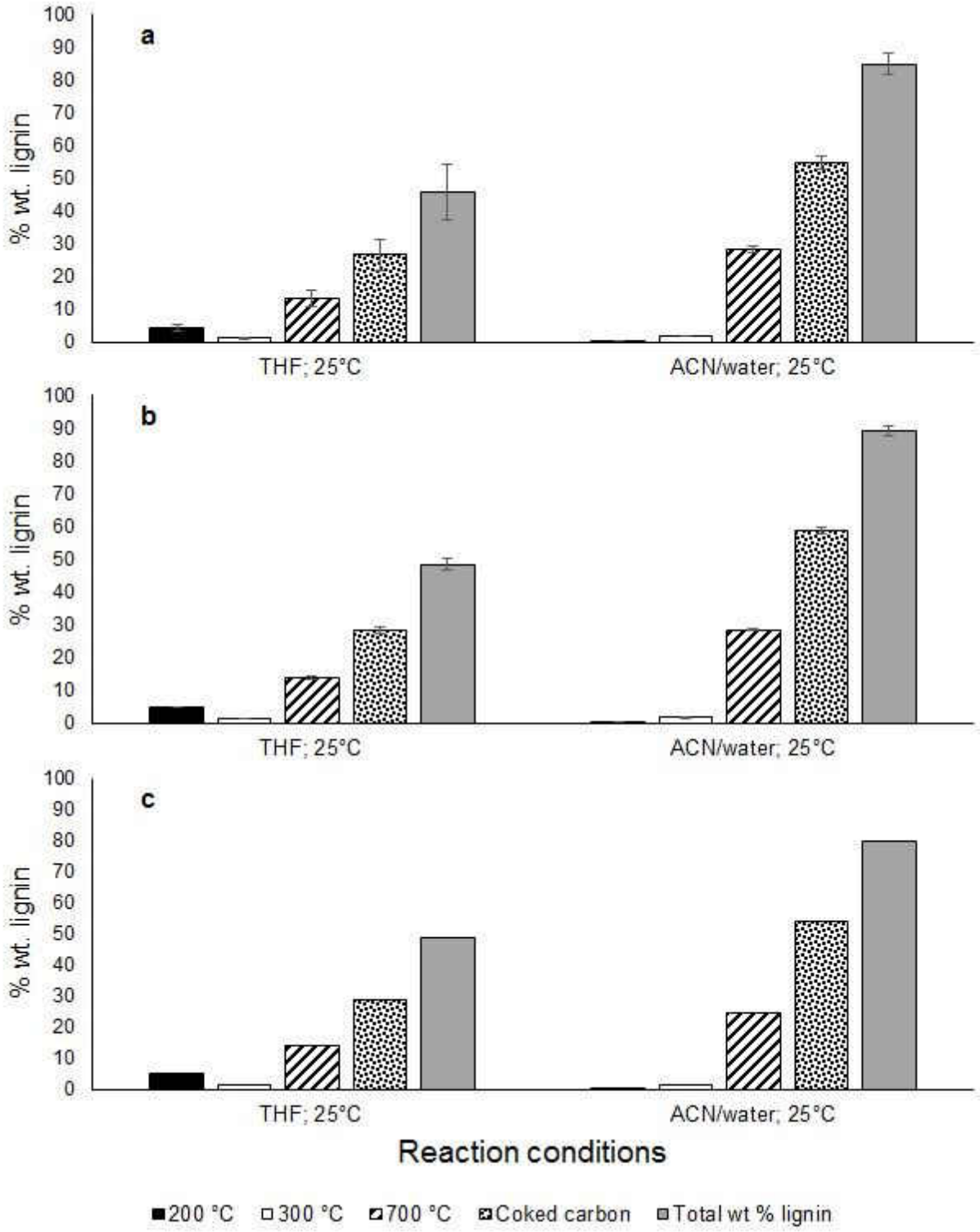

Figure 20: Lignin repolymerization in different solvent systems evaluated by using TCA, 2. mixture set, a) day 1, b) day 22, c) day 42

In order to initiate polymerization artificially, a catalytic amount of HCl was added after 61 days to one of the mixtures, while the second mixture was introduced to direct sunlight without shaking in order to form radical species. The last mixture from the triplicate, a control, was kept being shaken at the previous conditions. **Appendices XIX–XXIV** show that the introduction of additional polymerization initiators did not significantly affect the TCA profiles, suggesting that the mixtures' composition did not undergo any radical changes since they were prepared.

Finally, lignin dissolved in the THF/water 1:1 (v/v) mixture was tested for repolymerization at two different concentrations: 2,500 and 25,000 ppm. The mixture of THF/water 1:1 (v/v) was discovered to dissolve lignin completely, which was proven by a near-complete mass balance closure for both mixtures (**Fig. 21**). The weekly TCA screening did not show any changes in the C distribution profile as well, however the more concentrated mixture always evolved significantly more coked carbon at the expense of less pyrolyzed carbon than the less concentrated mixture. It is a similar trend as obtained with lignin model compounds and solid alkali lignin, where the amount of pyrolyzed fraction increased at lower C loadings, while the coked fraction was more pronounced at higher C loadings (**Fig. 12** and **16**). However, the shift was even more apparent in this experiment. The possible reason for this observation is that the repolymerization might have occurred immediately after the exposure to a specific solvent mixture.

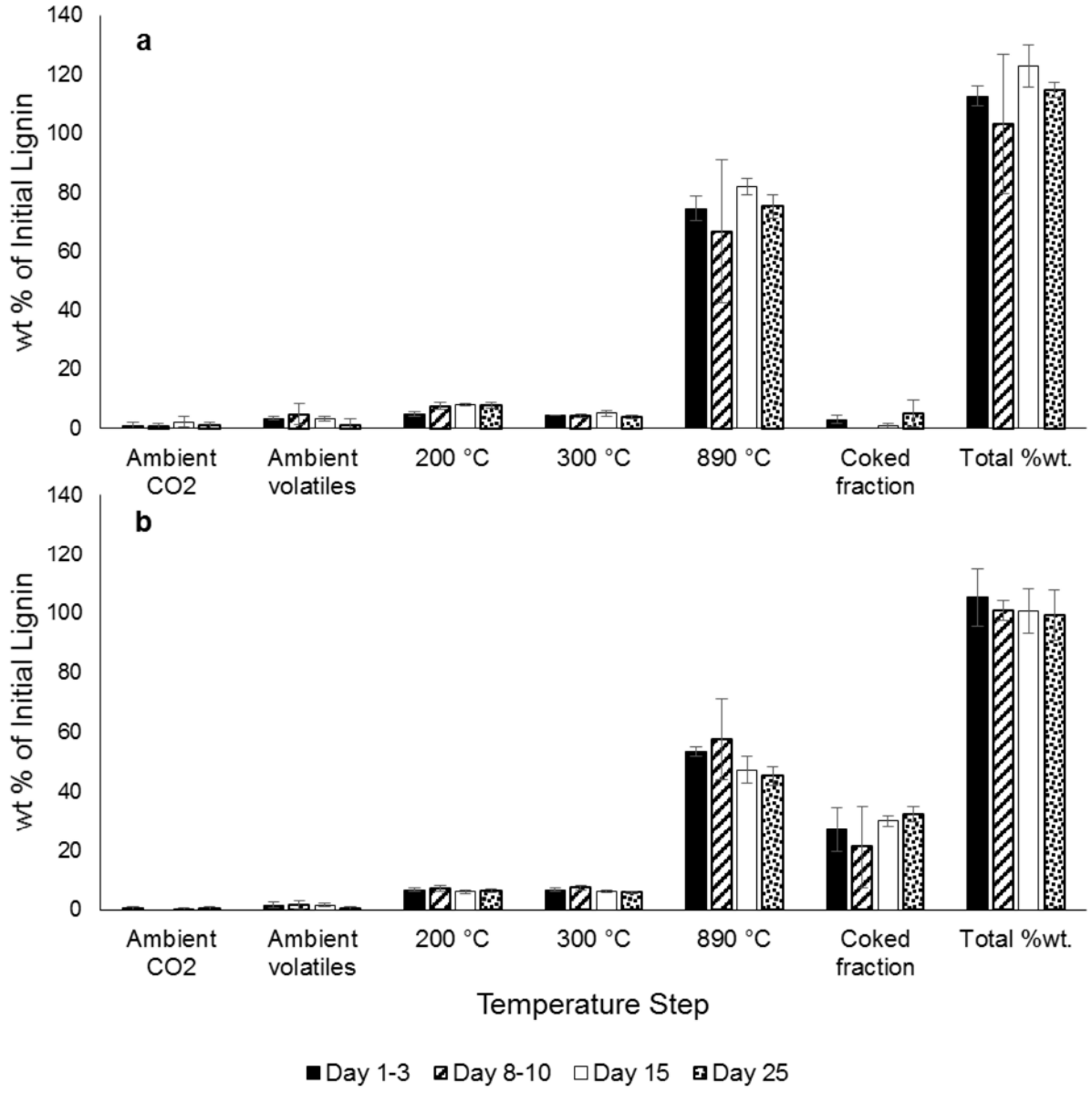

Figure 21: Lignin repolymerization evaluation by TCA, a) 2,500 ppm lignin in THF/water 1:1 (v/v), b) 25,000 ppm lignin in THF/water 1:1 (v/v).

3.3 Lignin hydrotreatment reactions

The main goal of the lignin degradation studies was to decompose lignin in a static batch reactor using solid Sigma alkali lignin in supercritical water as a solvent. Furthermore, catalytic activity of several transition metal catalysts was evaluated. Our intention was to optimize the reaction conditions and find the right catalyst in order to obtain the maximal yield of monomeric and dimeric products regardless of the product distribution. The main focus was on the nickel based catalysts, since together with water as a solvent they have a potential to be cheap and effective promoters of lignin degradation. The main project idea is summarized in **Fig. 22**.

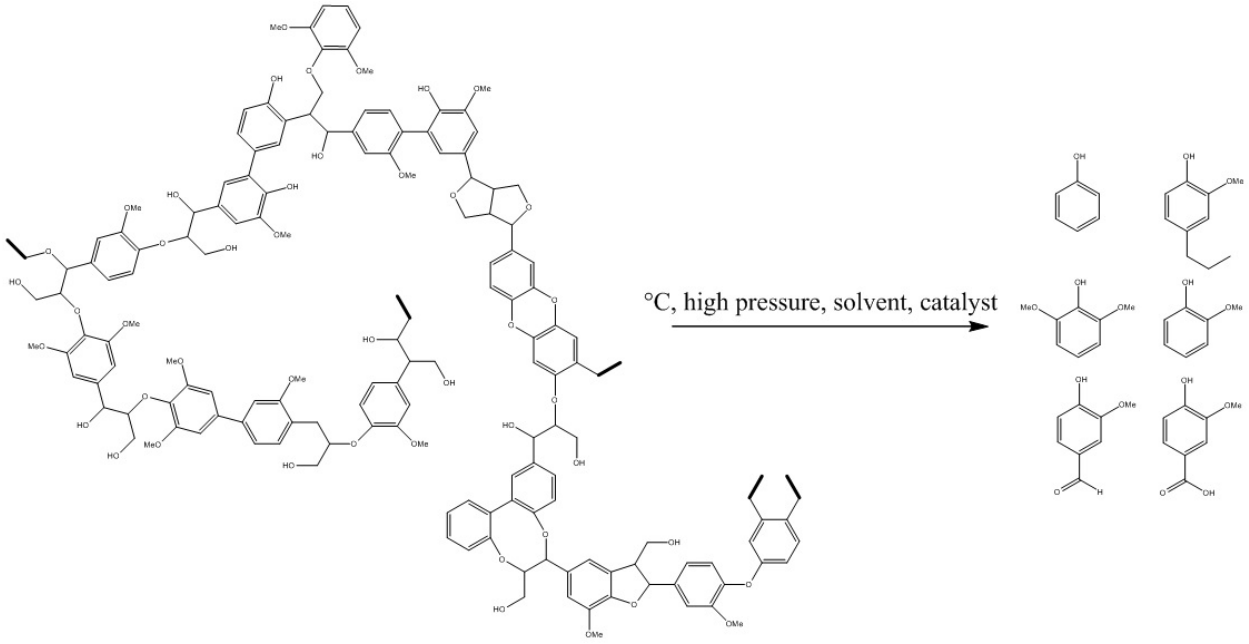

Figure 22: General scheme of lignin hydrotreatment

3.3.1 Non-catalyzed systems

3.3.1.1 Effect of mixing on the product yield and distribution

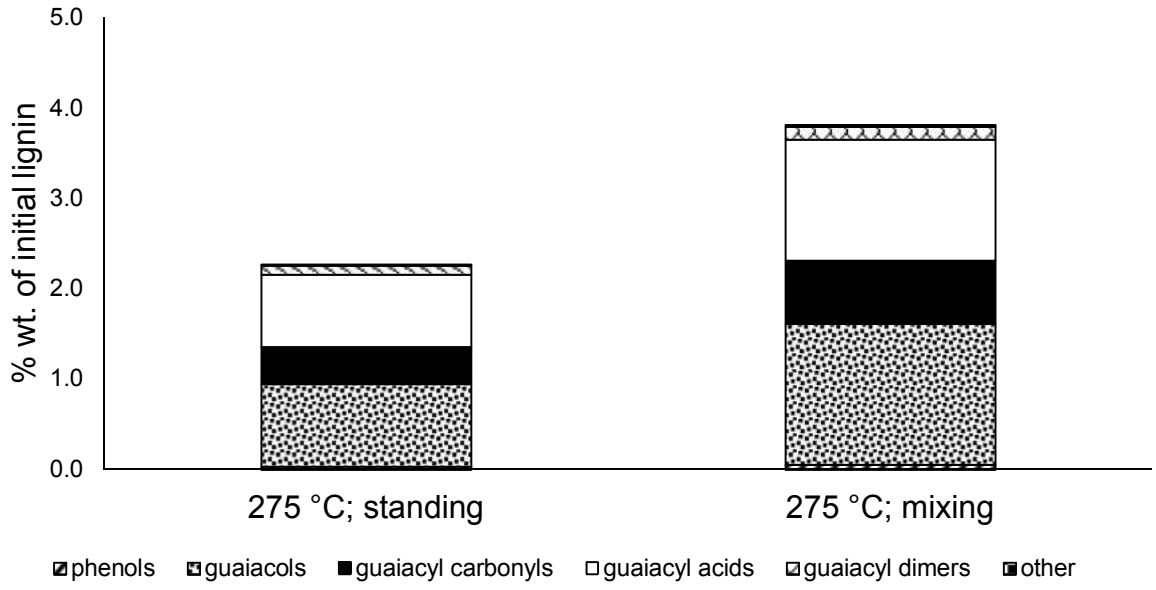

Figure 23: LLE GC-MS; Effect of mixing on the yield and distribution of lignin degradation products for non-catalyzed reactions conducted at 275 ¯C for 30 min (performed in duplicate, the difference between the two data sets was less than 10%)

The evaluation of the vessels' mixing provides an important information about the batch reactor performance. By placing additional vessels filled with reactants vertically next to the rotor with the stirred vessels, the reactor capacity can be increased However, **Fig. 23** exhibits an approximate 1.5-fold increase of the total product yield in the stirred vessels compared to the standing vessels, confirming the need of proper sample homogenization that affects especially the yield of guaiacols and guaiacyl acids.

3.3.1.2 Effect of unreacted lignin particles on the product yield and distribution

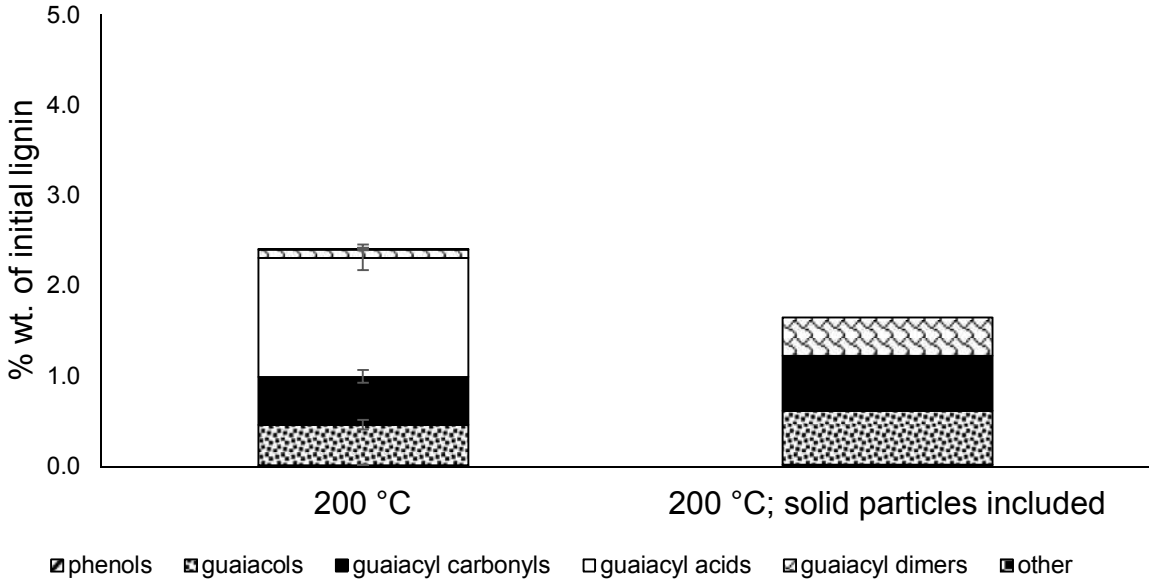

Figure 24: LLE GC-MS; Effect of solid unreacted lignin particles presence in the aqueous extract on the yield and distribution of lignin degradation products yield for non-catalyzed reactions performed at 200 °C for 30 min (experiment with solid particles performed in duplicate; the difference between the two data sets was less than 5%)

After the hydrotreatment the liquid-liquid extraction (LLE) was performed. The DCM extracts were prepared both from the liquid portion by itself and the combined liquid and solid portions. Then, the data were compared in order to determine the right approach for the future experiments. Unreacted lignin is one of the greatest technological obstacles in lignin hydrotreatment, since it decreases the reaction efficiency and complicates the sample preparation. In case of our experiments, the amount of unreacted lignin typically exceeded 40%wt. (section 4.3.1.6) of the initial lignin for both non-catalyzed and catalyzed systems. This observation corroborates other lignin degradation studies conducted in water, where the lowest amount of unreacted lignin/char was 38%wt.[5, 107, 111] **Fig. 24** shows that the additional unreacted lignin present in the test tube during LLE does not increase the amount of extracted products. The presence of solid particles had actually a negative effect, especially on the yield of homovanillic acid, which was not observed

in the enriched extract, probably due to increased adsorption. Thus, unfiltered liquid fraction was used for the sample preparation in the further optimization.

3.3.1.3 Effect of reaction temperature on the product yield and distribution

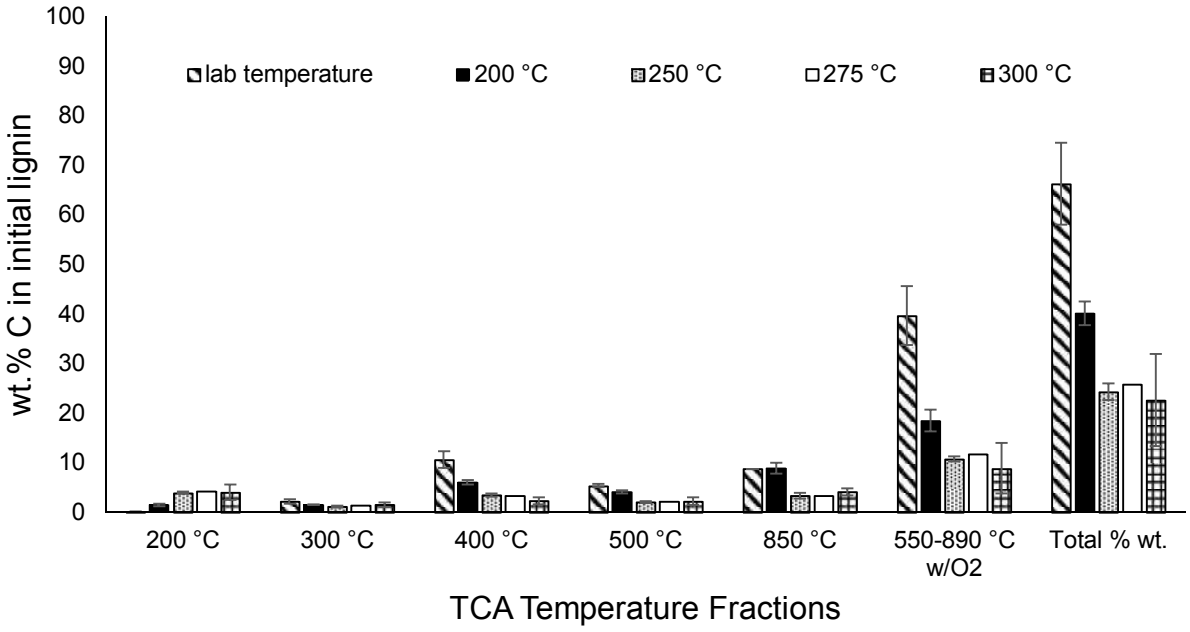

Figure 25: Effect of the reaction temperature on the TCA profile of unfiltered reaction mixtures from non-catalyzed reactions; 7 min drying and 2 min 40 s purging time was used, reaction conducted at 275 °C was performed in duplicate and the difference between the results was less than 5%.

The TCA results presented in **Fig. 25** show an increase of 200 °C fraction with temperature up to 250 °C, suggesting a higher production of low molecular weight products. The amount of pyrolyzed and coked carbon increases with decreased reaction temperature due to a less efficient bond cleavage. This observation is most apparent for the coked fraction for the reaction conducted at ambient temperature and 200 °C. At ambient temperature, the amount of the coked fraction reaches 39.6 ± 6.0 %wt. of C in the initial lignin. At 200 °C, the coked carbon amount decreases to 18.4 ± 2.2 %wt. of initial lignin, for 250, 275 and 300 °C the value oscillates at approximately 10% wt. The highest total %wt. yield of C in case of the experiment conducted at ambient temperature could be explained by a char formation from the unreacted lignin at higher

temperatures, since most of the char was not transferred to the solution and remained adsorbed on the walls of the reaction vessels.

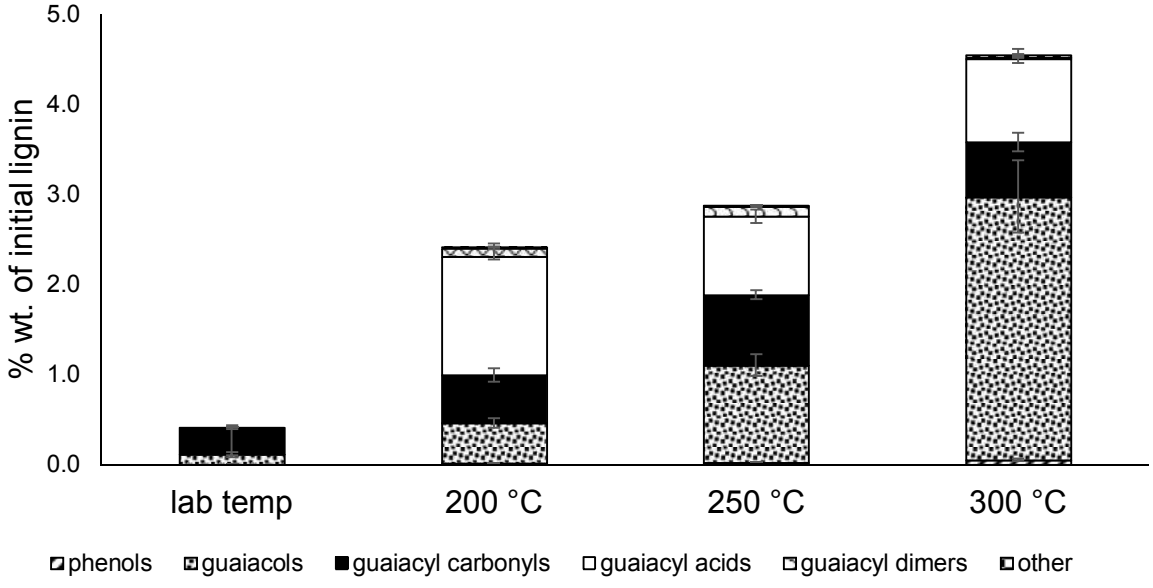

Figure 26: LLE GC-MS; Effect of reaction temperature on the product yield and distribution for non-catalyzed reactions

The LLE GC-MS results show a gradual increase of the total product yield with temperature. The effect of increased products' yield with increased temperature was previously described.[80, 111, 139] The final LLE GC-MS results presenting % wt. of initial lignin distribution for each group of degradation products are shown in **Fig. 26**. At ambient temperature, the only products detected were guaiacol, vanillin and homovanillyl alcohol, whereas no dimers were detected. The overall yield of products was 0.4 ± 0.1 % wt. of the initial lignin. The amount of products increased at higher reaction temperatures. At 200 and 250 °C, guaiacyl acids and guaiacyl carbonyls contributed the most to the final product recovery, especially homovanillic acid and vanillin. At 250 and 300 °C, guaiacols became the predominant product group, while the contribution of guaiacyl carbonyls and acids decreased. At 200 °C the guaiacyl carbonyls and acids contributed to

the final yield with 22.1 and 54.6%rel., respectively. At 300 °C their contribution decreases to 13.4 and 20.3%rel., respectively, while guaiacols contribute to the overall yield with 64.2%rel., especially due to high amounts of guaiacol (39.9%rel.) and ethylguaiacol (9.6%rel.).

The amount of monomers increased with temperature. The highest overall yield of products of non-catalyzed reactions was obtained for 300 °C reaction temperature and reached 4.6 ± 0.5 %wt. of the initial lignin, from which only 0.02 ± 0.01% wt. was accounted for by dimers, which were the most abundant at 275 °C. The amount of the quantified dimers is not large, since it is assumed that the monomeric units are connected by ether bonds, which are the weakest bonds occuring in the lignin structure. The temperature range of 200–300 °C should be sufficient to break both α and β-O-4 bonds with activation energies of 80–118 kJ/mol and 148–151 kJ/mol, respectively.[37] The observed decline of dimers at higher temperature might be explained by repolymerization processes. Grilc et al. claim that the bio-oil produced during the lignin degradation is thermally and chemically unstable and that the free radicals contained in the bio-oil might not be stabilized fast enough during fast heating rates, which results in increased char formation.[100]

3.3.1.4 LLE GC-MS analysis of underivatized vs. derivatized lignin extracts

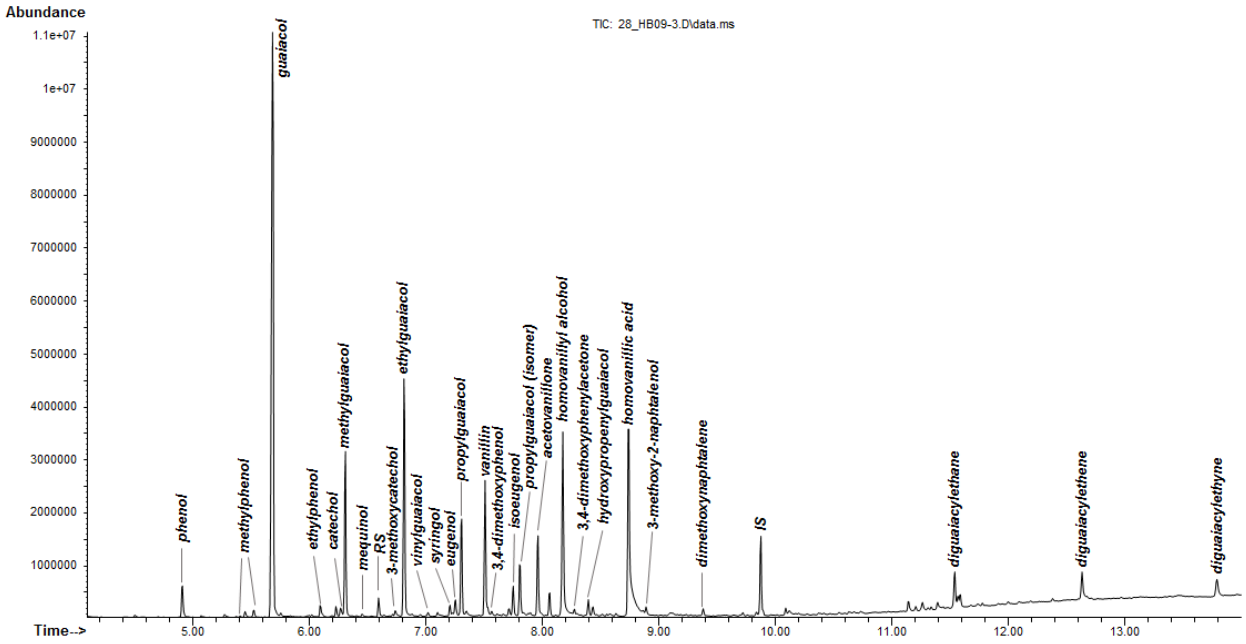

Figure 27: GC-MS chromatogram of underivatized DCM extract of lignin hydrotreated at 300 °C for 30 min without catalyst

The chromatogram of the underivatized DCM extract of lignin hydrotreated at 300 °C with labeled analytes is shown in **Fig. 27**. An important pattern of Fig**. 27** are several peaks observable after the IS peak, which are assumed to be phenolic dimers, however most of them were not identified. Five dimer structures and their molecular weights were predicted and calculated, respectively, before the experiments were conducted, i.e., molecular ions *m/z* 272, 274, 302, 316 and 314, of which the dimers of *m/z* 272 and 274 (bicreosol and TD-14) were synthetized and used as calibration standards for the dimers' quantification. Nevertheless, even the retention times and mass spectra of the quantified dimers did not match those of our synthetized standards. The main pattern missing in the mass spectra of the standards was *m/z* 137, which is one of the most abundant fragments observed among the lignin degradation products (see **Appendices XXV–XXVIII**). In order to determine the exact isomers' structure, new standards have to be synthetized and their GC

retention times and mass spectra should be matched to the products observed in the reaction mixtures.

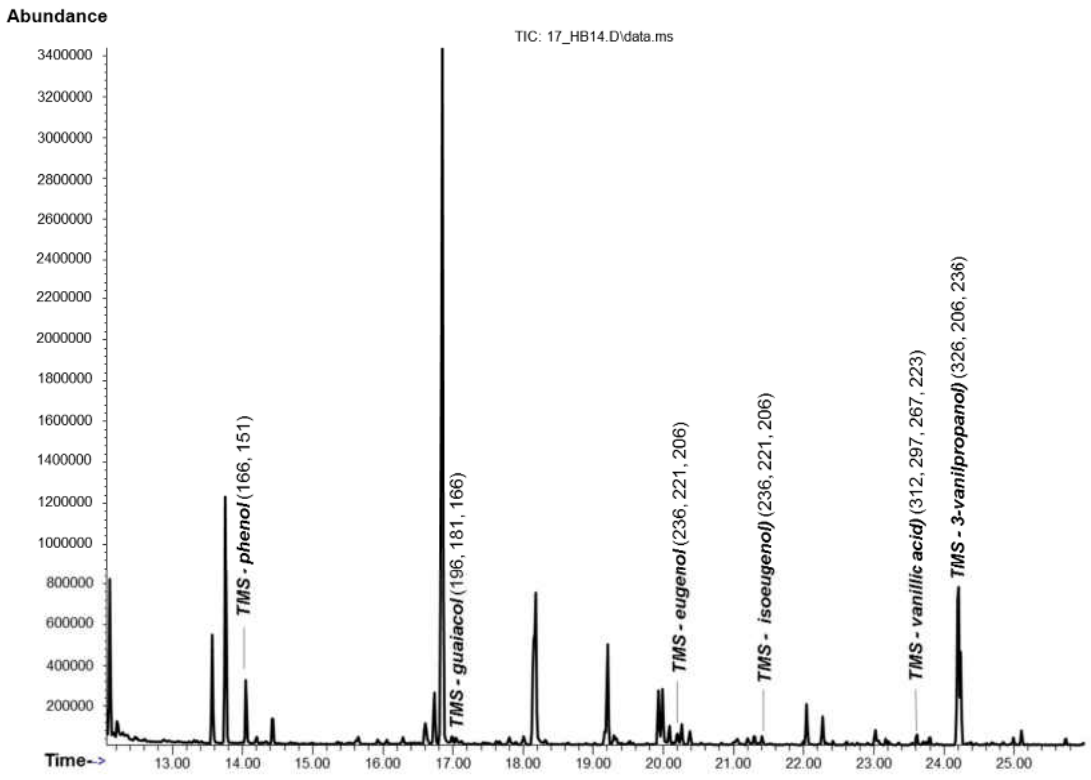

Figure 28: GC-MS chromatogram of BSTFA derivatized DCM extract of lignin hydrotreated at 300 °C for 30s without catalyst

Since the only hydroxy derivatives of degradation products observed in the DCM extracts by GC-MS were hydroxypropenylguaiacol and homovanillic acid, a derivatization by BSTFA of the sample treated at 300 °C was performed in order to detect other potential polar products. The derivatized forms of six products were identified: phenol, guaiacol, eugenol, isoeugenol, vanillic acid and 3-vinylpropanol. The GC-MS chromatogram of the DCM extract of lignin hydrotreatment products from the reaction conducted at 300 °C for 30 min without the catalyst derivatized by BSTFA is shown in **Fig. 28**.

3-vinylpropanol was not observed in the DCM extracts, unless derivatized. Vanillic acid was observed in the calibration mixtures, however its LOD was the highest from all the standards. In the last analysis performed, the vanillic acid LOD was 5.3 ppm and LOQ 17.7 ppm, respectively. In the samples, vanillic acid without the BSTFA derivatization was not observed at all. The second standard that has never been observed in the samples was syringaldehyde. Homovanillic acid was observed in the samples and even became one of the most abundant compounds, however its analysis sensitivity was second lowest with LOD of 4.3 ppm and LOQ of 14.2 ppm. The weak ionization efficiencies of carboxylic acids with derivatization in GC-MS were explained elsewhere.[148-149] The only other two compounds with increased LOQ compared to the others were homovanillyl alcohol and syringaldehyde, i.e., 8.1 and 8.6 ppm, respectively. The other standards exhibited LOQ <5ppm. The highest LOD obtained for phenols, guaiacols, syringols and guaiacyl carbonyls was obtained for acetovanillone, which was 1.4 ppm. Most of the alkylphenols and alkylguaiacols showed LOD <1ppm. Satisfactory values of extraction recoveries of 4-chloroacetophenone (RS) of 80–120% were obtained.

3.3.1.5 Comparison of LLE GC-MS vs. TCA results

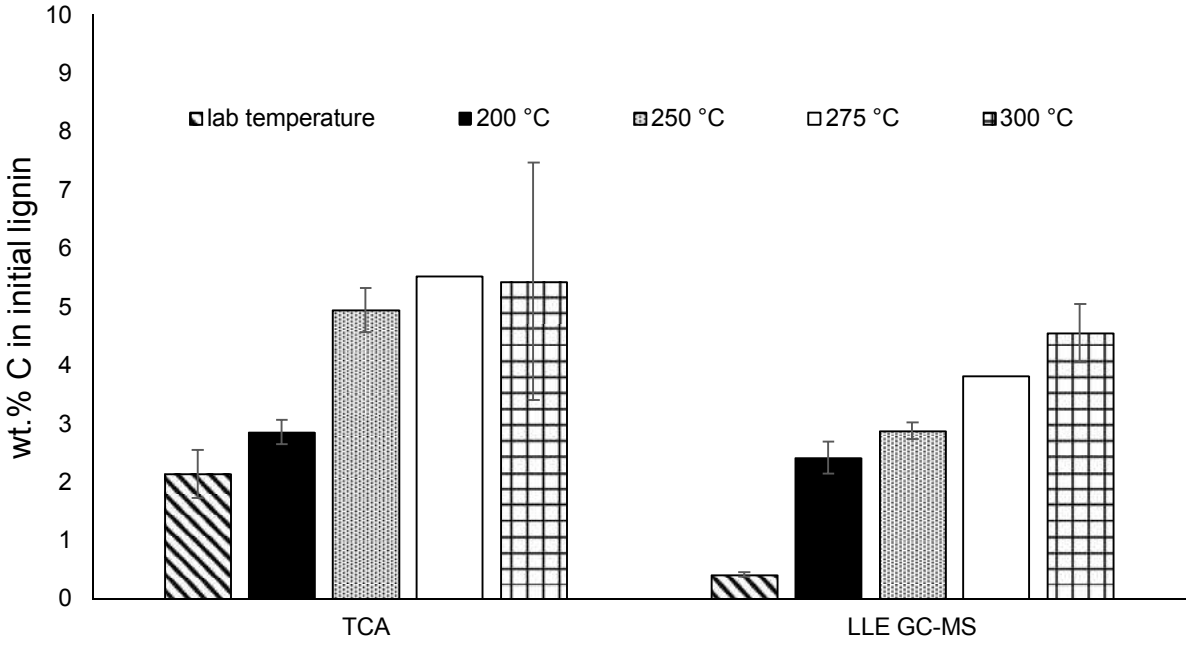

Figure 29: Comparison of TCA of the thermal desorption fraction (200 and 300 °C) vs. LLE GC-MS total %wt. yield of products for non-catalyzed reactions (for LLE GC-MS the data are presented in %wt. of initial feedstock); unfiltered aqueous samples were used for the TCA analysis and 7 min drying and min 40 s purging time were applied

The TCA %wt. of C in the initial lignin in TD fraction (200 and 300 °C), obtained using the old protocol with 7 min drying time and 2 min 402 s purging time, are in a good agreement with LLE GC-MS total yield of products including the increase of product yield with increased temperature (**Fig. 29**). The TCA %wt. of C initial lignin are slightly higher due to the complicated identification and lack of standards for some GC-elutable products, especially dimers (see section 4.3.1.5), therefore the proper quantification was not manageable. Another factor was that not all the compounds evolving in TCA at 200 and 300 °C are GC-elutable.

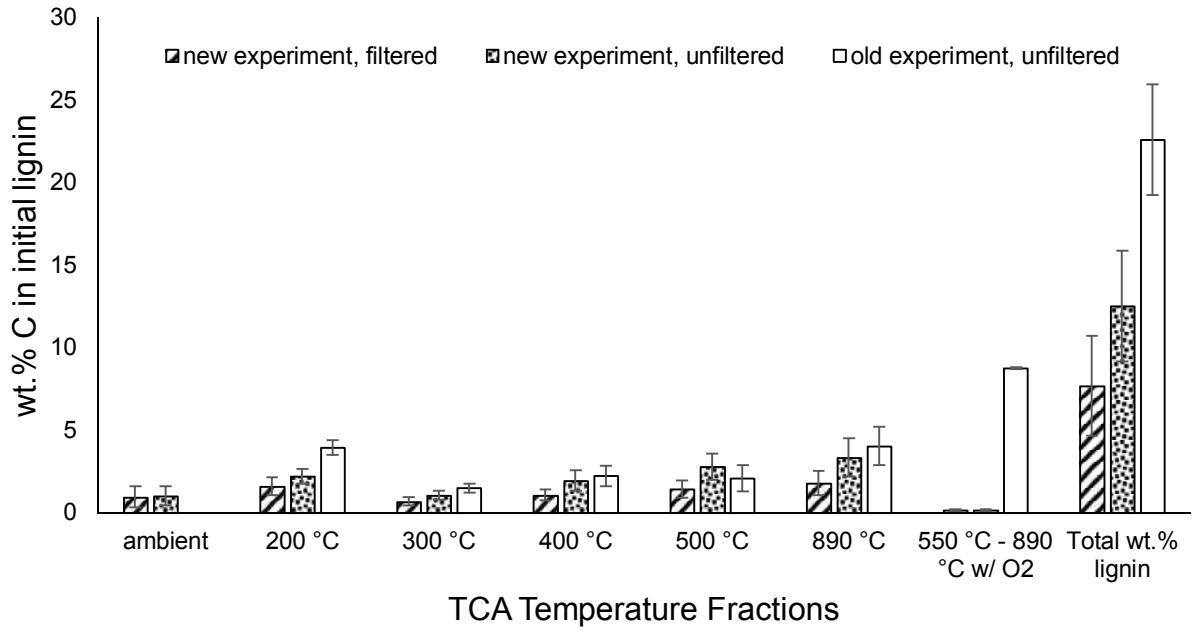

Figure 30: TCA profiles of lignin hydrotreated at 300 °C w/o catalyst for 30 min. Old analysis protocol included 7 min drying time and 2 min 40 s purging time. New protocol uses 4 s total purging time without a prior drying step.

The TCA data of lignin hydrotreated at 300 °C w/o catalyst obtained by using the old protocol with 7 min drying and 2 min 40 s purging time was compared to the TCA results of a fresh set of hydrotreated lignin samples analyzed by the upgraded method using 0 min drying time and 4 s purging time. Previously, the aqueous extracts were analyzed without a prior filtration. The TCA data obtained by the newly developed method were acquired using both unfiltered and filtered samples. The comparison of the TCA profiles is shown in **Fig. 30**. The amount of C evolved from the unfiltered sample at each temperature fraction is similar for both protocols, except the highest pyrolytic step, which may be explained by higher amount of char in the liquid fraction recovered from the reaction vessel.

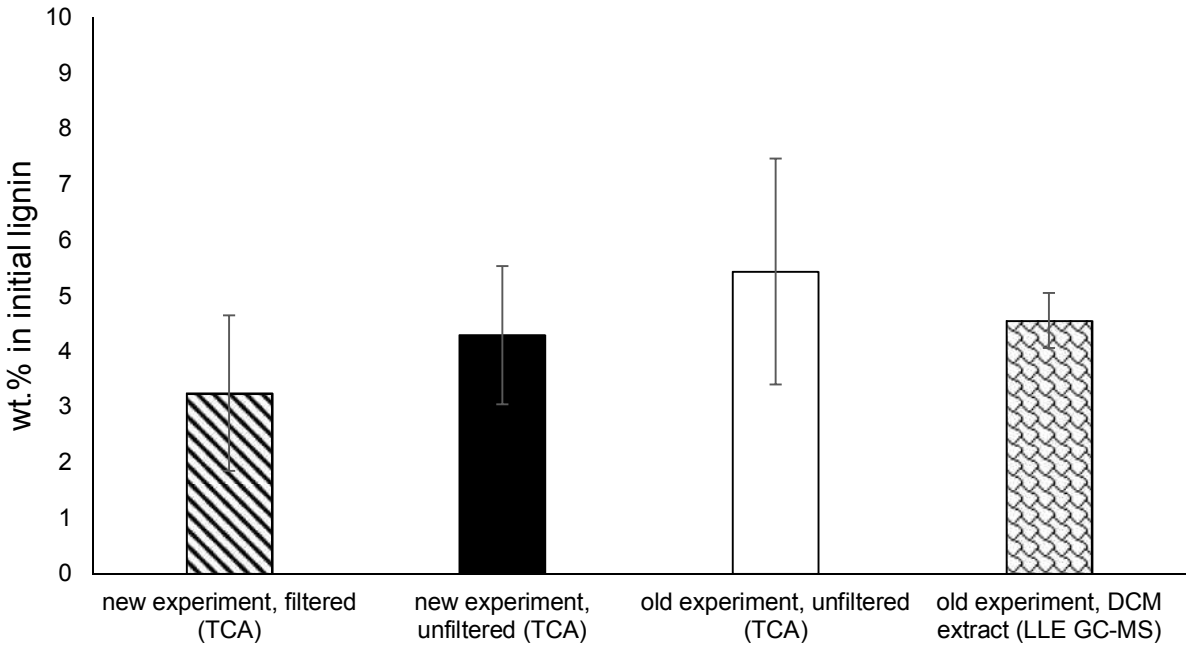

Figure 31: Comparison of TD fraction of TCA vs. LLE GC-MS total %wt. yield of products for lignin hydrotreated at 300 °C w/o catalyst for 30 min (TCA data are shown in %wt. of C in initial feedstock). Old analysis protocol included 7 min drying time and 2 min 40 s purging time. New protocol uses 4 s total purging time without a prior drying step.

Surprisingly, when the combined ambient and TD fraction from the new experiment were compared to the TD fraction of TCA and GC-MS results from the previously performed experiments, no statistical difference was observed (**Fig. 31**). This observation suggested that a lower amount of volatile species was lost using the old TCA protocol than expected. A possible reason may be analytes' interactions causing them to be less prompt to be vaporized. However this was not observed in section 4.1.2, where mixtures of lignin model compounds were tested at different drying times. Another explanation of such a behavior may be potential filter surface interactions with the analytes, which was observed for bicreosol (**Fig. 14).**

3.3.1.6 Mass balance closure

The mass balance was evaluated combining the results from the TCA analysis and gravimetric data of the unreacted lignin. A satisfactory mass balance closure in a range of 80–100 %wt. of initial lignin was obtained for the non-catalyzed reactions. The results are presented in **Fig. 32**, confirming that most of the lignin either remained unreacted, converted into char or its structure was modified into highly crosslinked polymers, which are not soluble in water. The most abundant TCA fractions were the highest pyrolytic (850 °C) and coked fraction, suggesting that the soluble products consist mainly of oligomers, water soluble cross-linked polymers and inorganic carbon.

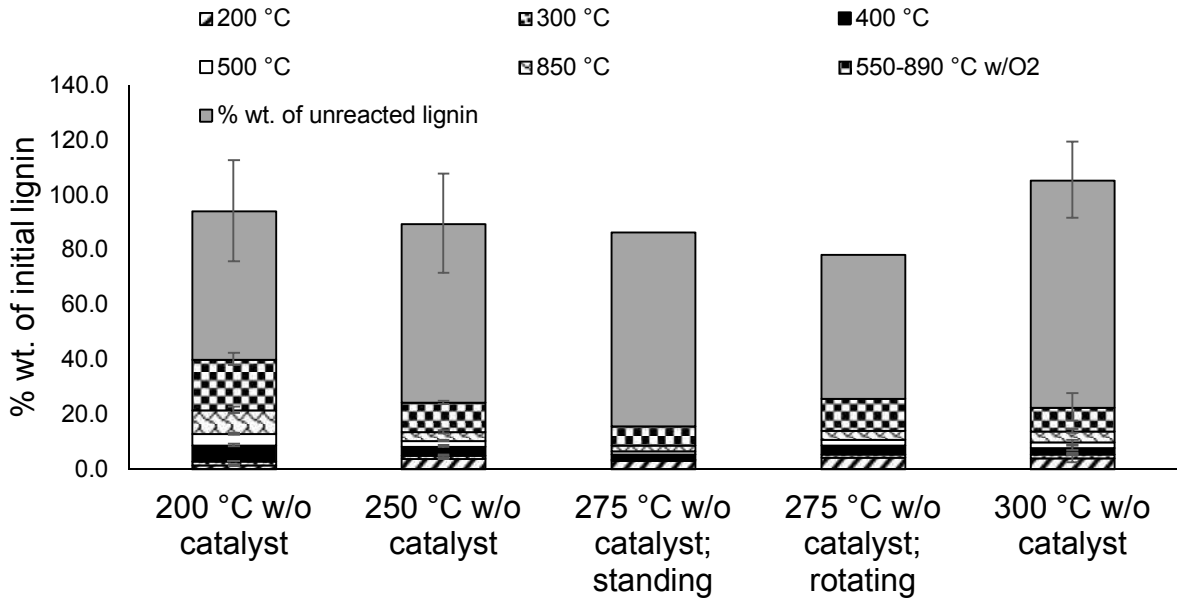

Figure 32: Mass balance closure for non-catalyzed lignin hydrotreatment reactions (TCA + gravimetry). The TCA analysis was conducted using unfiltered aqueous extracts dried at 40 °C for 7 min with 20 min 40 s purging time. The reactions conducted at 275 °C were performed in duplicate with an error of less than 10%.

3.3.2 Catalyzed systems

3.3.2.1 Nickel catalyzed systems

3.3.2.1.1 TCA vs. LLE GC-MS results comparison for experiments conducted in water

.

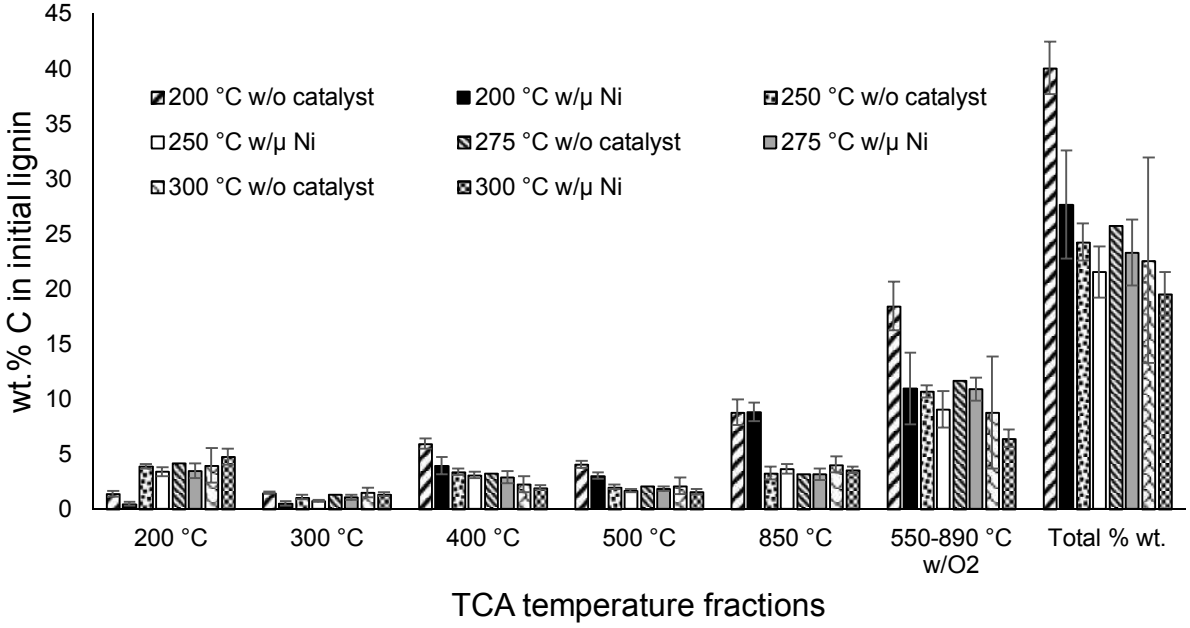

Figure 33: TCA profiles of unfiltered hydrotreated lignin samples; 7 min drying and 2 min 40 s purging time was used.

The TCA results of lignin hydrotreated samples with μNi demonstrate a similar trend as observed in section 4.3.1.3, which is an increase of the simple volatiles amount (TD fraction) with temperature (**Fig. 33)**. However, compared to the experiments conducted w/o catalyst, the catalyst presence did not provide a carbon increase in neither TD, pyrolytic or coked fraction, except for the experiments conducted at 200 °C.

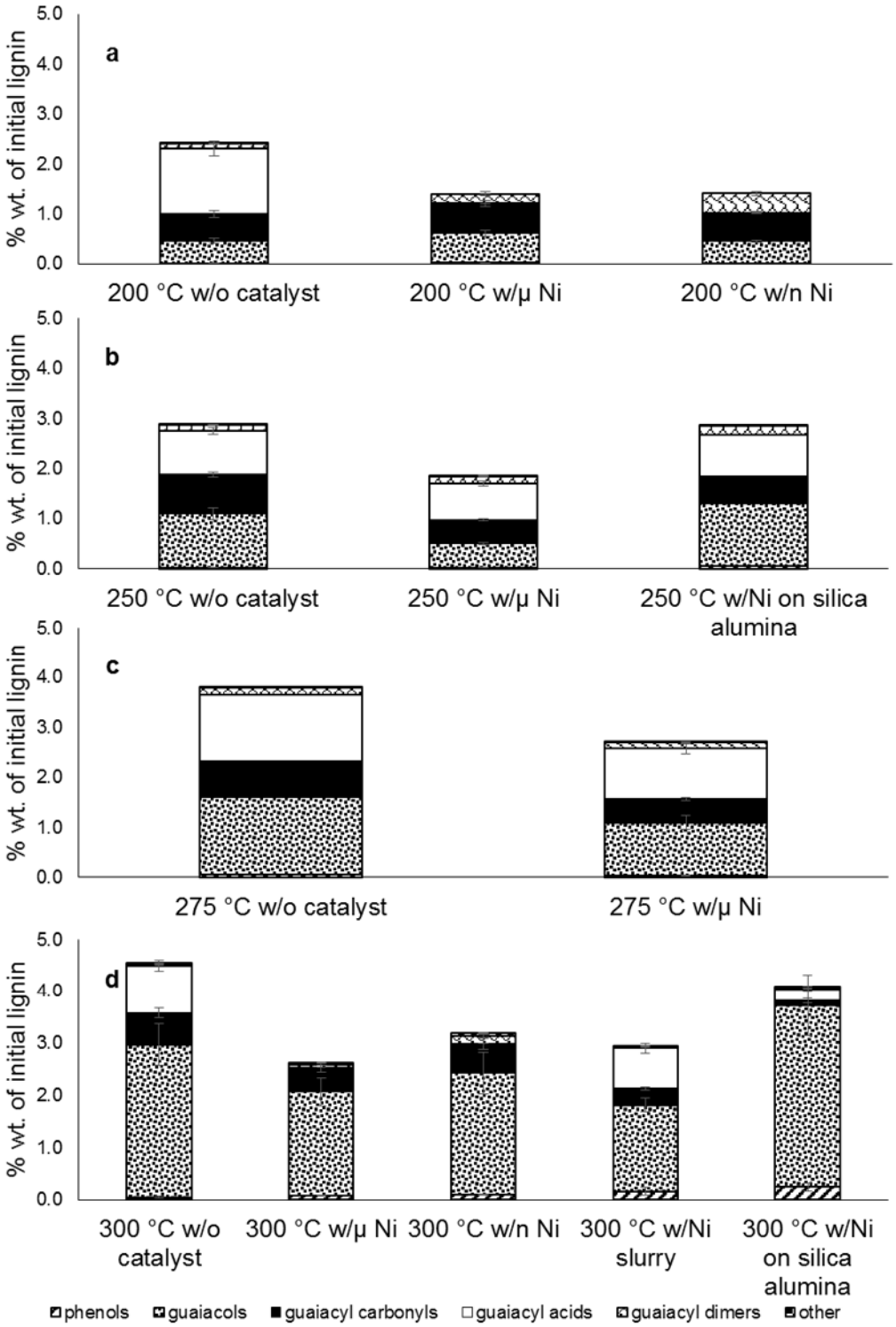

Figure 34: LLE GC-MS; comparison of non-catalyzed experiments with experiments catalyzed using Ni based catalysts at different reaction temperatures: a) 200 °C, b) 250 °C, c) 275 °C, d) 300 °C

At 200 °C, the LLE GC-MS analysis of the extract from a reaction conducted without a catalyst (2.4 ± 0.3 % wt.) showed higher overall yield of products than for the μm and nm Ni catalyzed reactions (**Fig. 34-a**). This is a similar observation as for the TCA where approximately three times higher %wt. of C in TD fractions was obtained for the non-catalyzed reaction (**Fig. 33**). The reaction yield for μm and nm Ni catalyzed reactions was similar (both 1.4 ± 0.1 %wt.). The lower values for catalyzed reactions are mainly caused by the absence of guaiacyl acids. The difference between the %wt. yield of other product groups was negligible.

Similar to non-catalyzed reactions, neither μNi nor nNi catalyzed reaction conducted at 200 °C the residual lignin portion in the aqueous extract increased the product yield. Moreover, the DCM extract prepared from the combined aqueous extract with unreacted lignin from the nm catalyzed reaction at 300 °C possessed almost a three times lower yield of products than the extract prepared from the experiment conducted without catalyst.

Even at 250 °C, the catalyst addition did not help to increase the product yield significantly compared to the non-catalyzed experiment (**Fig. 34-b**). The overall yields of degradation products for the non-catalyzed reaction and the experiment conducted with Si/Al were similar (~3.0%wt.). However, the yield of products in the experiment with μNi was lower by approximately 1%wt. The amount of guaiacols and guaiacyl carbonyls decreased by 0.5%wt. and 0.3%wt., respectively, compared to the experiment conducted without a catalyst. The recovery of phenols, guaiacyl acids, guaiacyl dimers and others were consistent throughout all three experiments and did not exceed 0.2%wt.

The results from the experiments conducted at 275 °C with and without μNi resemble those obtained at 250 °C (**Fig. 34-c**). The total yield of products in the reaction with μNi is lower by approximately 1%wt. Compared to the non-catalyzed reaction, the amount of guaiacols, guaiacyl

carbonyls and guaiacyl acids decreased by roughly 0.5, 0.3 and 0.2%wt., respectively. The reason for this observation might be that such temperatures are not sufficient to activate the catalyst. In addition, the micropores in the catalyst particles might entrap the products, which are small enough to fit in the pores, by the adsorption on the pore surface.

Similar to the experiments conducted at lower temperatures, the highest product yield at 300 °C was obtained for the non-catalyzed reaction (4.5 ± 0.5%wt.). Comparable yields were consequently gained only for the experiment conducted with Ni on Si/Al. For the other catalyzed systems, the overall yield ranged from 2.6 to 3.2%wt. of the initial feedstock. In **Fig. 34-d** it is apparent that the lower yields recovered in case of μNi, nNi and Ni slurry are mainly caused by lower production of guaiacols and guaiacyl acids, which were not observed for μNi and nNi catalyzed experiments at all. Phenols, guaiacyl dimers and other products exhibited similar yields throughout all the experiments and their yield did not exceed 0.2%wt. Comparison of thermal desorption fraction results obtained by the old TCA protocol with LLE GC-MS in **Fig. 35** shows statistically insignificant differences for the experiments conducted with nNi, Ni slurry and Ni on Si/Al. Interestingly, the TCA total carbon yield for μNi catalyzed experiment is significantly higher (approximately twice) than that obtained by LLE GC-MS, suggesting a production of monomers or dimers, which were not included in the GC-MS quantification method due to their complicated identification.

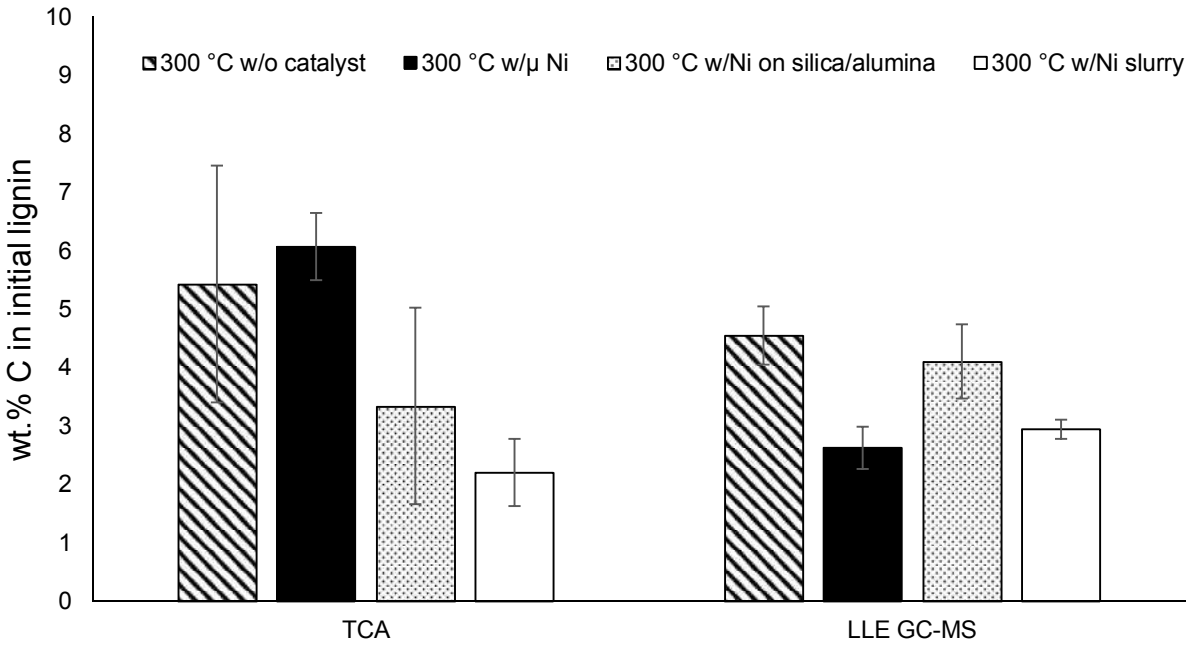

Figure 35: Comparison of TCA thermal desorption fraction vs. LLE GC-MS total %wt. yield of products comparison for reactions conducted at 300 °C catalyzed by Ni based catalysts. The TCA results were obtained using 2 min 40 s purging time.

In case of the lignin hydrotreated at 300 °C in presence of Ni on Si/Al catalyst, a good agreement of the TCA data of combined ambient and TD fraction obtained both with old and new protocol and LLE GC-MS was acquired (**Fig. 36**). Moreover, the similarity between the data from the non-catalyzed and μNi catalyzed reaction at 300 °C proves that the Ni on Si/Al addition does not significantly increase the total yield of low molecular degradation products.

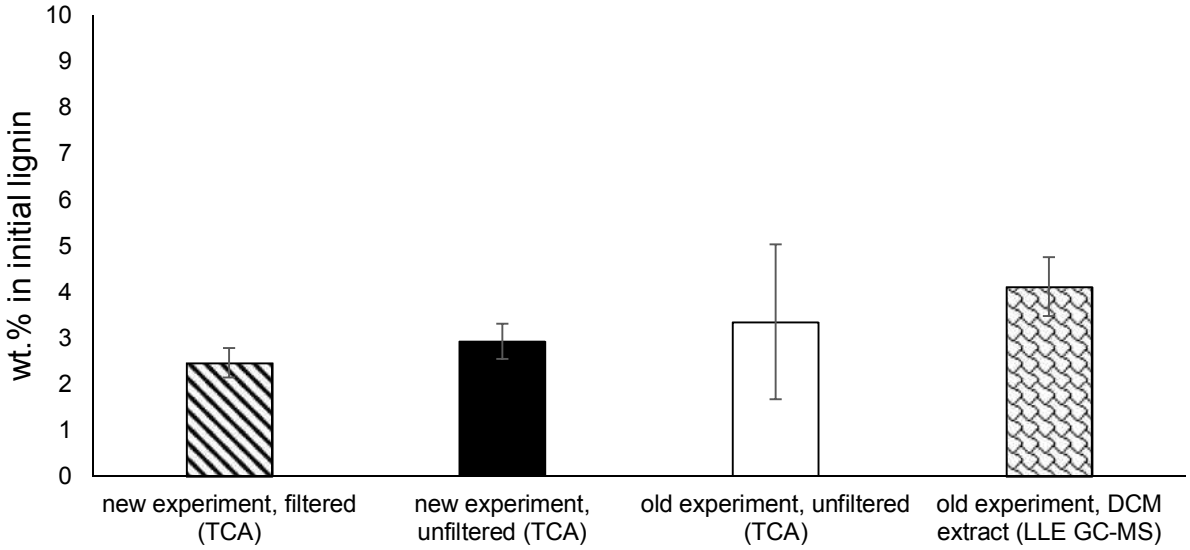

Figure 36: Comparison of TD fraction of TCA with LLE GC-MS data for lignin hydrotreated at 300 °C w/o catalyst for 30 min. Old experiment was analyzed by TCA using 7 min drying time and 2 min 40 s purging time. New experiment was analyzed by TCA without prior drying and using 4 s total purging time. The TCA results are presented in %wt. of C in initial lignin.

3.3.2.1.2 Lignin degradation at 275 °C in MeOH/water (5:2 v/v) w/ Ni slurry

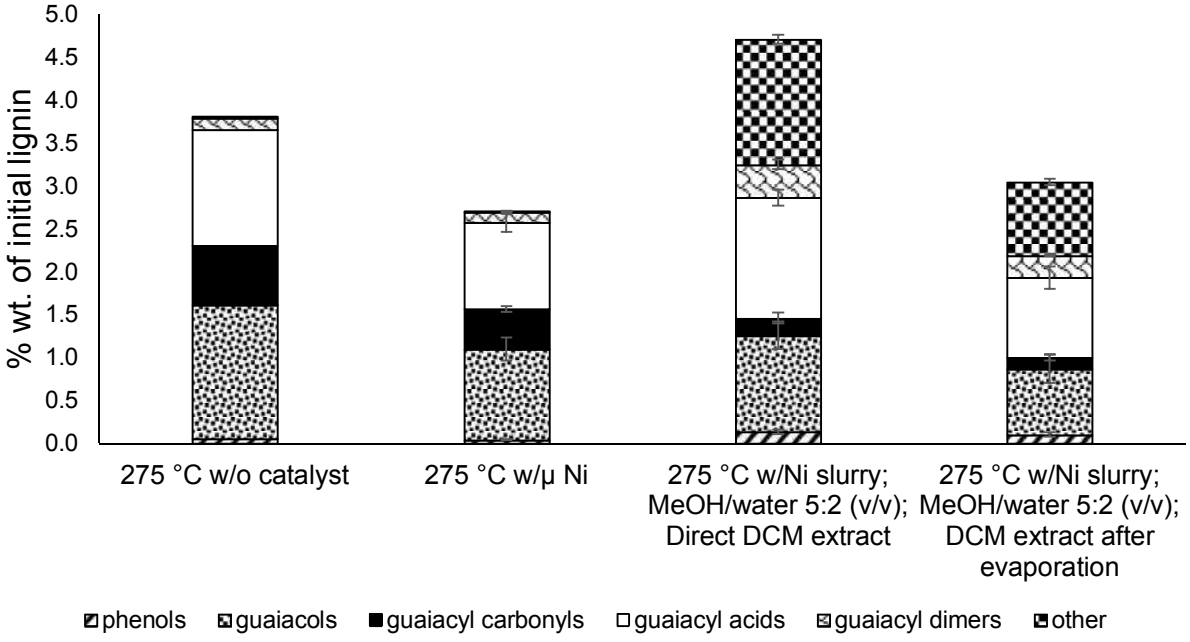

Figure 37: Comparison of LLE GC-MS %wt. yield of lignin degradation products for reactions performed at 275 °C

Since the experiments conducted in water did not yield promising results regarding a high production of monomeric and dimeric products, a different solvent system was evaluated. The work was inspired by Jiang et al.[98] The alkali lignin was treated in MeOH/water (5:2 v/v) mixture in presence of Ni slurry. The MeOH and EtOAc recovered after the vacuum evaporation were analyzed by GC-MS and the results showed a negligible amount of products (<0.1%wt.) consisting of trace levels of guaiacol, methylguaiacol, ethylguaiacol and propylguaiacol and the rest of the products was present in water/bio-oil fraction.

The GC-MS results of both non-catalyzed and catalyzed reactions performed at 275 °C are shown in **Fig. 37**. Apparently, the direct DCM extract from the reaction at 275 °C with MeOH/water 5:2 (v/v) with the addition of Ni slurry provides better results than the experiment conducted in water at the same temperature without a catalyst (3.8%wt. vs. 4.7 ± 0.3%wt.). The difference is made mainly by an increased amount of "others", especially homovanillyl alcohol. At 275 °C without a catalyst, the "others" amount was negligible (<0.1%wt.), whereas in the experiment with MeOH/water 5:2 (v/v) and Ni slurry the amount of homovanillyl alcohol was 1.4 ± 0.1%wt. For the DCM extract prepared from the bio-oil, the total yield decreased by approximately 1.7%wt., which may be related to a more sophisticated sample preparation.

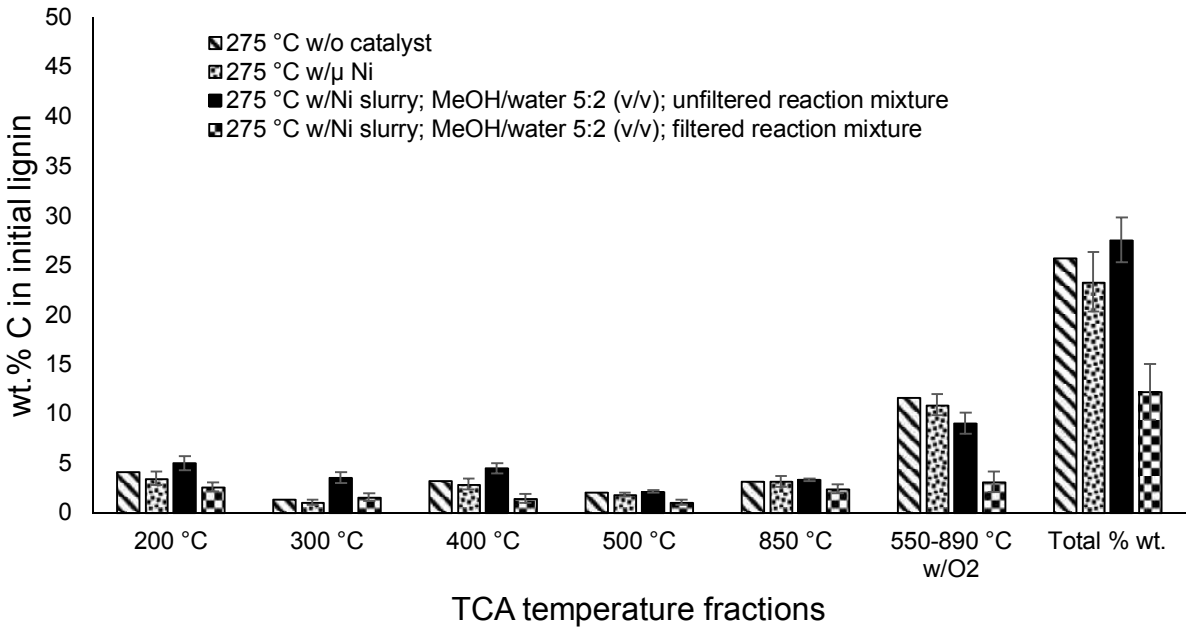

Figure 38: TCA %wt. of carbon in initial lignin for reaction catalyzed by Raney Ni at 275 °C

Fig. 38 shows a comparison of TCA obtained for an unfiltered reaction mixture and filtered mixture. Compared to LLE GC-MS results, the fresh unfiltered mixture shows a lower yield of products in TCA. Since the old TCA protocol was used for the analysis, the decrease is probably caused by longer drying and purging step. In **Fig. 38,** there is also a significant decrease of total carbon content for both filtered mixtures. Since the filtration separates higher molecular weight oligomers and polymers from the sample, a decreased carbon content can be observed for both the highest temperature pyrolytic fraction (850 °C) and coked fraction.

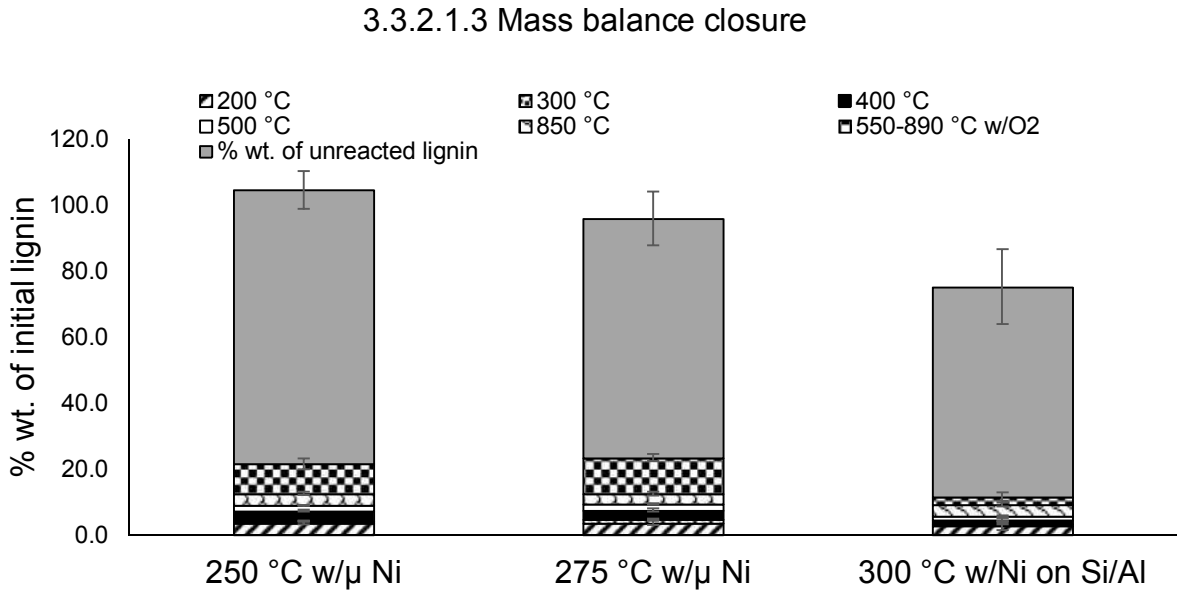

Figure 39: Mass balance closure for Ni catalyzed experiments; the data are a combination of the TCA data of unfiltered mixtures analyzed using old TCA protocol and gravimetric data

A satisfactory mass balance closure was obtained for the experiments catalyzed by μNi. **Fig. 39** summarizes the mass balance closure for the Ni catalyzed experiments. The incomplete mass balance for the Ni on Si/Al experiment is most probably affected by the volatiles' loss during the drying and purging step before the TCA analysis, since the amount of volatile was proven to increase with temperature and longer drying and purging time causes their lower yield.

3.3.2.2 Transition metal oxides doped activated carbon and zeolite catalyzed experiments

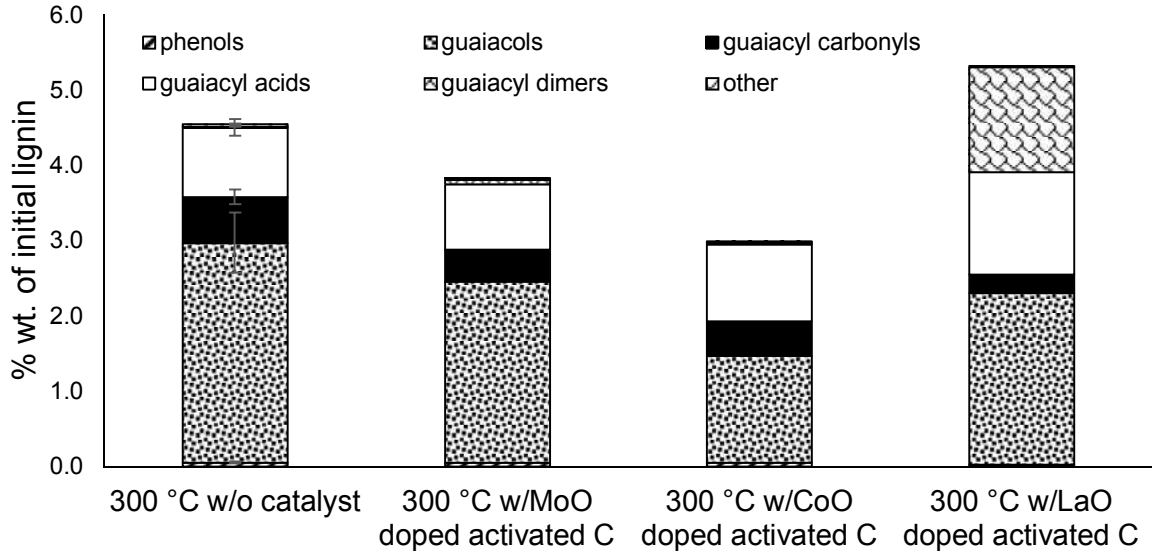

Figure 40: Comparison of GC-MS %wt. of lignin degradation products yield for transition metal oxides doped activated carbon catalyzed reactions performed at 300 °C (reactions with activated carbon performed in duplicate, the obtained error was lower than 10%)

MoO and CoO doped activated carbon catalyzed reactions provided a lower total product yield than the experiment without a catalyst (3.8%wt. and 3.0%wt. vs. 4.6 ± 0.5%wt.). The difference is mainly caused by the decreased amount of guaiacols, which is a similar trend as observed for Ni catalyzed reactions in Section 4.3.2.1. LaO catalysis increased the overall product recovery to 5.3%wt. Dimers contributed the most to this increase, particularly diguaiacylethene with an average recovery of 1.4%wt (see **Fig. 40**). Both in Ni and activated carbon catalyzed systems, the amount of dimers was marginal (<0.1%wt.). **Fig. 41** shows that the same trend of the product yield depending on the transition metal oxide type was obtained using both LLE GC-MS and TCA (LaO highest yield > MoO > CoO).

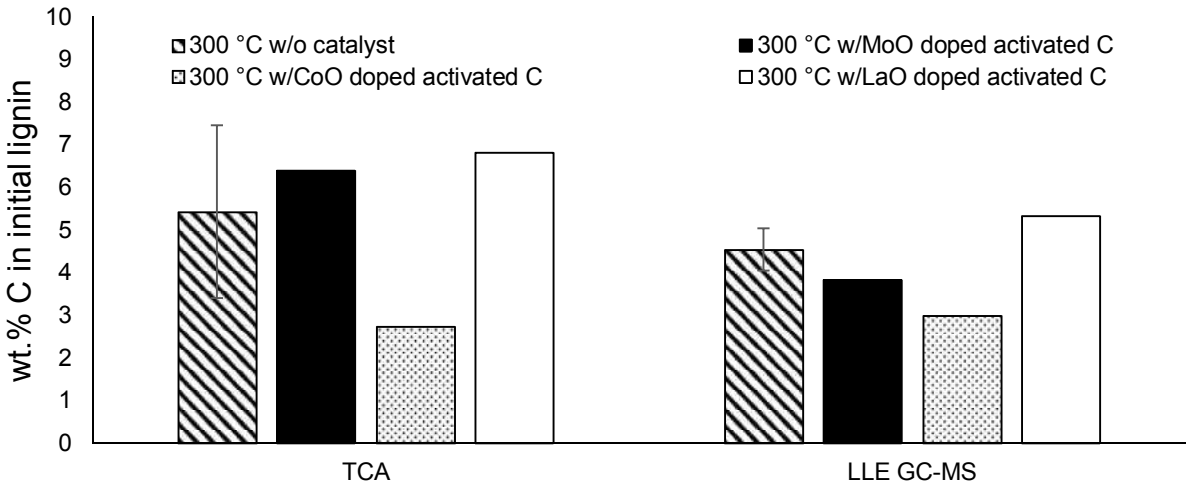

Figure 41: TCA thermal desorption fraction vs. LLE GC-MS total %wt. yield of products comparison for transition metal oxides doped activated carbon catalyzed reactions conducted at 300 °C (the data for LLE GC-MS are presented in %wt. of initial feedstock). The experiments with activated carbon catalysts were performed in duplicate and the error was lower than 10%.

Interestingly, the mass balance closure for the transition metal oxides catalyzed reactions ended up being significantly over 100% (see **Fig. 42**). Apparently, the greatest contributor was unreacted lignin measured by gravimetry. The most probable reason is that a small portion of the reaction solvent (water) remained adsorbed on the activated carbon particles and thus increased the weight of the unreacted residue.[150-152]

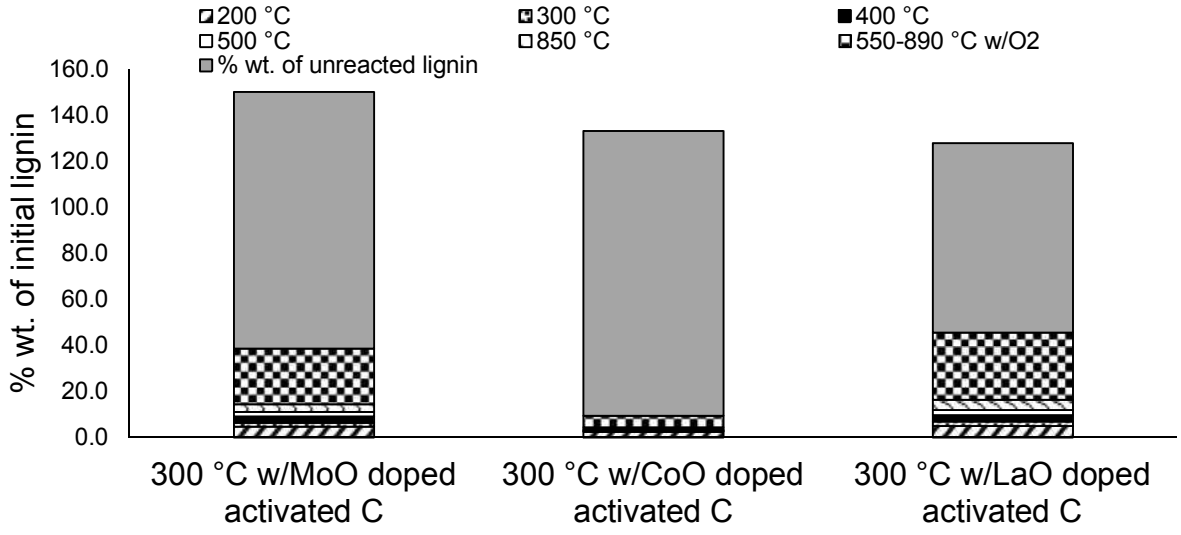

Figure 42: Mass balance closure for transition metal oxides doped activated carbon catalyzed lignin hydrotreatment reactions (TCA + gravimetry). The experiments were conducted in duplicate and the error was lower than 10%.

The LLE GC-MS results of zeolites catalyzed experiments resemble those of activated carbon catalyzed systems (see **Fig. 43**). The best results were obtained with the LaO doped zeolite (6.3%wt.), followed by MoO (3.8%wt.) and CoO (3.5%wt.). Moreover, similar as for the activated carbon catalyzed systems, the LaO doped zeolite promotes the formation of dimers, particularly diguaiacylethene (1.3%wt.). The TCA results of the TD fraction confirm a similar trend to the GC-MS results (**Fig. 44**), however the MoO and LaO zeolites showed higher yields on TCA than on GC-MS. Due to the increased dimers' content in case of LaO doped zeolite catalyzed reaction, it is possible that MoO and CoO also supported the dimers' production to some extent. As explained in chapter 4.3.1.4, the analytes eluting in GC after the IS are supposed to be dimers, however for most of them the identity was not confirmed. The difference between the TCA and the GC-MS might be attributed to such dimers, which were not quantified by GC-MS, but the TCA analysis accounted for them.

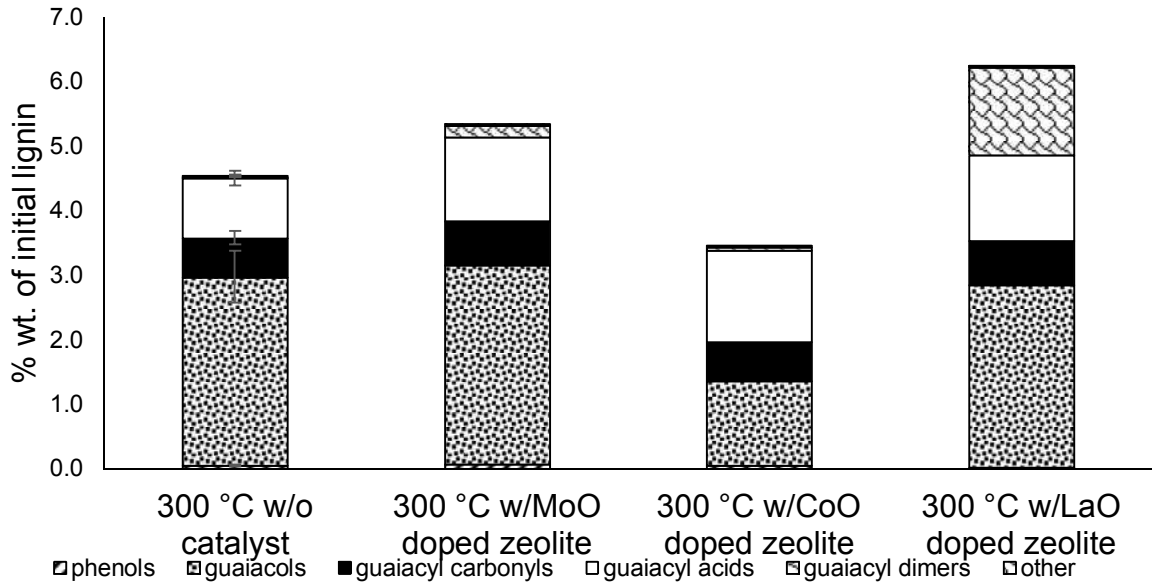

Figure 43: Comparison of LLE GC-MS %wt. of lignin degradation products yield for transition metal oxides doped zeolites catalyzed reactions performed at 300 °C (reactions with activated carbon performed in duplicate and the error was lower than 10%).

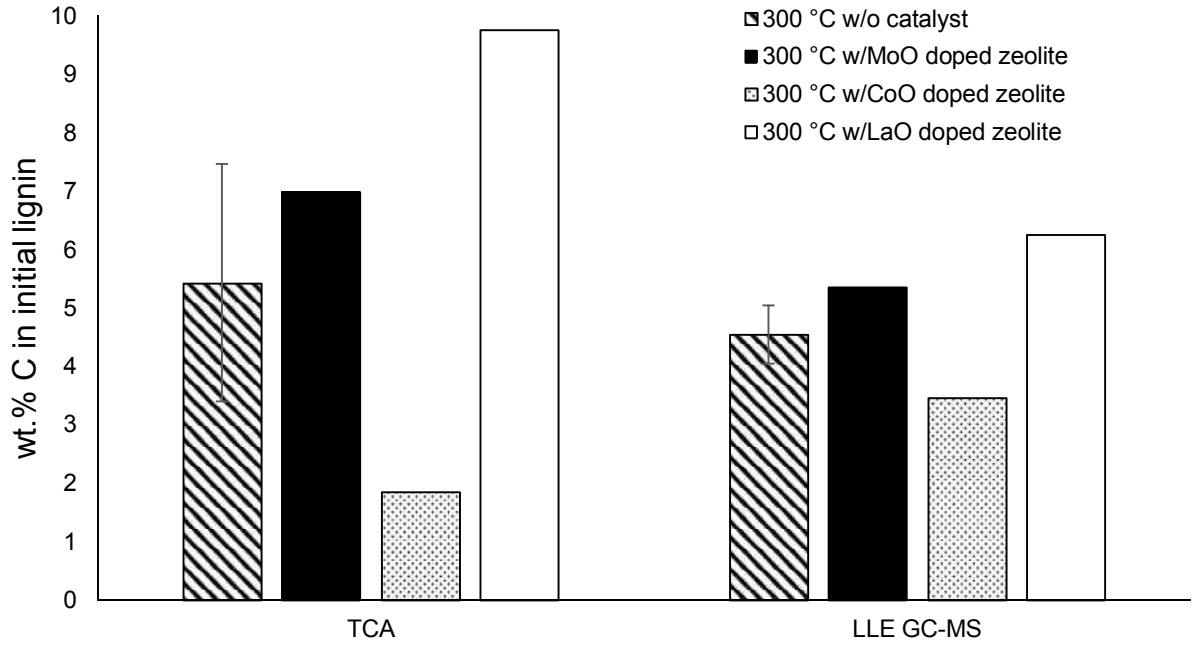

Figure 44: TCA thermal desorption fraction vs. LLE GC-MS total % wt. yield of products comparison for transition metal oxides doped zeolites catalyzed reactions conducted at 300 °C (the data for LLE GC-MS are presented in %wt. of initial feedstock). The experiments catalyzed with zeolites were conducted in duplicate and the error was lower than 5%.

3.3.2.3 Transition metal doped silica/alumina catalyzed experiments

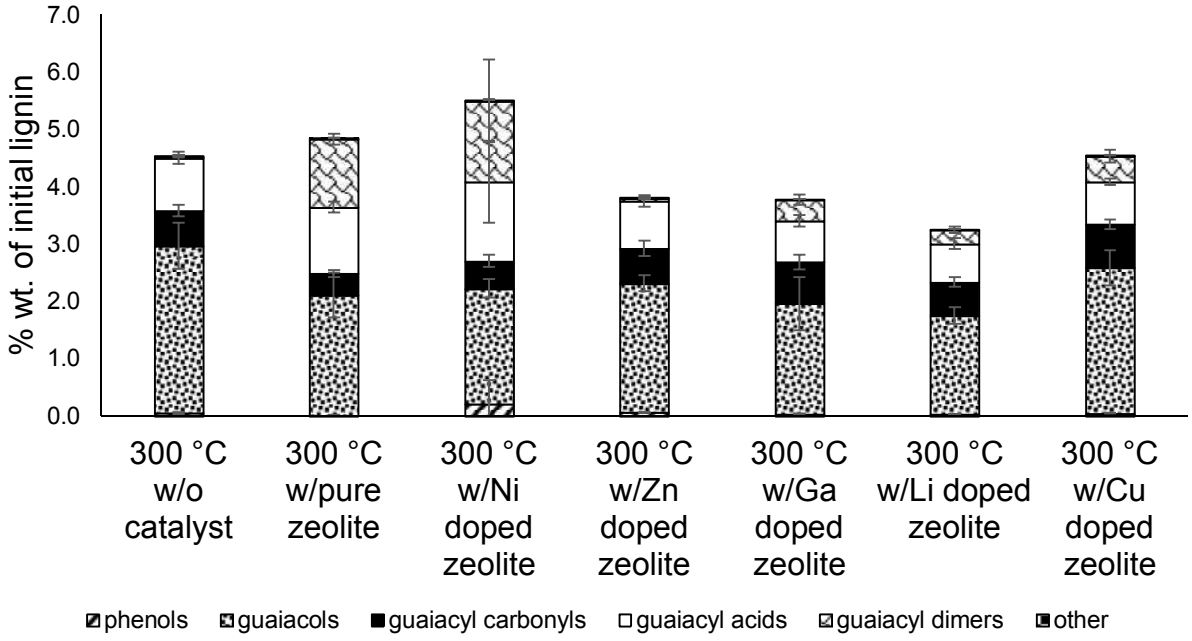

Figure 45: Comparison of LLE GC-MS %wt. of lignin degradation products yield for transition metals doped zeolites catalyzed reactions performed at 300 °C

Based on **Fig. 45**, the experiment conducted with pure Si/Al provides a similar product recovery as the non-catalyzed reaction (4.9 ± 0.6%wt. vs. 4.6 ± 0.5%wt.). In the pure zeolite catalyzed reaction, a lower amount of guaiacols was obtained (2.1 ± 0.4%wt. vs 2.9 ± 0.4%wt.), however the amount of guaiacyl acids increased by 0.3%wt. and the dimers yield was 1.2 ± 0.1%wt., while in non-catalyzed reaction the dimers production was negligible (<0.1%wt.).

Regarding the transition metal doping, the Ni doping contributed the most to the maximal production of monomers and dimers (5.5 ± 1.9%wt.), however compared to the pure Si/Al catalyzed reaction the product yield increase was not statistically significant. From all the doped Si/Al, the Ni doping promoted the most pronounced formation of guaiacyl acids (1.4 ± 0.7%wt.) and guaiacyl dimers (1.4 ± 0.7%wt.). Thus, it can be claimed that the doping does not lead to radical changes in LLE GC-MS profiles, which was also confirmed by TCA measurements, where

significant yield improvements were obtained for neither of the temperature fractions, compared to the experiment without a catalyst (see **Fig. 46**). The yields of phenols, guaiacols, guaiacyl carbonyls and others are relatively consistent throughout all the zeolite catalyzed experiments (0.1–0.2%wt., 1.7–2.5%wt., 0.4–0.8%wt. and <0.1%wt., respectively). The yields of the guaiacyl acids and dimers fluctuate more and vary in a range of 0.7–1.4%wt. and 0.1–1.4%wt.

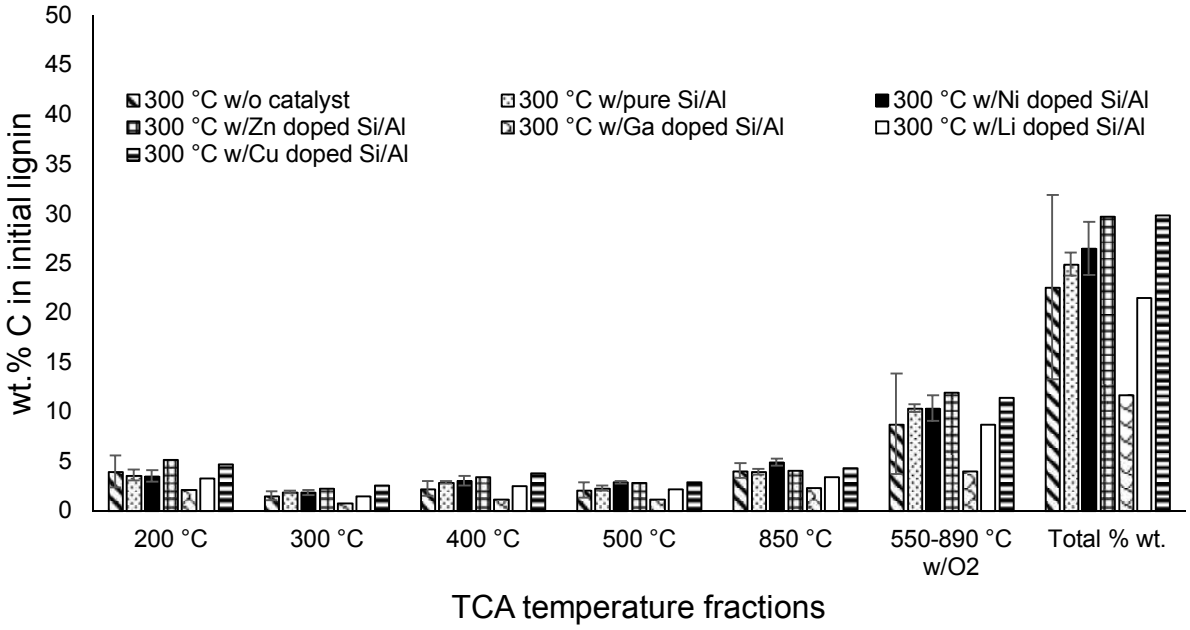

Figure 46: TCA %wt. of C in initial lignin for transition metals doped Si/Al catalyzed reactions conducted at 300 °C (reaction catalyzed by Zn, Ga, li and Cu doped Si/Al were performed in duplicate and the error was lower than 10%).

3.3.2.4 Summary of catalyzed lignin hydrotreatment reactions

In conclusion, in most of the catalyzed lignin hydrotreatment reactions the catalyst addition did not promote a significant increase of the overall product yield. The comparison of the LLE GC-MS and TCA data of the catalyst screening conducted at 300 °C is summarized in **Table 7**. In some experiments, particularly those catalyzed by Ni and Si/Al catalysts, the catalyst addition had mostly a negative effect. We consider activated carbon and zeolites as promising for future

optimization, particularly LaO doped ones. Besides a relatively high total yield of products, which was also confirmed by TCA (TD fraction), the occurrence of guaiacyl acids (1.3–1.4%wt.) and mainly guaiacyl dimers (both ~1.4%wt.) was significantly more pronounced than in other catalyzed reactions. Even though the reactions with Raney Ni in MeOH/water mixture did not provide higher yields than the experiments conducted in pure water, we consider the increased contribution of the organic solvent and longer reaction time to be important factors for future optimization.

Table 7: Summary of LLE GC-MS and TCA results for catalyst screening conducted at 300 °C. The TCA analysis was performed using unfiltered mixtures dried for 7 min with 2 min 40 s purging time

Type of catalyst		LLE GC-MS %wt. of initial feedstock														TCA %wt. of carbon in initial feedstock											
		phenols		*guaiacols*		*guaiacyl carbonyls*		*guaiacyl acids*		*guaiacyl dimers*		*other*		*total*		*200 °C w/o O_2*		*300 °C w/o O_2*		*400 °C w/o O_2*		*500 °C w/o O_2*		*850 °C w/o O_2*		*550–890 °C w/ O_2*		*total*	
		mean	*SD*	*mean*	*SD*	*mean*	*SD*	*mean*	*SD*	*mean*	*SD*	*mean*	*SD*	*mean*	*SD*	*mean*	*SD*	*mean*	*SD*	*mean*	*SD*	*mean*	*SD*	*mean*	*SD*	*mean*	*SD*	*mean*	*SD*
none		0.05	0.01	2.92	0.40	0.61	0.10	0.92	0.11	0.02	0.01	0.03	0.01	4.55	0.50	3.95	1.59	1.48	0.46	2.24	0.72	2.10	0.77	4.03	0.75	8.76	5.09	22.56	9.31
Ni catalysts	µNi	0.09	0.01	1.97	0.26	0.47	0.08	0.00	0.00	0.05	0.00	0.05	0.00	2.62	0.36	4.75	0.72	1.32	0.18	1.94	0.18	1.57	0.23	3.53	0.28	6.42	0.79	19.53	1.98
	nNi	0.10	0.01	2.32	0.40	0.55	0.11	0.00	0.00	0.16	0.03	0.06	0.01	3.20	0.55	–	–	–	–	–	–	–	–	–	–	–	–	–	–
	Ni on Si/Al	0.24	0.08	3.49	0.58	0.09	0.05	0.23	0.03	0.04	0.02	0.02	0.00	4.11	0.64	2.65	1.37	0.69	0.32	1.17	0.45	0.99	0.26	3.58	0.57	2.41	1.20	11.49	3.99
	Ni slurry	0.16	0.08	1.66	0.13	0.32	0.03	0.77	0.09	0.02	0.00	0.02	0.00	2.94	0.16	1.81	0.49	0.39	0.10	0.64	0.16	0.62	0.16	1.47	0.20	1.26	0.83	6.19	1.74
Activated carbon doped w/	MoO	0.06	*	2.41	*	0.42	*	0.87	*	0.07	*	0.02	*	3.83	*	4.67	*	1.73	*	2.77	*	1.85	*	3.35	*	24.15	*	38.51	*
	CoO	0.05	*	1.43	*	0.46	*	1.02	*	0.02	*	0.02	*	3.00	*	2.54	*	0.19	*	0.35	*	0.44	*	0.83	*	4.97	*	9.32	*
	LaO	0.02	*	2.28	*	0.24	*	1.37	*	1.39	*	0.02	*	5.33	*	5.00	*	1.82	*	2.82	*	2.15	*	4.56	*	29.13	*	45.48	*
Zeolite doped w/	MoO	0.07	*	3.09	*	0.68	*	1.30	*	0.18	*	0.03	*	5.35	*	5.10	*	1.89	*	3.03	*	2.02	*	3.66	*	26.40	*	42.10	*
	CoO	0.05	*	1.31	*	0.60	*	1.42	*	0.05	*	0.02	*	3.46	*	1.57	*	0.29	*	0.48	*	0.47	*	0.81	*	4.54	*	8.17	*
	LaO	0.02	*	2.83	*	0.69	*	1.32	*	1.36	*	0.03	*	6.25	*	6.78	*	2.97	*	4.09	*	2.58	*	5.09	*	35.71	*	47.36	*
Si/Al doped w/	–	0.01	0.00	2.09	0.39	0.38	0.06	1.16	0.09	1.19	0.10	0.02	0.00	4.85	0.64	3.60	0.56	1.89	0.12	2.84	0.15	2.27	0.28	3.92	0.29	10.35	0.38	24.86	1.16
	Ni	0.21	0.42	2.02	0.16	0.48	0.10	1.38	0.71	1.41	0.72	0.02	0.00	5.52	1.86	3.49	0.58	1.82	0.23	3.03	0.48	2.86	0.16	4.90	0.34	10.34	1.29	26.44	2.68
	Zn	0.06	0.01	2.25	0.14	0.61	0.13	0.83	0.10	0.04	0.01	0.02	0.00	3.81	0.34	5.17	*	2.30	*	3.43	*	2.83	*	4.07	*	11.93	*	29.72	*
	Ga	0.03	0.00	1.92	0.46	0.73	0.13	0.72	0.10	0.37	0.09	0.01	0.00	3.79	0.74	2.14	*	0.79	*	1.20	*	1.18	*	2.37	*	4.04	*	11.71	*
	Li	0.03	0.00	1.72	0.14	0.59	0.08	0.67	0.09	0.24	0.06	0.01	0.00	3.26	0.30	3.31	*	1.46	*	2.49	*	2.15	*	3.39	*	8.71	*	21.50	*
	Cu	0.05	0.00	2.54	0.31	0.76	0.08	0.74	0.06	0.45	0.12	0.02	0.00	4.55	0.48	4.73	*	2.57	*	3.81	*	2.91	*	4.37	*	11.46	*	29.86	*

* reaction conducted in duplicate, the % error did not exceed 10%

3.4 Thermal Desorption Pyrolysis-GC-MS

The comparison of TCA and Py-GC-MS profiles of the three characteristic lignin model compounds, i.e., guaiacol, vanillic acid and bicreosol, is shown in **Fig. 47**. Comparison of the same analyte amount analyzed by TCA and Py-GC-MS revealed a good agreement for guaiacol. Most of the C (mass) was evolved at 200 °C with the rest evolved at 300 °C. However, a minimal amount of analyte was evolved at 890 and 1,200 °C, which may be caused by the low residual amount of target compounds close or below the LOD. A similar observation was made also for mequinol, syringol and levoglucosan. The Py-GC-MS profiles of guaiacol, mequinol, syringol and levoglucosan are shown in **Appendices XXIX–XXXII**. However, during the initial testing conducted at a split ratio of 10:1 at higher dose, a relatively high portion (~20%) of levoglucosan evolved at 890 °C (**Appendix XXXIII**), whereas at 20 µg of C all the levoglucosan is evolved at 200 °C with a fairly low detector response (**Appendix XXXII**). This behavior may due to the presence of three hydroxyl groups in the levoglucosan structure leading to its low ionization efficiency. Regarding the less volatile lignin standards, vanillic acid and bicreosol, the discrepancies between the TCA and Py-GC-MS were more apparent, however the data showed the same trend of decreasing TD and increasing pyrolytic fraction. A similar adsorption effect of less volatile analytes, especially bicreosol, on glass wool was observed as in case of TCA, where bicreosol spiked on the quartz filter evolved less C at 200 °C than when spiked on the glass boat (**Fig. 14**). The Py-GC-MS profiles of vanillic acid and bicreosol are shown in **Appendices XXXIV–XXXV**.

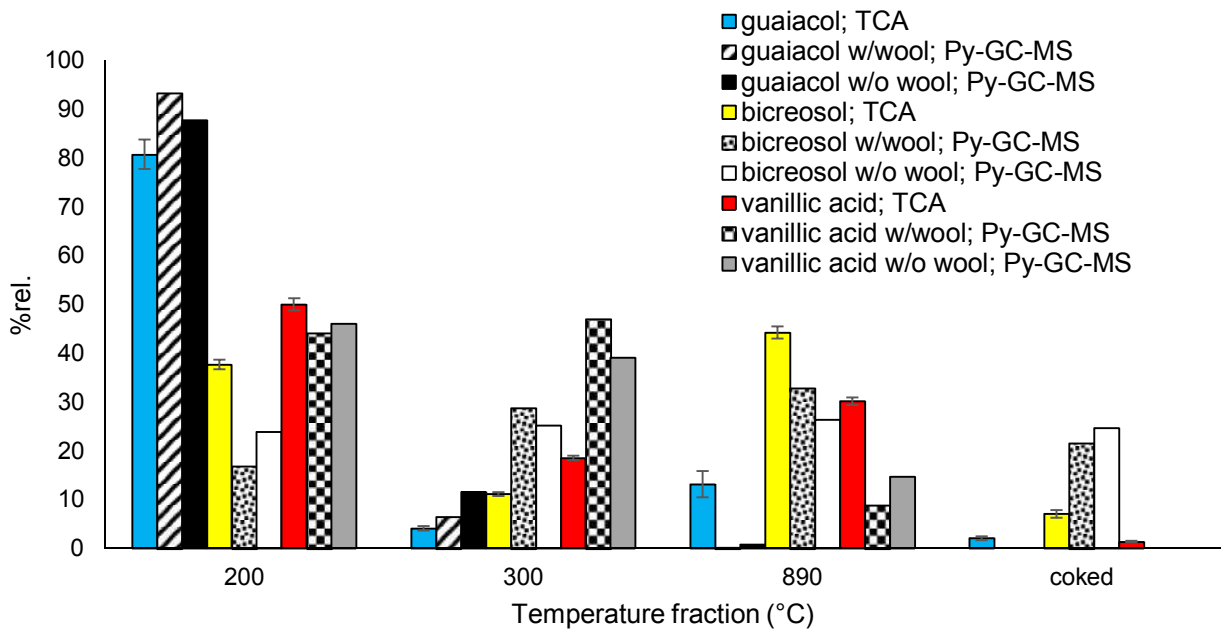

Figure 47: TCA vs. Py-GC-MS comparison of %rel. of C (mass) evolved at different temperature steps; The spiked sample volume for both methods was 5µL, which corresponded to 5µg of C. Analysis was performed in split ratio of 50:1.

An important feature of the Py-GC-MS chromatograms is a presence of an air peak, resulting from the air introduction to the system during the valve switching between the interface heating and the sample loading steps (**Fig. 48**). After the air peak, a combined peak of CO_2 and water appears on the chromatogram. A little portion of CO_2 and water could probably be introduced by air, however they may also be products of sample oxidation. In addition, water may be naturally present in the sample and simply vaporize when the temperature increases. **Appendix XXXVI** shows the extracted *m/z* of 18 and 44 ions from solid alkali lignin analysis, which are expected to be related mainly to water and CO_2, respectively. Interestingly, with increased temperature both water and CO_2 elute later, suggesting a different origin of the two species. At the first step (200 °C), air is probably the major contributor in the CO_2 peak, whereas water originates both from air and sample moisture. At higher temperatures, CO_2 and water are most likely produced during combustion processes. This theory is also supported by the decreased abundance of *m/z* 18 and the

increased abundance of *m/z* 44 with temperature in solvent control analysis (**Appendix XXXVII**) Since CO_2 and water partially evolve from the lignin samples, it is crucial to evaluate controls in order to subtract CO_2 and water of external origin for potential mass balance closure.

Solid alkali lignin was analyzed using Py-GC-MS in the inert He atmosphere with a goal to identify the degradation products characteristic for each temperature fraction, in parallel to TCA providing mainly quantification data. **Table 8** summarizes the identified products and **Fig. 48** shows thermograms for each temperature fraction with the analyte distribution. A relatively low abundance of volatiles was observed at 200 °C, similar to the TCA analysis (**Fig. 17**). The most pronounced peaks belonged to guaiacol, vanillin, acetovanillone and homovanillic acid. The greatest portion of lignin degradation products evolved at 300 °C and 400 °C steps. It consisted mainly of guaiacols, guaiacyl carbonyls, guaiacyl alcohols, guaiacyl dimers and homovanillic acid. At 500 °C and 890 °C steps, lignin was further disintegrated into lower molecular weight species, i.e., phenols and aromatic hydrocarbons, whereas the abundance of the higher molecular weight products decreased.

Table 8: Compounds identified by TD-Py-GC/MS including retention times (tR) and major MS ions

Label	t_R (min)	Compound Name	Formula	Major Ions (*m/z*)	Compound Class	Identification*
A_1	3.033	Benzene	C_6H_6	78, 52	Aromatic hydrocabons	S
A_2	3.211	Toluene	C_7H_8	91, 92, 65	Aromatic hydrocabons	S
A_3	3.746	Xylene	C_8H_{10}	91, 106, 105	Aromatic hydrocabons	T
P_1	4.158	Phenol	C_6H_6O	94, 66, 39	Phenols	S
P_2	4.631	Methylphenol	C_7H_8O	107, 108, 77	Phenols	S
P_3	4.736	Methylphenol	C_7H_8O	107, 108, 77	Phenols	T
G_1	4.859	Guaiacol	$C_7H_8O_2$	109, 124, 81	Guaiacols	S
P_4	5.191	Dimethylphenol	$C_8H_{10}O$	107, 122, 121	Phenols	T
P_5	5.277	Ethylphenol	$C_8H_{10}O$	107, 122, 77	Phenols	S
P_6	5.455	Benzenediol	$C_6H_6O_2$	110, 64, 81	Phenols	T
G_2	5.474	Methylguaiacol	$C_8H_{10}O_2$	138, 123, 95	Guaiacols	S
A_4	5.707	Dimethoxytoluene	$C_9H_{12}O_2$	152, 137, 121	Aromatic hydrocabons	T
P_7	5.824	Methylbenzenediol	$C_7H_8O_2$	124, 123, 78	Phenols	T
G_3	5.966	Ethylguaiacol	$C_9H_{12}O_2$	137, 152, 122	Guaiacols	S
G_4	6.169	Vinylguaiacol	$C_9H_{10}O_2$	150, 135, 107	Guaiacols	S
P_8	6.335	Dimethylbenzenediol	$C_8H_{10}O_2$	123, 138	Phenols	T
G_5	6.396	Eugenol	$C_{10}H_{12}O_2$	164, 149, 103	Guaiacols	S
P_9	6.488	Dimethylbenzenediol	$C_8H_{10}O_2$	123, 138	Phenols	T
C_1	6.642	Vanillin	$C_8H_8O_3$	151, 152, 81	Guaiacyl Carbonyls	S
G_6	6.888	Isoeugenol	$C_{10}H_{12}O_2$	164, 149, 131	Guaiacols	S
G_7	6.943	Propylguaiacol	$C_{10}H_{14}O_2$	137, 166, 122	Guaiacols	S
C_2	7.085	Acetovanillone	$C_9H_{10}O_3$	151, 166, 123	Guaiacyl Carbonyls	S
L_1	7.306	Homovanillyl alcohol	$C_9H_{12}O_3$	137, 180, 122	Guaiacyl Alcohols	S

Table 8 continues: Compounds identified by TD-Py-GC/MS including retention times (tR) and major MS ions

Label	t_R (min)	Compound Name	Formula	Major Ions (*m/z*)	Compound Class	Identification*
G_8	7.558	Propionylguaiacol	$C_{10}H_{12}O_3$	151, 180, 123	Guaiacols	T
D_1	7.860	Homovanillic acid	$C_9H_{10}O_4$	137, 182, 122	Guaiacyl Acids	S
C_3	8.265	Coniferyl aldehyde	$C_{10}H_{14}O_3$	178, 135, 147	Guaiacyl Carbonyls	T
L_2	8.278	Coniferyl alcohol	$C_{10}H_{12}O_3$	137, 180, 124	Guaiacyl Alcohols	T
R_1	10.356	Diguaiacylmethane	$C_{15}H_{16}O_4$	137, 260	Guaiacyl Dimers	T
R_2	10.405	Diguaiacylmethane	$C_{15}H_{16}O_4$	137, 260	Guaiacyl Dimers	T
R_3	10.620	Diguaiacylethane	$C_{16}H_{18}O_4$	137, 274	Guaiacyl Dimers	T
R_4	10.676	Diguaiacylethane	$C_{16}H_{18}O_4$	137, 274	Guaiacyl Dimers	T
R_5	11.764	Diguaiacylethene	$C_{16}H_{16}O_4$	211, 272	Guaiacyl Dimers	T

*Identification is confirmed by standards (S) or reported as tentative (T) based on the literature and mass spectrum at least 80% match with NIST library

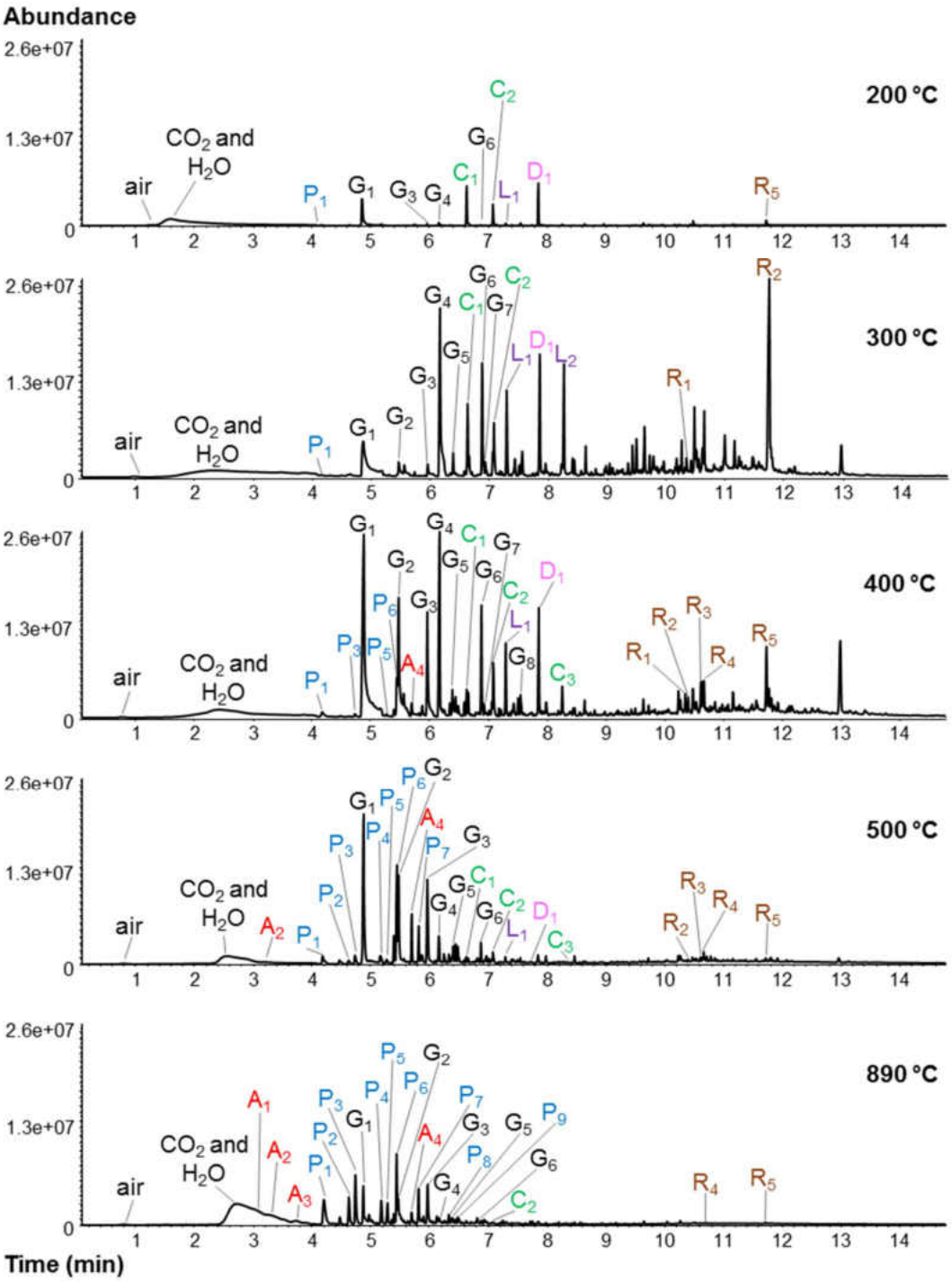

Figure 48: TD-Py-GC-MS analysis of solid alkali lignin

A characteristic marker of lignin related compounds is the ion with *m/z* 137. **Appendix XXXVIII** shows a distribution of extracted *m/z* 137 throughout the Py-GC-MS profile of solid alkali lignin and highlights the products with a mass spectra with a high abundance of the ion with *m/z* 137.

A comparison of %rel. of C analyzed by TCA and normalized peak areas of analytes evolved by Py-GC-MS was made for the lignin hydrotreated at 300 °C w/o catalyst. The data are shown in **Appendix XXXIX**. Contradictory to TCA data, where pyrolyzed C is the main contributor in the final yield, TD fraction is predominant in Py-GC-MS. It is assumed that the product fraction evolving at pyrolytic temperatures consists mainly of lignin derived oligomers, which may not be GC-elutable, whereas the unique TCA protocol is able to detect and quantify all the C containing forms.

CONCLUSIONS

A novel method for the analysis of lignin and its degradation products by TCA was developed. The current TCA protocol ensures close to 100% recovery of all the potential lignin degradation products, including the most volatile ones, such as guaiacol or phenol. After the successful testing on the lignin model compounds, the final method was applied on the solid alkali lignin with a full mass balance closure. The results were compared to the routinely used TGA and the analytes evolving at each temperature were identified by TD-Py-GC-MS. In addition, a good agreement was obtained in between the results obtained by TCA and LLE GC-MS for both non-catalyzed and catalyzed lignin hydrotreatment experiments.

Three main parameters had to be addressed in order to create a reliable TCA method, which guarantees the maximum recovery of each analyte at each temperature step. The volatiles' vaporization losses were minimized by limiting the drying and purging time and particular temperature steps' lengths were extended to avoid carryovers. For solid lignin samples and aqueous hydrotreated lignin samples from the batch reactor, the purging time is set to 4 s without a prior drying. The final temperature program consisted of an ambient temperature step, two thermal desorption steps (200 and 300 °C), three pyrolytic steps (400, 500 and 890 °C) and oxygenation step (890 °C w/O_2). The length of all the steps was adjusted at 6 min, except for the last pyrolytic step at 890 °C, which is 12 min long.

The purging time minimization and the ambient step implementation not only decreased the vaporization losses of analytes, but also allowed for the detection of the analytes evolving at

ambient step, including CO_2 from air. The impact of CO_2 and other carbon containing impurities can be easily eliminated by the analysis of sufficient amount of solvent controls.

The initial step temperature does not seem to have a significant effect on the TCA profile of lignin model compounds. However, an interaction between the analyte and the filter surface, shifting the amount of evolved carbon towards the higher temperature fractions, was observed. Also, more pyrolyzed carbon evolved at lower loadings (<5 μg of carbon). This observation was made both for lignin standards and solid alkali lignin. However, there was a significant shift towards the coked fraction observed at high lignin loadings.

The TGA analysis of lignin showed higher mass losses in low temperature fractions than the TCA, thus confirming the TCA sensitivity for carbon containing (lignin derived) compounds, since the difference was most probably caused by the presence of water, sulfur and other carbon free moieties. The TD-Py-GC-MS analysis of lignin demonstrated that guaiacols and guaiacyl carbonyls together with homovanillyl alcohol and homovanillic acid were the most abundant degradation products at TD temperature. With increased temperature, phenols became more abundant.

Lignin repolymerization was studied in seven different reaction systems. Each mixture was analyzed weekly by TCA for at least one month and even the application of polymerization initiators, such as catalytic amount of acid or UV light, did not cause any significant change in the TCA profiles.

The LLE GC-MS results of the hydrotreated lignin showed a need of the reaction vessel homogenization in order to obtain higher yield of products. On the other hand, the presence of unreacted lignin particles during LLE did not provide any increase in the overall yield. The total product yield increased with the reaction temperature. A satisfactory mass balance was closed for

the non-catalyzed systems. The nickel based catalysts did not seem to promote any significant yield increase. An interesting results was obtained for the reactions performed at 300 °C in the presence of LaO doped activated carbon and zeolite catalysts. The average overall yield of products reached 5.3 and 6.3%wt., respectively, with a surprisingly high yield of dimers, around 1.4%wt. The TCA results of TD fraction obtained by both old and newly developed TCA protocol were similar to LLE GC-MS overall yield of products.

APPENDICES

Appendix I: Determination of the internal vessel pressure and percentage of the liquid phase during the lignin hydrotreatment reactions

First, the theoretical volume of the empty vessel had to be determined. Using the vessel dimensions, i.e. internal diameter of 0.71 cm and length of 6.325 cm, and the formula for the cylinder volume calculation, the theoretical vessel volume of 2.5 cm^3 was determined. The weight of water in the vessel closed by cap on one side was 3.57 g. Assuming water density at lab temperature (~20 °C) to be 0.998 g/cm^3, the water volume was calculated to be 3.58 mL. From the difference between the theoretical volume of the empty vessel and the volume of water in the capped vessel the approximate cap volume of 1.1 mL was calculated.

Consequently, saturation properties of the reaction solvent (water) were obtained for the four tested temperatures: 200, 250, 275 and 300 °C. The information is available online on the National Institute of Standards and Technology (NIST) web page webbook.nist.gov and the values are presented in the following table.

Reaction temperature (°C)	200	250	275	300
Pressure (bar)	15.55	39.76	59.46	85.88
Liquid phase density (g/cm^3)	0.8647	0.7989	0.7590	0.7121
Vapor density (g/cm^3)	0.0079	0.0200	0.0305	0.0461

Since the reaction mixture is not water by itself, but water with lignin, it was necessary to determine the density of lignin and consequently the density of water in the mixture. For the reaction experiments conducted in the range of 250–300 °C 0.25±0.01 g of lignin was used. The approximate volume of 0.25 g of lignin was experimentally determined to be 0.5 mL. Assuming that lignin is not compressible and water fills the remainder of the internal vessel space, the density of water in the mixture with lignin can be calculated the following way:

$$\rho_{water} = \frac{m_{water}}{V_{vessel} - V_{lignin}} = \frac{2.9\ g}{4.7\ mL - 0.5\ mL} = 0.690\ g/mL$$

Due to the fact that the calculated water density at 300 °C is lower than the water density at saturation condtions at 300 °C, we are sure that we operate at subcritical water conditions at safe pressure below 85.88 bar. The percentage of the liquid phase inside the vessel at 300 °C can be then calculated the following way:

$$\%\ of\ liquid\ phase = \frac{\rho_{water,sample} - \rho_{vapor}}{\rho_{water,saturation} - \rho_{vapor}} X\ 100 = \frac{0.690 - 0.0461}{0.7121 - 0.0461} X\ 100 = 96.7\%$$

The final table summarizes the operation conditions at each reaction temperature.

Reaction temperature (°C)	200	250	275	300
Lignin loading (g)	0.1	0.25	0.25	0.25
Water loading (mL)	3.2	2.9	2.9	2.9
Vessel pressure (bar)	<15.55	<39.76	<59.46	<85.88
% of liquid phase in vessel	88.1	86.0	90.5	96.7

Appendix II: TCA flow schematics; Standby and cleaning mode

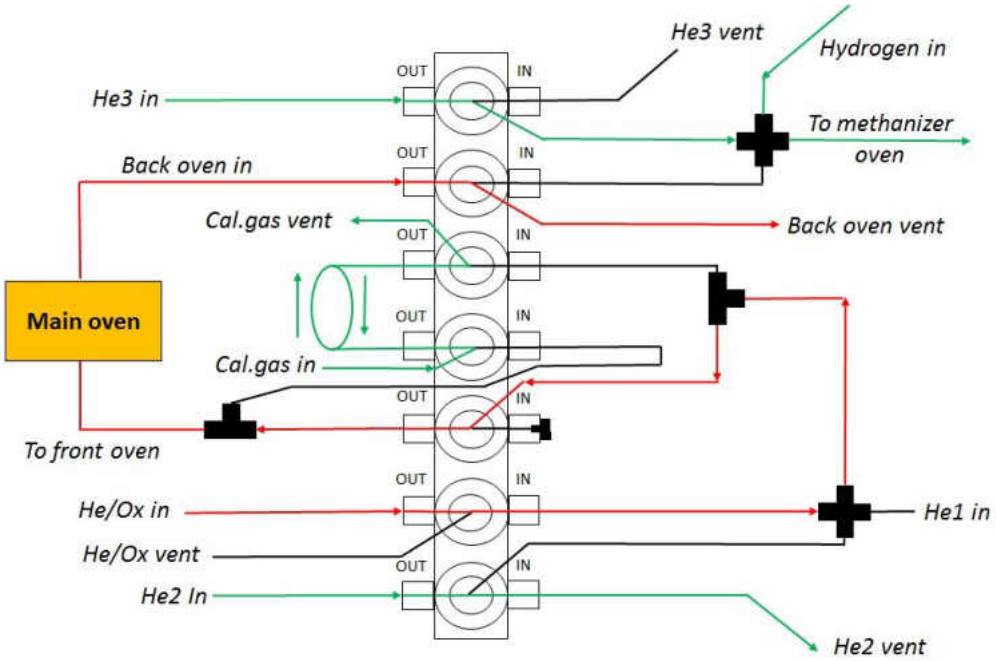

Appendix III: TCA flow schematics; Off and Idle mode (Purge Offline)

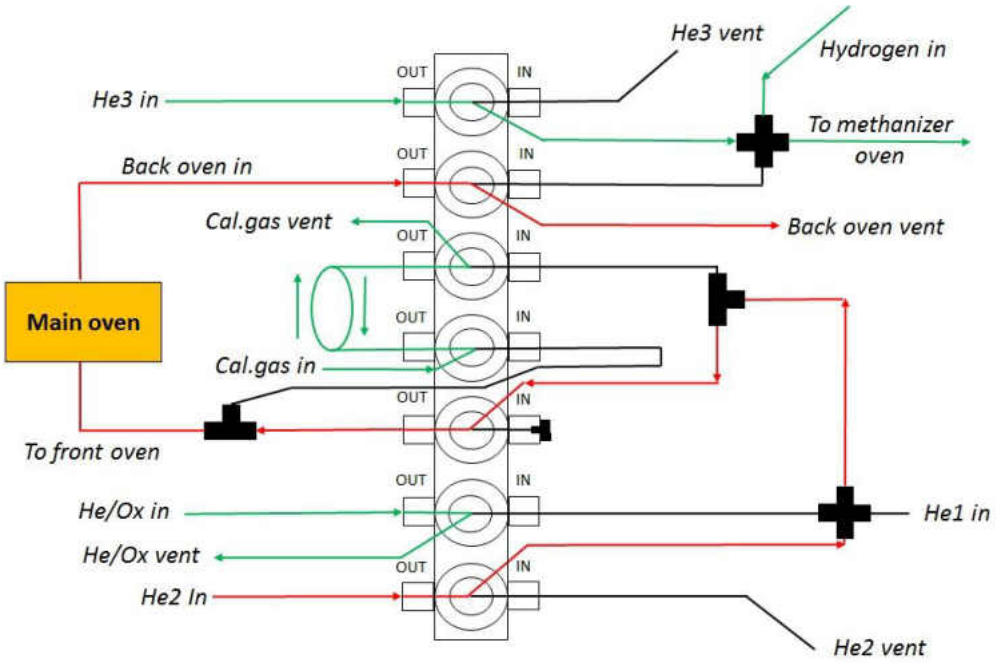

Appendix IV: TCA flow schematics; Helium phase (Purge Online)

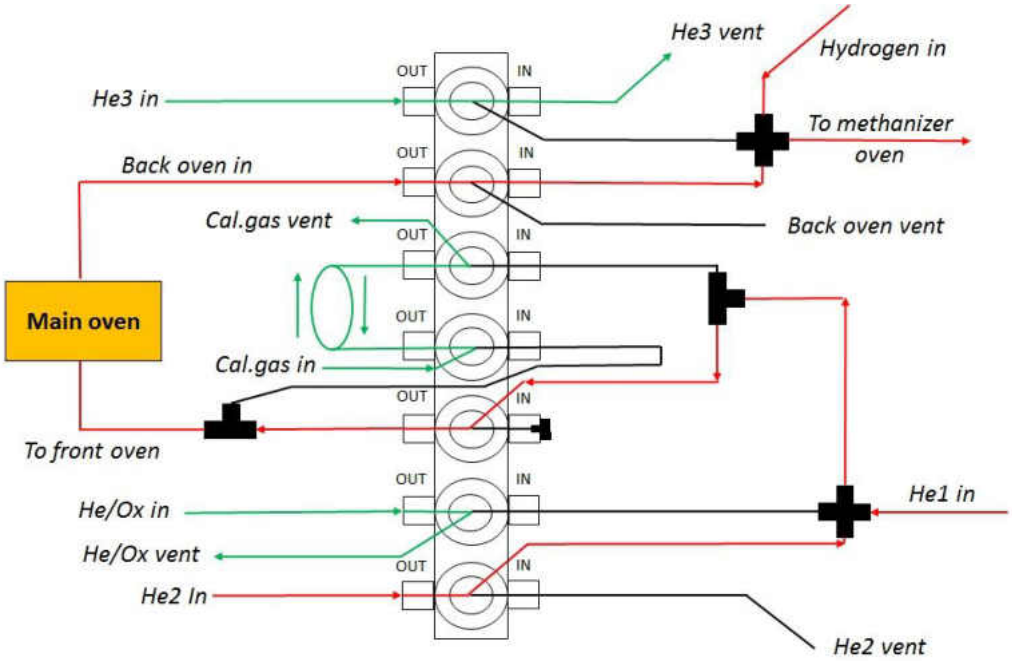

Appendix V: TCA flow schematics; Oxygen phase

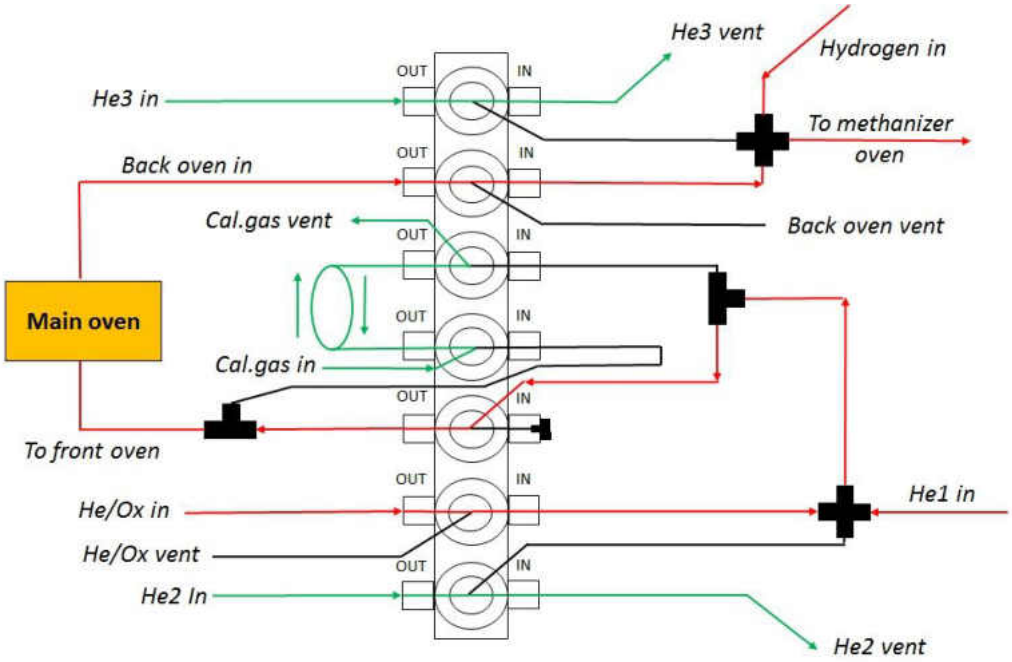

Appendix VI: TCA flow schematics; Calibration phase

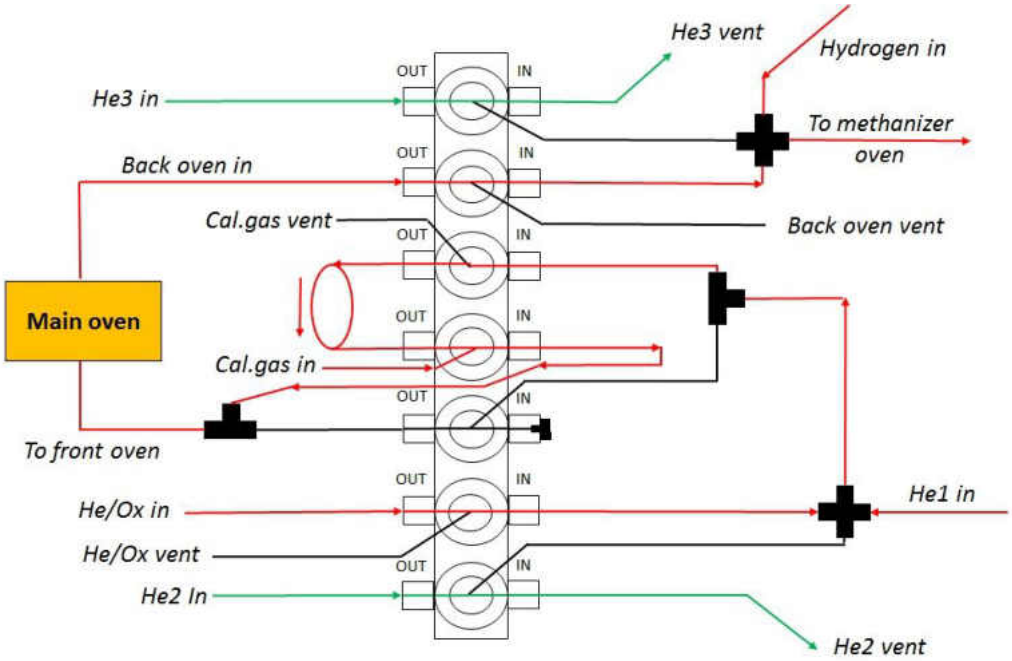

Appendix VII: TCA operational manual and guide for data processing in Excel templates and Calc software

OCEC Start Up (if completely off)

- The 5 gas tanks are located between the first and the second bench next to the wall in lab 309. Open all gas tanks by opening the **secondary (on/off)** valve. Open the valve completely and then turn it slightly back, so the knob does not stuck. **Don't manipulate with the main valve and the regulator valve!!! When the pressure in any gas tank drops under 200 psi replace the tank! The gas tanks consisting of a mixture of more than one gas, i.e. 5% methane in He and He/Ox have to be ordered in advance (~at least 6 weeks before the expected replacement corresponding to pressure of approximately 500 psi), since they are not readily available in Airgas storage**. Air, N_2 and H_2 should be delivered the next work day after placing the order.

- Turn on OCEC by pressing the red power button on the white extension cord (power cord located behind instrument)
- On the computer open the "OCEC 828" program located in the C drive, **see section "Software selection"**
- ***Slowly*** adjust all the gas flow rates by turning the needle valves until gas flows are within ranges indicated on PC (the table with flow rates is located on the right side of the software window), **adjust the hydrogen flow rate as the last one due to safety reasons!!!**
- Turn on FID, H_2 flow rate within the range indicated by the window should be sufficient to light the FID by pressing the red button, if having issues, adjust the H_2 flow by an extra 20-30 psi (70-80 total) and ignite with red button, ignition of the FID detector is indicated by a popping noise
- After FID is lit (check with metal piece – vapor) readjust H_2 back within the optimal range if an additional flow was needed

OCEC Start Up from STAND BY

- Unclick the **"Standby"** button at the top of the OCEC828 software and change "desired CH_4 oven temperature" in the bottom panel of the OCEC828 software to **500°C**. Back oven temperature will raise back to 870°C automatically.
- The air, hydrogen and methane/helium (calibration gas) valves might be closed, then you have to open them before you start adjusting the flow rates. The 5 gas tanks are located between the first and the second bench next to the wall in lab 309. Open all gas tanks by opening the **secondary (on/off)** valve. Open the valve completely and then turn it slightly back, so the knob does not stuck. **Don't manipulate with the main valve and the**

regulator valve!!! When the pressure in any gas tank drops under 200 psi replace the tank! The gas tanks consisting of a mixture of more than one gas, i.e. 5% methane in He and He/Ox have to be ordered in advance (~at least 6 weeks before the expected replacement corresponding to pressure of approximately 500 psi), since they are not readily available in Airgas storage. Air, N_2 and H_2 should be delivered the next work day after placing the order.

- ***Slowly*** adjust all the gas flow rates by turning the needle valves until gas flows are within ranges indicated on PC (the table with flow rates is located on the right side of the software window), **adjust the hydrogen flow rate as the last one due to safety reasons!!!**
- Turn on FID, H_2 flow rate within the range indicated by the window should be sufficient to light the FID by pressing the red button, if having issues, adjust the H_2 flow by an extra 20-30 psi (70-80 total) and ignite with red button, ignition of the FID detector is indicated by a popping noise
- After FID is lit (check with metal piece – vapor) readjust H_2 back to indicated range if additional flow was needed

Software selection

- In C:\Program files\OCEC828 there are 3 different softwares present. They can be also found in Dropbox\AK group\Instrument Protocols and Manuals\software. They differ in the purging time. The original software is called "OCEC828" and has approximately 40 s offline purging and 2 min online purging programmed. "OCEC828NoPurge" has both offline and online purging set to 2 s, unless some volatile sample is being run. In such case the online purging has a variable length depending how long it takes the FID signal to get

stabilized. “OCEC828NoPurge_2+2 uses 2 s offline and online purging, regardless the sample properties.

- There isn’t any apparent visual difference between the 3 softwares when they are open. If you aren’t sure, which one is open, close it by selecting “Exit” in the upper left corner and “Exit (all off)”. After that open the desired software.

OCEC Operation

- Cut a piece from a prebaked quartz filter with the black filter cutter (500 °C over night), remove the metal clamp, put the front oven glass cap onto the upper left corner of the paper/aluminum foil board and insert the freshly cut filter piece (rough part on the top) to the main oven. Manipulate with the filter by using the sharp end tweezer, for manipulation with the glass boat use the Teflon tweezer with rubber ends.
- Connect the front oven glass cap back to the TCA machine and tighten the connection with the metal clamp. Clean the oven by selecting “Action” and “Clean Oven”
- While the main oven is being cleaned, fill out the log book. Record transmittance and reflectance signal, hydrogen and calibration gas flow rates and absolute pressure after the oven has finished cleaning
- Create a folder for your data in “Output raw data file”, the preferred way of naming is “initials_date_sample”. The folder path will be D:\OCEC\Data\your_name. In order to process the data in the Excel quantification spreadsheet it is better to first create a folder in D:\OCEC\Data\your_name and call it “initials_date_sample” and then create a separated text file for each analysis in “Output raw data file”. This way you will have a folder for each day of analysis, which will contain separated text files with data from each run.

- For every run including blanks and calibration make sure that the pressure after closing the oven is **above 0.1 PSIG**!!! The common value is approximately 0.2 PSIG. To be able to start a new analysis, the oven temperature has to be below 75 °C, in that case you will see a notice "Safe to put a new sample" in a green field. For every run you also need to fill the "Analyst name", "Sample ID" and "Punch area". Always set 1 cm^2 for "Punch area". Press "Start" to run.
- For the data processing it is strongly recommended to use the Excel data spreadsheets located either in Dropbox\AK group\Instrument Protocols & Manuals\OCEC or in the PC operating the TCA in D:\OCEC\TCA_Lignin_Templates. For a brief quantification Calc316 software can be used. For the details see section "Data Processing in Calc software". However, the Excel templates are the primary way of quantification, alternatively the Origin software can be used, for details see "HB_Origin_Guide" located in Dropbox\AK group\Instrument Protocols & Manuals\OCEC. Remember, if you want to use Calc software for the brief quantification of, e.g., filter blank or sucrose calibration, it is necessary to use the original "OCEC828" software", otherwise the Calc software calculates odd carbon amounts, since the minimized purging time causes issues with the proper FID baseline setting.
- After oven cleaning with the filter still in the oven run blank, in "parameter file" choose folder D:\OCEC\methods\Default and select "HB_Blank Run", for blank baseline FID signal should be obtained.
- After running the blank a sucrose calibration solution of known carbon content should be run. In "parameter file" select D:\OCEC\methods\Default and "pyroprobe_ac2". The expected amount of C ± 5% (see processing in Excel templates) should be obtained in order

to continue with the analysis of samples. If the value calculated in Excel template does not fall within the 5% of the expected value run duplicate analysis for repeatability. After running the calibration contact the person in charge (Honza or Brett). You should get a permission of the person in charge to continue in the analysis.

- **For every set of samples at least 1 solvent blank has to be run in order to subtract the carbon amount, which is not part of the sample!** Use the solvent that you have your samples dissolved in and also use the same loading volume as you use for your samples.
- Load sample (5-10 µL) on the center of the filter paper on its rough side. If wet, allow to dry (use hot plate with aluminum foil on the top. Heat it up to 40° C. For water, unless allowed by the person in charge (Honza), 7 min will be the drying time used, for DCM and other organic solvents 4 min. Use timer to measure the exact drying time.
- The regular lignin ramp for lignin samples including an ambient temperature step and then 200, 300, 400, 500, 890 (all w/o oxygen) and 890 °C step w/oxygen can be found in D:\OCEC\Methods\Default and "HB_Lignin Ramp_amb_long_890_170712". All temperature steps are 6 min long, except the 890 °C w/o oxygen, which is 12 min long. Using this method together with the "OCEC828NoPurge_2+2" and minimized drying time depending on the type solvent ensures maximum recoveries of lignin and lignin degradation products and enough for their elution in every temperature step.
- Run a duplicate sample about every tenth sample.

Standby mode

- **NOTE: Use the standby mode when using the instrument regularly (every day) or when interrupting your work for less than one week, otherwise shut down the instrument completely (see "Instrument shut down")**

- Click on "Standby" in upper left corner of the OCEC828 software, set "desired CH_4 oven temperature" and "standby back oven temperature" in the bottom OCEC828 software panel to **300°C**.
- **Slowly adjust** the flow rates the following way: air 5-10 ccm, H_2 5-10 ccm, He1 6-10 ccm, He2 4-6 ccm, He3 6-10 ccm, He/Ox 4-6 ccm, Cal. Gas 5-10 ccm. **Due to safety reasons, start with hydrogen!** There is no manipulation with the FID detector. When the flow rates are decreased, the FID extinguishes automatically.
- After the flow rates are adjusted, air, hydrogen and calibration gas (methane/helium) secondary valves on the gas tanks can be closed completely during standby mode. **Don't touch the main and regulator valves!!!**
- **The PC operating the TCA stays turned on and the operational software stays open during the standby mode!**

Instrument Shut Down (Reverse order of Start Up)

- **NOTE: Turn off the instrument completely only when not planning to use the machine for week or more. If you plan to use the instrument regularly, set the instrument to standby mode (see "Standby mode")**
- After oven is cooled all gasses should be ***SLOWLY*** reduced to a flow rate 5-10 mL/min by first starting with H_2 due to safety reasons. There is no manipulation with the FID detector. When the flow rates are decreased, the FID extinguishes automatically.
- Once gasses have been reduced turn off power supply located behind instrument by pressing the red button on the extension cord
- Close the secondary valves on the gas tanks. **Don't touch the main and regulator valves!!!**

- **The PC operating the TCA stays turned on and the operational software stays open when the TCA is turned off! If you come to the instrument and the PC is turned off or the software is closed, first, turn on the instrument before opening the OCEC828 software!**

Data processing in Excel templates

- The Excel templates are the primary way of data processing and they are located either in D:\OCEC\TCA_Lignin_Templates or in Dropbox\Lignin\TCA_Lignin_Templates.
- The folders contain following templates:

HB-OCECTemplate_pyroprobe_ac2_170712 used for pyroprobe_ac_2 parameter. This parameter with the corresponding template are used for the sucrose calibration mixtures analysis.

HB-OCECTemplate_hb_Lignin Ramp_amb_long_890_170712 used for Lignin Ramp_amb_long890_170418 parameter. This parameter with the corresponding template are used for the complete analysis of lignin related samples.

HB_OCECTemplate_repolymerization_170712 used for HB_repolymerization_170627 parameter. This parameter with the corresponding template are used for a brief analysis of lignin related samples. The parameter contains two 6 min long TD steps at 200 an 300 °C, one 12 min long pyrolytic step at 890 °C and the oxygenation step.

- Both directories also contain the last version of the sucrose calibration with the calibration curves. All the slopes, intercepts and calibration constants are linked to this file.
- As mentioned in section "OCEC operation", in order to process the data in Excel templates it is better to have all the analyses saved in separated text files
- Open the text file, highlight the whole content (Ctrl+A), right click and "Copy" (or Ctrl+C)

- Open the desired Excel template and save it under different name in you data folder (preferably “Initials_date_sample”)
- Create a new sheet following the sheet with the template and call it “raw_data_sample_label”, right click and “Paste” the data there (or Ctrl+V). Therefore, for one day of TCA analysis you will have one quantification Excel file and for one analysis you will have the quantification template followed by the analysis raw data
- The copied raw data will probably not be separated into the single columns. In order to do that, click on the first cell, on the top panel select “Data” > “Text to columns” > “Delimited” > “Comma” > “Finish”, now all the parameters are separated in different columns.
- When the different parameters are separated in the different columns, highlight the raw data set by starting in the cell with word “Sample” and highlight the whole row till column O, then highlight the rest of the data set by pushing Ctrl+Shift+↓ and copy.
- Go to the template sheet (the previous one before the raw data sheet) and paste the data starting in cell **D1**. The D1 cell should contain the word “Sample”.
- When the data are pasted, the template automatically calculates all the results. The original templates were modified for the lignin researchers, so they stress especially the FID results. However, the laser results are kept in the template, if needed.
- The most important information is shown on the right side of the template. The large blue box on the top with a smaller orange box show slopes and intercepts and the calibration constant, respectively, linked from the recent calibration file

- The yellow box under the calibration data contains the final integrated peak areas and amounts of carbon calculated using external calibration, internal calibration and calibration constant (from top to bottom)
- The chart under the yellow box shows the temperature profile (yellow line) with the FID signal obtained for that particular sample. The FID signal range (y-axis values) is automatically adjusted to the peak with the highest abundance. The next chart shows the maximized FID used for the integration and the closest area to the baseline.
- For the data processing of the next sample, copy the template and the raw data spreadsheet behind the two spreadsheets with already processed sample, rename based on the sample labeling and repeat the process. The newly copied raw data of the next sample should be already separated into the single columns.
- For more details about the quantification templates, e.g., how to modify the template when the analysis parameter was modified, see Brett's videos in Dropbox\AK group\Instrument Protocols & Manuals\OCEC\Videos

Data Processing in CALC software

- **Reminder:** Calc software is not the primary way how to process the data. It is used just for a brief evaluation of the total carbon evolved. In addition, when a software with a limited purging is used, the data cannot be trust at all.
- Open program "Calc 316" located on the desktop and select the data file
- Click on "Calculate all samples"
- Laser and FID graph scales can be adjusted on the right hand side, it's possible to switch between samples by clicking on the sample ID in the upper right corner

- In order to calculate new data, the software has to be closed and opened again. The software does not allow the user to use the "Calculate all samples" function twice, while being already open
- To open in Excel, open the text file with your data, select the data to be transferred, copy and paste to Excel
- In Excel select "Data" > "Text to columns" > "Delimited" > "Comma" > "Finish", now all the parameters are separated in different columns
- To process in Origin see HB_Origin_Guide_170308

Appendix VIII: Guide for data processing in Origin

Prior to Origin:

- In order to process your data in Origin you need to have the .txt file with your data. Your data are saved in the file selected in "Output raw data file" in OCEC828 software when you were running the analysis. The preferred directory for saving the text files is D:\OCEC\Data\your_name. Each text file is a set of files from one day, the new dataset always starts with "sample".
- Before copying the data from the text file open an Excel spreadsheet and create a column called "Time". The TCA machine collects the data every second, therefore the time difference in min between every two points will be 1/60 (0.0167). You can also plot the time in seconds, just remember to **use the same time units both for calibration and sample**, because it affects the peak area!!!
- Open the text file and highlight the data of **one** sample starting from "FID1" and continue highlighting the set of data until next "sample"

- Copy the highlighted data and paste it in the first cell of the second column next to the "Time" column.
- To distribute into multiple columns highlight the second column you've just pasted and select "Data" → "Text to columns" → select "Delimited" → "Next" → select "Comma" → "Finish"
- Now all the data columns are separated, 1. Column is "Time", the second one is "FID1".
- Drag down the time values and make sure that every FID1 value is attributed to a time value in order to make a thermogram in Origin
- It's recommended to create one spreadsheet for one sample. Label each spreadsheet the same way as you labeled your samples. Copy the "Time" column into spreadsheets for the following samples. Call the whole Excel file as Initials_Analysis date_TCA_raw_data.

Guide for OriginPro 2016 32bit use

- Origin software is installed on the first PC along the left wall in the PC lab
- Open OriginPro 2016 32bit software
- In Book1 highlight first 4 rows labeled with yellow color and delete them
- In your Excel file select first two columns ("Time" and "FID1"), copy them, go back to Origin, click on A1 cell and paste
- Erase the first row with column names, otherwise you'll make the software confused
- Click on the very upper left cell of Book1 (not labeled one), this way you highlight the whole data set
- On the top line of the software select **"Plot"** → **"Line"** → **"Line"** and you'll get a thermogram of your sample

- In order to magnify the baseline area of your thermogram right click on the y axis and select "Scale", in "from" line type 2850 and in "to" line type 3200. In case you don't see the separation of all the temperature fractions in this magnified area increase the "to" value

Creating a baseline for the curve

- Go to **"Analysis" → "Peaks and Baseline" → "Peak Analyzer" → "Open Dialog"**. This brings up the *Peak Analyzer* window. On the top pane of the window the wizard is shown highlighting the steps you will take in the process of creating the baseline for your curve. In the first step you will select the goal of this process:

  Recalculate "Manual"

  Goal "Create Baseline"

  Input Your graph/curve (Example: [Graph1]1!1"Heat Flux")

- **The only thing you have to select is "goal" → "Create baseline", otherwise "recalculate" and input" are already set**
- Select "Next" to move onto the next step of the *Peak Analyzer* wizard: "*Baseline Mode"*. In this pane select the following:

  Baseline Mode "User Defined"

  Snap to Spectrum Uncheck

  Baseline Anchor Points

  Method "2nd Derivative"

  Smoothing Window Size 1

  Threshold 0.05 Keep "Auto" checked

  Current # of points 0

  Enable Auto Find Check (only for initial peak find)

Number of pts to find 2

- **The only parameters you have to change from the default are "smoothing window size" and "number of points to find", for the rest you use the default settings**
- Now push the "Next" button. You will see the baseline anchor points appear along your curve. If you are satisfied with the placement of these points you may go on to integrating the peak areas of the curve by pressing "Finish". However, you will probably have to correct the baseline for every sample. In that case you do the following:
  1) To move an already existing anchor point select "Modify/Del", bringing you back to your graph window. Select the point you wish to move by clicking and holding down either the left mouse button or using the keyboard arrows (better, more precise). Move the point to the desired location and release the left mouse button to set the new location.
  2) You can view the anchor point info at anytime by selecting the "Anchor Points Info.." button (not necessary).
  3) If you are satisfied with your baseline select "Done" and "Finish"

Integrating Peak Areas (Using a User Defined Baseline)

- This procedure is for integrating peak areas of a curve based on a user defined baseline that is already added to the curve (see section above for instruction on creating the user defined baseline).
- Go to "**Gadgets" → "Integrate…",** this brings up the *Data Exploration: "addtool_curve_integ"* window. In the *Integration Tab* set the following:

  Fit Limits To "Data Points"

  Area Type "Mathematical Area" (algebraic sum of trapezoids) or

"Absolute Area" (sum of absolute trapezoid values)

Show

Show Integrated Area Leave checked

Integral Curve None

- **The only parameters you have to change are "Fit limits to" → "Data points" and "Area type" → "Absolute area" (so far for TCA data processing we've always used absolute area), otherwise for the remaining parameters you use the default setup**
- In the *Baseline* tab select the following:

  Mode "Use Existing Dataset"

  Dataset Select the baseline you created (Example: [Graph2]1!2"Baseline of Heat Flux"), **if you don't call it anyway it will be called "Plot 2: Baseline of B"**

  Range "Curve within ROI" (default setup)

- Don't worry about the other tabs and push OK. This will now bring you to your graph and a new yellow box (the ROI box) is shown. All peaks in this box will be integrated and the peak areas summed. Therefore if you wish to have the area of a single peak move the sides of the box to change the range so that only a single peak is integrated.
- The preferential way of moving the box is using the keyboard arrows. You can either decrease or increase the integrated area (the yellow box size) by clicking on the green arrows on the edge of the yellow box and moving them either left or right.
- If you don't see a clear fraction separation and you don't remember your temperature program, go to your raw data file (the Excel file including all the parameters separated in individual columns copied from the text file) and based on the columns called "desired

temperature" and "sample temperature" (the actual temperature) you can figure out the beginning of each temperature fraction.

- At the top of the thermogram the absolute area of the chosen part of the thermogram is provided.
- When you are done with processing of one sample, close the Graph1 and erase the content of columns C and D in Book1 in order to continue with another sample.

Appendix IX: TCA thermogram of syringol (7.9 µg of C) in water; analysis was performed without prior drying with 2 min 40 s purging time

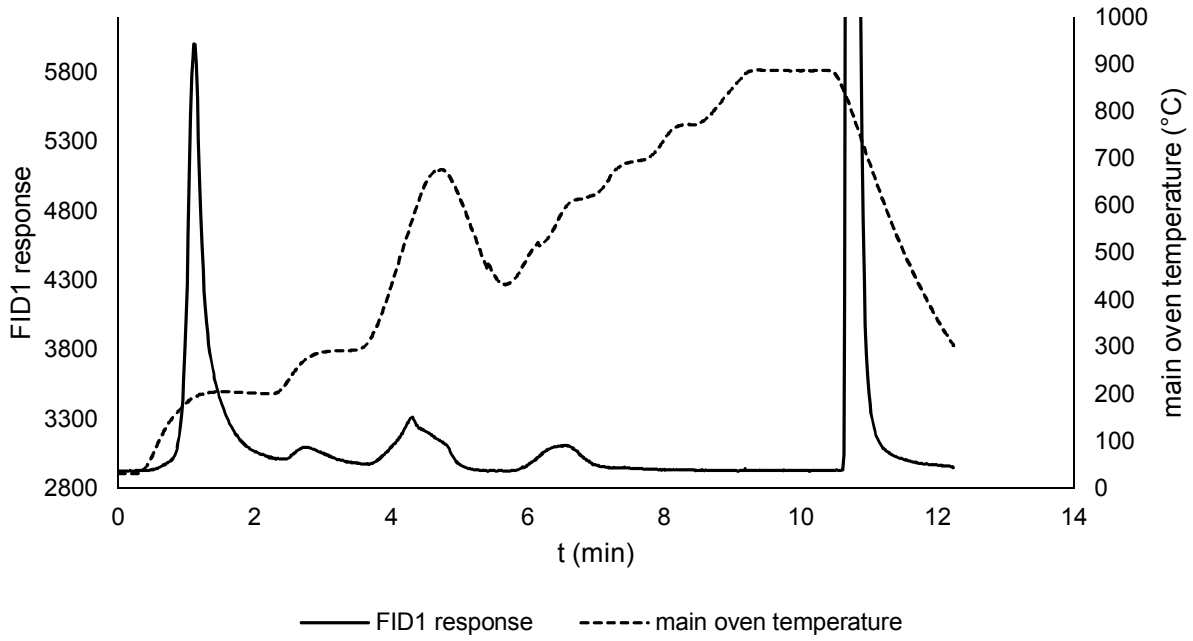

Appendix X: TCA analysis of DCM solvent controls; µg of C evolved at 700 °C and in the oxygenation phase

Analysis parameters	µg of C evolved in TCA temperature fraction	
	700 °C	**550–890 °C w/O_2**
DCM; 5 µL; 4 min drying time; 200 °C initial step	0.7	0.2
	0.4	0.1
DCM; 5 µL; 1.5 min drying time; 200 °C initial step	0.2	0.1
	0.1	0.1
DCM; 5 µL; 1 min drying time; 200 °C initial step	0.3	0.1
	0.1	0.0
DCM; 5 µL; 30 s drying time; 200 °C initial step	0.1	0.1
	0.5	0.1
DCM; 10 µL; 30 s drying time; 200 °C initial step	0.9	0.0
	0.0	0.0
DCM; 2.5 µL; 30 s drying time; 200 °C initial step	0.1	0.2
	0.2	0.1
DCM; 5 µL; 30 s drying time; 100 °C initial step	0.6	0.1
	0.0	0.0
DCM; 5 µL; 30 s drying time; 300 °C initial step	0.1	0.0
	0.1	0.0

Appendix XI: Interday evaluation of TCA blanks; a) filter blank, b) 5 µL of DCM, c) 10 µL of DCM. 2 min 30 s purging time and 30 s drying time (DCM blanks) was used.

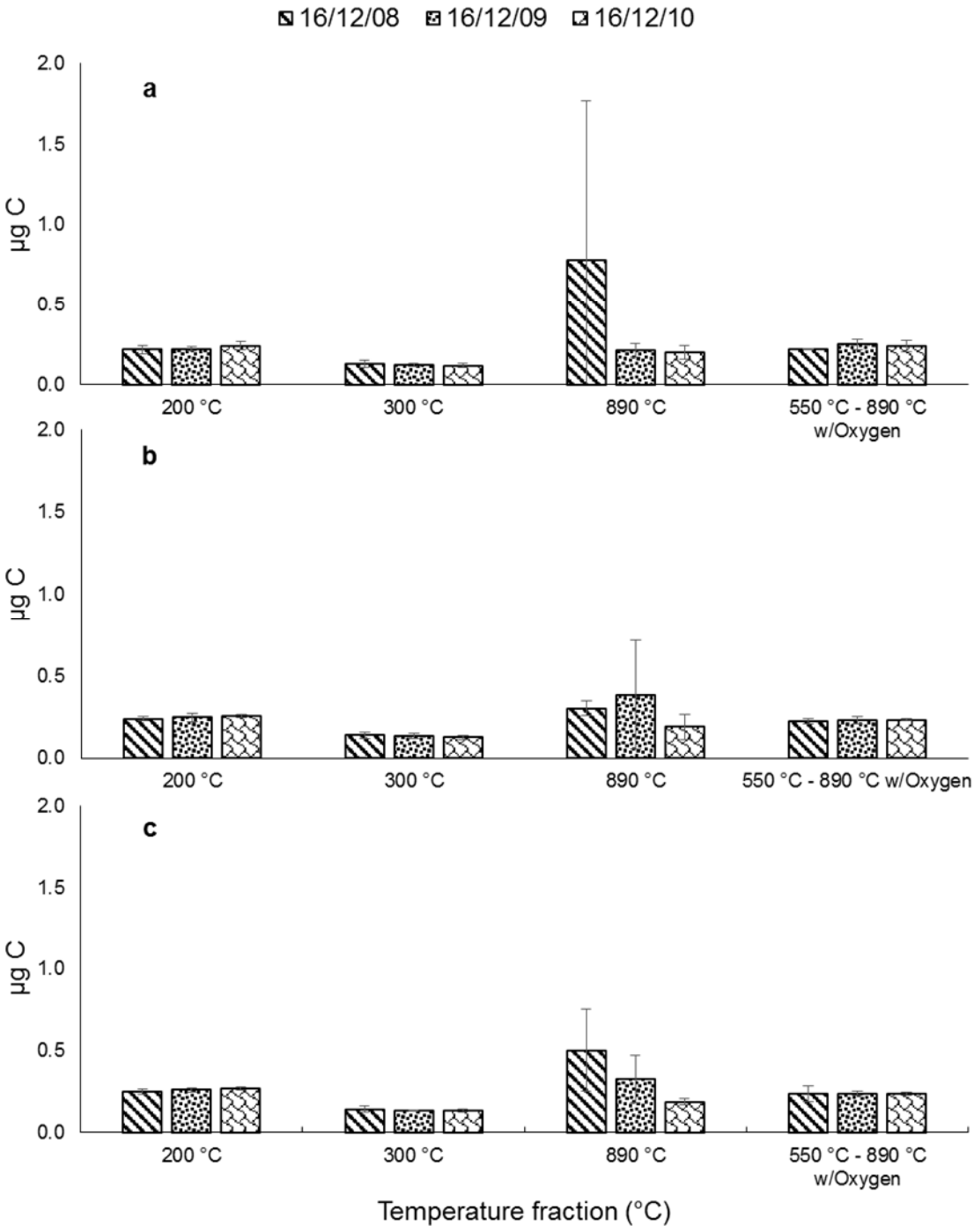

Appendix XII: Blank evaluation, intraday comparison 12/10/16; 200 °C initial step

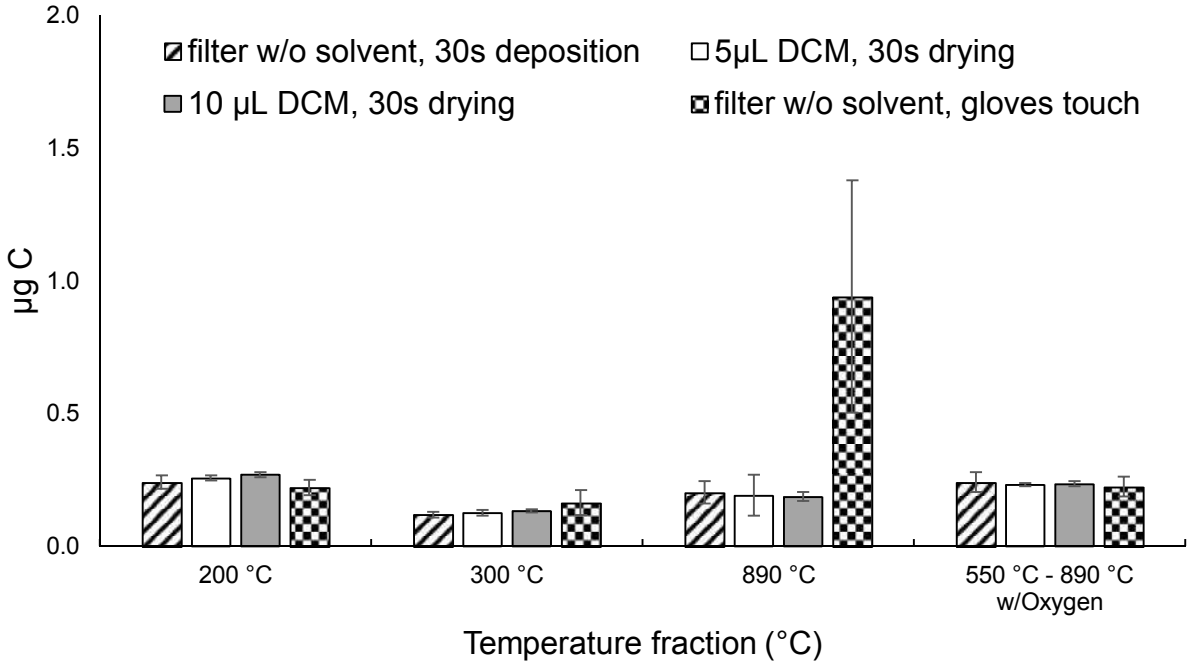

Appendix XIII: TCA profiles of a) syringol, b) methylguaiacol, c) guaiacol. Approximately 20 µg of C was introduced. Solutions were prepared in DCM and dried for 4 min at 40 °C. 2 min 30 s purging time was used.

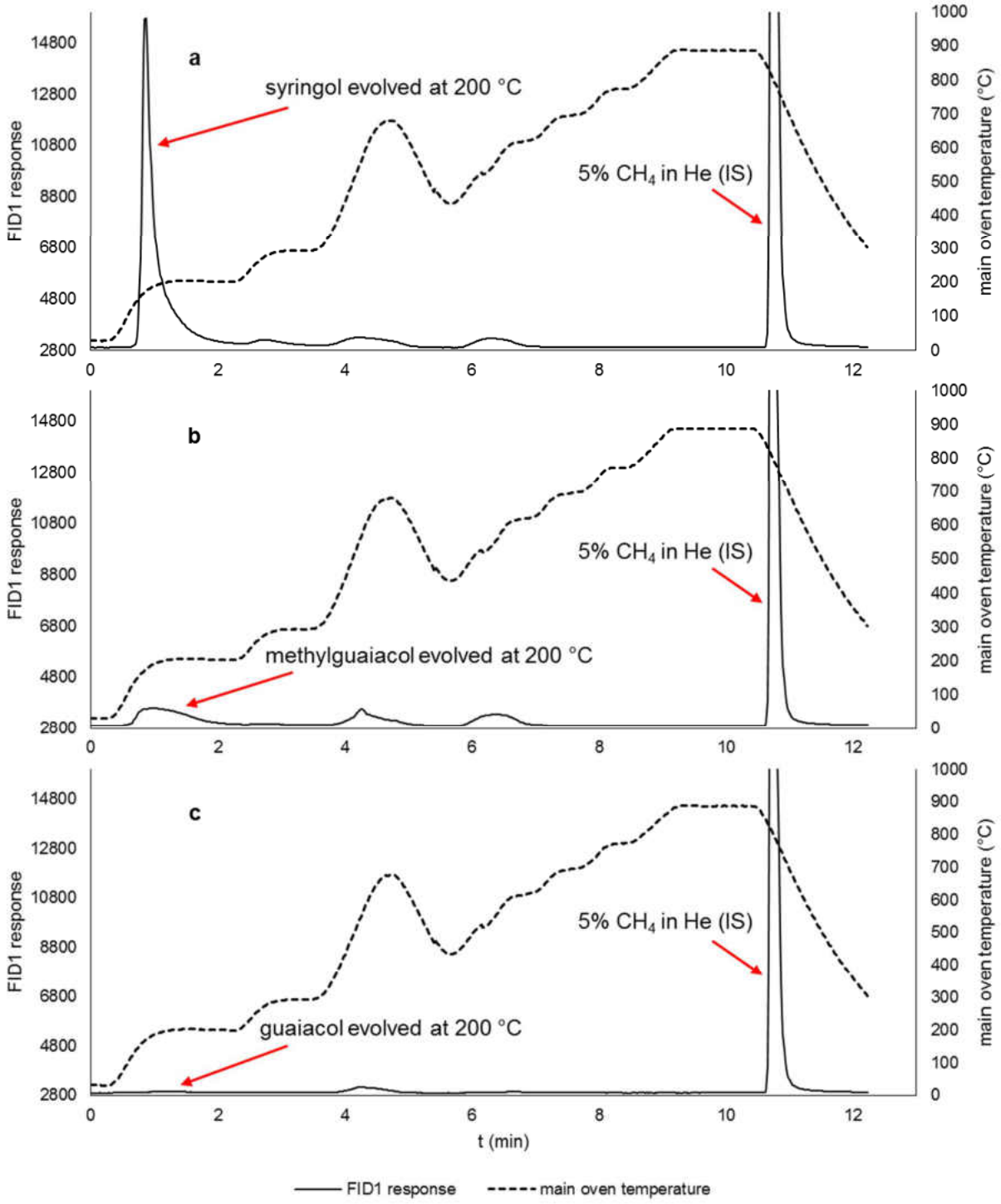

Appendix XIV: TCA thermogram of phenol in water (20.2 µg of C); no drying, 4 s total purging time, blower constant 0

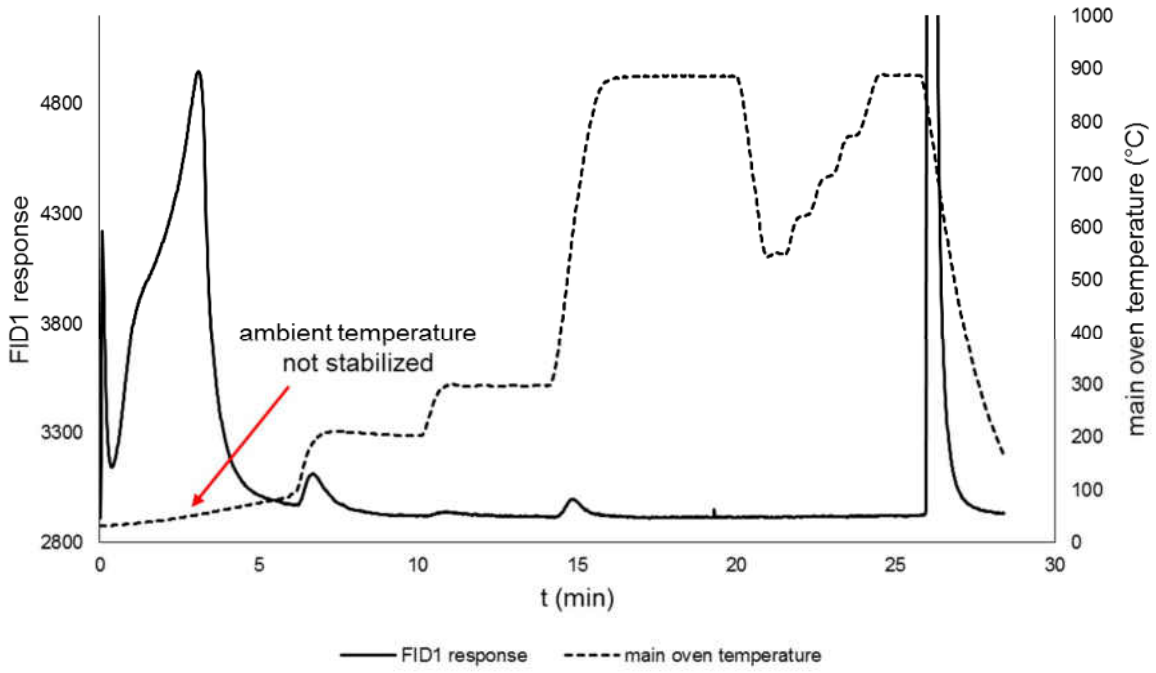

Appendix XV: TCA thermogram of phenol in water (20.2 µg of C); no drying, 4 s total purging time, blower constant 8

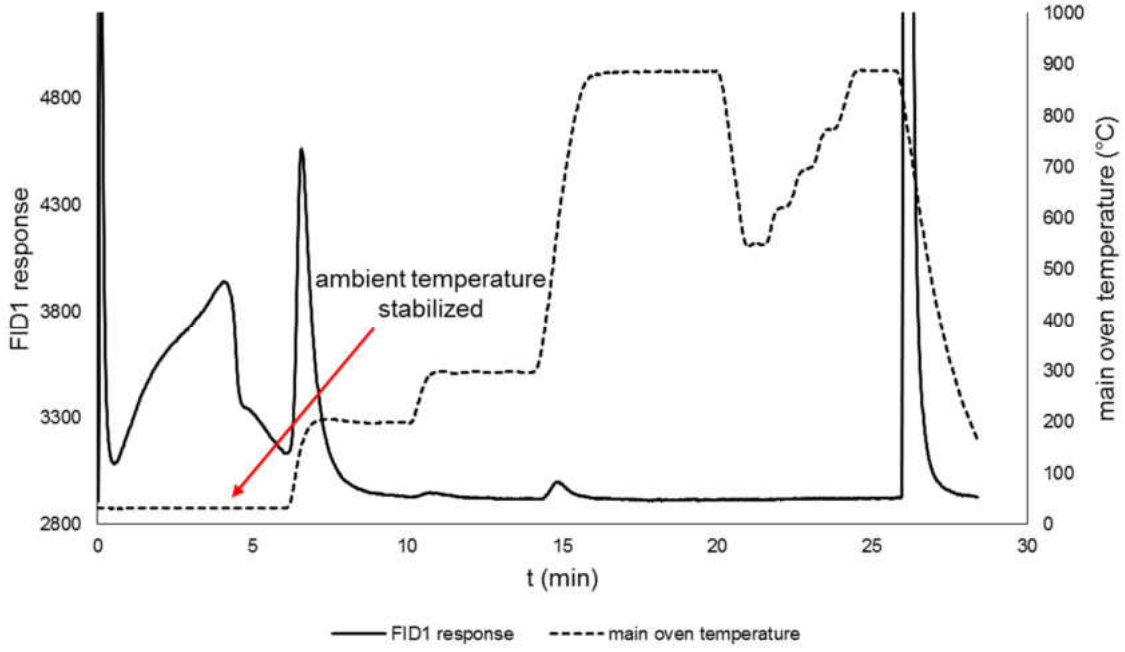

Appendix XVI: TCA mequinol in DCM thermogram (20.1 µg of C); 30 s drying at 40 °C, 4 s total purging time

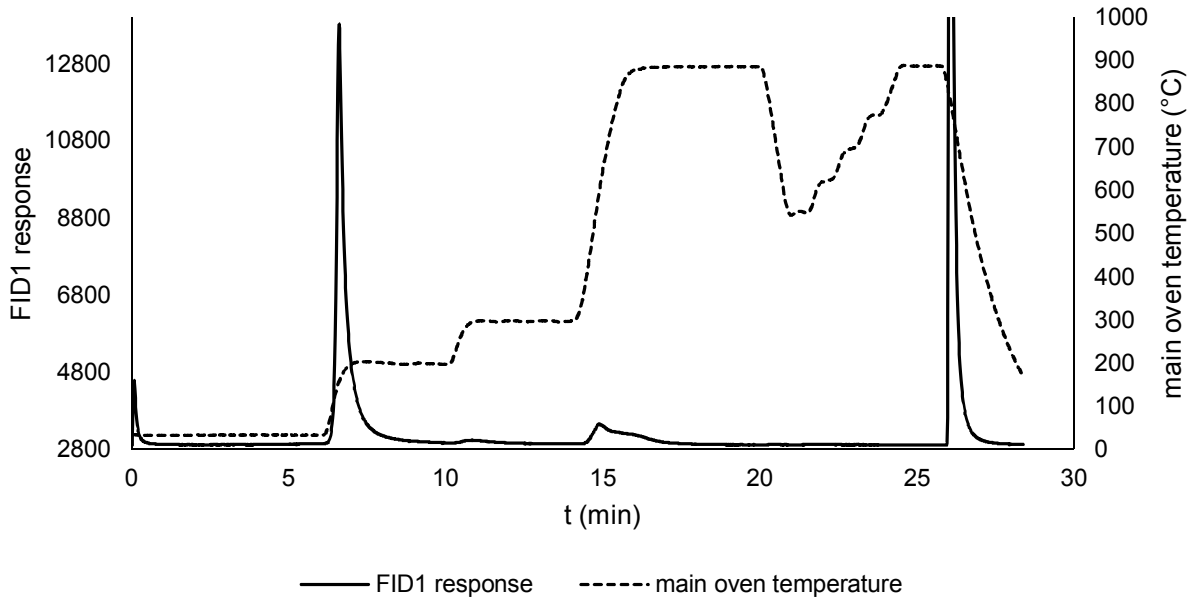

Appendix XVII: TCA thermogram of a) pure solid alkali lignin with 6 min 890 °C w/o O_2 step (37.8 µg of C), b) solid alkali lignin hydrotreated at 300 °C w/µNi without the extract filtration with 12 min 890 °C w/o O_2 step (12.2 µg of C)

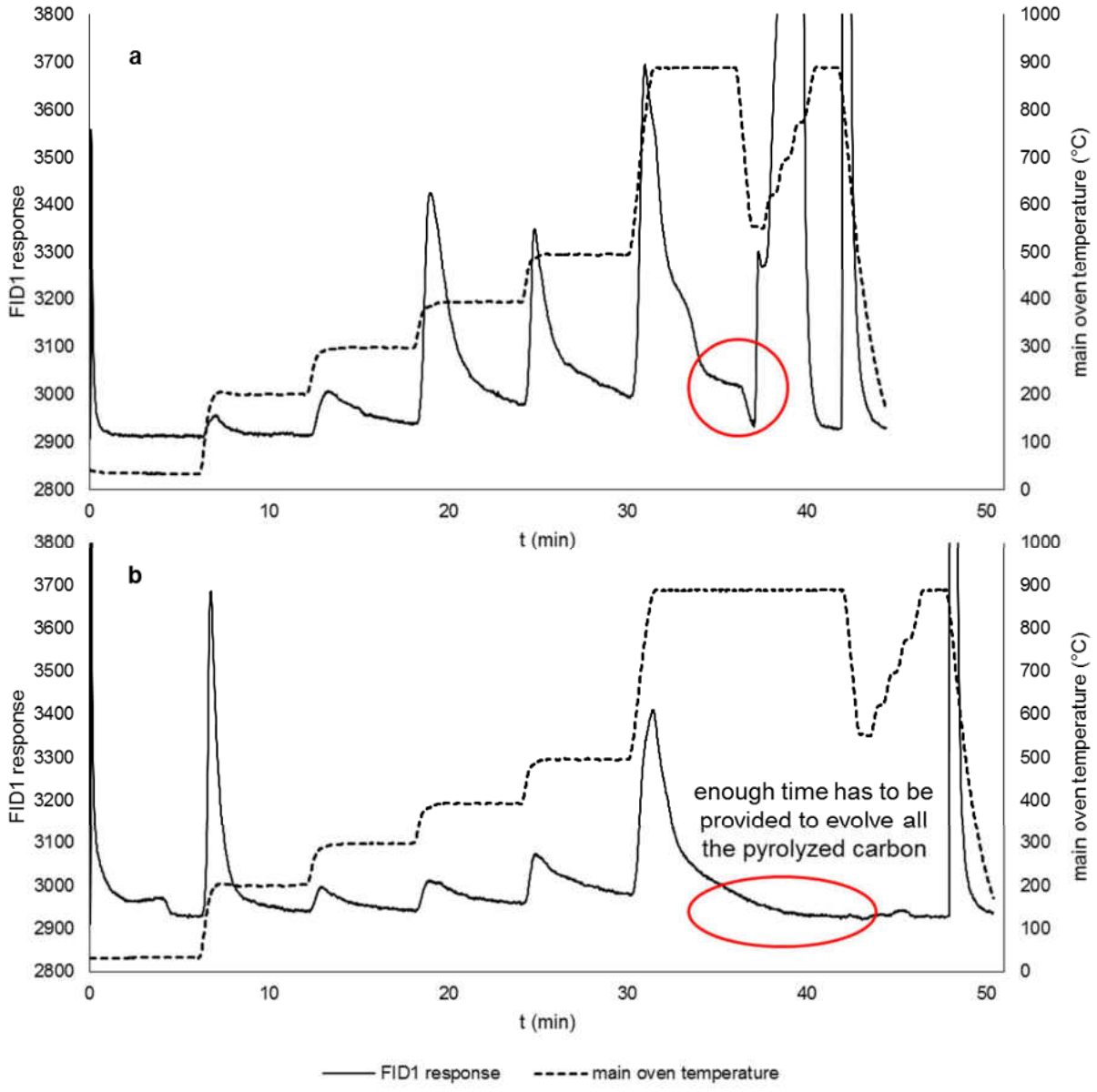

Appendix XVIII: TGA profile of solid alkali lignin analyzed in triplicate (average loading 20.3 µg of lignin); solid lines represent the oven temperature, dash lines represent the individual mass losses.

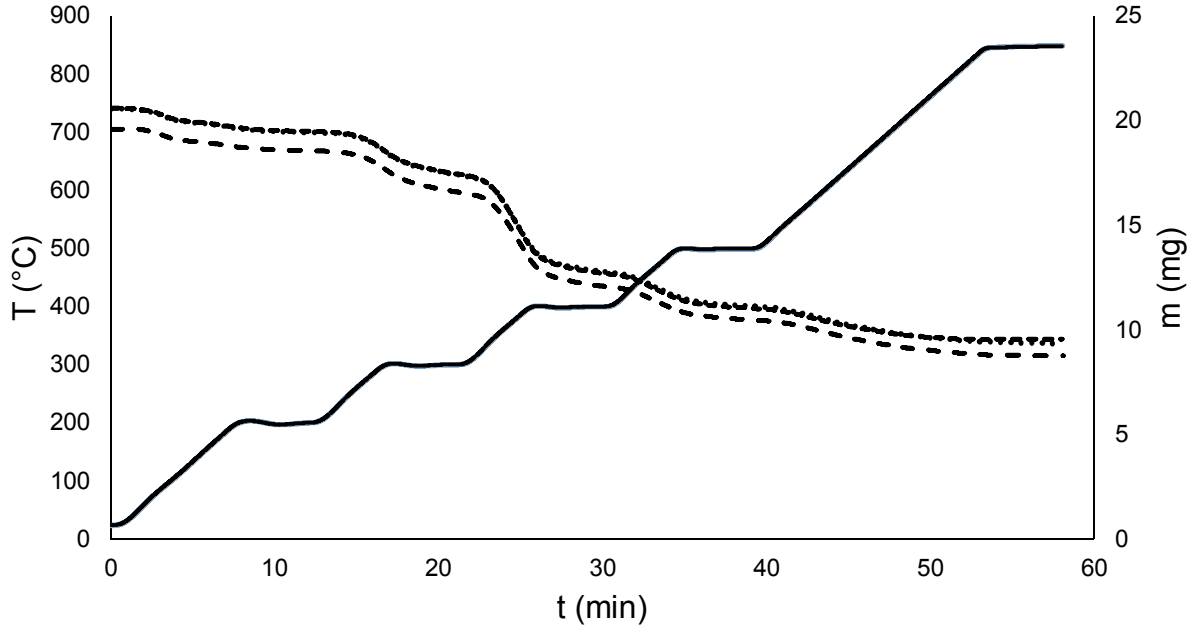

Appendix XIX: Lignin repolymerization evaluated by TCA; lignin dissolved in water at 25 °C, a) day 1, b) day 13, c) day 20

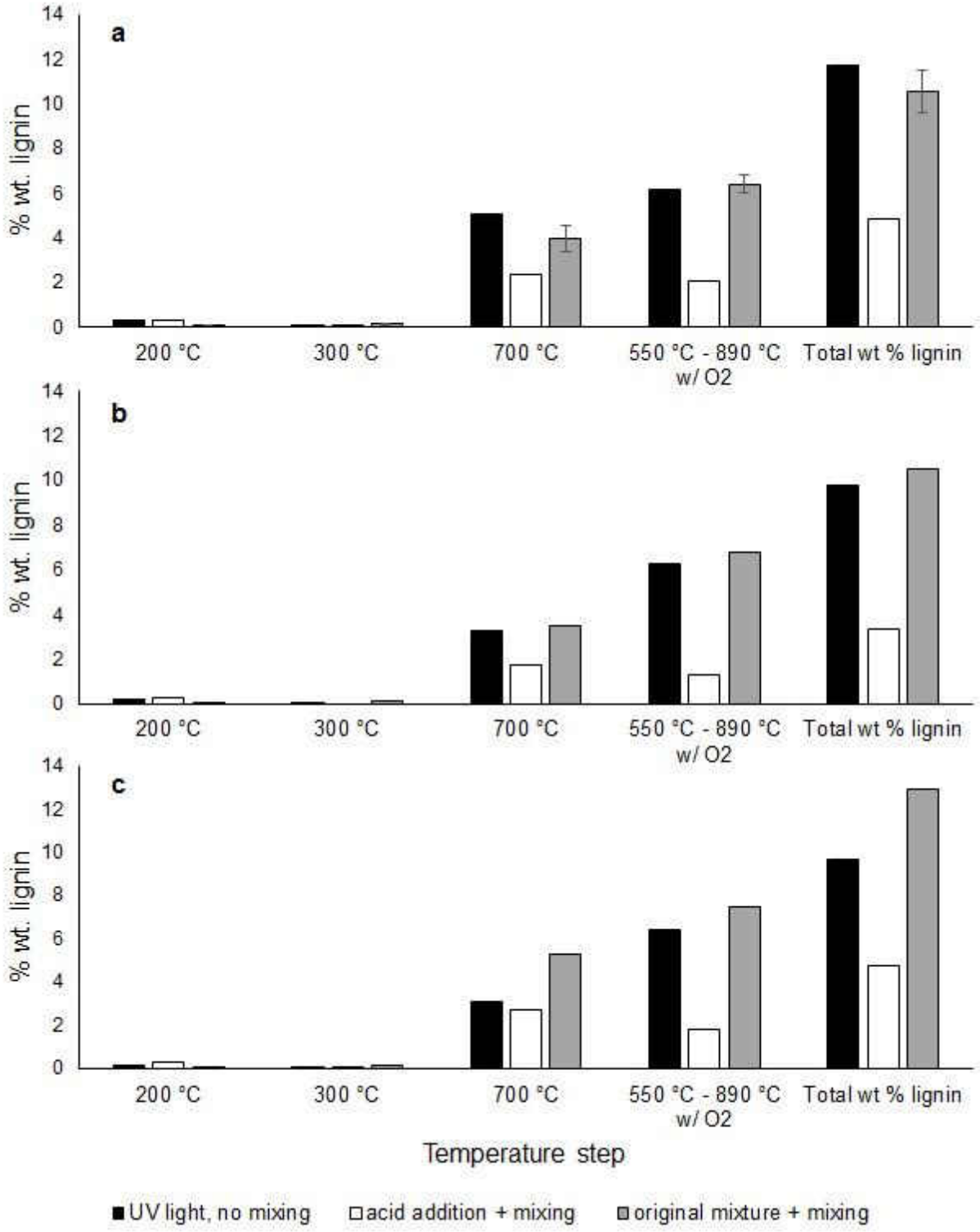

Appendix XX: Lignin repolymerization evaluated by TCA; lignin dissolved in MeOH/water 5:2 (v/v) at 25 °C, a) day 1, b) day 13, c) day 20

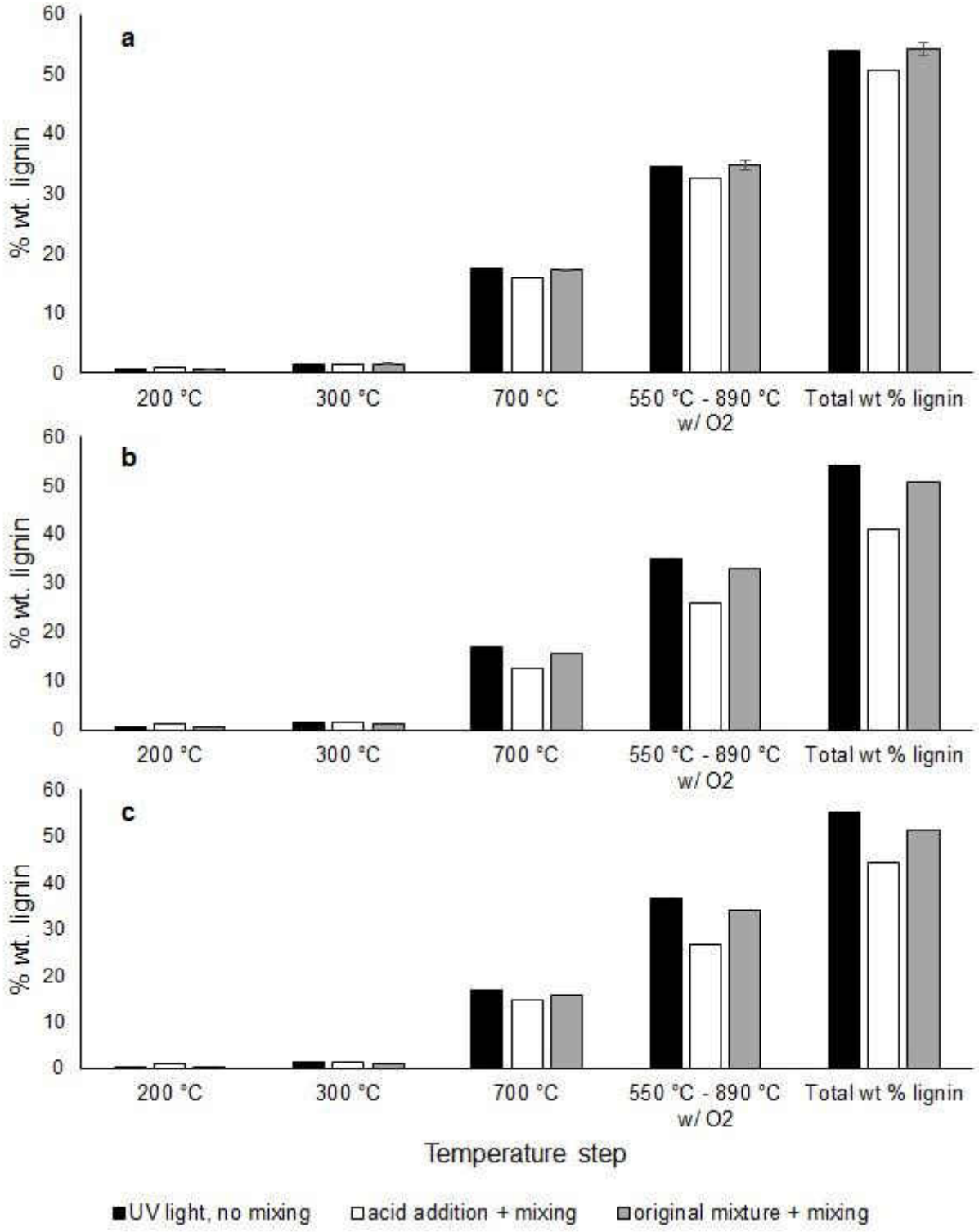

Appendix XXI: Lignin repolymerization evaluated by TCA; lignin treated in water at 300 °C, a) day 1, b) day 13, c) day 20

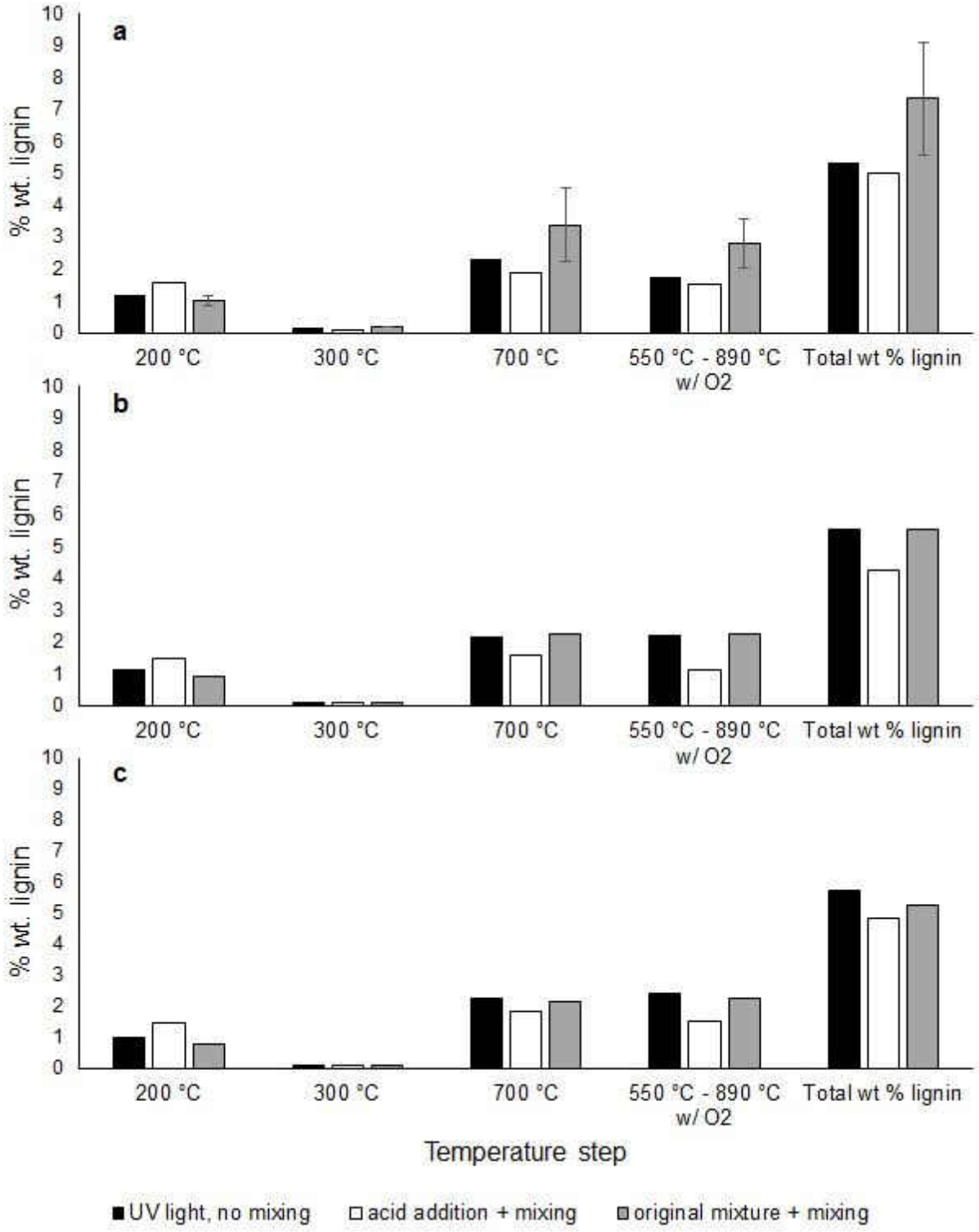

Appendix XXII: Lignin repolymerization evaluated by TCA; lignin treated in MeOH/water 5:2 (v/v) at 300 °C, a) day 1, b) day 13, c) day 20

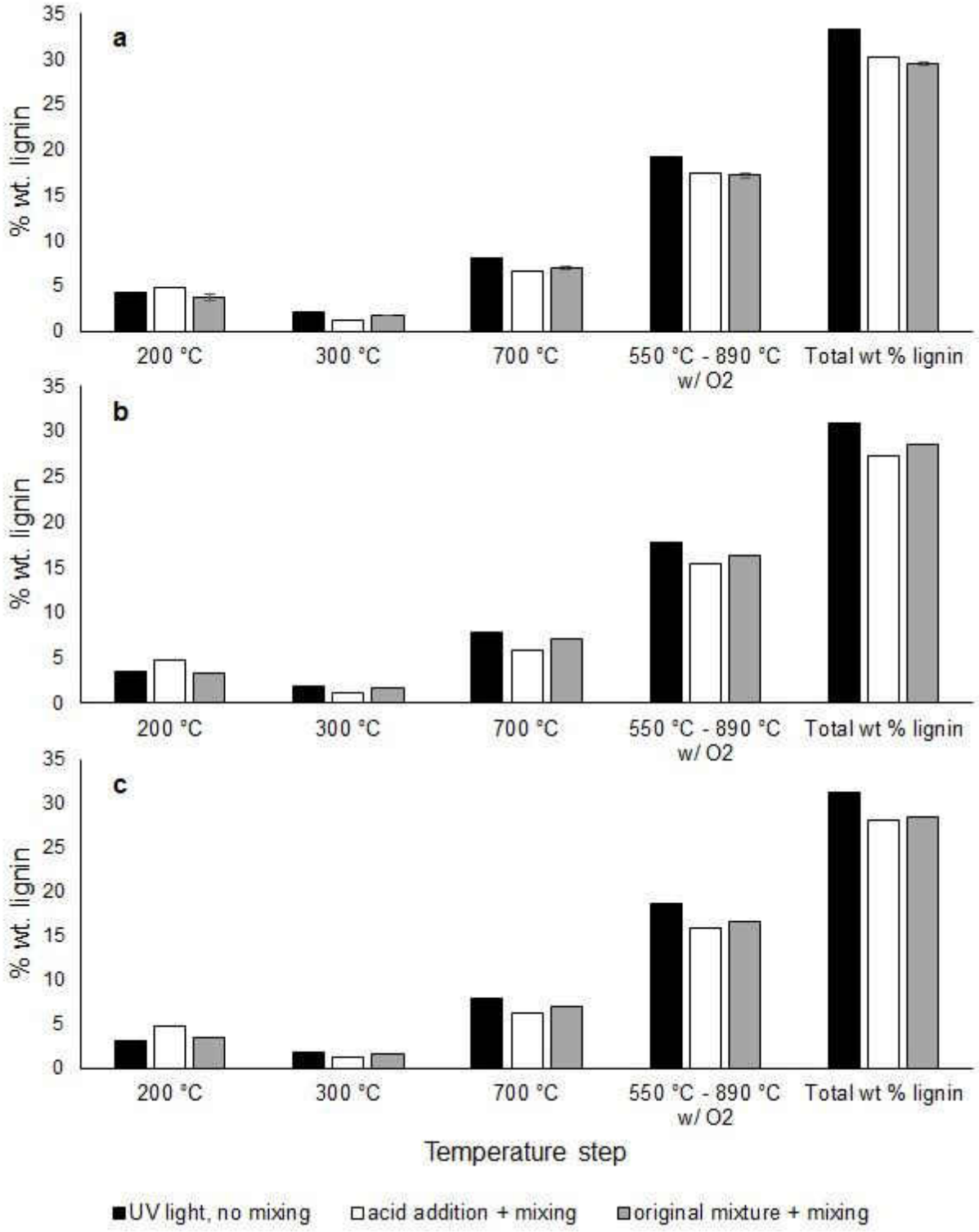

Appendix XXIII: Lignin repolymerization evaluated by TCA; lignin dissolved in THF at 25 °C, a) day 1, b) day 13, c) day 20

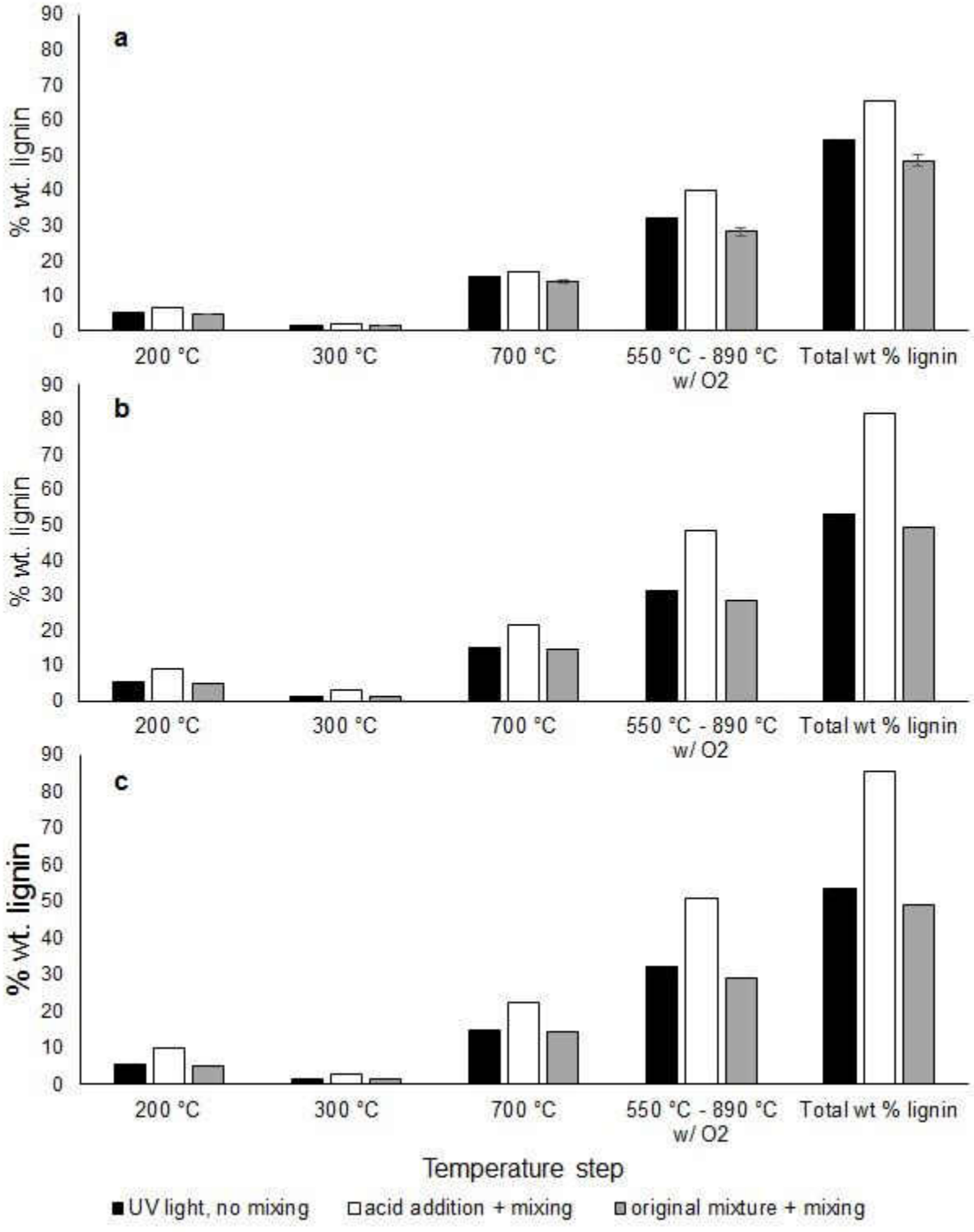

Appendix XXIV: Lignin repolymerization evaluated by TCA; lignin dissolved in ACN/water 1:1 (v/v) at 25 °C, a) day 1, b) day 13, c) day 20

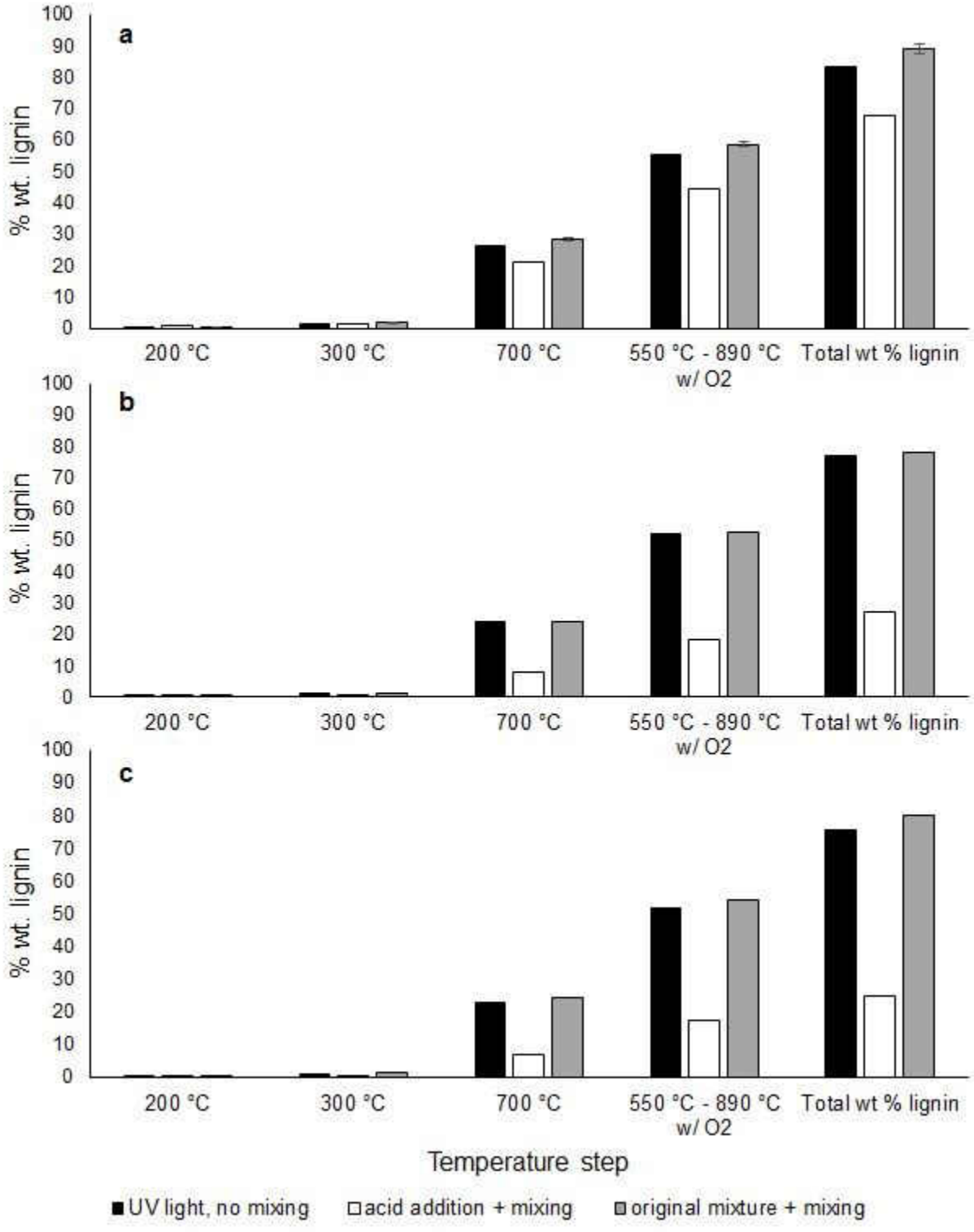

Appendix XXV: Mass spectrum of bicreosol (*m/z* 274); synthetized lignin standard

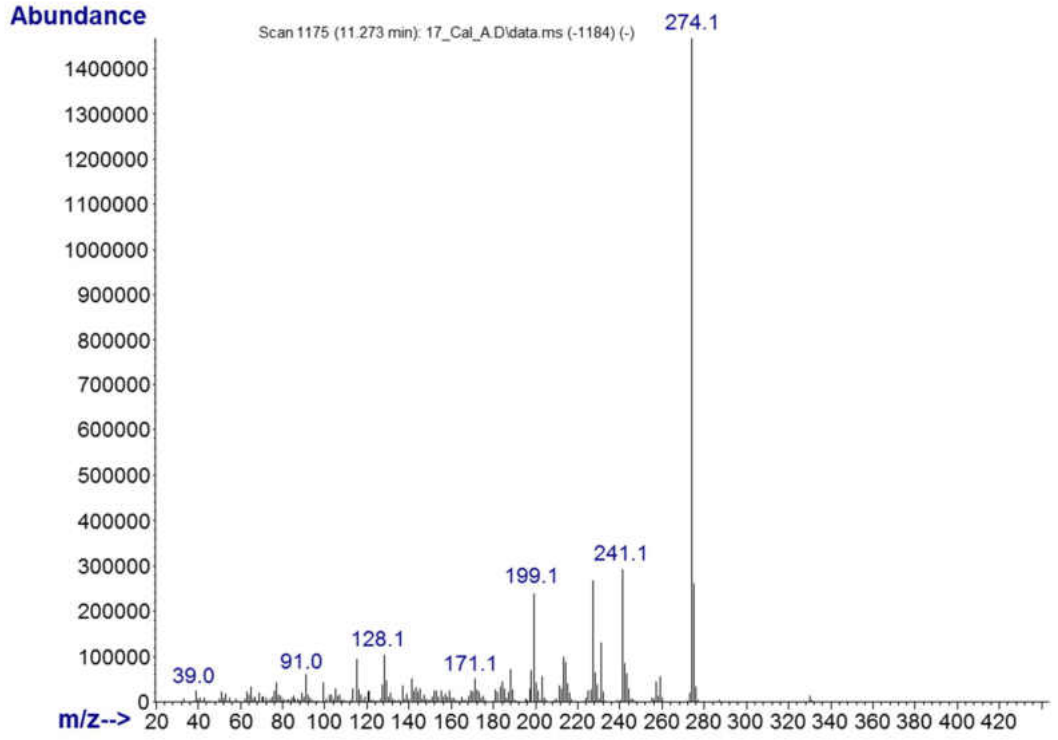

Appendix XXVI: Mass spectrum of TD-14 (*m/z* 272); synthetized lignin standard

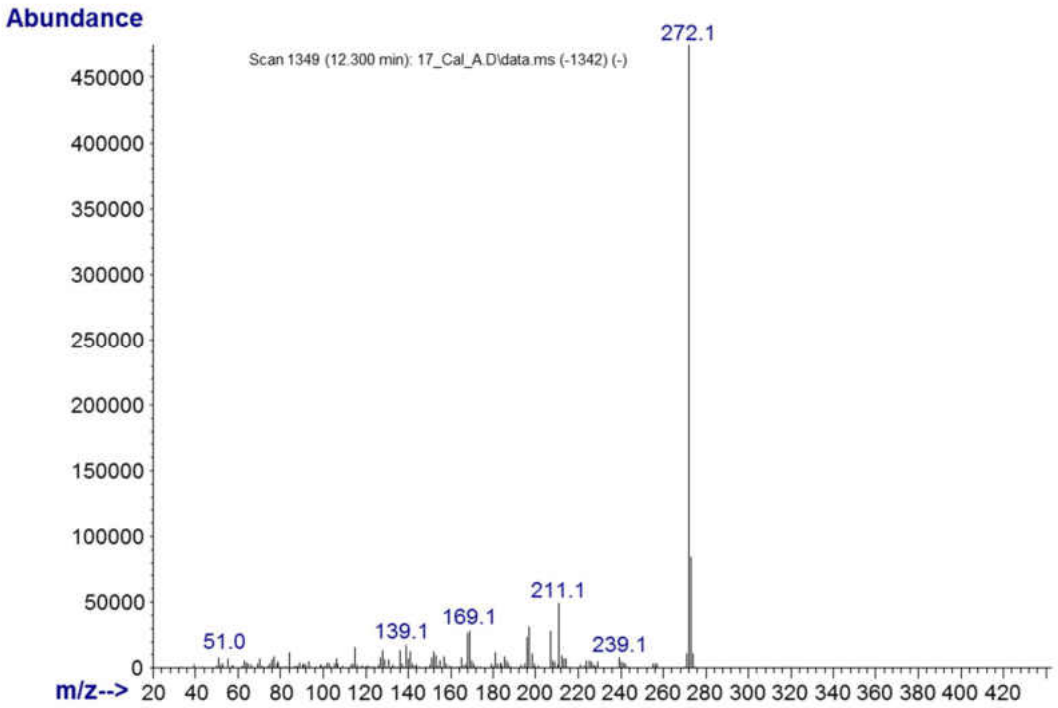

Appendix XXVII: Mass spectrum of diguaiacylethane (*m/z* 274); lignin degradation product

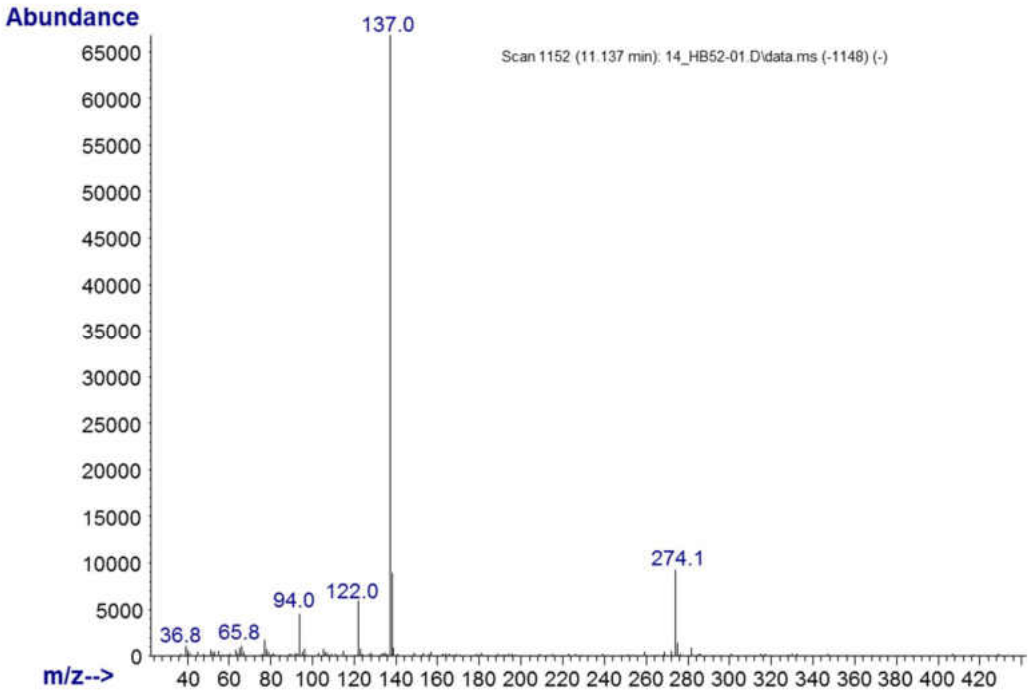

Appendix XXVIII: Mass spectrum of diguaiacylethene (*m/z* 272); lignin degradation product

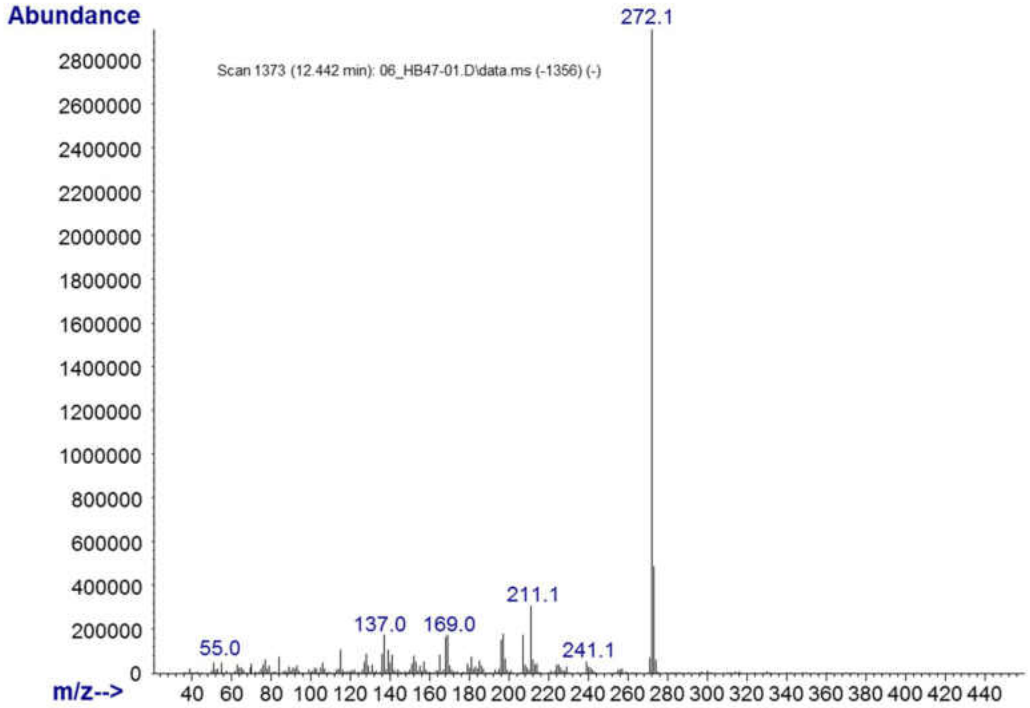

Appendix XXIX: Py-GC-MS profile of guaiacol spiked on the glass wool, a) guaiacol (109, 124, 81), b) benzodioxole (121, 122, 63); 5 µL (20 µg) of sample was loaded. The analysis was performed in 50:1 split ratio.

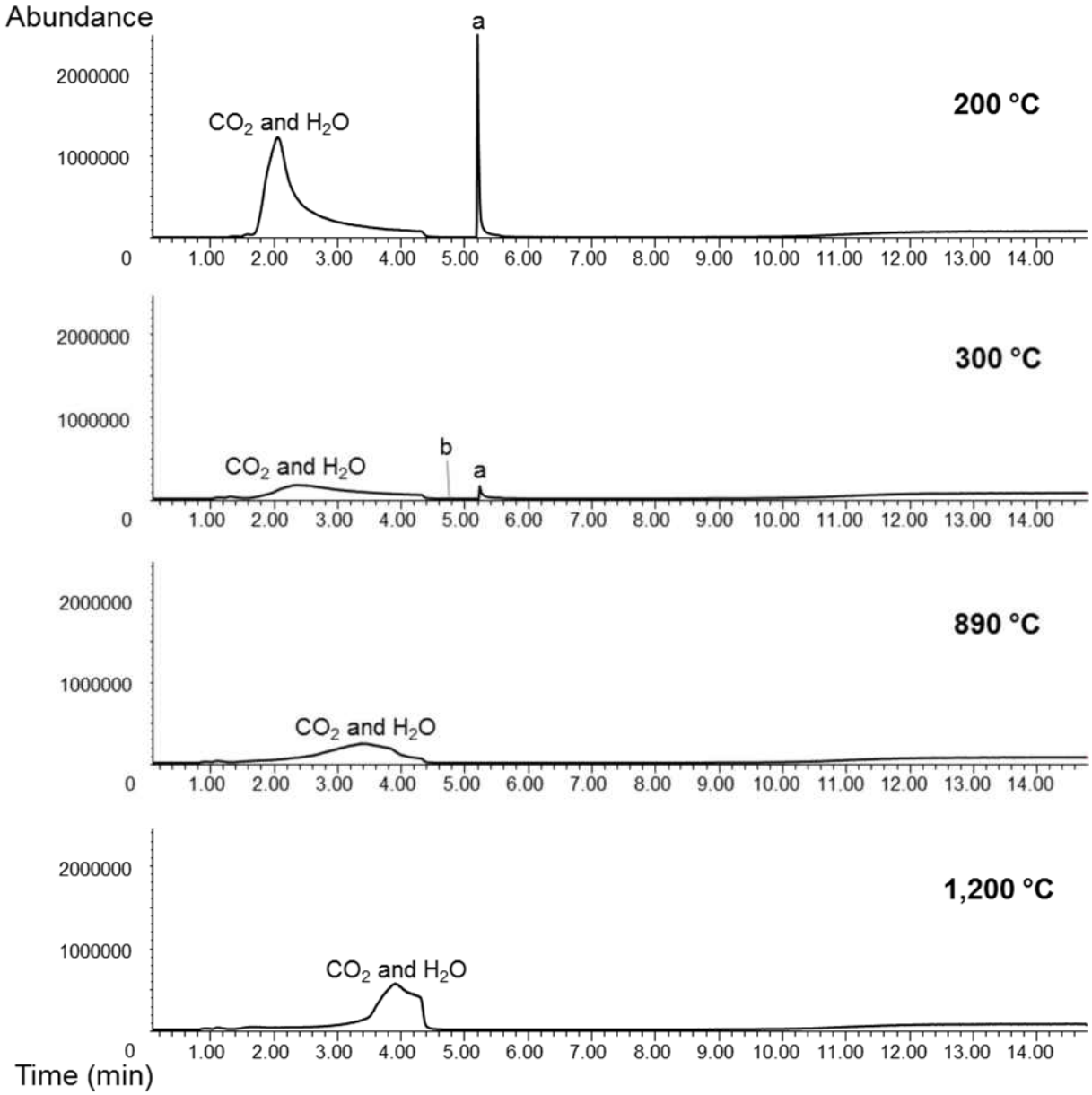

Appendix XXX: Py-GC-MS profile of mequinol spiked on the glass wool, a) mequinol (109, 124, 81), b) dimethoxybenzene (123, 138, 95); 5 µL (20 µg) of sample was loaded. The analysis was performed in 50:1 split ratio.

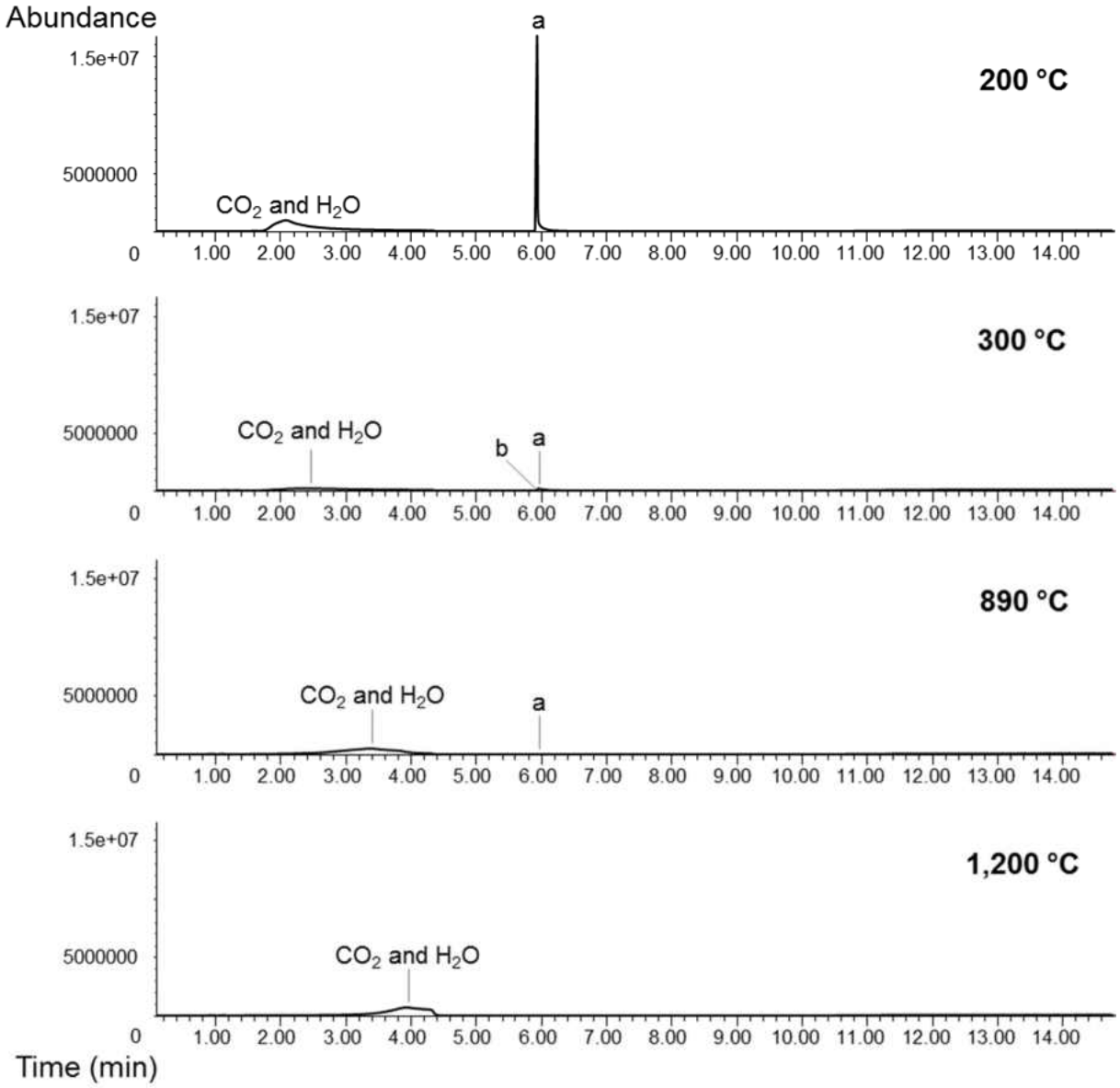

Appendix XXXI: Py-GC-MS profile of syringol spiked on the glass wool, a) syringol (154, 139, 111, 96), b) methylenedioxyanisole (152, 151, 107, 137), c) trimethoxybenzene (168, 153, 110, 125); 5 µL (20 µg) of sample was loaded. The analysis was performed in 50:1 split ratio.

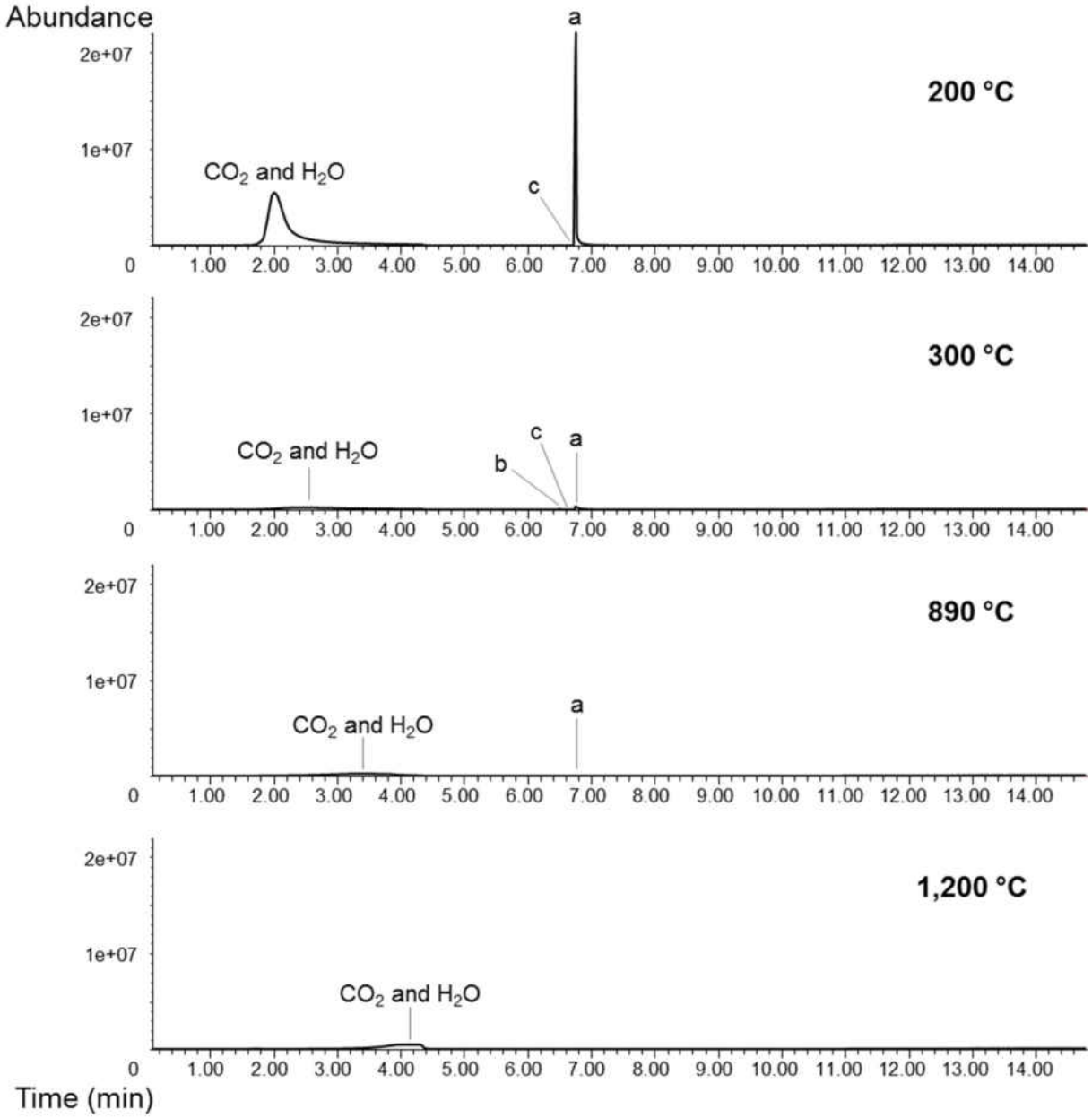

Appendix XXXII: Py-GC-MS profile of levoglucosan spiked on the glass wool, a) levoglucosan (60, 73, 57); 5 µL (20 µg) of sample was loaded. The analysis was performed in 50:1 split ratio.

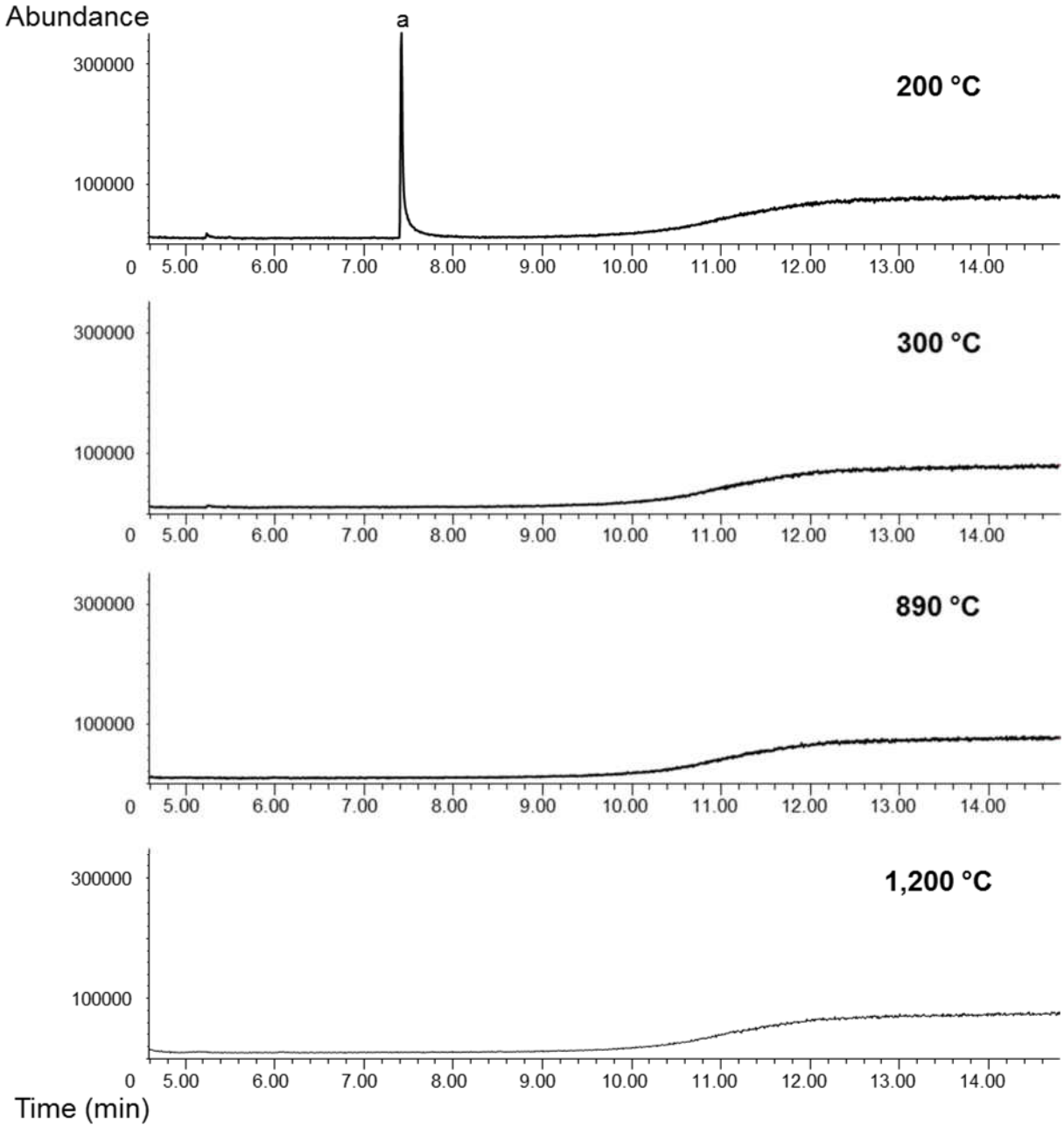

Appendix XXXIII: TCA vs. Py-GC-MS comparison of %rel. of evolved C (mass) of lignin model compounds; The amount of C introduced in mequinol and syringol was approximately 4 µg (1 µL spiked), for levoglucosan 12 µg (3 µl spiked). The analysis was performed using 10:1 split ratio.

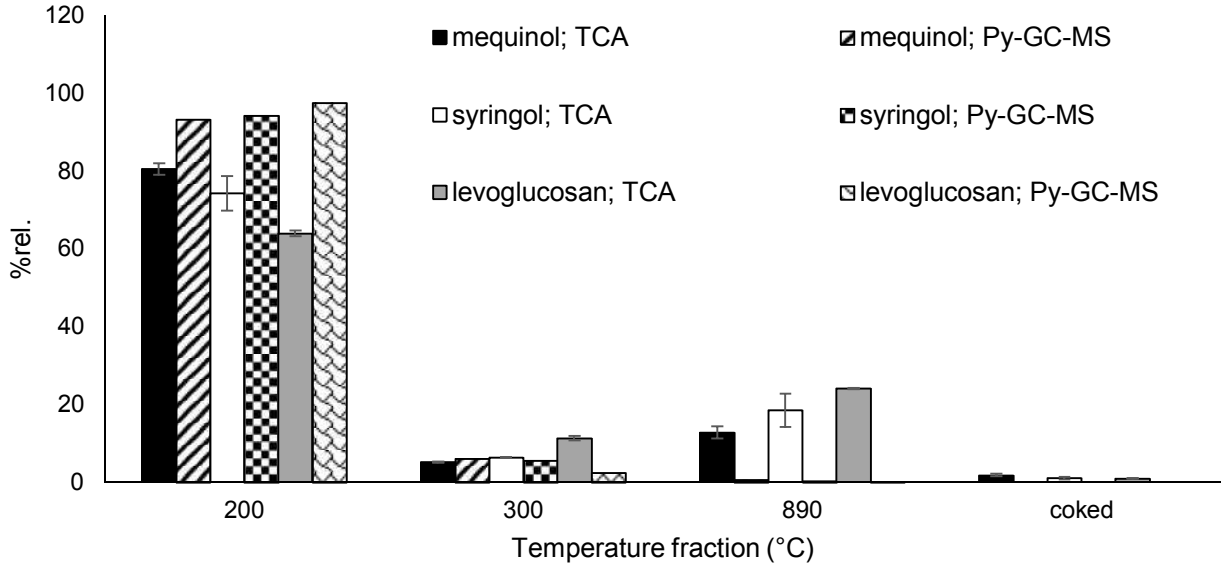

Appendix XXXIV: Py-GC-MS profile of vanillic acid spiked on the glass wool, a) vanillic acid (168, 153, 97, 125), b) guaiacol (190, 124, 81), c) methylester of vanillic acid (151, 182, 123), d) methylester of dimethoxybenzoic acid (165, 196, 168); 5 µL (20 µg) of sample was loaded. The analysis was performed in 50:1 split ratio.

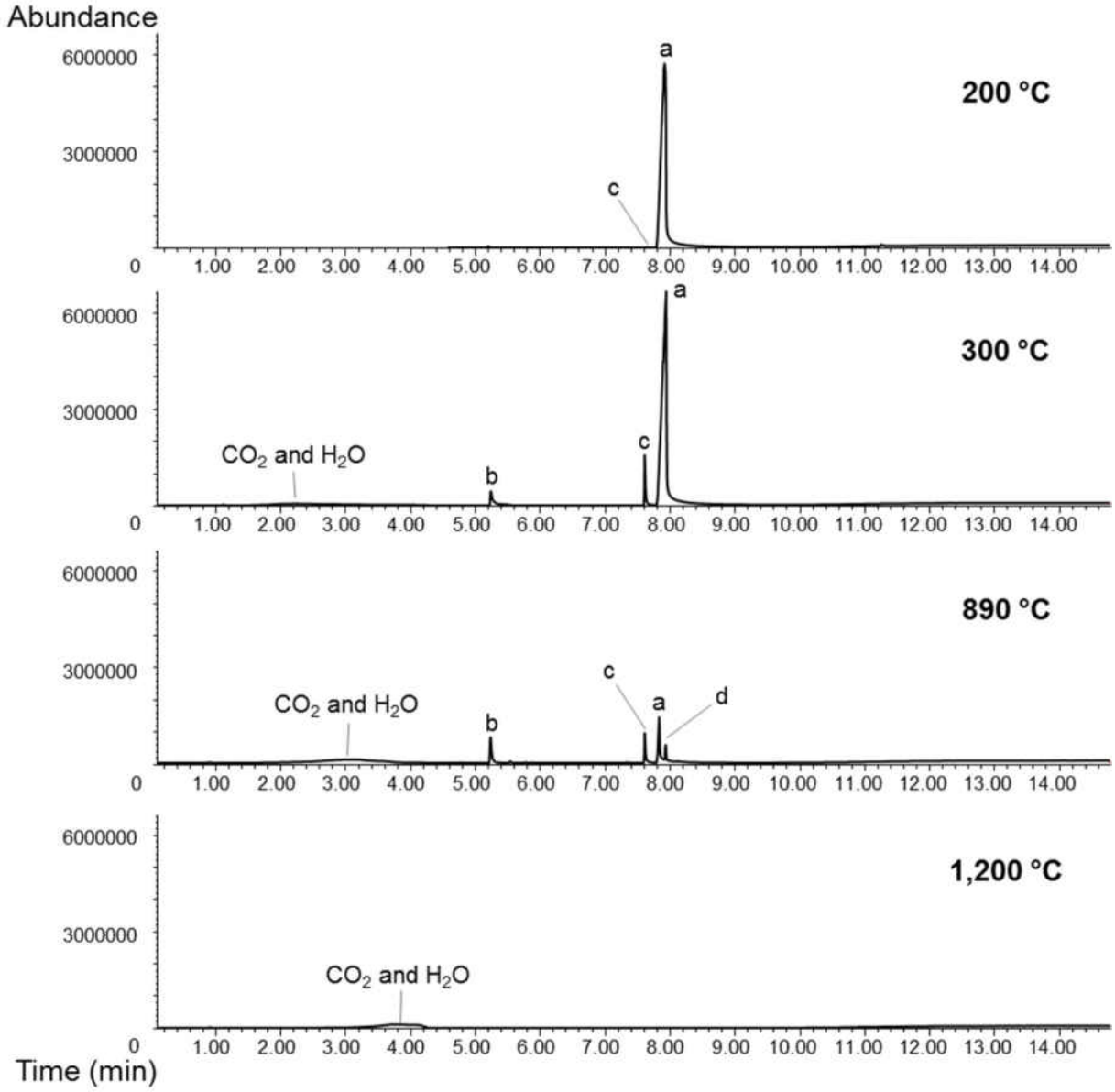

Appendix XXXV: Py-GC-MS profile of bicreosol spiked on the glass wool, a) bicreosol (274, 241, 227), b) not identified (256, 288, 241, 213), c) not identified (272, 227, 199), d) not identified (272, 257, 214, 229); 5 µL (20 µg) of sample was loaded. The analysis was performed in 50:1 split ratio.

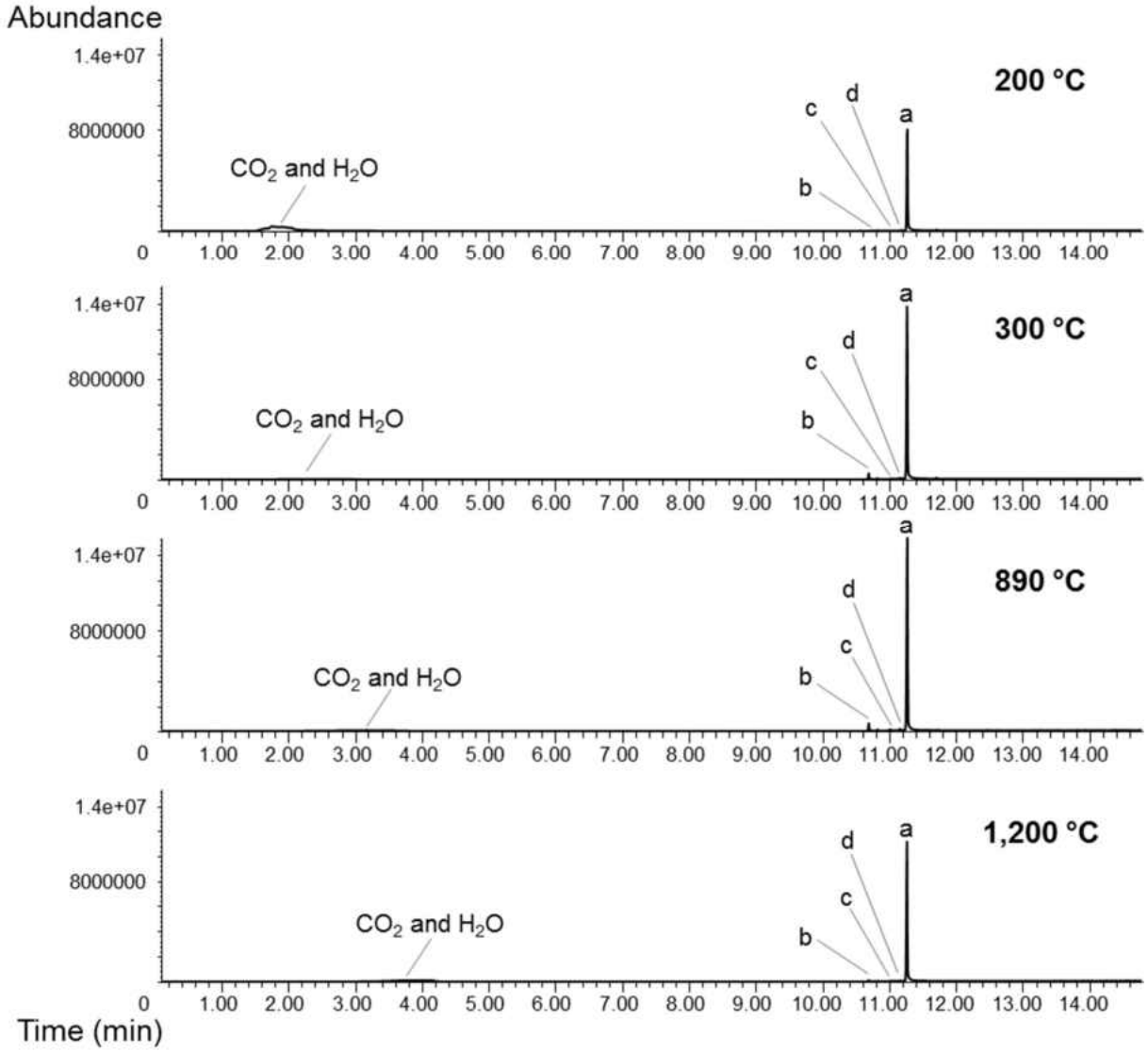

Appendix XXXVI: Py-GC-MS analysis of solid alkali lignin; extracted *m/z* 18 and 44

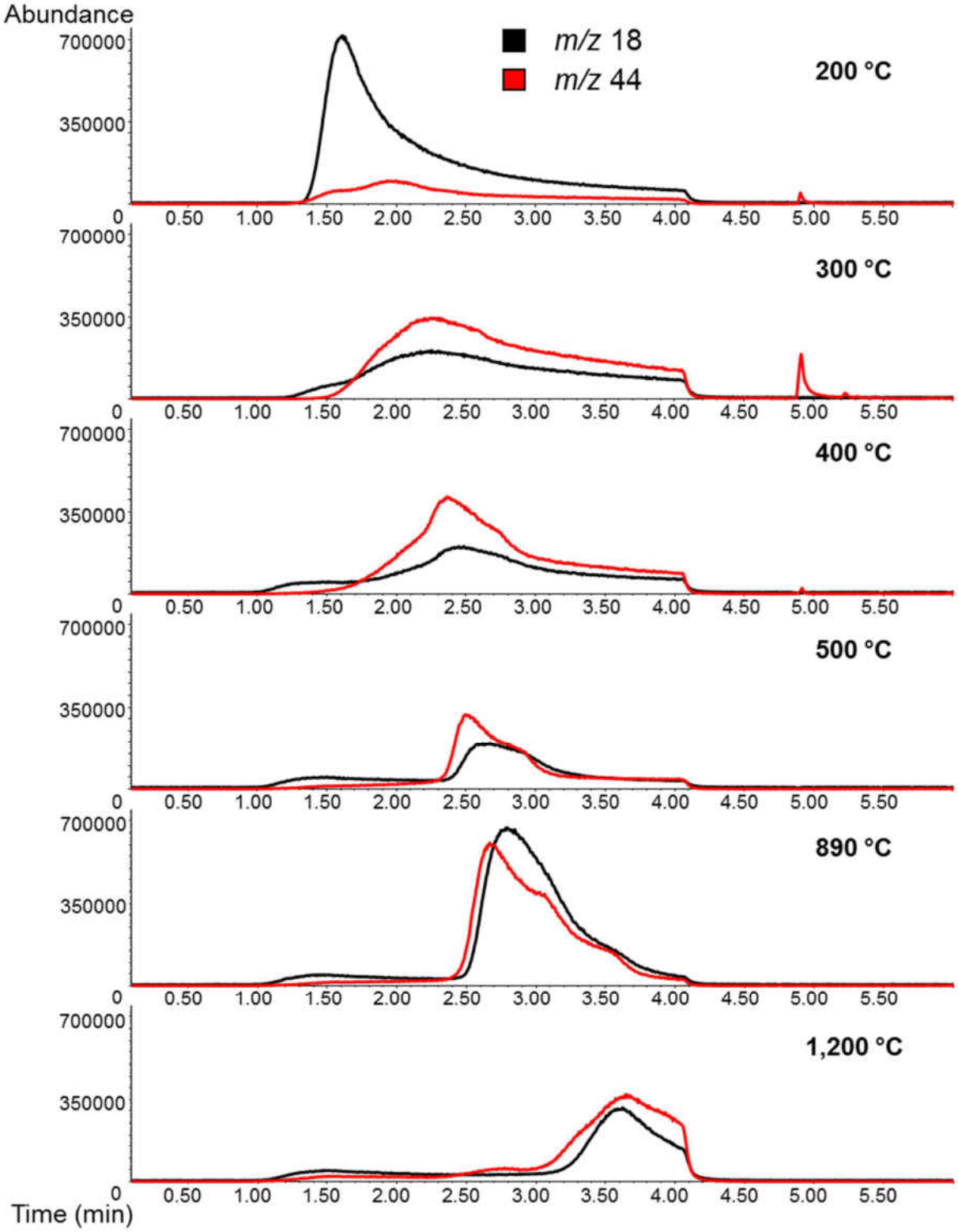

Appendix XXXVII: Py-GC-MS analysis of solvent control (water); extracted *m/z* 18 and 44

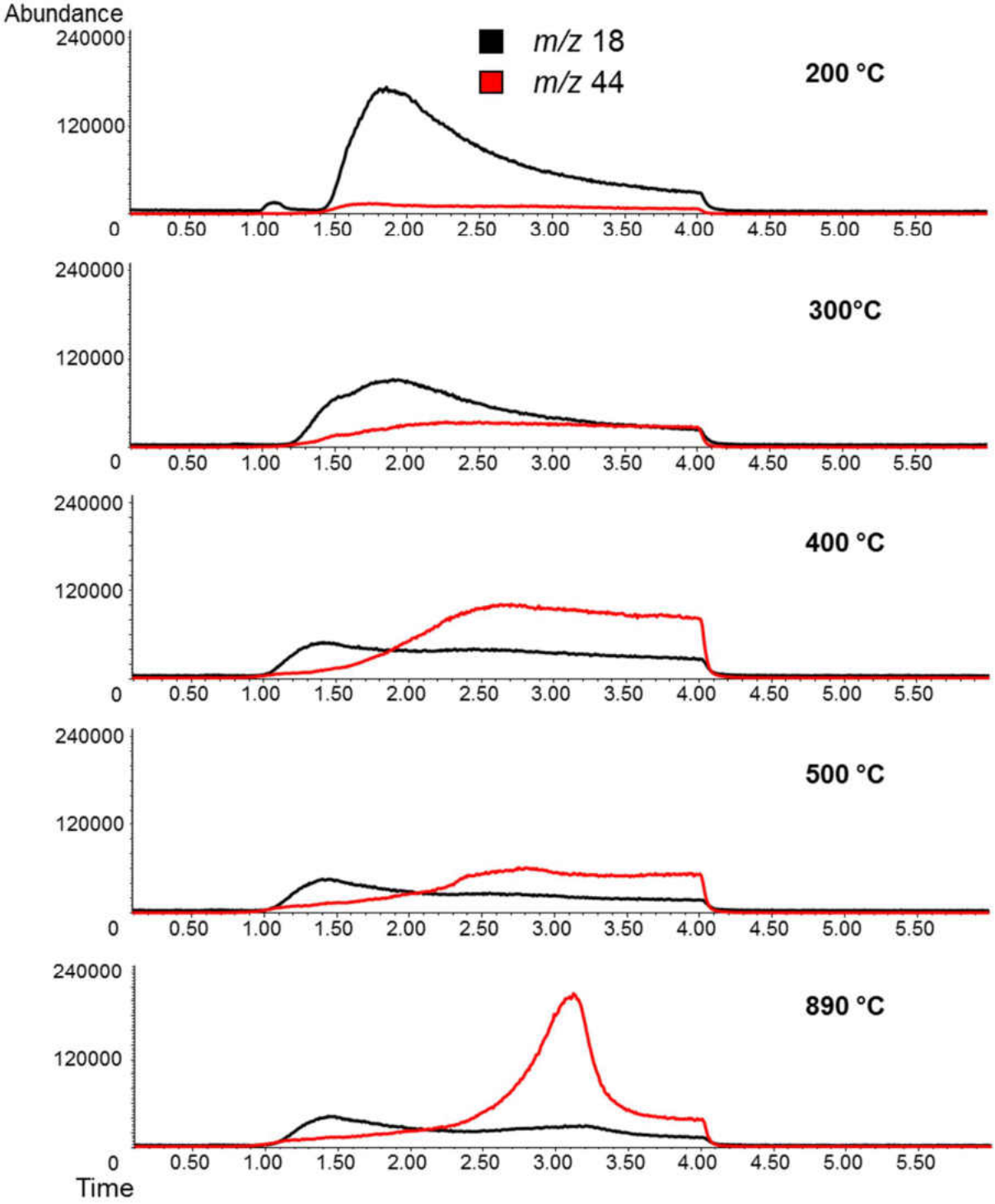

Appendix XXXVIII: Py-GC-MS analysis of solid alkali lignin; extracted *m/z* 137

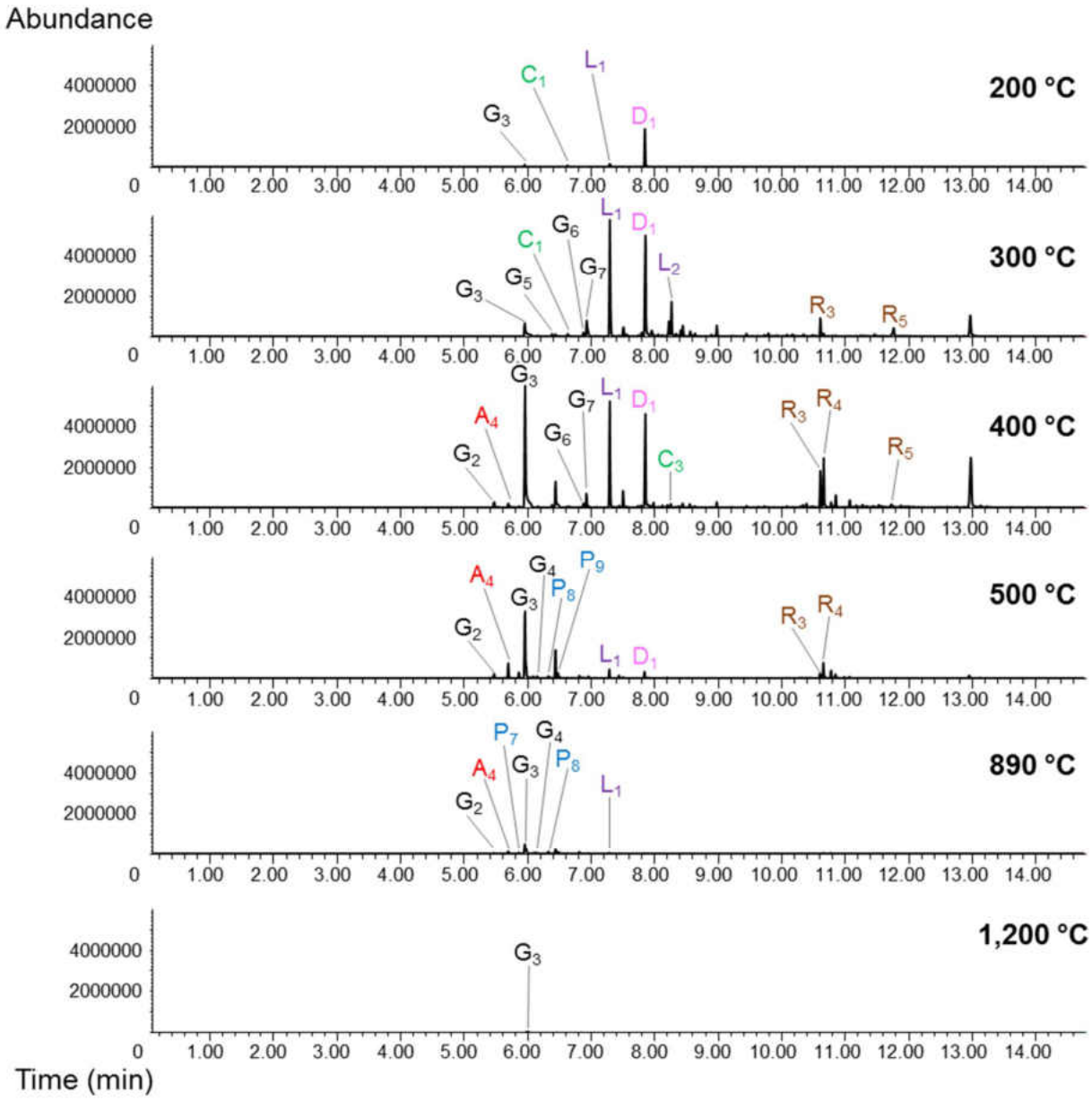

Appendix XXXIX: Py-CG-MS (% of normalized peak areas) vs. TCA (%rel. of C evolved) comparison of solid alkali lignin analysis

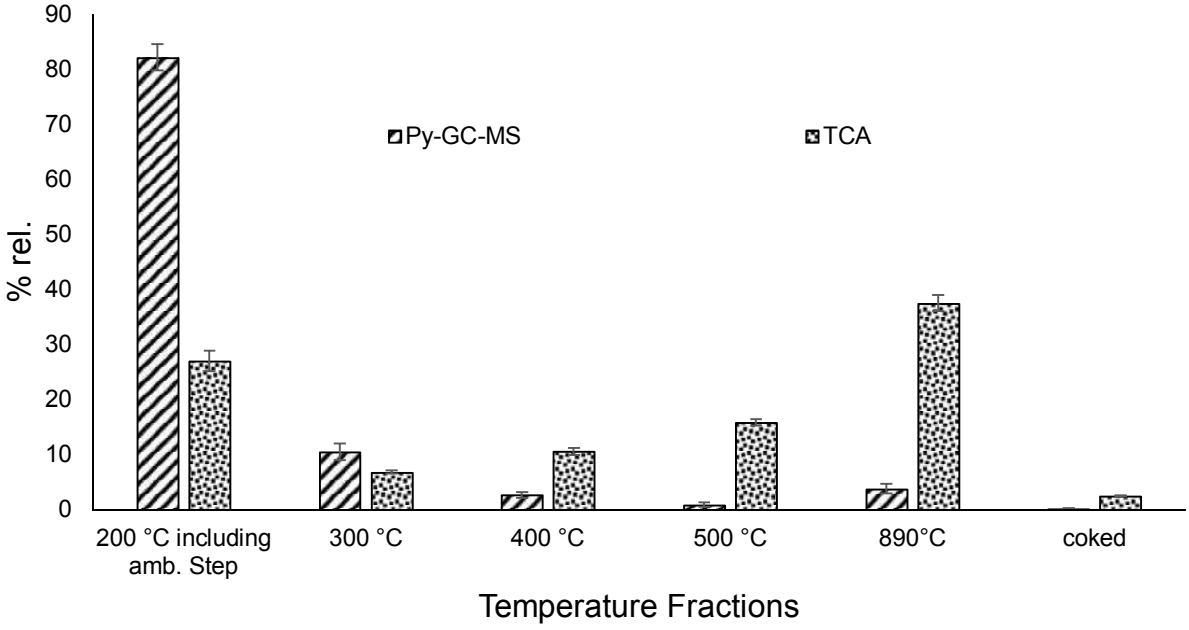

REFERENCES

1. Oregui Bengoechea, M.; Hertzberg, A.; Miletić, N.; Arias, P. L.; Barth, T. Simultaneous catalytic de-polymerization and hydrodeoxygenation of lignin in water/formic acid media with Rh/Al2O3, Ru/Al2O3 and Pd/Al2O3 as bifunctional catalysts. *Journal of Analytical and Applied Pyrolysis* **2015,** *113*, 713-722.
2. Long, J.; Zhang, Q.; Wang, T.; Zhang, X.; Xu, Y.; Ma, L. An efficient and economical process for lignin depolymerization in biomass-derived solvent tetrahydrofuran. *Bioresour Technol* **2014,** *154*, 10-7.
3. Yu, J.; Paterson, N.; Blamey, J.; Millan, M. Cellulose, xylan and lignin interactions during pyrolysis of lignocellulosic biomass. *Fuel* **2017,** *191*, 140-149.
4. Erdocia, X.; Prado, R.; Corcuera, M. Á.; Labidi, J. Base catalyzed depolymerization of lignin: Influence of organosolv lignin nature. *Biomass and Bioenergy* **2014,** *66*, 379-386.
5. Zhang, J.; Teo, J.; Chen, X.; Asakura, H.; Tanaka, T.; Teramura, K.; Yan, N. A series of NiM (M = Ru, Rh, and Pd) bimetallic catalysts for effective lignin hydrogenolysis in water. *ACS Catalysis* **2014,** *4* (5), 1574-1583.
6. Vanholme, R.; Demedts, B.; Morreel, K.; Ralph, J.; Boerjan, W. Lignin biosynthesis and structure. *Plant Physiol* **2010,** *153* (3), 895-905.
7. Yuan, T.-Q.; Xu, F.; Sun, R.-C. Role of lignin in a biorefinery: separation characterization and valorization. *Journal of Chemical Technology & Biotechnology* **2013,** *88* (3), 346-352.
8. Zakzeski, J.; Bruijninckx, P. C. A.; Jongerius, A. L.; Weckhuysen, B. M. The Catalytic Valorization of Lignin for the Production of Renewable Chemicals. *Chemical Reviews* **2010,** *110* (6), 3552-3599.
9. Vishtal, A.; Kraslawski, A. Challenges in Industrial Applications of Technical Lignins. *BioResources* **2011,** *6* (3), 3547-3568.
10. Rinaldi, R.; Jastrzebski, R.; Clough, M. T.; Ralph, J.; Kennema, M.; Bruijnincx, P. C.; Weckhuysen, B. M. Paving the Way for Lignin Valorisation: Recent Advances in Bioengineering, Biorefining and Catalysis. *Angew Chem Int Ed Engl* **2016,** *55* (29), 8164-215.
11. Rashed, M. M. A.; Tong, Q.; Nagi, A.; Li, J.; Khan, N. U.; Chen, L.; Rotail, A.; Bakry, A. M. Isolation of essential oil from Lavandula angustifolia by using ultrasonic-microwave assisted method preceded by enzymolysis treatment, and assessment of its biological activities. *Industrial Crops and Products* **2017,** *100*, 236-245.
12. Schwiderski, M.; Kruse, A.; Grandl, R.; Dockendorf, D. Comparison of the influence of a Lewis acid AlCl3 and a Brønsted acid HCl on the organosolv pulping of beech wood. *Green Chemistry* **2014,** *16* (3), 1569.
13. Jonsson, L. J.; Martin, C. Pretreatment of lignocellulose: Formation of inhibitory by-products and strategies for minimizing their effects. *Bioresour Technol* **2016,** *199*, 103-12.

14. Klinke, H. B.; Ahring, B. K.; Schmidt, A. S.; Thomsen, A. B. Characterization of Degradation Products from Alkaline Wet Oxidation of Wheat Straw. *Bioresource Technology* **2002,** *82*, 15-26.
15. Li, J.; Gellerstedt, G.; Toven, K. Steam explosion lignins; their extraction, structure and potential as feedstock for biodiesel and chemicals. *Bioresour Technol* **2009,** *100* (9), 2556-61.
16. Martin-Sampedro, R.; Capanema, E. A.; Hoeger, I.; Villar, J. C.; Rojas, O. J. Lignin changes after steam explosion and laccase-mediator treatment of eucalyptus wood chips. *J Agric Food Chem* **2011,** *59* (16), 8761-9.
17. Mathew, A. K.; Parameshwaran, B.; Sukumaran, R. K.; Pandey, A. An evaluation of dilute acid and ammonia fiber explosion pretreatment for cellulosic ethanol production. *Bioresour Technol* **2016,** *199*, 13-20.
18. Lee, J. M.; Jameel, H.; Venditti, R. A. A comparison of the autohydrolysis and ammonia fiber explosion (AFEX) pretreatments on the subsequent enzymatic hydrolysis of coastal Bermuda grass. *Bioresour Technol* **2010,** *101* (14), 5449-58.
19. Yang, H.; Xie, Y.; Zheng, X.; Pu, Y.; Huang, F.; Meng, X.; Wu, W.; Ragauskas, A.; Yao, L. Comparative study of lignin characteristics from wheat straw obtained by soda-AQ and kraft pretreatment and effect on the following enzymatic hydrolysis process. *Bioresour Technol* **2016,** *207*, 361-9.
20. Nasser, R. A.; Hiziroglu, S.; Abdel-Aal, M. A.; Al-Mefarrej, H. A.; Shetta, N. D.; Aref, I. M. Measurement of some properties of pulp and paper made from date palm midribs and wheat straw by soda-AQ pulping process. *Measurement* **2015,** *62*, 179-186.
21. Chakar, F. S.; Ragauskas, A. J. Review of current and future softwood kraft lignin process chemistry. *Industrial Crops and Products* **2004,** *20* (2), 131-141.
22. Mansouri, N.-E. E.; Salvadó, J. Structural characterization of technical lignins for the production of adhesives: Application to lignosulfonate, kraft, soda-anthraquinone, organosolv and ethanol process lignins. *Industrial Crops and Products* **2006,** *24* (1), 8-16.
23. Berlin, A.; Balakshin, M. Industrial Lignins: Analysis, Properties and Applications. *Bioenergy Reserach: Advances and Applications* **2014,** *18*, 315-336.
24. Joffres, B.; Lorentz, C.; Vidalie, M.; Laurenti, D.; Quoineaud, A. A.; Charon, N.; Daudin, A.; Quignard, A.; Geantet, C. Catalytic hydroconversion of a wheat straw soda lignin: Characterization of the products and the lignin residue. *Applied Catalysis B: Environmental* **2014,** *145*, 167-176.
25. Zhang, F.; Lin, J.; Zhao, G. Preparation and Characterization of Modified Soda Lignin with Polyethylene Glycol. *Materials* **2016,** *9* (10), 822.
26. Matsushita, Y. Conversion of technical lignins to functional materials with retained polymeric properties. *Journal of Wood Science* **2015,** *61* (3), 230-250.
27. Xin, J.; Zhang, P.; Wolcott, M. P.; Zhang, X.; Zhang, J. Partial depolymerization of enzymolysis lignin via mild hydrogenolysis over Raney Nickel. *Bioresour Technol* **2014,** *155*, 422-6.
28. Guerra, A.; Filpponen, I.; Lucia, L. A.; Saquing, C.; Baumberger, S.; Argylopoulos, D. S. Toward a Better Understanding of the Lignin Isolation Process from Wood. *J. Agric. Food. Chem.* **2006,** *54*, 5939-5947.
29. Achinivu, E. C.; Howard, R. M.; Li, G.; Gracz, H.; Henderson, W. A. Lignin extraction from biomass with protic ionic liquids. *Green Chem.* **2014,** *16* (3), 1114-1119.

30. Pang, Z.; Lyu, W.; Dong, C.; Li, H.; Yang, G. High selective delignification using oxidative ionic liquid pretreatment at mild conditions for efficient enzymatic hydrolysis of lignocellulose. *Bioresour Technol* **2016,** *214*, 96-101.
31. Tanahashi, M.; Tamabuchi, K.; Goto, T.; Aoki, T.; Karina, M.; Higuchi, T. Characterization of Steam-Exploded Wood II. *Wood Research: Bulletin of the Wood Research Institute Kyoto Univeristy* **1988,** *75*, 1-12.
32. Marchessault, R. H.; Coulombe, S.; Morikawa, H. Characterization of aspen exploded wood. *Can J. Chem.* **1982,** *60*, 2372-2382.
33. Liu, C.; Hu, J.; Zhang, H.; Xiao, R. Thermal conversion of lignin to phenols: Relevance between chemical structure and pyrolysis behaviors. *Fuel* **2016,** *182*, 864-870.
34. Kozliak, E. I.; Kubátová, A.; Artemyeva, A. A.; Nagel, E.; Zhang, C.; Rajappagowda, R. B.; Smirnova, A. L. Thermal Liquefaction of Lignin to Aromatics: Efficiency, Selectivity, and Product Analysis. *ACS Sustainable Chemistry & Engineering* **2016,** *4* (10), 5106-5122.
35. Long, J.; Xu, Y.; Wang, T.; Yuan, Z.; Shu, R.; Zhang, Q.; Ma, L. Efficient base-catalyzed decomposition and in situ hydrogenolysis process for lignin depolymerization and char elimination. *Applied Energy* **2015,** *141*, 70-79.
36. Joffres, B.; Laurenti, D.; Charon, N.; Daudin, A.; Quignard, A.; Geantet, C. Thermochemical Coversion of Lignin for Fuels and Chemicals: A Review. *Oil & Gas Science and Technology – Revue d'IFP Energies nouvelles* **2013,** *68* (4), 753-763.
37. Li, C.; Zhao, X.; Wang, A.; Huber, G. W.; Zhang, T. Catalytic Transformation of Lignin for the Production of Chemicals and Fuels. *Chem Rev* **2015,** *115* (21), 11559-624.
38. Pineda, A.; Lee, A. F. Heterogeneously catalyzed lignin depolymerization. *Applied Petrochemical Research* **2016,** *6* (3), 243-256.
39. Chang, G.; Huang, Y.; Xie, J.; Yang, H.; Liu, H.; Yin, X.; Wu, C. The lignin pyrolysis composition and pyrolysis products of palm kernel shell, wheat straw, and pine sawdust. *Energy Conversion and Management* **2016,** *124*, 587-597.
40. Mu, W.; Ben, H.; Ragauskas, A.; Deng, Y. Lignin Pyrolysis Components and Upgrading—Technology Review. *BioEnergy Research* **2013,** *6* (4), 1183-1204.
41. Saiz-Jimenez, C.; De Leeuw, J. W. Lignin Pyrolysis Products: Their Structures and their Significance as Biomarkers. *Advances in Organic Geochemistry* **1986,** *10*, 869-876.
42. Zhang, M.; Resende, F. L. P.; Moutsoglou, A.; Raynie, D. E. Pyrolysis of lignin extracted from prairie cordgrass, aspen, and Kraft lignin by Py-GC/MS and TGA/FTIR. *Journal of Analytical and Applied Pyrolysis* **2012,** *98*, 65-71.
43. Collard, F.-X.; Blin, J. A review on pyrolysis of biomass constituents: Mechanisms and composition of the products obtained from the conversion of cellulose, hemicelluloses and lignin. *Renewable and Sustainable Energy Reviews* **2014,** *38*, 594-608.
44. Nair, V.; Vinu, R. Production of guaiacols via catalytic fast pyrolysis of alkali lignin using titania, zirconia and ceria. *Journal of Analytical and Applied Pyrolysis* **2016,** *119*, 31-39.
45. Kawamoto, H. Lignin pyrolysis reactions. *Journal of Wood Science* **2017,** *63* (2), 117-132.
46. Jiang, W.; Wu, S.; Lucia, L. A.; Chu, J. A comparison of the pyrolysis behavior of selected β-O-4 type lignin model compounds. *Journal of Analytical and Applied Pyrolysis* **2017,** *125*, 185-192.
47. Huang, J.; He, C. Pyrolysis mechanism of α-O-4 linkage lignin dimer: A theoretical study. *Journal of Analytical and Applied Pyrolysis* **2015,** *113*, 655-664.

48. Nakagawa-Izumi, A.; H'ng, Y. Y.; Mulyantara, L. T.; Maryana, R.; Do, V. T.; Ohi, H. Characterization of syringyl and guaiacyl lignins in thermomechanical pulp from oil palm empty fruit bunch by pyrolysis-gas chromatography-mass spectrometry using ion intensity calibration. *Industrial Crops and Products* **2017,** *95*, 615-620.
49. Guo, D.; Wu, S.; Lyu, G.; Guo, H. Effect of molecular weight on the pyrolysis characteristics of alkali lignin. *Fuel* **2017,** *193*, 45-53.
50. Wang, S.; Ru, B.; Lin, H.; Sun, W.; Luo, Z. Pyrolysis behaviors of four lignin polymers isolated from the same pine wood. *Bioresour Technol* **2015,** *182*, 120-7.
51. Zhou, S.; Garcia-Perez, M.; Pecha, B.; McDonald, A. G.; Westerhof, R. J. M. Effect of particle size on the composition of lignin derived oligomers obtained by fast pyrolysis of beech wood. *Fuel* **2014,** *125*, 15-19.
52. Ojha, D. K.; Viju, D.; Vinu, R. Fast pyrolysis kinetics of alkali lignin: Evaluation of apparent rate parameters and product time evolution. *Bioresour Technol* **2017,** *241*, 142-151.
53. Bai, X.; Kim, K. H.; Brown, R. C.; Dalluge, E.; Hutchinson, C.; Lee, Y. J.; Dalluge, D. Formation of phenolic oligomers during fast pyrolysis of lignin. *Fuel* **2014,** *128*, 170-179.
54. Ma, Z.; van Bokhoven, J. A. Deactivation and Regeneration of H-USY Zeolite during Lignin Catalytic Fast Pyrolysis. *ChemCatChem* **2012,** *4* (12), 2036-2044.
55. Shen, D.; Zhao, J.; Xiao, R.; Gu, S. Production of aromatic monomers from catalytic pyrolysis of black-liquor lignin. *Journal of Analytical and Applied Pyrolysis* **2015,** *111*, 47-54.
56. Zhang, M.; Resende, F. L. P.; Moutsoglou, A. Catalytic fast pyrolysis of aspen lignin via Py-GC/MS. *Fuel* **2014,** *116*, 358-369.
57. Ohra-aho, T.; Linnekoski, J. Catalytic pyrolysis of lignin by using analytical pyrolysis-GC–MS. *Journal of Analytical and Applied Pyrolysis* **2015,** *113*, 186-192.
58. Geng, J.; Wang, W. L.; Yu, Y. X.; Chang, J. M.; Cai, L. P.; Shi, S. Q. Adding nickel formate in alkali lignin to increase contents of alkylphenols and aromatics during fast pyrolysis. *Bioresour Technol* **2017,** *227*, 1-6.
59. Peng, C.; Zhang, G.; Yue, J.; Xu, G. Pyrolysis of lignin for phenols with alkaline additive. *Fuel Processing Technology* **2014,** *124*, 212-221.
60. Jia, S.; Cox, B. J.; Guo, X.; Zhang, Z. C.; Ekerdt, J. G. Cleaving the beta--O--4 bonds of lignin model compounds in an acidic ionic liquid, 1-H-3-methylimidazolium chloride: an optional strategy for the degradation of lignin. *ChemSusChem* **2010,** *3* (9), 1078-84.
61. Deuss, P. J.; Scott, M.; Tran, F.; Westwood, N. J.; de Vries, J. G.; Barta, K. Aromatic monomers by in situ conversion of reactive intermediates in the acid-catalyzed depolymerization of lignin. *J Am Chem Soc* **2015,** *137* (23), 7456-67.
62. Güvenatam, B.; Heeres, E. H. J.; Pidko, E. A.; Hensen, E. J. M. Lewis acid-catalyzed depolymerization of soda lignin in supercritical ethanol/water mixtures. *Catalysis Today* **2016,** *269*, 9-20.
63. Güvenatam, B.; Heeres, E. H. J.; Pidko, E. A.; Hensen, E. J. M. Lewis-acid catalyzed depolymerization of Protobind lignin in supercritical water and ethanol. *Catalysis Today* **2016,** *259*, 460-466.
64. Hepditch, M. M.; Thring, R. W. Degradation of Solvolysis Lignin Using Lewis Acid Catalysts. *The Canadian Journal of Chemical Engineering* **2000,** *78*, 226-231.
65. Binder, J. B.; Gray, M. J.; White, J. F.; Zhang, Z. C.; Holladay, J. E. Reactions of lignin model compounds in ionic liquids. *Biomass and Bioenergy* **2009,** *33* (9), 1122-1130.

66. Oregui Bengoechea, M.; Miletic, N.; Vogt, M. H.; Arias, P. L.; Barth, T. Analysis of the effect of temperature and reaction time on yields, compositions and oil quality in catalytic and non-catalytic lignin solvolysis in a formic acid/water media using experimental design. *Bioresour Technol* **2017,** *234*, 86-98.
67. Kristianto, I.; Limarta, S. O.; Lee, H.; Ha, J. M.; Suh, D. J.; Jae, J. Effective depolymerization of concentrated acid hydrolysis lignin using a carbon-supported ruthenium catalyst in ethanol/formic acid media. *Bioresour Technol* **2017,** *234*, 424-431.
68. Kloekhorst, A.; Shen, Y.; Yie, Y.; Fang, M.; Heeres, H. J. Catalytic hydrodeoxygenation and hydrocracking of Alcell® lignin in alcohol/formic acid mixtures using a Ru/C catalyst. *Biomass and Bioenergy* **2015,** *80*, 147-161.
69. Narani, A.; Chowdari, R. K.; Cannilla, C.; Bonura, G.; Frusteri, F.; Heeres, H. J.; Barta, K. Efficient catalytic hydrotreatment of Kraft lignin to alkylphenolics using supported NiW and NiMo catalysts in supercritical methanol. *Green Chem.* **2015,** *17* (11), 5046-5057.
70. Liguori, L.; Barth, T. Palladium-Nafion SAC-13 catalysed depolymerisation of lignin to phenols in formic acid and water. *Journal of Analytical and Applied Pyrolysis* **2011,** *92* (2), 477-484.
71. Roberts, V. M.; Stein, V.; Reiner, T.; Lemonidou, A.; Li, X.; Lercher, J. A. Towards quantitative catalytic lignin depolymerization. *Chemistry* **2011,** *17* (21), 5939-48.
72. Toledano, A.; Serrano, L.; Labidi, J. Improving base catalyzed lignin depolymerization by avoiding lignin repolymerization. *Fuel* **2014,** *116*, 617-624.
73. Katahira, R.; Mittal, A.; McKinney, K.; Chen, X.; Tucker, M. P.; Johnson, D. K.; Beckham, G. T. Base-Catalyzed Depolymerization of Biorefinery Lignins. *ACS Sustainable Chemistry & Engineering* **2016,** *4* (3), 1474-1486.
74. Beauchet, R.; Monteil-Rivera, F.; Lavoie, J. M. Conversion of lignin to aromatic-based chemicals (L-chems) and biofuels (L-fuels). *Bioresour Technol* **2012,** *121*, 328-34.
75. Schmiedl, D.; Endisch, S.; Pindel, E.; Ruckert, D.; Reinhardt, S.; Unkelbach, G.; Schweppe, R. Base Catalyzed Degradation of Lignin for the Generation of oxy-Aromatic Compounds - Possibilities and Challenges. *Erdoel Erdgas Kohle* **2012,** *128* (10), 357-363.
76. Jia, S.; Cox, B. J.; Guo, X.; Zhang, Z. C.; Ekerdt, J. G. Decomposition of a phenolic lignin model compound over organic N-bases in an ionic liquid. *Holzforschung* **2010,** *64* (5).
77. Kim, J. Y.; Oh, S.; Hwang, H.; Cho, T. S.; Choi, I. G.; Choi, J. W. Effects of various reaction parameters on solvolytical depolymerization of lignin in sub- and supercritical ethanol. *Chemosphere* **2013,** *93* (9), 1755-64.
78. Shafaghat, H.; Rezaei, P. S.; Daud, W. M. A. W. Using decalin and tetralin as hydrogen source for transfer hydrogenation of renewable lignin-derived phenolics over activated carbon supported Pd and Pt catalysts. *Journal of the Taiwan Institute of Chemical Engineers* **2016,** *65*, 91-100.
79. Kim, K. H.; Brown, R. C.; Kieffer, M.; Bai, X. Hydrogen-donor-assisted solvent liquefaction of lignin to short-chain alkylphenols using a micro reactor/gas chromatography system. *Energy & Fuels* **2014,** *28* (10), 6429-6437.
80. Thring, R. W.; Breau, J. Hydrocracking of solvolysis lignin in a btach reactor. *Fuel* **1996,** *75* (7), 795-800.
81. Toledano, A.; Serrano, L.; Pineda, A.; Romero, A. A.; Luque, R.; Labidi, J. Microwave-assisted depolymerisation of organosolv lignin via mild hydrogen-free hydrogenolysis: Catalyst screening. *Applied Catalysis B: Environmental* **2014,** *145*, 43-55.

82. Wang, H.; Tucker, M.; Ji, Y. Recent Development in Chemical Depolymerization of Lignin: A Review. *Journal of Applied Chemistry* **2013,** *2013*, 1-9.
83. Wahyudiono; Sasaki, M.; Goto, M. Recovery of phenolic compounds through the decomposition of lignin in near and supercritical water. *Chemical Engineering and Processing: Process Intensification* **2008,** *47* (9-10), 1609-1619.
84. Takami, S.; Okuda, K.; Man, X.; Umetsu, M.; Ohara, S.; Adschiri, T. Kinetic Study on the Selective Production of 2-(Hydroxybenzyl)-4-methylphenol from Organosolv Lignin in a Mixture of Supercritical Water andp-Cresol. *Industrial & Engineering Chemistry Research* **2012,** *51* (13), 4804-4808.
85. Pińkowska, H.; Wolak, P.; Złocińska, A. Hydrothermal decomposition of alkali lignin in sub- and supercritical water. *Chemical Engineering Journal* **2012,** *187*, 410-414.
86. Hidajat, M. J.; Riaz, A.; Park, J.; Insyani, R.; Verma, D.; Kim, J. Depolymerization of concentrated sulfuric acid hydrolysis lignin to high-yield aromatic monomers in basic sub- and supercritical fluids. *Chemical Engineering Journal* **2017,** *317*, 9-19.
87. Kim, H.-Y.; Jang, S.-K.; Hong, C.-Y.; Choi, J. W.; Choi, I.-G. Relationship between characteristics of ethanol organosolv lignin and the productivity of phenolic monomers by solvolysis. *Fuel* **2016,** *186*, 770-778.
88. Mahmood, N.; Yuan, Z.; Schmidt, J.; Xu, C. C. Hydrolytic depolymerization of hydrolysis lignin: Effects of catalysts and solvents. *Bioresour Technol* **2015,** *190*, 416-9.
89. Li, Q.; Liu, D.; Hou, X.; Wu, P.; Song, L.; Yan, Z. Hydro-liquefaction of microcrystalline cellulose, xylan and industrial lignin in different supercritical solvents. *Bioresour Technol* **2016,** *219*, 281-8.
90. Riaz, A.; Kim, C. S.; Kim, Y.; Kim, J. High-yield and high-calorific bio-oil production from concentrated sulfuric acid hydrolysis lignin in supercritical ethanol. *Fuel* **2016,** *172*, 238-247.
91. Warner, G.; Hansen, T. S.; Riisager, A.; Beach, E. S.; Barta, K.; Anastas, P. T. Depolymerization of organosolv lignin using doped porous metal oxides in supercritical methanol. *Bioresour Technol* **2014,** *161*, 78-83.
92. Gosselink, R. J.; Teunissen, W.; van Dam, J. E.; de Jong, E.; Gellerstedt, G.; Scott, E. L.; Sanders, J. P. Lignin depolymerisation in supercritical carbon dioxide/acetone/water fluid for the production of aromatic chemicals. *Bioresour Technol* **2012,** *106*, 173-7.
93. Numan-Al-Mobin, A. M.; Kolla, P.; Dixon, D.; Smirnova, A. Effect of water–carbon dioxide ratio on the selectivity of phenolic compounds produced from alkali lignin in sub- and supercritical fluid mixtures. *Fuel* **2016,** *185*, 26-33.
94. Kim, J.-Y.; Park, J.; Hwang, H.; Kim, J. K.; Song, I. K.; Choi, J. W. Catalytic depolymerization of lignin macromolecule to alkylated phenols over various metal catalysts in supercritical tert-butanol. *Journal of Analytical and Applied Pyrolysis* **2015,** *113*, 99-106.
95. Jin, S.; Xiao, Z.; Li, C.; Chen, X.; Wang, L.; Xing, J.; Li, W.; Liang, C. Catalytic hydrodeoxygenation of anisole as lignin model compound over supported nickel catalysts. *Catalysis Today* **2014,** *234*, 125-132.
96. Forchheim, D.; Hornung, U.; Kempe, P.; Kruse, A.; Steinbach, D. Influence of RANEY Nickel on the Formation of Intermediates in the Degradation of Lignin. *International Journal of Chemical Engineering* **2012,** *2012*, 1-8.

97. Tsodikov, M. V.; Ellert, O. G.; Nikolaev, S. A.; Arapova, O. V.; Konstantinov, G. I.; Bukhtenko, O. V.; Vasil'kov, A. Y. The role of nanosized nickel particles in microwave-assisted dry reforming of lignin. *Chemical Engineering Journal* **2017,** *309*, 628-637.
98. Jiang, Y.; Li, Z.; Tang, X.; Sun, Y.; Zeng, X.; Liu, S.; Lin, L. Depolymerization of cellulolytic enzyme lignin for the production of monomeric phenols over Raney Ni and acidic zeolite catalysts. *Energy & Fuels* **2015,** *29* (3), 1662-1668.
99. Konnerth, H.; Zhang, J.; Ma, D.; Prechtl, M. H. G.; Yan, N. Base promoted hydrogenolysis of lignin model compounds and organosolv lignin over metal catalysts in water. *Chemical Engineering Science* **2015,** *123*, 155-163.
100. Grilc, M.; Likozar, B.; Levec, J. Hydrotreatment of solvolytically liquefied lignocellulosic biomass over NiMo/Al2O3 catalyst: Reaction mechanism, hydrodeoxygenation kinetics and mass transfer model based on FTIR. *Biomass and Bioenergy* **2014,** *63*, 300-312.
101. Grilc, M.; Likozar, B.; Levec, J. Hydrodeoxygenation and hydrocracking of solvolysed lignocellulosic biomass by oxide, reduced and sulphide form of NiMo, Ni, Mo and Pd catalysts. *Applied Catalysis B: Environmental* **2014,** *150-151*, 275-287.
102. Finch, K. B. H.; Richards, R. M.; Richel, A.; Medvedovici, A. V.; Gheorghe, N. G.; Verziu, M.; Coman, S. M.; Parvulescu, V. I. Catalytic hydroprocessing of lignin under thermal and ultrasound conditions. *Catalysis Today* **2012,** *196* (1), 3-10.
103. Song, Q.; Wang, F.; Xu, J. Hydrogenolysis of lignosulfonate into phenols over heterogeneous nickel catalysts. *Chem Commun (Camb)* **2012,** *48* (56), 7019-21.
104. Kim, J.-Y.; Park, J.; Kim, U.-J.; Choi, J. W. Conversion of Lignin to Phenol-Rich Oil Fraction under Supercritical Alcohols in the Presence of Metal Catalysts. *Energy & Fuels* **2015,** *29* (8), 5154-5163.
105. Wang, X.; Rinaldi, R. Solvent effects on the hydrogenolysis of diphenyl ether with Raney nickel and their implications for the conversion of lignin. *ChemSusChem* **2012,** *5* (8), 1455-66.
106. Chen, P.; Zhang, Q.; Shu, R.; Xu, Y.; Ma, L.; Wang, T. Catalytic depolymerization of the hydrolyzed lignin over mesoporous catalysts. *Bioresour Technol* **2017,** *226*, 125-131.
107. Strüven, J. O.; Meier, D. Hydrocracking of Organosolv Lignin in Subcritical Water to Useful Phenols Employing Various Raney Nickel Catalysts. *ACS Sustainable Chemistry & Engineering* **2016,** *4* (7), 3712-3721.
108. Klein, I.; Saha, B.; Abu-Omar, M. M. Lignin depolymerization over Ni/C catalyst in methanol, a continuation: effect of substrate and catalyst loading. *Catal. Sci. Technol.* **2015,** *5* (6), 3242-3245.
109. Singh, S. K.; Ekhe, J. D. Towards effective lignin conversion: HZSM-5 catalyzed one-pot solvolytic depolymerization/hydrodeoxygenation of lignin into value added compounds. *RSC Advances* **2014,** *4* (53), 27971.
110. Milovanović, J.; Rajić, N.; Romero, A. A.; Li, H.; Shih, K.; Tschentscher, R.; Luque, R. Insights into the Microwave-Assisted Mild Deconstruction of Lignin Feedstocks Using NiO-Containing ZSM-5 Zeolites. *ACS Sustainable Chemistry & Engineering* **2016,** *4* (8), 4305-4313.
111. Klamrassamee, T.; Laosiripojana, N.; Cronin, D.; Moghaddam, L.; Zhang, Z.; Doherty, W. O. Effects of mesostructured silica catalysts on the depolymerization of organosolv lignin fractionated from woody eucalyptus. *Bioresour Technol* **2015,** *180*, 222-9.
112. Toledano, A.; Serrano, L.; Balu, A. M.; Luque, R.; Pineda, A.; Labidi, J. Fractionation of organosolv lignin from olive tree clippings and its valorization to simple phenolic compounds. *ChemSusChem* **2013,** *6* (3), 529-36.

113. Ma, X.; Tian, Y.; Hao, W.; Ma, R.; Li, Y. Production of phenols from catalytic conversion of lignin over a tungsten phosphide catalyst. *Applied Catalysis A: General* **2014,** *481*, 64-70.
114. Zhang, G.; Wen, Y.; Liu, Z.; Zhang, S.; Li, G. Acid-catalyzed hydrolysis of conifer lignosulfonate in black liquor for the production of value-added chemicals. *Applied Catalysis A: General* **2017,** *542*, 1-9.
115. Luo, H.; Klein, I. M.; Jiang, Y.; Zhu, H.; Liu, B.; Kenttämaa, H. I.; Abu-Omar, M. M. Total Utilization of Miscanthus Biomass, Lignin and Carbohydrates, Using Earth Abundant Nickel Catalyst. *ACS Sustainable Chemistry & Engineering* **2016,** *4* (4), 2316-2322.
116. Sturgeon, M. R.; O'Brien, M. H.; Ciesielski, P. N.; Katahira, R.; Kruger, J. S.; Chmely, S. C.; Hamlin, J.; Lawrence, K.; Hunsinger, G. B.; Foust, T. D.; Baldwin, R. M.; Biddy, M. J.; Beckham, G. T. Lignin depolymerisation by nickel supported layered-double hydroxide catalysts. *Green Chem.* **2014,** *16* (2), 824-835.
117. Molinari, V.; Clavel, G.; Graglia, M.; Antonietti, M.; Esposito, D. Mild Continuous Hydrogenolysis of Kraft Lignin over Titanium Nitride–Nickel Catalyst. *ACS Catalysis* **2016,** *6* (3), 1663-1670.
118. Jeong, S.; Jang, G. H.; Kim, D. H. Decomposition of Lignin Using MO–MgAlOy Mixed Oxide Catalysts (M=Co, Ni and Cu) in Supercritical Ethanol. *Topics in Catalysis* **2017,** *60* (9-11), 637-643.
119. Korányi, T. I.; Hensen, E. J. M. Preparative Aspects of Supported Ni2P Catalysts for Reductive Upgrading of Technical Lignin to Aromatics. *Catalysis Letters* **2017,** *147* (7), 1722-1731.
120. Koranyi, T. I.; Huang, X.; Coumans, A. E.; Hensen, E. J. Synergy in Lignin Upgrading by a Combination of Cu-Based Mixed Oxide and Ni-Phosphide Catalysts in Supercritical Ethanol. *ACS Sustain Chem Eng* **2017,** *5* (4), 3535-3543.
121. Rajappagowda, R.; Numan-Al-Mobin, A. M.; Yao, B.; Cook, R. D.; Smirnova, A. Toward Selective Lignin Liquefaction: Synergistic Effect of Hetero- and Homogeneous Catalysis in Sub- and Supercritical Fluids. *Energy & Fuels* **2017,** *31* (1), 578-586.
122. Regmi, Y. N.; Mann, J. K.; McBride, J. R.; Tao, J.; Barnes, C. E.; Labbé, N.; Chmely, S. C. Catalytic transfer hydrogenolysis of organosolv lignin using B-containing FeNi alloyed catalysts. *Catalysis Today* **2017**.
123. Shen, X.-J.; Wen, J.-L.; Huang, P.-L.; Zheng, K.; Wang, S.-F.; Liu, Q.-Y.; Charlton, A.; Sun, R.-C. Efficient and Product-Controlled Depolymerization of Lignin Oriented by Raney Ni Cooperated with $Cs_xH_{3-x}PW_{12}O_{40}$

BioEnergy Research **2017**.
124. Wang, H.; Ruan, H.; Feng, M.; Qin, Y.; Job, H.; Luo, L.; Wang, C.; Engelhard, M. H.; Kuhn, E.; Chen, X.; Tucker, M. P.; Yang, B. One-Pot Process for Hydrodeoxygenation of Lignin to Alkanes Using Ru-Based Bimetallic and Bifunctional Catalysts Supported on Zeolite Y. *ChemSusChem* **2017,** *10* (8), 1846-1856.
125. Zhai, Y.; Li, C.; Xu, G.; Ma, Y.; Liu, X.; Zhang, Y. Depolymerization of lignin via a non-precious Ni–Fe alloy catalyst supported on activated carbon. *Green Chem.* **2017,** *19* (8), 1895-1903.
126. Agarwal, S.; Chowdari, R. K.; Hita, I.; Heeres, H. J. Experimental Studies on the Hydrotreatment of Kraft Lignin to Aromatics and Alkylphenolics Using Economically Viable Fe-Based Catalysts. *ACS Sustain Chem Eng* **2017,** *5* (3), 2668-2678.

127. Yoshikawa, T.; Yagi, T.; Shinohara, S.; Fukunaga, T.; Nakasaka, Y.; Tago, T.; Masuda, T. Production of phenols from lignin via depolymerization and catalytic cracking. *Fuel Processing Technology* **2013,** *108*, 69-75.
128. Abdelaziz, O. Y.; Brink, D. P.; Prothmann, J.; Ravi, K.; Sun, M.; Garcia-Hidalgo, J.; Sandahl, M.; Hulteberg, C. P.; Turner, C.; Liden, G.; Gorwa-Grauslund, M. F. Biological valorization of low molecular weight lignin. *Biotechnol Adv* **2016,** *34* (8), 1318-1346.
129. Shen, D.; Liu, N.; Dong, C.; Xiao, R.; Gu, S. Catalytic solvolysis of lignin with the modified HUSYs in formic acid assisted by microwave heating. *Chemical Engineering Journal* **2015,** *270*, 641-647.
130. Asikkala, J.; Tamminen, T.; Argyropoulos, D. S. Accurate and reproducible determination of lignin molar mass by acetobromination. *J Agric Food Chem* **2012,** *60* (36), 8968-73.
131. Karimi, K.; Taherzadeh, M. J. A critical review of analytical methods in pretreatment of lignocelluloses: Composition, imaging, and crystallinity. *Bioresour Technol* **2016,** *200*, 1008-18.
132. Jarrell, T. M.; Marcum, C. L.; Sheng, H.; Owen, B. C.; O'Lenick, C. J.; Maraun, H.; Bozell, J. J.; Kenttämaa, H. I. Characterization of organosolv switchgrass lignin by using high performance liquid chromatography/high resolution tandem mass spectrometry using hydroxide-doped negative-ion mode electrospray ionization. *Green Chem.* **2014,** *16* (5), 2713-2727.
133. Tolbert, A.; Akinosho, H.; Khunsupat, R.; Naskar, A. K.; Ragauskas, A. J. Characterization and analysis of the molecular weight of lignin for biorefining studies. *Biofuels, Bioproducts and Biorefining* **2014,** *8* (6), 836-856.
134. Greving, M. P.; Patti, G. J.; Siuzdak, G. Nanostructure-Initiator Mass Spectrometry Metabolite Analysis and Imaging. *Anal Chem* **2011,** *83*, 2-7.
135. Marvin, L. F.; Roberts, M. A.; Fay, L. B. Matrix-assisted laser desorption/ionization time-of-flight mass spectrometry in clinical chemistry. *Clinica Chimica Acta* **2003,** *337* (1-2), 11-21.
136. Watkins, D.; Nuruddin, M.; Hosur, M.; Tcherbi-Narteh, A.; Jeelani, S. Extraction and characterization of lignin from different biomass resources. *Journal of Materials Research and Technology* **2015,** *4* (1), 26-32.
137. Wang, K.; Xu, F.; Sun, R. Molecular characteristics of Kraft-AQ pulping lignin fractionated by sequential organic solvent extraction. *Int J Mol Sci* **2010,** *11* (8), 2988-3001.
138. Capanema, E. A.; Balakshin, M. Y.; Kadla, J. F. A Comprehensive Approach for Quantitative Lignin Characterization by NMR Spectroscopy. *J. Agric. Food Chem.* **2004,** *52*, 1850-1860.
139. Shu, R.; Long, J.; Yuan, Z.; Zhang, Q.; Wang, T.; Wang, C.; Ma, L. Efficient and product-controlled depolymerization of lignin oriented by metal chloride cooperated with Pd/C. *Bioresour Technol* **2015,** *179*, 84-90.
140. Zakis, G. F., *Synthesis of Lignin Model Compounds*. Zinatne: Riga, 1980.
141. Voeller, K. M. Characterization of Kraft alkali lignin and products of its thermal degradation by fractional pyrolysis methods. University of North Dakota, 2015.
142. Chakraborty, A.; Gupta, T.; Tripathi, S. N. Combined effects of organic aerosol loading and fog processing on organic aerosols oxidation, composition, and evolution. *Sci Total Environ* **2016,** *573*, 690-698.
143. Parvez, F.; Lamancusa, C.; Wagstrom, K. Primary and secondary particulate matter intake fraction from different height emission sources. *Atmospheric Environment* **2017,** *165*, 1-11.

144. Evans, M.; Kholod, N.; Kuklinski, T.; Denysenko, A.; Smith, S. J.; Staniszewski, A.; Hao, W. M.; Liu, L.; Bond, T. C. Black carbon emissions in Russia: A critical review. *Atmospheric Environment* **2017,** *163*, 9-21.
145. Feng, X.; Wang, S. Influence of different weather events on concentrations of particulate matter with different sizes in Lanzhou, China. *Journal of Environmental Sciences* **2012,** *24* (4), 665-674.
146. Zhang, B.; Jiao, L.; Xu, G.; Zhao, S.; Tang, X.; Zhou, Y.; Gong, C. Influences of wind and precipitation on different-sized particulate matter concentrations (PM2.5, PM10, PM2.5–10). *Meteorology and Atmospheric Physics* **2017**.
147. Naron, D. R.; Collard, F. X.; Tyhoda, L.; Görgens, J. F. Characterisation of lignins from different sources by appropriate analytical methods: Introducing thermogravimetric analysis-thermal desorption-gas chromatography–mass spectroscopy. *Industrial Crops and Products* **2017,** *101*, 61-74.
148. Viidanoja, J. Determination of short chain carboxylic acids in vegetable oils and fats using ion exclusion chromatography electrospray ionization mass spectrometry. *J Chromatogr A* **2015,** *1383*, 96-103.
149. Stavova, J.; Beranek, J.; Nelson, E. P.; Diep, B. A.; Kubatova, A. Limits of detection for the determination of mono- and dicarboxylic acids using gas and liquid chromatographic methods coupled with mass spectrometry. *J Chromatogr B Analyt Technol Biomed Life Sci* **2011,** *879* (17-18), 1429-38.
150. Do, D. D.; Junpirom, S.; Do, H. D. A new adsorption–desorption model for water adsorption in activated carbon. *Carbon* **2009,** *47* (6), 1466-1473.
151. Do, D. D.; Do, H. D. A model for water adsorption in activated carbon. *Carbon* **2000,** *38*, 767-773.
152. Brennan, J. K.; Thomson, K. K.; Gubbins, K. K. Adsoprtion of Water in Activated Carbons: Effects of Pore Blocking and Connectivity. *Langmuir* **2002,** *18*, 5438-5447.